Adsorbent assisted drying of spiral and flotation coal fines

R. Erlank

Dissertation accepted in fulfilment of the requirements for the degree *Master of Engineering in Chemical Engineering* at the North-West University

Supervisor: Prof M. le Roux

Co-supervisor: Prof Q.P. Campbell

Graduation: Aug 2021

Student number: 24312614

orcid.org/0000-0002-4999-2421

DISSERTATION DETAILS

Author:	Ruan Erlank
Student Number:	24312614
Highest Qualification:	Bachelor of Engineering in Chemical Engineering
Obtained at:	Northwest-University: Potchefstroom Campus

Project title:	Adsorbent assisted drying of spiral and flotation coal fines
Submitted for:	Master of Engineering in Chemical Engineering
Institute:	Northwest-University: Potchefstroom Campus School of Chemical and Minerals Engineering

Supervisor:	Prof Marco le Roux
Co-supervisor:	Prof Quentin Peter Campbell

DECLARATION

The author, **Ruan Erlank**, solemnly declares that this dissertation is a presentation of his original work.

Whenever others' contributions were involved, every effort was made to indicate this clearly, with due reference to the literature.

No part of this work has been submitted in the past or submitted for a degree or examination at any other university or course.

Signed on Wednesday, 24th of March, 2021, in Centurion, South Africa

R. Erlank

ACKNOWLEDGEMENTS

The author would like to acknowledge and extend his sincere gratitude to the following:

- First, and with utmost gratitude, I would like to thank our Heavenly Father, God Almighty, for His grace and the privileges He has blessed me with; to follow and achieve my dreams. I am sincerely humbled.
- To the North-West University and, specifically, the School of Chemical and Minerals Engineering, allowing me to further my studies.
- A special thanks to Coaltech Research Association for funding this project and my postgraduate studies.
- A sincere thanks to my supervisor and co-supervisor, Professors Marco le Roux and Quentin Campbell, for their insight, support and mentorship throughout my studies.
- A warm thanks to my parents, Andre Snr and Margaret Erlank, for raising me with love and guidance and to my brother, Andre Jnr Erlank, for his support, love and care.
- Last but not least, heartfelt gratitude to the love of my life, Tipharah van Dyk for her love, continuous support and care. You are dear to me.

ABSTRACT

Collieries inevitably have ever-increasing wet coal fines, which cannot be sold since it is difficult to handle, has a consequently lower heating value and relates to higher transportation costs. Recently, due to the energy industry leaning toward greener technologies, more emphasis has been placed on drying these coal fines as opposed to merely discarding them. Adsorbent assisted drying is one such proposed method that has proven promising in previous studies.

This study investigated the drying of spiral and flotation coal filter cakes using activated alumina as an adsorbent. The spiral product has a larger particle size (d_{50}:434 µm) than the flotation product (d_{50}:21 µm), and its effects were evaluated. Spiral product was also compared to spiral tailings to see the mineral content's effect on how the coal is dewatered.

The experiments were done on a laboratory-scale rotating bed with the coal being dried in a cascading motion inside cylindrical vessels. The adsorbent-to-coal mass ratio, adsorbent particle size and adsorbent state (new, used or regenerated) were varied to study each variable's effect on the drying performance. The coal's heating values were measured at significant intervals during drying to do an energy balance on the process, determining the feasibility thereof from an economical and energy perspective. Supplementary experiments included the use of molecular sieves to dewater flotation product.

The study found that the spiral and flotation coal fines could be dried swiftly to a market specified moisture content of 10% w/w within two minutes' contact sorption, experiencing overall moisture reductions in the vicinity of 91%. The majority of the coals' moisture reduction occurred in the first two minutes of dewatering, signifying the technology's fast dewatering. The spiral and flotation product experienced 17% and 30% increases in calorific value due to moisture reduction.

The main driving force for optimal drying was the contact surface area between the adsorbent and coal particles. Drying efficiencies can be optimised using either smaller adsorbent particle sizes or higher adsorbent-to-coal mass ratios or both. Nevertheless, larger adsorbent particle sizes and some lower adsorbent-to-coal mass ratios still showed sufficient dewatering of the coal fines.

Spent and regenerated adsorbents were able to deliver adequate drying of the coal fines. Fresh adsorbents' dewatering performance was followed closely by regenerated adsorbents' performance, which showed considerable improvement over the spent adsorbents' performance. Spent adsorbents were able to dry spiral product until the fifth cycle of use and flotation product until the second cycle of use, without regeneration. The spent adsorbent moisture loads confirmed that regenerated adsorbents need not be bone-dry to dewater coal efficiently in continuous use.

The regenerated adsorbents dewatered the spiral and flotation product to market specifications within at least 4 and 6 minutes, irrespective of adsorbent particle size.

The spiral product and tailings' dewatering behaved similarly to one another. Although similar in dewatering behaviour, the spiral tailings experienced slightly higher moisture reductions than the spiral product, suggesting that the mineral matter in coal tailings did not retain moisture stronger than the carbon-containing coal products.

Spiral and flotation coal vastly differed in particle size and initial moisture contents, yet their dewatering behaved very similarly, experiencing almost identical moisture desorption rates and moisture reductions. Flotation reagents were thus found to have little to no effects on flotation coal's dewatering. Flotation coal experienced less weak drying effects than spiral coal when using lower adsorbent-to-coal mass ratios and larger adsorbent particle sizes attributed to flotation coal's ultrafine particle size, which aided with good contact surface area between the coal and adsorbents.

Molecular sieves showed extraordinarily fast dewatering, significantly faster than activated alumina, having the coal dewatered to near bone-dry moisture contents within two minutes. However, spent molecular sieves showed poor coal dewatering, while its regenerated version showed meagre improvement suggesting molecular sieves' ineligibility for industrial use.

The regeneration of spent adsorbents showed sufficient moisture load reductions for activated alumina and molecular sieves. The main driving force for optimal regeneration times is the bed mass to regeneration column area ratio, which stressed the importance of intelligent regeneration column design.

Qualitative observations showed the spiral and flotation coal having affinities for caking and forming lumps, which inhibit dewatering performance, signifying the necessity for suitable materials handling before dewatering. Capillary pore blinding of the adsorbents was encountered, which may have played a role in the adsorbents' drying performance during continuous use without regeneration. Activated alumina was found to be a robust adsorbent with little to no particle breakage or attrition encountered during drying and regeneration. Molecular sieves showed brittleness and severe particle breakage during operation.

The adsorbent assisted drying of spiral and flotation coal fines were found to be an energy-positive and economically feasible process on a high level, while the use of activated alumina as adsorbent proved suitability for industrial application. A concept design of a continuous adsorbent assisted drying plant was draughted and described.

Keywords: coal processing; fine coal dewatering; fine coal drying

TABLE OF CONTENTS

LIST OF FIGURES

LIST OF TABLES

LIST OF ABBREVIATIONS & ACRONYMS

Abbreviation/ Acronym	Description	Unit
ad	air-dried basis	n/a
ar	as-received basis	n/a
daf	dry ash-free basis	n/a
db	dry basis	n/a
CV	calorific value	MJ/kg
ID	inner diameter	mm
NDT	Nano Drying Technology	n/a
PSA	Pressure swing adsorption	n/a
PSD	particle size distribution	n/a
PDT	Parsepco Drying Technology	n/a
RH	relative humidity	%
ROM	run-of-mine	n/a
SAP	super absorbent polymer	n/a
TGA	thermogravimetric analyser	n/a
SACPS	The Southern African Coal Processing Society	n/a
IEA	The International Energy Agency	n/a
SANEDI	South African National Energy Development Institute	n/a
VSA	Vacuum swing adsorption	n/a

LIST OF SYMBOLS

Symbol	Description	Unit
Al_2O_3	Aluminium(III) oxide (alumina)	n/a
CO_2	Carbon dioxide	n/a
H_2O	Water	n/a
H_2SO_4	Sulphuric acid	n/a
Na_2O	Sodium oxide	n/a
SiO_2	Silicon dioxide (silica)	n/a

LIST OF UNITS

Unit Symbol	Unit	Measurement
% w/w	percentage of weight per weight base	Moisture content; composition
g	gram	Mass
kg	kilogram	Mass
t	metric tonne	Mass
Mt	million tonnes	Mass
min	minutes	Time
s	seconds	Time
h	hours	Time
tph	ton per hour	Mass flow rate
m	metre	Length
mm	millimetre	Length
µm	micrometre	Length
kJ	kilojoule	Energy
MJ	megajoule	Energy
GJ	gigajoule	Energy
kWh	kilowatt-hour	Energy
W	watt	Power
kW	kilowatt	Power
MW	megawatt	Power
GW	gigawatt	Power
GHz	gigahertz	Frequency
°C	degree Celsius	Temperature

m^2/g	square metre per gram	Surface area
cm^3/g	cubic centimetre per gram	Pore volume
kg/m^3	kilogram per cubic metre	Density
$g_{moisture}/g_{coal}.min$	gram moisture per gram wet coal per minute	Desorption rate
$g_{moisture}/g_{ads}.min$	gram moisture per gram wet adsorbent per minute	Adsorption rate
$kJ/mol_{adsorbed}$	kilojoule per mol H_2O adsorbed	Adsorption enthalpy
$kWh/g_{moisture}$	kilowatt-hour per gram moisture removed	Dewatering energy

Chapter 1 Introduction

1.1 Background and motivation

South Africa's coal mining history stretches for about 150 years and plays a vital role in the economy (Venter & Naude, 2015). Annually, South Africa produces on average 224 million tonnes of marketable coal, exports 25% of the production, and is the seventh-largest coal producing country in the world (Baruya, 2018; Eskom, 2016). For only the first quarter of 2016, coal sales accounted for R25.5 billion, of which R11.6 billion was export sales (Department of Mineral Resources (RSA), 2016).

Of the domestic-use coal in South Africa, 53% is used for electricity generation, 33% is used for petrochemical industries, and 12% is used for metallurgical industries (Eskom, 2016). Coal-fired electricity generation represents 83.3% (39,342 MW of a total 47,201MW) of the South African energy mix (Eskom, 2017a). As a steam coal user, Eskom ranks first globally, and as a coal-to-chemical producer, Sasol ranks first in the world (Department of Energy (RSA), 2018).

Thermal grade coal and synthetic fuel-grade coal, as the two largest consuming industries in South Africa, have coal specifications that their respective coal suppliers must meet. Table 1-1 shows the coal specifications for thermal grade and synthetic fuel, respectively.

Table 1-1 South African thermal-grade vs synthetic fuel coal specification, adapted from (Steyn & Minnit, 2010)

Parameter	Thermal-grade	Synthetic fuel-grade
Calorific value (MJ/kg)	21	20-22.64
Total moisture (% w/w)	10	10
Ash (%)	25-33	20-29.7
Volatile matter (%)	20	21-26.9
Sulphur (%)	1.0	>1.0

Coal fines have become more abundant in the coal industry, mainly because of more mechanised mining technology (Peters, 2016). Up to 15% of run-of-mine coal can be in the -500 µm particle size range, and 6% of ROM coal can be in the -200 µm particle size range (SACPS, 2015; Venter & Naude, 2015).

Fine coal has a larger surface area per mass unit than its coarser counterparts, which causes it to retain more moisture, which holds inordinate challenges for the coal industry due to the difficulty of fine coal dewatering.

High moisture levels in fine coal hold several problems, including combustion, transportation, handling, and marketability (Tao *et al*., 2000). In 2000, the economic benefit of fine coal dewatering was reported, stating that a 1 % w/w moisture reduction can hold a saving of US $100 per kiloton of clean coal (Figures in 2000) in terms of transportation costs (Tao *et al*., 2000). For perspective purposes, a typical coal-fired power station in South Africa burns 50,000 tonnes of coal every day (Eskom, 2017b).

Because of its higher moisture content and consequently lower calorific value, South African coal-fired power stations discard -200 µm coal fines (Venter & Naude, 2015). Coal beneficiation causes 65 Mt of fine coal to be discarded every year (Department of Energy (RSA), 2018). It is estimated that over 150 years, South Africa has discarded a total of one billion tonnes of thermal-grade coal fines (ESI Africa, 2014).

Current mechanical dewatering methods at coal preparation plants (filter presses, screen-bowl centrifuges, or vacuum disc filters) can lower fine coal's moisture content down to approximately 18-30 % w/w. Filter presses are also applied to dewater flotation concentrates, delivering moisture contents of 15-20 % w/w (Prat, 2012). Still, more drying is necessary to achieve coal specifications of below 10 % w/w.

A computer simulation was done on a typical coal preparation plant and revealed that the annual revenue of the plant could potentially be increased by 5.7% if the moisture content of the clean coal product can be reduced by 50%, typically from 18 % w/w to 9 % w/w (Mohanty *et al*., 2012).

Two emerging drying technologies, Parsepco Drying Technology (PDT) and Nano Drying Technology (NDT), have shown the feasibility to yield the desired moisture reduction of fine coal from 18 % w/w to 9 % w/w (Mohanty *et al*., 2012). The PDT method dries the fine coal on a woven steel conveyor belt under vacuum conditions, while the NDT method uses molecular sieves to adsorb moisture from the fine coal (Mohanty *et al*., 2012).

Some researchers reported that activated alumina adsorbents were contacted with mechanically dewatered fine coal for approximately five minutes and reduced the moisture content from 19 % w/w to 9 % w/w (Yang, 2015).

Some workers studied the drying ability of run-of-mine coal in the -2 mm +0.25 mm particle size range by using adsorbents to dry fine coal from 15-20 % w/w to below 8 % w/w within 10 minutes (Peters, 2016). The author used spherically shaped activated alumina and activated silica

adsorbents and dried the fine coal in a fixed bed and rotating bed (cascading motion) setup. The rotating bed (cascading motion) and the activated alumina proved to yield the best results.

Considering the figures listed above, it is evident that fine coal dewatering is more critical than ever before. For more than a decade, extensive research has been done to improve the way fine coal is dried. Conventional methods of dewatering fine coal (mechanical dewatering) do not dewater sufficiently down to market specifications. Thermal drying is uneconomical and has detrimental effects on the environment. Thus, fine coal dewatering is a challenge from a technical, economic and environmental point of view. It is now needed to study if adsorbent assisted drying is feasible for spiral and flotation coal fines.

1.2 The scope of this study

To date, the drying ability of run-of-mine coal fines by using activated alumina, as adsorbent, in a cascading motion is known (Peters, 2016). In this study, the drying ability of spiral coal product and tailings and flotation coal product will be studied using activated alumina on a laboratory-scale batch process.

The laboratory-scale batch process entails a rotational bed with cylindrical vessels in which the coal will be mixed with activated alumina adsorbents. Conditions such as adsorbent-to-coal mass ratio, adsorbent particle sizes, and the adsorbent state (fresh, spent or regenerated) will be varied to investigate each condition's influence on the drying ability. The calorific values of the coal will be analysed at predetermined time intervals during the drying procedure.

The regeneration ability of these adsorbents will be studied to test industrial applicability. The degradation of the adsorbents during operation will be studied, whether significant or not. Finally, the economic feasibility and industrial applicability of this process will be studied.

1.3 Objectives of this study

1.3.1 Primary objectives

1. What is the drying ability of spiral coal (product and tailings) using activated alumina as an adsorbent in a cascading motion, and how does the dewatering affect the calorific value under the following conditions?
    a. Atmospheric conditions
    b. Various adsorbent-to-coal mass ratios
    c. Various adsorbent particle sizes
    d. Using new, used, and regenerated adsorbents
2. What is the drying ability of flotation coal product using activated alumina as an adsorbent in a cascading motion, and how does the dewatering affect the calorific value under the following conditions?
    a. Atmospheric conditions
    b. Various adsorbent-to-coal mass ratios
    c. Various adsorbent particle sizes
    d. Using new, used, and regenerated adsorbents
3. What is the regeneration ability of activated alumina adsorbents using a packed bed column under the following conditions?
    a. 22°C and 70% relative humidity

1.3.2 Secondary objectives

1. Is adsorbent degradation significant (attrition) during operation?
2. Does a low pH lead to degradation of the adsorbents?
3. How does activated alumina compare to molecular sieves' adsorption performance?
4. Are other means of regeneration effective?
5. What is the economic feasibility and energy consumption of a continuous adsorbent assisted fine coal dryer?
6. What is the industrial applicability of a continuous adsorbent assisted coal fines dryer?

1.4 Beneficiaries of this study

If this project is proven to be feasible, the coal industry, locally and internationally, will benefit from this by yielding more acceptable fine coal for specifications. As the annual and historic fine coal discards are mentioned in Section 1.1, it will positively influence the environment, causing less fine coal to be discarded and previously discarded wet fine coal to be reclaimed and dried for utilisation.

1.4.1 Environmental

Previously discarded product fine coal can be reclaimed, dried, and sold again. This reclamation may positively affect the environment as these slurry ponds, where the coal is discarded, take up large land areas where some natural habitats might have been found. Reducing these slurry ponds' footprint by reclaiming the coal and rehabilitating the area might avail the land area for recreational purposes where natural habitats occur or could be used for agricultural purposes.

Furthermore, this drying technology may substitute current effective dewatering practices, which are harmful to the environment due to high energy consumption, and when implemented, may reduce/ eliminate the detrimental effects that the previous technologies had on the environment.

1.4.2 Economic

If the drying technology discussed in this study is feasible and could be implemented industrially, it may contribute to the coal industry's economy. This means that fine and ultra-fine coal products would not have to be discarded anymore but may be sold to the market and even for higher prices due to lower moisture contents. Power stations would be able to buy more fine coal because the challenges of higher moisture and poor handleability associated with fine coal may be abridged.

In short, coal producers would be able to sell more product coal due to product coal fines, also accounting to sales, generating more revenue. Power stations would be able to buy the coal fines. Previously discarded product grade coal may be reclaimed and dried. Eventually, this reclaimed and dried coal may cause an influx in the coal supply, leading to lower coal prices and cheaper electricity. The abovementioned scenarios may eventually impact the broader economy positively.

Chapter 2 Literature review

2.1 Introduction to coal

2.1.1 History

2.1.1.1 United Kingdom

Coal appeared to have received the first attention in England and Scotland before the close of King William the Lion (1210-1214 AD) when carboniferous strata were exposed on the seashores (Galloway, 1882). Favourable conditions for coal working, which included that the coal seams came out to the surface and could be easily conveyed to the market, existed on the seacoast of Northumberland and the south shore of the Frith of Forth. Historians record these localities as the cradles of the coal trade (Galloway, 1882).

Holyrood Abbey's monks received grants (tithes) from the Carriden colliery, near Blackness, Edinburgh. These grants were confirmed by King William (Galloway, 1882). During King William's reign, Newbottle Abbey's monks also received grants from a colliery and quarry on the seashore at Preston, Tranent's lands, a district well known for its coal production (Galloway, 1882). In 1228, a lane in a suburb of the metropolis, London, was named "Sacoles Lane", which meant "Sea Coals Lane", which clearly stated that some coal trading was going on in London (Galloway, 1882).

2.1.1.2 United States of America

In 1908, President Theodore Roosevelt reminded those in attendance at the White House Conference that coal's dominance in America was a relatively recent occurrence. Roosevelt said that in George Washington's time (1789-1797), anthracite was known as useless black stones and the vast bituminous coal fields were yet to be discovered (Buckley, 2004). Steam to electricity generation was unknown, and moving water was the only power source (Buckley, 2004).

At the start of the 19th century, coal was mainly used as domestic heating fuel and blacksmiths' forging. In the following years, it became useful as a fuel for salt and iron furnaces, brick and pottery kilns, and finally, steam engines (Buckley, 2004). Between 1800 and 1860, the United States' annual coal production increased from 100,000 tonnes to 20 Mt (Buckley, 2004).

The post-Civil War years, between 1863 and 1877, caused tremendous growth in coal production and consumption. In 1885, the annual production of coal increased to 110 Mt. Coal was now increasingly being used as fuel for steamship travel and steam locomotives and to stoke the furnaces of an arising steel industry (Buckley, 2004).

By 1900, coal was responsible for nearly 70% of the national energy market, and the United States was the world's leading coal producer with an annual production of 243 Mt (Buckley, 2004).

2.1.1.3 Australia

In 1796, George Bass and Matthew Flinders discovered coal in the Wollongong district on the Illawarra coastal plain, south of Sydney, while they were on a voyage southward in the Tom Thumb II. Flinders wrote, "…under the cliffs were lying black lumps, apparently of slaty stone rounded by attrition" (Young, 2017).

In 1848, the first coal mine opened at Mount Keira, west of Wollongong, Australia, while coal was transported to the port for steamers or shipped to Sydney. Rising coal prices initiated a second coal mine at Mount Keira in 1857 (Young, 2017). By 1862, five coal mines were operating at the lower slopes of the mountain, and by 1894 12 mines were operating in the coalfield with railways running to the Wollongong port (Young, 2017).

Six significant firms in the smelting, metal manufacturing and fertiliser industry were developed between 1908 and 1938 in Wollongong and made this region the primary centre of heavy industry in Australia. Wollongong was recognised as "Steel Town" in Australia (Young, 2017).

2.1.1.4 South Africa

Coal was first used by the indigenous people of South Africa many years before commercial mining began. By 1852, steamships were supplied with bunker coal in Natal, and coal was scarcer nearer to the coast, while the transportation costs to the coast made this resource very expensive (SACPS, 2015).

Vast reserves of coal were found in the Witbank area, and so, large scale mining began. The discovery of gold in the Witwatersrand area and its need for coal energy caused the Springs/ Boksburg area to develop even faster, and by 1887, it was producing more coal than the Witbank coalfield (SACPS, 2015). As the gold industry declined, the development swung back to Witbank, and indeed, Witbank's coal met the needs of the export market and the power generation market (SACPS, 2015).

With the South African government's sanction to export 27 Mt of low-ash coking coal to Japanese steel mills for ten years in the late 1960s, the industry had to find a suitable port (Dunn, 1980). Richards Bay was chosen as the suitable deep-water port, and on the 1st April 1976, the first phase of the Richards Bay Coal Terminal was commissioned, handling 11 Mt per annum and 11 grades of coal. By April 1979, the second phase was commissioned with a throughput of 24 Mt per annum (Dunn, 1980).

Today, the Richards Bay Coal Terminal, with its fifth phase commissioned in 2010, has a throughput of 91 Mt per annum and a stockyard capacity of 8.2 Mt with 36 grades of coal stockpiled (Richards Bay Coal Terminal, 2018). Figure 2-1 shows the stockyard of the Richards Bay Coal Terminal with ships in the background.

Figure 2-1 Richards Bay Coal Terminal, taken from (Richards Bay Coal Terminal, 2018)

2.1.2 Coal formation

Various kinds of coal exist, and understanding these differences between the coal types and their qualities, allows one to comprehend when and where to use the coal. What better way is there to understand the types of coal than to understand how the coal was formed in the first place.

Coal is a sedimentary rock formed from the maturation and compaction of altered remains of luxuriant vegetation in another geological time (Osborne, 1988). Coal consists of more than 70% by volume and 50% by mass carbonaceous material (SACPS, 2015). Further, the variety of vegetation will determine the "type" of the coal, the range of impurities that will determine the "grade" of the coal and the degree of metamorphism that will determine the "rank" of the coal (SACPS, 2015).

Under a microscope, coal is composed of many distinct organic constituents called macerals and parallel to these macerals are the inorganic minerals found in the coal (Falcon & Snyman, 1986). Falcon and Snyman define macerals as: "… entities which evolve from different organs or tissues of the original plant material during primary accumulation and the early stages of biochemical degradation and early coalification".

Several factors play a part in the maceral formation, including vegetation, climate, ecological conditions, pH and the redox (Eh) value. These factors play a prominent role in the degradation of plant matter, especially the redox value (Falcon & Snyman, 1986). During peat formation or peatification, bacteria and fungi will feed on the organic material, producing hydrogen-poor humates, the plant sap will dissipate, and the cell walls will dry out and darken, leaving the vegetation to look like light to dark strings of wood (Falcon & Snyman, 1986).

While the peat is submerged and peatification progresses under limited oxygen supply, the enrichment of cell wall matter and resistant plant matter occur while humic acids are produced because of the biochemical degradation. These humic acids form a precipitate gel which causes gelification or vitrinization of the woody plant tissue (Falcon & Snyman, 1986).

When the peat is buried at depths below 1 m, the peatification process stops because of sedimentation. Through time, with high temperatures and high pressures, coalification occurs, which entails the metamorphosis of peat through the progressive ranks of lignite (brown coal), sub-bituminous and bituminous coal and finally anthracite (Falcon & Snyman, 1986).

2.1.3 Coal classification

2.1.3.1 Rank

The maturity state to which coal has metamorphosed during the coalification process is termed the coal RANK (Falcon & Snyman, 1986). The rank of coal increases as it matures from peat to anthracite. Figure 2-2 illustrates the different coal ranks.

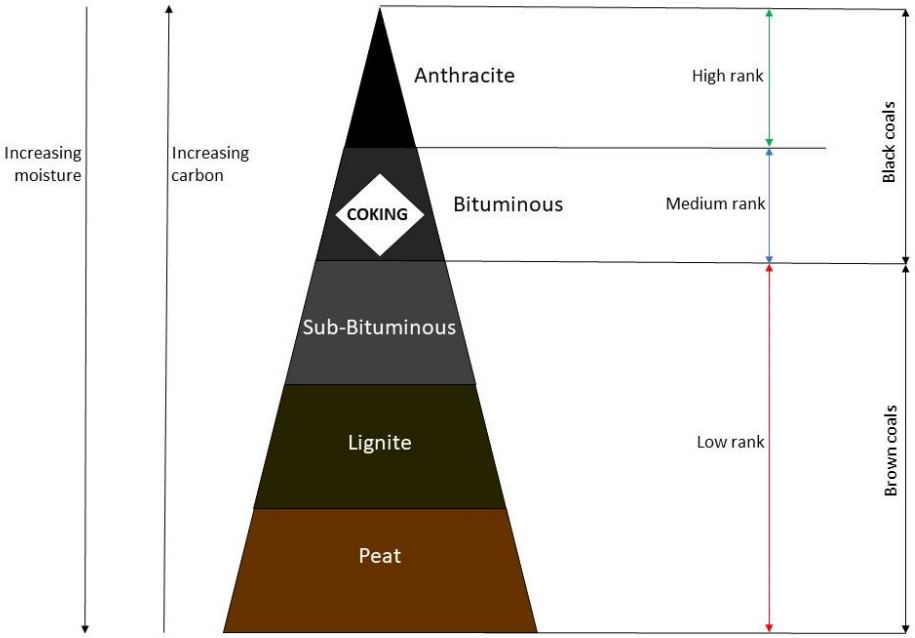

Figure 2-2 Coal classification by rank, adapted from (Osborne, 1988)

The carbon content and calorific value of the coal increases as the rank increases, and the moisture and volatile content of the coal decreases as the rank increases (Osborne, 1988). Furthermore, the geological complexity, cost of extraction and the unit realisation price of the coal also increase as the rank increases (Osborne, 1988).

Lignite is primarily light brown to near black and may be incoherent and woody. Anthracite is hard to very hard, has no caking properties and burns smokeless (SACPS, 2015). In Table 2-1, the vitrinite reflectance and volatile matter of the different coal ranks can be seen.

Table 2-1 Changes accompanying coal rank, adapted from (SACPS, 2015)

Rank	Vitrinite reflectance (%)	Volatile matter (%)
Sub-bituminous coal	<0.6	>40
Bituminous coal	0.6 – 2	>16.5
Semi-anthracite	2 – 2.5	12.5 – 16.5
Anthracite	2.5 – 6	<12.5

2.1.3.2 Type

The coal TYPE (also called petrographic or maceral composition) refers to the composition of the organic constituents formed during biochemical degradation (Falcon & Snyman, 1986). The proportions in which these organic constituents are consolidated affect the coal's physical and chemical properties of a given rank. In essence, the maceral content of coal plays a significant role in technological properties and coal usage (SACPS, 2015).

Microlithotypes are the microscopic layers (usually greater than 50µm in width) formed from the organic and inorganic constituents of coal combined in various associations. The succession of these microlithotypes form layers of 5 mm or more called lithotypes (Falcon & Snyman, 1986). These layers or bands can be distinguished from one another based on lustre, fracture pattern, the colour of the coal, the colour of the band, texture, and stratification (Falcon & Snyman, 1986).

Lithotypes are further divided into sapropelic and humic coals:

Sapropelic coals are non-banded, dull and have an even granular surface and conchoidal fracture. Sapropelic coals originate from open or deeper water and are formed from accumulated algae and aquatic detrital organic matter (Falcon & Snyman, 1986).

Humic coals are banded with layers of alternating lustre, originating from humic matter accumulation found near or in peat swamps (Falcon & Snyman, 1986).

In South Africa, three main maceral groups exist in bituminous and anthracitic coals:

Vitrinite is formed initially from woody trunks, branches, twigs, stems, leaf tissue and shoots (Falcon & Ham, 1988). Vitrinite plays a significant role in the coking properties of coal (SACPS, 2015). A specific coal's rank can be determined by measuring polished vitrinite reflectance (SACPS, 2015). Vitrinite is oxygen-rich, combusts rapidly, and is essential for coking, pyrolysis and liquefaction (Falcon & Ham, 1988).

Liptinite includes plant and seed remnants that are mainly resistant to biochemical degradation and therefore slightly metamorphoses from the original material. It consists primarily of cuticles, spores, resins and algae (Falcon & Ham, 1988). Liptinite is hydrogen-rich, combusts very rapidly and is vital for pyrolysis, liquefaction and bitumen production (Falcon & Ham, 1988).

Inertinite includes the most highly-altered plant remains in coal (SACPS, 2015) and oxidised detrital organic humus (Falcon & Ham, 1988). Usually, inertinite has a lower volatile matter than vitrinite (SACPS, 2015). Inertinite is carbon-rich, combusts slowly and is relatively inert in coking, liquefaction and pyrolysis (Falcon & Ham, 1988).

2.1.3.3 Grade

The coal GRADE refers to the quality concerning the mineral matter or range of impurities within the coal (Falcon, 2013).

Mineral matter within coal refers to the inert solid material in coal, which lowers the coal's heating value by dilution. When coal is combusted, the mineral matter does not combust and remains ash after combustion (SACPS, 2015).

Inherent mineral matter refers to the minerals intimately mixed within the coal, mainly from the minerals present in the original plant material from which the coal was formed. Pyrites, carbonates, quartz and finely dispersed clays are the main inherent minerals groups found in South African coals (SACPS, 2015). Extraneous mineral matter refers to sedimentary bands, sandstones, siltstones and intermediate rocks in the coal seam (SACPS, 2015).

The different grades of coal being sold in South Africa can be seen in Table 2-2.

Table 2-2 Coal grades being sold in South Africa, adapted from (Falcon, 2013)

Grade	Gross Calorific Value (MJ/kg) (*ad*)
Special	>28.5
Grade A	27.5 – 28.5
Grade B	26.5 – 27.5
Grade C	25.5 – 26.5
Grade D	<25.5

2.2 Coal in South Africa

2.2.1 South African coal geology

In South Africa, nineteen coalfields, covering approximately 9.7 million hectares, have been defined based on geographic considerations and variation in origin, quality, sedimentation, formation and distribution (Hancox & Götz, 2014; SACPS, 2015).

However, most coal mined in South Africa to date comes from only six or seven of these coalfields (Hancox & Götz, 2014). A map of the different coalfields in South Africa can be seen in Figure 2-3.

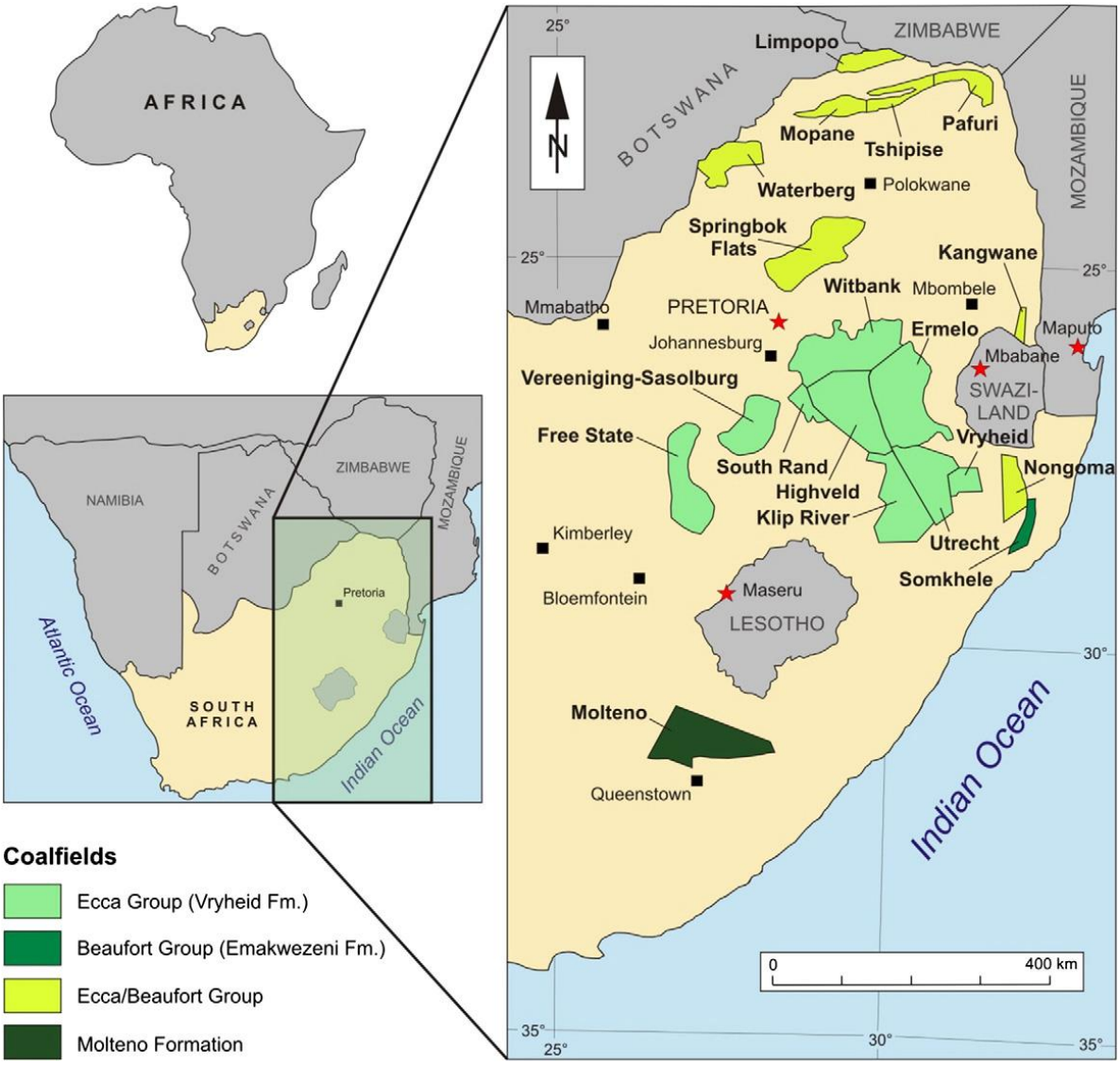

Figure 2-3 Map of the South African Coalfields, taken from (Hancox & Götz, 2014)

2.2.1.1 Witbank Coalfield

As early as 1889, four small collieries were mining on the Witbank Coalfield (Falconer, 1990). Today, the Witbank Coalfield is still one of the most vital coalfields in South Africa, as it supplies more than 50% of the South African coal economy. This coalfield produces both metallurgical and thermal coal for the local and export market. Many of the significant coal-fired power stations in South Africa are situated near the Witbank Coalfield (Hancox & Götz, 2014).

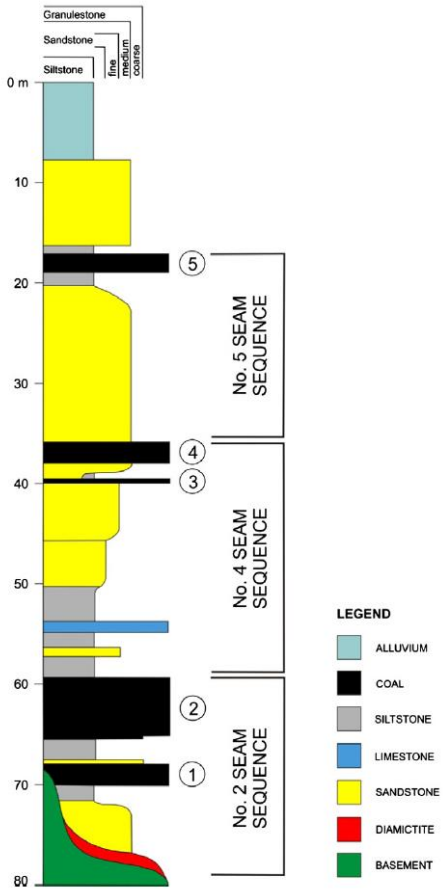

Figure 2-4 Stratigraphic column for the Vryheid Formation in the Witbank Coalfield, taken from (Hancox & Götz, 2014)

As illustrated in Figure 2-4, five coal seams are present in the Witbank Coalfield where No. 1 Seam is at the base and No. 5 Seam is at the top. The No. 1 Seam has an average thickness of 1.5-3 m and is a source of A and B-grade thermal coal and metallurgical coal. No. 1 Seam and No. 2 Seam merges in some parts, forming a composite seam up to 17 m thick (SACPS, 2015).

The No. 2 Seam accounts for approximately 69% of the Witbank Coalfield's remaining coal resources and is the central economic seam with an average thickness of 6.5 m. It consists mainly of dull coal but has some of the best quality coal with bright coal at the bottom and bright bands at other seam levels (SACPS, 2015). The No. 3 Seam is usually thinner than 0.5 m and is therefore not economically mined (SACPS, 2015).

The no. 4 Seam's thickness varies between 2.5 m and 6.5 m in some parts and is primarily a source of thermal-grade coal and, to some extent, used for coal to liquids processes. This seam consists mainly of dull coal, with only a few bright bands (SACPS, 2015). The No.5 Seam's thickness varies between 0.5 m and 2 m, and the seam has relatively high-quality coal, generally vitrinite-rich bituminous coal, which is mainly used as metallurgical coal (Hancox & Götz, 2014).

2.2.1.2 Other significant coalfields

The Highveld Coalfield is similar to the Witbank Coalfield in many ways, including the general stratigraphy. The Highveld Coalfield's coal resources are vital to South Africa's coal to liquid or synthetic fuel industry, where this industry consumes about 50 million tonnes of coal per annum (Hancox & Götz, 2014).

The Free State Coalfield is the single largest coalfield in South Africa but is less popular than the other coalfields. It has a 25-50 m thick coal zone at depths of 50-100 m in the north and even deeper in the coalfield's southern parts (Hancox & Götz, 2014; Stavrakis, 1986). The Vereeniging-Sasolburg Coalfield is essential for South Africa's history as it is the original coalfield that supplied South Africa's first coal-to-liquid plant in the 1950s built by Sasol (SACPS, 2015).

The Klip River Coalfield played the most critical role in the anthracite and coking coal industry in South Africa. The Waterberg Coalfield contains approximately 40-50% of the remaining coal resources in South Africa and hosts the world's largest opencast coal mine, which extracts approximately 38 million tonnes of run-of-mine coal (SACPS, 2015).

2.2.2 Coal industry and economy

Annually, South Africa produces on average 224 million tonnes of marketable coal, exports 25% of the production and is the seventh-largest coal producing country in the world (Baruya, 2018; Eskom, 2016). In 2013, the coal industry contributed R51 billion to the South African economy, compared to the R31 billion contribution of gold in the same year, which established coal as a more important commodity for the South African economy (Motengwe & Alagidede, 2017).

In 2017, coal production reached 252 Mt, generating revenue of R130 billion. In the same year, the coal industry employed approximately 82,248 people, delivering total wages of R22 billion to employers (Minerals Council South Africa, 2019).

South Africa's coal exports consist, to a more considerable extent, of thermal grade coal (75.8 Mt, 2017) and to a smaller extent of metallurgical coal (1.6 Mt) (Baruya, 2018). Of the domestic-use coal, 53% is used for electricity generation, 33% is used for petrochemical industries, and 12% is used for metallurgical industries (Eskom, 2016). Coal-fired electricity generation represents 83.3% (39,342 MW of a total 47,201 MW) of the South African energy mix (Eskom, 2017a).

As a steam coal user, Eskom ranks first globally, and as a coal-to-chemical producer, Sasol ranks first in the world (Department of Energy (RSA), 2018). Two major coal-fired power stations are currently under construction, which will add an extra 9,564 MW of electricity to the total energy mix of South Africa, once fully commissioned (Eskom, 2017a).

Even though the world is moving towards greener, renewable energy alternatives, coal will still be in demand for the next couple of decades, as illustrated in Figure 2-5. Electricity generation will, to a more considerable extent, be dependent on coal for decades to come (Figure 2-6). At the current production and consumption rates in South Africa, only half of the recoverable coal reserves would have been mined by 2070 (Baruya, 2014).

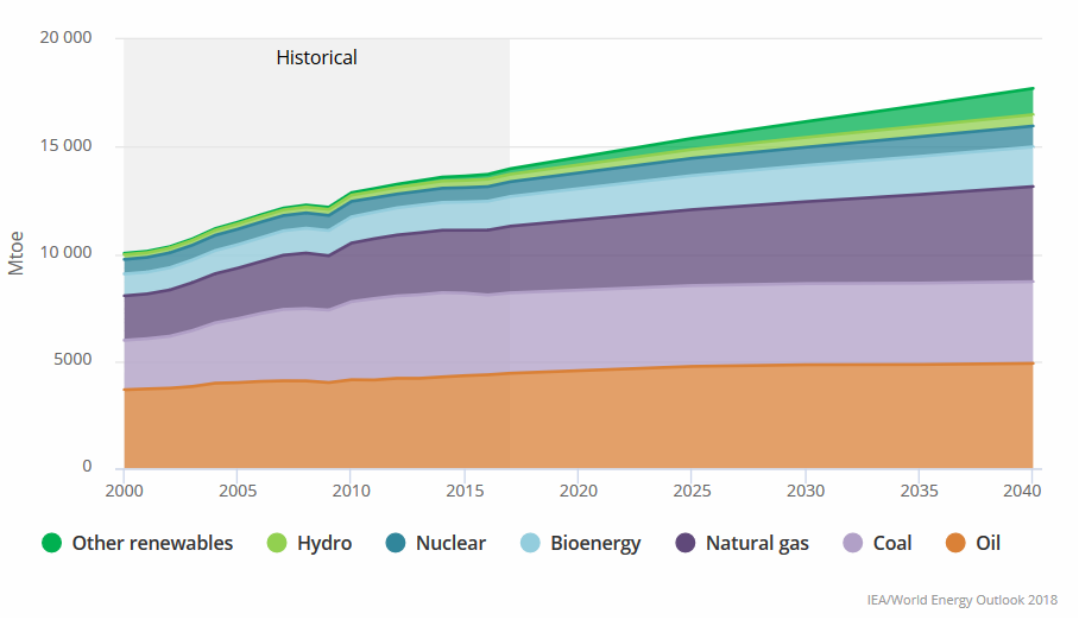

Figure 2-5 Total global primary energy demand forecast, taken from (IEA, 2018)

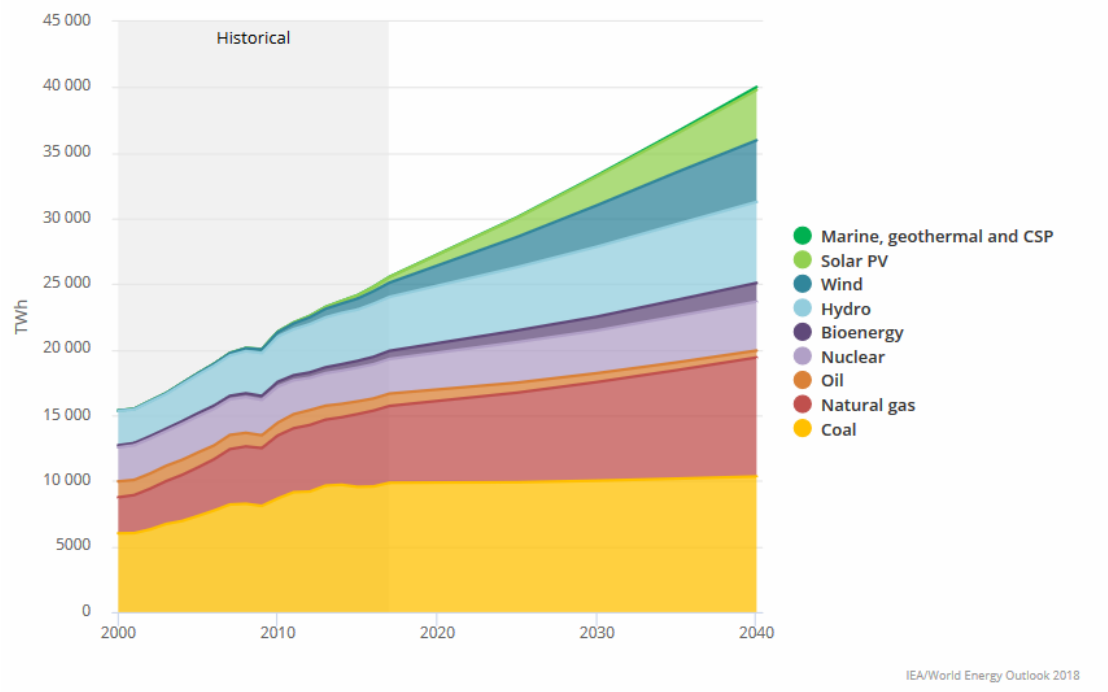

Figure 2-6 Global electricity generation by technology, taken from (IEA, 2018)

2.3 Coal preparation

2.3.1 Conventional coal preparation

In a conventional wet coal beneficiation plant, the main objective is to separate good quality coal from lower-quality coal through their density differences. Denser coals contain more mineral matter and impurities and consequently yield more ash and lower heating values when combusted. Less dense coals contain less mineral matter and impurities and higher carbon contents, yielding less ash and higher heating values when combusted (Laskowski, 2001).

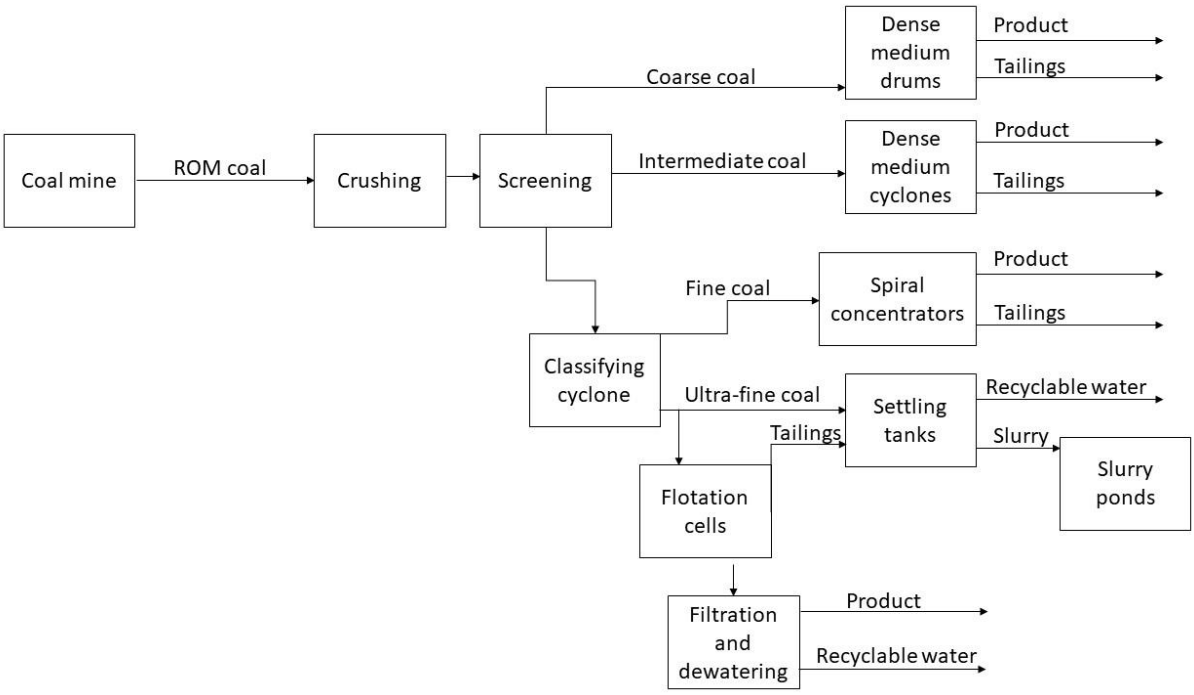

Figure 2-7 Conventional wet coal beneficiation plant, adapted from (SANEDI, 2011)

As illustrated in Figure 2-7, the run-of-mine coal is first liberated or crushed and then screened into the respective particle size portions suitable for beneficiation and market requirements (SACPS, 2015). Coarse coal is then beneficiated in dense medium drums where valuable low ash coal (lighter coal) is considered a product, and denser high ash coals are considered discards or tailings. The medium coals are beneficiated with dense medium cyclones. Finer coals are then separated using classifying cyclones where fine coal is beneficiated with spiral concentrators. The ultra-fine coal is beneficiated with flotation cells, or it is discarded in slurry ponds if the colliery does not have flotation cells. Water, reclaimed from the settling tanks, slurry ponds and dewatering processes, is recycled for beneficiation of more ROM coal.

2.3.2 Spiral concentrator

Over the years, spiral concentrators have found numerous applications in various mineral processing industries, including fine coal recovery. The spiral concentrator consists of a helical conduit that is modified semi-circular in cross-sectional view (Wills & Napier-Munn, 2006). Figure 2-8 shows a bank of coal spiral concentrators working in parallel.

Figure 2-8 Coal spiral concentrators, taken from (FLSmidth, 2019)

At the top of the spiral, a feed slurry of 15 to 45% solids within the particle size range of -3 mm +75µm is introduced. The solids content should be around 35% for coal spirals, and the particle sizes around -500 µm and +150 µm (SACPS, 2015). The slurry flows spirally downwards, and due to centrifugal force, interstitial trickling and differential particle settling rates, the particles stratify between the inner edge and the outer edge of the stream (Wills & Napier-Munn, 2006).

Some researchers reported that hindered settling is the primary separation effect with the largest, densest particles that report to the stream's inner edge (Mills, 1978). Other workers reported that reverse classification is the net effect with smaller, denser particles reporting to the stream's inner edge (Bonsu, 1983). Figure 2-9 illustrates a typical spiral concentrator's cross-sectional view where the denser particles end in the stream's inner edge while the lower density material (coal product) will end in the outer edges.

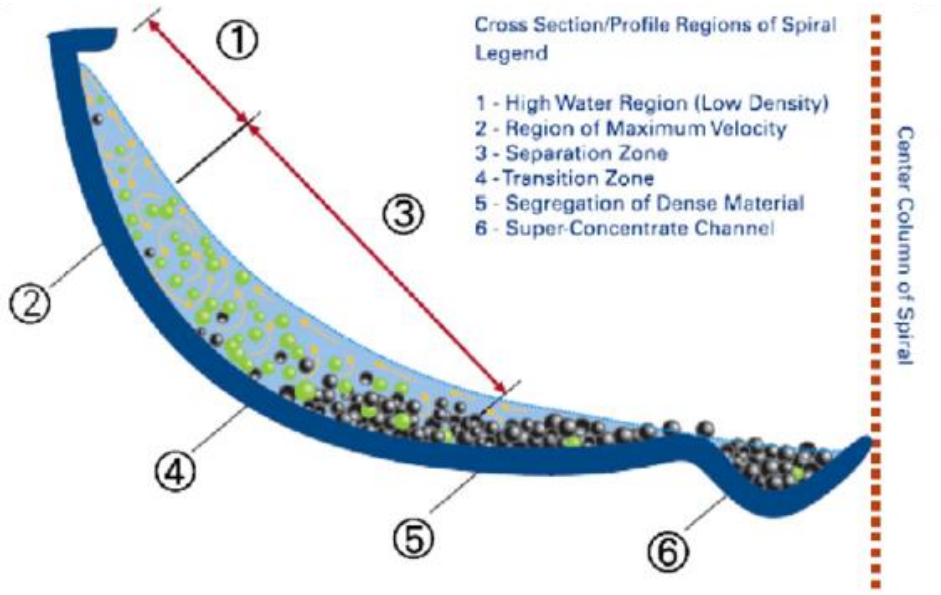

Figure 2-9 Cross-sectional view of spiral concentrator, taken from (Doheim, et al., 2013)

At the bottom of the spiral concentrator, ports are located for the removal of the different specific gravity particles, with the higher density particles exiting at the inner edge of the stream (the lowest point in cross-sectional view), middling range exiting at the middle of the stream and the lowest density particles exiting at the outer edge of the stream (Wills & Napier-Munn, 2006).

The angle of the steepness of a spiral affects the specific gravity of separation, hence the fact that various spirals are constructed with various slope steepnesses, depending on the specific mineral processing requirements. In coal processing, shallow angles are used to separate coal from shale compared to the steepest angles used to separate heavy minerals (specific gravity of 4.7) from heavy waste minerals (specific gravity of 3.6) (Wills & Napier-Munn, 2006). The uniformity in the feeding stream has a significant effect on the operating efficiency and recovery of the desired product, especially with coal spiral concentrators (Holland-Batt, 1993).

2.3.3 Flotation cell

Flotation is a physicochemical process that entails the selective attachment of some mineral matter to air bubbles and the simultaneous wetting of other mineral matter by water (Osborne, 1988). Hydrophobic species attach to the air bubbles, floating, while hydrophilic species attach to the water, which will sink.

Coal flotation is the most widely used beneficiation method to treat fine bituminous coal, especially metallurgical coking coal, to treat coal finer than 1 mm in top size (Osborne, 1988). In South Africa, the use of spiral concentrators meant that the -150 µm coal fractions, being too small in particle size for spiral concentrators, could be processed with froth flotation (SACPS, 2015).

Coal's hydrophobicity increases significantly as its rank increases but reaches a peak at almost 90% carbon content for bituminous coal. The increase in hydrophobicity is because of the gradual elimination of hydrophilic polar groups and increasing carbon content in the coal during the coalification process (Osborne, 1988). As the hydrophobicity of the coal increases, its rate of flotation increases. Another phenomenon is that the hydrophobicity or floatability of the coal is affected by the macrolithotypes increasing order from fusain, durain, and clarain to vitrain (Laskowski, 2001; Osborne, 1988).

Even though coal is naturally hydrophobic, exhibiting large contact angles when submerged in pure water, coal's froth flotation process still requires some flotation reagents to enhance the flotation process. Reagents include collectors for selective wetting, frothers, promoters for collector spreading over coal surface, modifiers for pH control and depressants to inhibit the flotation of certain minerals such as pyrites (Laskowski, 2001).

Two main froth flotation methods are used in South Africa, namely mechanical and pneumatic flotation cells. Mechanical flotation cells entail vertical hollow shafts driven by electric motors to draw air through the shaft (SACPS, 2015). At the top of the shaft, the rotor draws air for mixing with the slurry; in the middle section, a dispenser breaks the air into tiny bubbles; and the lower section draws the slurry upwards to mix with the bubbles. The air bubbles attach to the hydrophobic coal and float to the top of the cell, where sweeping paddles sweep the coal froth into a product launder (SACPS, 2015).

There are two types of pneumatic flotation cells: column cell and short column cell (better known as Jameson Cell). With the column cell, the air is introduced through spargers at the column's base, while coal is fed closer to its top. The coal and air bubbles meet in counter-current flow, while coal descends and air bubbles rise (SACPS, 2015).

With the Jameson Cell, the air and coal feed meet in a downcomer pipe where most contact occurs. The air is also induced in the downcomer pipe due to the coal feed and needs no air blowers. The downcomer pipe enters the flotation cell to a relatively low point where the froth exits and floats to the top (SACPS, 2015).

2.4 Coal fines

2.4.1 Mechanised mining technology

In the early stages of coal mining, coal fines were rejected and treated as tailings, which meant that it would end up in tailing ponds, awaiting reclamation when interest was shown in coal fines.

It was not until the 1980s when coal fines and its dewatering techniques started receiving attention because of more mechanised mining, the urge to close coal preparation plants' water circuits and more advanced petrographic studies, revealing the potential value of fine coal (Osborne, 2012).

Fine and ultra-fine coal has become more plentiful in the coal industry due to more mechanised mining. Up to 15% of ROM coal can be in the -500 µm size range, and up to 6% of ROM coal can be in the -200 µm range (SACPS, 2015; Venter & Naude, 2015).

Coal beneficiation causes 65 Mt of coal to be discarded every year (Department of Energy (RSA), 2018). It is estimated that for 150 years, South Africa has discarded a total of one billion tonnes of thermal-grade coal fines (ESI Africa, 2014).

2.4.2 Moisture associated with coal

High moisture levels in fine coal hold several problems, including combustion, transportation, handling and marketability (Tao *et al*., 2000). As illustrated in Figure 2-10, three categories exist in which moisture is associated with coal (SACPS, 2015).

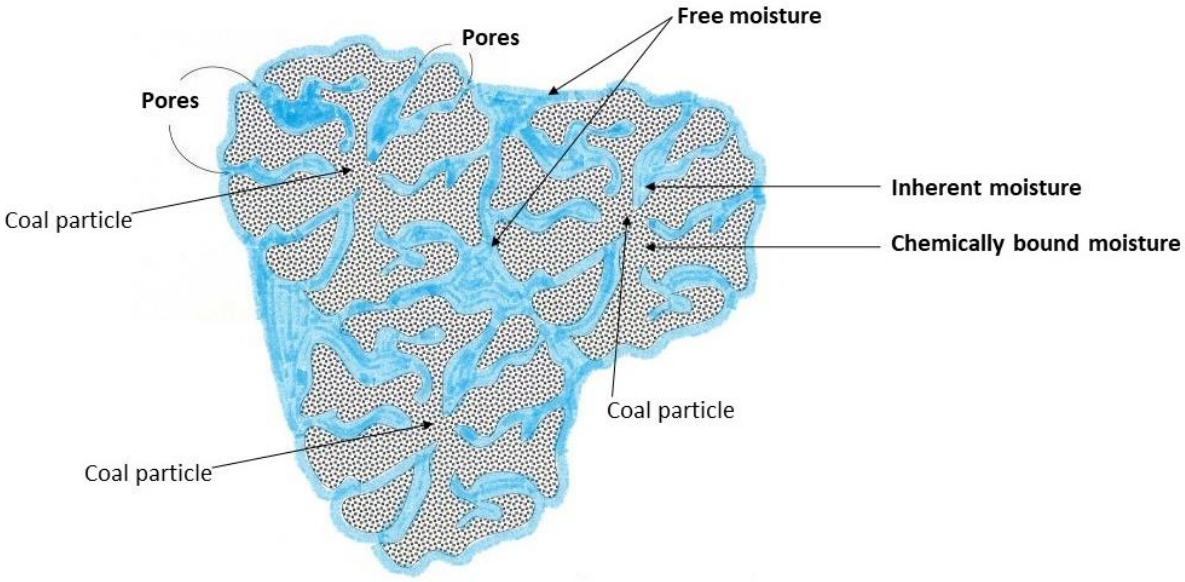

Figure 2-10 Illustration of moisture associated with coal, adapted from (Lemley *et al*., 1995)

2.4.2.1 Surface moisture

The moisture adhering to a coal particle's surface, internally and externally, including the moisture between coal particles in a heap, is known as the surface or free moisture (Le Roux, 2003; Petrick, 1969). Free moisture adheres to the film of inherent moisture due to cohesive forces between the water molecules. In industry, dewatering coal is mainly concerned with removing most surface

moisture (SACPS, 2015). The total moisture content of coal refers to the free moisture and the inherent moisture content in total, the former usually accounting for the majority of the moisture (Bland & McDaniel, 2011; Campbell, 2006).

2.4.2.2 Inherent moisture

Inherent moisture, also known as capillary bound moisture, is the moisture bound internally and externally onto the surface area of the pore network of coal. Capillary forces or adhesion forces hold the moisture inside the pore network. This moisture cannot be removed using mechanical dewatering but can be removed utilising thermal drying (Campbell, 2006).

2.4.2.3 Chemically bound moisture

The moisture captured inside the crystalline structure of a coal particle, usually as crystal water, is known as the chemically bound moisture. This moisture cannot be removed mechanically or with thermal drying and can only be removed through pyrolysis (Campbell, 2006). Chemically bound moisture is not considered when considering coal's total moisture content (Le Roux, 2003).

2.4.3 Market specifications

The selling price of coal depends mainly on its moisture content, and coal producers also pay penalties when not delivering coal on contract specifications (Bland & McDaniel, 2011; Hand, 2000).

Some workers report that an economically appealing coal moisture content is 8 % w/w. In South Africa, thermal-grade coal's market specifications are a product with less than 15% of -1 mm coal with a moisture content below 9% w/w. Furthermore, for synthetic fuel coal specifications in South Africa, the moisture content should be lower than 10 % w/w. Export markets call for a coal moisture content below 12 % w/w (Bland & McDaniel, 2014; De Korte, 2019b; Steyn & Minnit, 2010).

South Africa's flotation coal product is mainly sold to the export market due to its ultra-fine particle size, which is undesirable in the thermal-grade coal market (De Korte, 2019b). Currently, South Africa's coal-fired power stations pay on average R40/GJ for coal, provided the moisture content is below 9 % w/w (De Korte, 2019a).

2.4.4 Challenges associated with wet coal fines

Fine coal has a larger surface area per mass unit than its coarser brethren causing it to retain more free moisture than coarser coals, making the dewatering process more challenging. From a technical and economic point of view, dewatering fine and ultra-fine coal easily and cost-effectively remain a great challenge for the coal industry.

Coal fines (+150 µm -500 µm) can retain water to such an extent that its total moisture content can be between 20-25 % w/w after filtration and ultra-fine coal (-150 µm) can have total moisture contents up to 30 % w/w after filtration (Bourgeois & Barton, 1998; Van Rensburg *et al.*, 2018). In the coal mining industry, producers blend wet coal fines with drier, coarser coals to reduce the final product's moisture content by dilution (Reddick *et al*., 2007).

2.4.4.1 Economic

Moisture in coal reduces its heating value and reduces a power station's boiler and overall efficiencies, which is detrimental to its economics. Moisture also adds to the total weight of a coal product, leading to increased transportation costs.

Because of its higher moisture content and consequently lower calorific value, South African coal-fired power stations discard -200 µm coal fines (Venter & Naude, 2015). In South Africa, approximately 10 Mt of ultrafine coal (-150 µm) is discarded each year because its dewatering costs exceed its market value, even though it is still moderate to good quality coal (Reddick *et al*., 2007).

For perspective, a typical coal-fired power station in South Africa burns 50,000 tonnes of coal per day (Eskom, 2017b). Some workers reported the economic benefit of fine coal moisture reduction, in the sense that a 1 % w/w moisture reduction can hold a saving of US $100 per kiloton of clean coal (Figures in 2000) when considering transportation costs (Tao *et al.*, 2000). Coal producers in South Africa can spend on average R2.40 per ton of dewatered coal (Figures in 2001) to dewater coal to approximately 15-16 % w/w moisture content (De Korte, 2001).

A computer simulation revealed that the overall plant yield of a typical coal preparation plant could be increased by roughly 6% when the fine clean coal's moisture content can be reduced by half, typically from 18 % w/w to 9 % w/w moisture content (Mohanty *et al*., 2012).

2.4.4.2 Environmental

The abundance of wet coal fines and the discarding of it into tailing ponds is detrimental to the environment. Coal is a sulphur bearing sedimentary rock, and when it is discarded in large slurry ponds, it causes the ponds to become acidic, leading to environmental problems such as acid mine drainage (Reddick *et al*., 2007).

The discarded coal fines could also cause other environmental problems such as dust release and spontaneous dust explosions (Reddick *et al*., 2007). These tailing ponds take up large land areas that could alter natural habitats and need to be rehabilitated before being developed or used for agriculture.

From the statistics mentioned in Sections 2.4.1, 2.4.3 and 2.4.4, it is clear how imperative the dewatering of fine coal is for the coal industry, economically and environmentally.

2.5 Drying techniques

2.5.1 Mechanical drying

The most used method of moisture reduction in the coal mining industry remains mechanical drying. The most common mechanical drying technologies include dewatering screens, centrifuges and filters.

Usually, dewatering screens can be used quite effectively for coal larger than 12 mm in size and can achieve moisture reduction in coal with top sizes of 25 mm down to 12-15 % w/w (SACPS, 2015). A large variety of centrifuges and filters exist for coal dewatering. The most common centrifuges include vibrating basket centrifuges, scraper basket centrifuges, solid-bowl centrifuges and screen-bowl centrifuges. Screen-bowl centrifuges can reduce fine coal's surface moisture down to 15 % w/w (SACPS, 2015).

Filters are subdivided into two genres: vacuum and pressure filters. The most common vacuum filters include rotary drum filters, rotary disc filters and horizontal belt filters. Vacuum filters were initially designed for dewatering coarser slurries than pressure filters (Bourgeois & Barton, 1998).

The most common pressure filters include filter presses, belt presses and hyperbaric filters. Filter presses' filter cake can reach the final total moisture contents of 20-35 % w/w (SACPS, 2015). Pressure filters are more effective than vacuum filters in moisture reduction but has higher capital and operating costs (Tao *et al*., 2000).

Current mechanical dewatering methods at coal preparation plants can lower the fine coal moisture content down to approximately 18-30 % w/w (Prat, 2012). Filter presses are also applied to dewater flotation concentrates and delivers a moisture content of 23-25 % w/w. These mechanically dewatered coal moisture contents indicate the necessity of alternative means of fine coal dewatering to reach market specifications of below 10 % w/w moisture content.

2.5.2 Thermal drying

Various thermal drying technologies, from laboratory-scale to industrial-scale, exist today. However, it is not the most economical means of drying because of its energy-consuming heat or heated air.

Drytech Engineering supplies an extensive variety of thermal dryers, ranging from the food industry, mining to other chemical or commercial industries. Their thermal dryers include cabinet dryers, conveyor dryers, flash dryers, fluid bed dryers, infrared dryers, rotary cascade dryers, spray dryers, indirect dryers, calciners and custom-designed dryers (Drytech Engineering, 2008).

(Badenhorst, 2009) reported thermal drying to be a feasible alternative to other employed drying methods. Fine coal in the particle size range of -600 µm +425 µm was analysed with a TGA (thermogravimetric analyser), and the results showed that the moisture reduction rates are at a maximum between 150°C and 200°C. Dewatering rates decrease above 200°C up to 350°C and 450°C, where primary devolatilisation starts. It was also reported that the coal's porosity is affected at temperatures as low as 250°C (Badenhorst, 2009).

The most popular means of thermal drying is the fluidised bed dryer, which uses oil, gas or coal as a heating source for the fluidising air. These fluidised bed dryers can dry the coal product down to 6 % w/w moisture content. However, this technology involves high capital costs, high maintenance costs, high operating costs, and adversely affects the environment in the long run (Bratton *et al*., 2012).

2.5.3 Emerging drying technologies

2.5.3.1 Flocculation filtration

The addition of anionic and cationic flocculants to flotation concentrate slurries can enhance ultra-fine coal's dewatering performance when using a vacuum and centrifugal filtration. A study was conducted in which anionic and cationic flocculants were added to a 14% solids content slurry consisting of ultrafine coal (d_{50} particle size of 29.5 µm). Vacuum, centrifugal and hyperbaric filtration were used for dewatering the slurry (Tao *et al*., 2000).

The filtration rate increased when adding anionic or cationic flocculant to the slurry using vacuum filtration. Consequently, the cake moisture was also reduced significantly when cake thickness is effectively controlled (Tao *et al*., 2000). Adding 15 g/t anionic flocculant using vacuum filtration reduced cake moistures from 30 % w/w to 18 % w/w and 39 % w/w to 24 % w/w with 4.5 mm and 13 mm cake thicknesses, respectively (Tao *et al*., 2000).

Anionic flocculant performed better than cationic flocculant reducing cake moistures when using vacuum filtration. When using centrifugal and hyperbaric filtration, cationic flocculant performed better than anionic flocculant dewatering the coal (Tao *et al*., 2000).

2.5.3.2 Super absorbent polymers (SAPs)

Super absorbent polymers, which entails granular cross-linked hydrophilic polymers, are considered to provide sufficient dewatering of fine coal slurries. Depending on their chemical composition, the polymers can absorb tens to several hundreds of times their mass in water. The drying occurs in four consecutive steps: 22 hours of passive contact, 2 hours of mixed contact, a further 4 hours of passive contact and a final 48 hours of passive contact (Dzinomwa *et al*., 1997).

Coal slurries of varying moisture contents (30 %, 45 % and 60 % w/w) were dried using 0.5%, 1.0% and 2.0% polymer dosage. The polymers were inserted in sachets, each consisting of 1g of dry polymers, for better handleability. Results showed that the 2.0% polymer dosage dewatered the different coal slurries below 10 % w/w moisture after the fourth step (Peer & Venter, 2003).

Further investigation showed that a 10% polymer dosage mixing for 25.5 hours and passive contact for 53.5 hours dewatered the 30 % w/w and 45 % w/w moisture coal slurries below 10 % w/w moisture contents within 7 hours of mixing. It was also concluded that 7 hours of mixing contact time is the maximum time required (Peer & Venter, 2003).

Regeneration of these SAPs is done by temperature-induction or pH-induction (Dzinomwa *et al*., 1997). In the study, SAPs were thermally dried at 70°C and which removed most of their moisture. For the pH-induced regeneration, HCl was added to the sachets to release 80% of its absorbed water. The pH of the SAP must be neutral for it to absorb moisture optimally. Therefore, the SAPs are neutralised with NaOH after regeneration (Peer & Venter, 2003).

2.5.3.3 Improved vacuum filtration

An improved method of vacuum filtration was conceived by (Le Roux & Campbell, 2003). This improved vacuum filtration method entails the deliberate interruption in the vacuum applied, which causes a sudden increase in airflow through the filter cake leading to better dewatering performances than an increase in the applied vacuum (Le Roux & Campbell, 2003).

Le Roux & Campbell also reported that the sudden interruption in the applied vacuum caused cracks to form at the bottom of the filter cake, which caused higher airflow rates through the filter cake. This hypothesis was tested by deliberately damaging the filter cake with cuts made with a

spatula. The results showed the deliberately damaged filter cake to have lower saturation levels and faster dewatering rates.

The researchers studied the vacuum filtration of a fine coal slurry with a d_{50} particle size of -212 µm. A bench-scale filter was used with an applied vacuum of 45kPa. Once the filtration had reached 100% saturation, the applied vacuum was interrupted either after 15, 30, 45 or 60 s. The interruption duration in applied vacuum was also varied between 15, 30 or 60 s (Le Roux & Campbell, 2003).

The results showed that the filter cake's moisture content could be reduced from 32 % w/w to 25 % w/w. The dewatering rate increased significantly after an interruption in the applied vacuum, yielding a drier product in less time. The researchers concluded that the airflow increase through the filter cake was more beneficial than increasing the pressure differential over the filter cake (Le Roux & Campbell, 2003).

Further investigation on this method was done considering the effect of the filter cake's deliberate damage on the drying performance (Le Roux *et al*., 2005). It was found that the deliberate damage of the filter cake should be done as close as possible to, or at, 100% saturation level. Furthermore, the filter cake's damage should be so that the cracking could take higher airflow through the cake.

2.5.3.4 Selective microwave heating

A study was conducted on the selective microwave heating and drying of fine coal slurries using conventional microwave ovens (Seehra *et al*., 2007). Microwave drying of coal is based on the fact that the absorption of microwave energy by water molecules is significantly higher than the absorption by dry carbonaceous matter (Marland *et al*., 2001). Other researchers also reported that microwave radiation did not have significant effects on the proximate composition, rank or reactivity of coal (Lester & Kingman, 2004)

A fine coal slurry at 52 % w/w moisture, consisting of bituminous coal, with particles being in the -440 µm +120 µm size range, was dried using microwave energy. A conventional 2.45 GHz microwave oven with a power output of 800W was used. The workers also measured the power usage of the microwave drying system. The microwave drying was done on a laboratory batch scale and semi-continuous bench scale (Seehra *et al*., 2007).

For the laboratory scale microwave drying, moisture loss was measured in intervals of 10 and 30 s. It was found that the dewatering power usage related to 1.33×10^{-3} kWh/$g_{moisture}$ and 9.8×10^{-4} kWh/$g_{moisture}$ for the 10 s and 30 s interval dewatering procedures, respectively. Further, it was

found that microwave dewatering is 73% efficient for 30 s interval dewatering calculated against the theoretical energy needed to remove water (Seehra *et al*., 2007).

The semi-continuous bench-scale microwave drying process, with controlled mass feed and belt speed, correlated to a moisture loss of 1.16 kg/ kWh power used. This process was calculated to be 83% efficient compared to the theoretical energy needed to remove water (Seehra *et al*., 2007).

The workers also compared the microwave dewatering with thermal drying using TGA analysis and found the microwave drying to be significantly more efficient, with almost ten times shorter drying times than thermal heating. The coal slurry moisture was reduced to 10 % w/w moisture. The workers also estimated the approximate running cost of a microwave dewatering unit to be in the vicinity of $3/ ton coal, assuming an 83% efficiency (Seehra *et al*., 2007).

2.5.3.5 Parsepco Drying Technology

The Parsepco Drying Technology entails the drying of coal fines using MIR (medium-wave infrared radiation) and a woven steel conveyor belt under a vacuum. Wet fine coal is transported on a woven steel conveyor belt which passes under ceramic MIR emitters above the belt in a negative pressure environment generated from below the belt. The Parsepco Drying Technology can dewater fine wet coal from moisture contents of approximately 25 % w/w to below 10 % w/w (Mohanty *et al*., 2012).

2.5.3.6 Nano Drying Technology

Nano Drying Technology is a drying technique that uses molecular sieves to adsorb moisture from fine wet coal. Molecular sieves contain pores of precise and uniform size, depending on the crystal composition (Tien, 2019), which is large enough for water molecules to be adsorbed into the sieves but too small for fine coal particles to enter and blind the pores (Bratton *et al*., 2012). This novel process is protected by patent rights and owned by Nano Drying Technologies, LLC (Bland & McDaniel, 2014).

The molecular sieves are mixed with fine wet coal and are agitated to increase contact surface area. The molecular sieves then adsorb the free moisture from the fine coal. The molecular sieves and coal are then separated through standard screening. The workers also reported that the molecular sieves yielded a significantly drier coal product with even single-digit moisture contents, regardless of the coal particle size (Bratton *et al*., 2012).

The workers investigated the use of the NDT system on a bench-scale experimental setup. The coal being dried consisted of metallurgical coal with 100% 600 µm and 100% 150 µm particle sizes. The coals' feed moisture was in the vicinity of 22 % w/w and 26 % w/w for the 600 µm and 150 µm feed. Results showed that the 600 µm, as well as 150 µm coal, could be dewatered within 5 minutes to moisture contents below 9 % w/w (Bratton *et al*., 2012). The workers also regenerated the molecular sieves employing microwave drying and reused the regenerated sieves in the drying process and found no significant difference in effectiveness between new (fresh) or regenerated molecular sieves.

Further investigation was done using a continuous pilot-scale experimental setup with a throughput capacity of 0.5 tph. A 0.5 tph coal feed, consisting of 100% 150µm particle size and a feed moisture of about 31.8 % w/w, could be dried down to 3.2 % w/w moisture (Bratton *et al*., 2012). This process proves to be successful and has a greener effect on the environment than thermal drying processes.

2.5.4 Adsorbent assisted drying

2.5.4.1 Adsorption vs absorption

A clear definition between adsorption and absorption is required to eliminate confusion, as these two terms are often used interchangeably, even though a significant difference exists. Adsorption is defined as "the preferential concentration of species onto surfaces of adsorbing solids" (Tien, 2019). Absorption is defined as "a diffusional operation in which a liquid phase absorbs some components of a gas phase" (Zarzycki & Chacuk, 1993).

Adsorption is a surface phenomenon, limited by the relevant adsorption isotherm, whereas absorption is a bulk phenomenon, limited by the solubility of the gases involved. Furthermore, adsorption is usually considered an inherently non-steady state process where absorption is treated as a steady-state process (Tien, 2019).

2.5.4.2 Adsorption

Adsorption can be subdivided into liquid-phase adsorption (applicable to this study) and gas-phase adsorption. The first notable use of adsorbents is dated as far as two millennia back where charcoal was used to purify water. Adsorption is applied in various fields today. A partial list of the various applications and respective detail can be found elsewhere (Tien, 2019).

Today, many adsorbents exist, of which the most commonly used ones include: activated carbon, activated alumina, activated silica, molecular sieve zeolites and polymeric adsorbents, each having an industry or application by which it is prefered. Most adsorbents' pore sizes vary throughout the pore network, with molecular sieve zeolites being the exception. Molecular sieves' pore sizes are uniform throughout the pore network, and the pore size depends on the sieve's crystal composition (Tien, 2019).

As mentioned, adsorption is governed by the relevant adsorption isotherm. The water adsorption isotherm gives the relationship between the equilibrium amount of water adsorbed on a solid and the fluid's water content at constant temperature and pressure. The number of available sites within an adsorbent and water's chemical affinity for the adsorbent's composition limits the amount of water that can be adsorbed (Ducreux & Nedez, 2011).

Water adsorption comprises three consecutive stages: chemisorption, physisorption and capillary condensation (Ducreux & Nedez, 2011). These stages of adsorption on activated alumina are summarised in Table 2-3.

Table 2-3 Adsorption stages on activated alumina, adapted from (Ducreux & Nedez, 2011)

Stage	Illustration	Description
1. Chemisorption	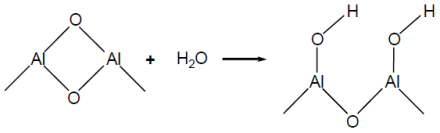	Water molecules are added, which dissociate and attach to aluminium oxide sites.
2. Physisorption	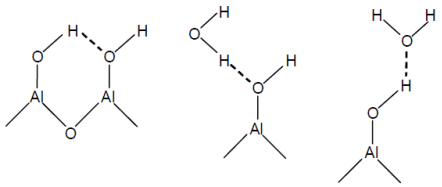	Hydrogen bonding occurs with surface species (Van der Waals' forces), and multiple layers of water molecules form by hydrogen bonding.
3. Capillary condensation	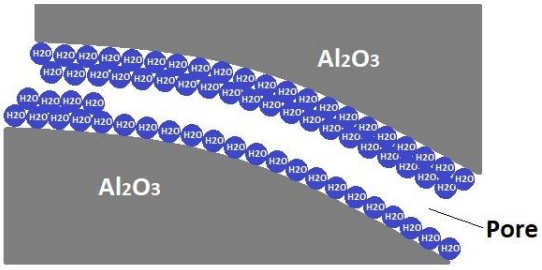	Multilayers of water grow (Kelvin's law), where the water starts condensing locally at temperatures above that of the bulk fluid's dew point.

In the initial stage of adsorption, water is rapidly adsorbed during the chemisorption stage, and a monomolecular water layer is formed. The net enthalpy of this monolayer formation

(chemisorption) is the highest at 25 to 38 kJ/mol$_{adsorbed}$, whereas physisorption has a significantly lower net enthalpy of 2 kJ/mol$_{adsorbed}$ (Ducreux & Nedez, 2011). No net enthalpy is reported for the capillary condensation stage.

The water adsorption isotherm with its relevant subdivided stages' isotherms can be seen in Figure 2-11 to understand the different stages better.

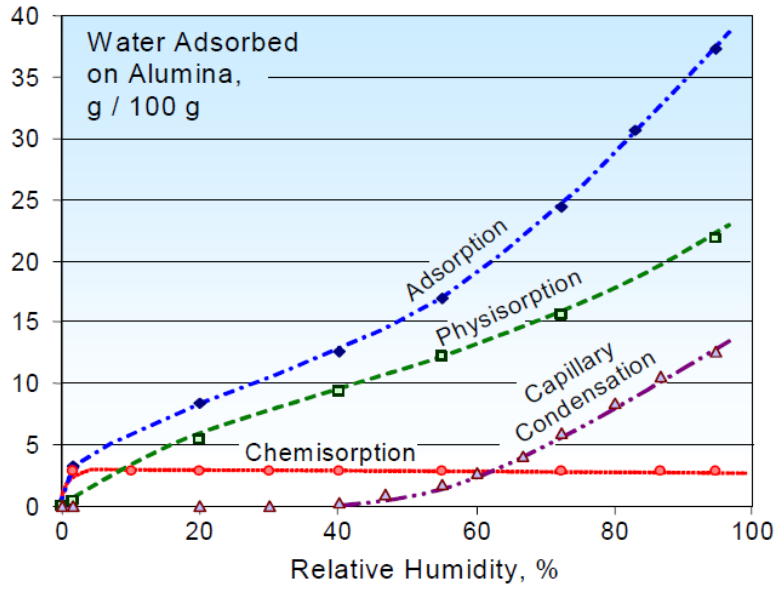

Figure 2-11 Static water adsorption isotherms using activated alumina, taken from (Ducreux & Nedez, 2011)

2.5.4.3 Activated alumina

The primary raw material to produce activated alumina is bauxite. Bauxite reacts with soda to form, via the Bayer process, sodium aluminates. The sodium aluminates are washed to remove impurities, and gibbsite is obtained. The gibbsite is calcinated at 400 to 600°C to form activated alumina. Two species, gibbsite and boehmite, is found in bauxite ores. The composition of these two species has a considerable influence on the activated alumina's quality, including its specific surface areas and total pore volume (Ducreux & Nedez, 2011).

Ducreux & Nedez reports that the advantage activated alumina has compared to other adsorbents is that its structural integrity is not destroyed by capillary condensation or free water. Activated alumina is also chemically inert against most gases and liquids. Furthermore, it is reported that activated alumina has strong resistance against hydrothermal ageing (gradual, irreversible changes in alumina structure) that mainly depends on the number of regeneration cycles. It is important to note that extending the regeneration cycle time to longer intervals extends the adsorbents' lifetime compared to more intensive, short regeneration cycles (Ducreux & Nedez, 2011).

2.5.4.4 Adsorbent assisted drying

Contact-sorption drying is the mechanism that describes adsorbent assisted drying. Contact-sorption drying is defined as the process whereby dry adsorbents are brought into physical contact with wet material for some time to allow moisture transport to occur (Kudra & Mujumdar, 2009).

Adsorbent assisted drying of coal entails fine wet coal's dewatering utilizing physical contact between the wet fine coal and the adsorbents as illustrated in Figure 2-12. With high water adsorptive capacities, the adsorbents adsorb the moisture from the fine wet coal and deliver a drier coal product. The contact surface area between the coal and adsorbents is increased by mixing it in a cascading motion.

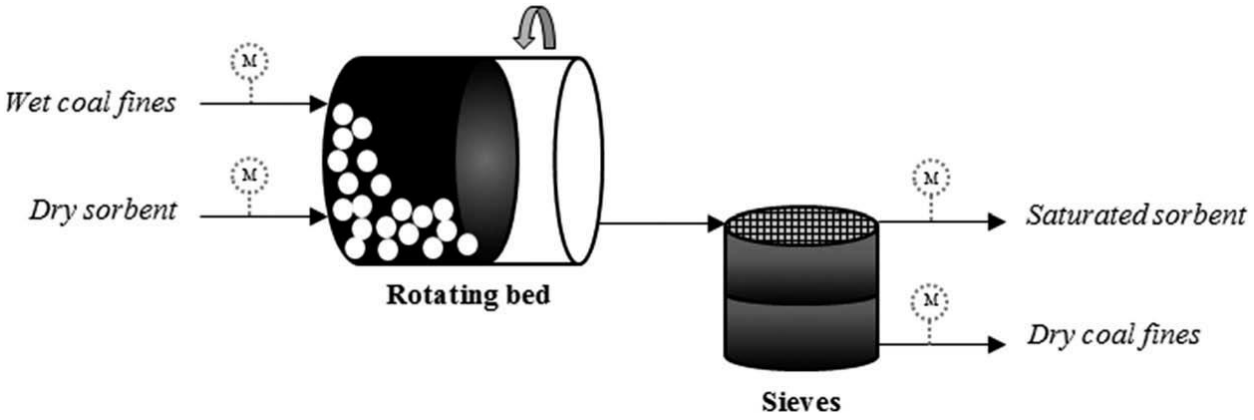

Figure 2-12 Illustration of the adsorbent assisted drying of coal, taken from (Van Rensburg *et al.*, 2018)

Recent studies investigated the adsorbent assisted drying of mechanically dewatered run-of-mine coal in the particle size range -2 mm + 0.25 mm using activated alumina and activated silica (Peters, 2016). The study was conducted on sub-bituminous coal using three different particle size ranges, -2 mm +1 mm, -1 mm +0.5 mm and -500 µm +250 µm with 18, 25 and 29 % w/w moisture contents, respectively.

The coal was dried using a fixed-bed setup and a rotating bed setup (to induce a cascading motion). For the fixed-bed setup, the wet coal was brought into contact with the adsorbents in cylindrical vessels that remained stationary. For the rotating bed setup, the wet coal was mixed with the adsorbents in cylindrical vessels that rotated on rollers (Peters, 2016).

Furthermore, the adsorbent-to-coal mass ratio (3:1; 2:1; 1:1; 0.75:1 and 0.5:1), adsorbent particle size (3 mm and 5 mm) and adsorbent condition (new, used and regenerated) were varied in an attempt to study its effect on the drying performance (Peters, 2016).

Results showed that the fine coal’s moisture content could be reduced by 60-80% within 10 minutes of drying. Using the 3 mm activated alumina and activated silica adsorbents, the coal's

moisture could be reduced to 8 % w/w within 2.5 minutes of drying. Target moistures of 8 % w/w could not easily be reached with the fixed-bed setup due to the lack of motion. The rotating-bed setup significantly reduced the time need for sufficient drying.

It was found that an increasing adsorbent-to-coal mass ratio led to increasing initial desorption rates and, consequently, lower final moisture contents of the coal. Furthermore, the 3 mm adsorbents yielded higher initial desorption rates than the 5 mm adsorbents. No significant difference in performance was found between the activated alumina and activated silica during the rotating bed experiments.

The adsorbents could easily be regenerated with air drying through a packed bed and reduced the adsorbents moisture by almost half. (Peters, 2016) also found that the adsorbents could be reused up to six times without regeneration and still provide efficient drying of the fine coal when using a 3:1 adsorbent-to-coal mass ratio. Degradation (attrition) of the adsorbents during operation was found to be insignificant.

Further studies found that the drying mechanism for coal using contact sorption is limited by the liquid moisture transport (Van Rensburg *et al.*, 2018). Direct contact between the coal and the adsorbents is imperative for moisture transport to occur. Increased contact surface areas between the coal and adsorbents led to increased liquid moisture transport and consequently increased desorption rates.

2.6 Conclusion

Even though the world promotes a green revolution, considering greener, renewable energies, coal will still be part of the global energy mix for decades to come. The focus on coal has only shifted to more efficient coal utilisation, more efficient, leaner, environmentally friendlier beneficiation methods, and using or wasting less water. Part of this new focus on coal shows that dewatering of coal fines remains a challenge for the coal industry from a technical, economic and environmental point of view.

The increased generation of coal fines is an inevitable case that indirectly leads to higher product coal moisture contents. Mechanical dewatering methods remains ineffective in dewatering coal fines to market specifications. Thermal drying does provide enough drying but remains uneconomical with detrimental effects on the environment. It is senseless to burn coal to dry coal.

Some emerging drying technologies provide better dewatering performances than current mechanical methods, but still not enough dewatering. Other drying technologies may provide sufficient drying but entails a challenging process in handling the drying medium. Finally, some drying technologies provide excellent drying performance and prove to be less challenging in terms of handleability, but they still need proper investigation to determine, whether they are economically viable and environmentally friendlier means of drying.

Chapter 3 Experimental methodology

3.1 Material

3.1.1 Coal

The origin of the coal being used in this study is Medium Rank C No. 4 Seam of the Witbank Coalfield, South Africa. Filter cakes of spiral beneficiated coal (product and tailings) and flotation beneficiated coal product were investigated. The coal was sampled directly after filtration from the spiral and flotation plants of a colliery mining on No. 4 and No. 5 Seam of the Witbank Coalfield.

The coal samples received from the mine are reduced to 15 kg samples with the cone and quartering method (SACPS, 2015). Whenever samples were taken for experimental runs, cone and quartering were used again to reduce the samples to 1 kg.

The reduced 15 kg samples were stored in airtight sealed plastic buckets, and the reduced 1 kg samples were stored in airtight sealed glass jars before experimental runs. The coal was stored in airtight containers to eliminate any moisture transport from the samples so that experiments could be done on the coal using moisture contents that are as close as possible to that received from the plant after filtration.

Table 3-1 Average particle sizes of coals being investigated

Coal	**d_{10} (µm)**	**d_{50} (µm)**	**d_{90} (µm)**
Spiral product	81.3	434.3	1002.9
Spiral tailings	77.5	397.1	954.4
Flotation product	2.3	21.2	136.0

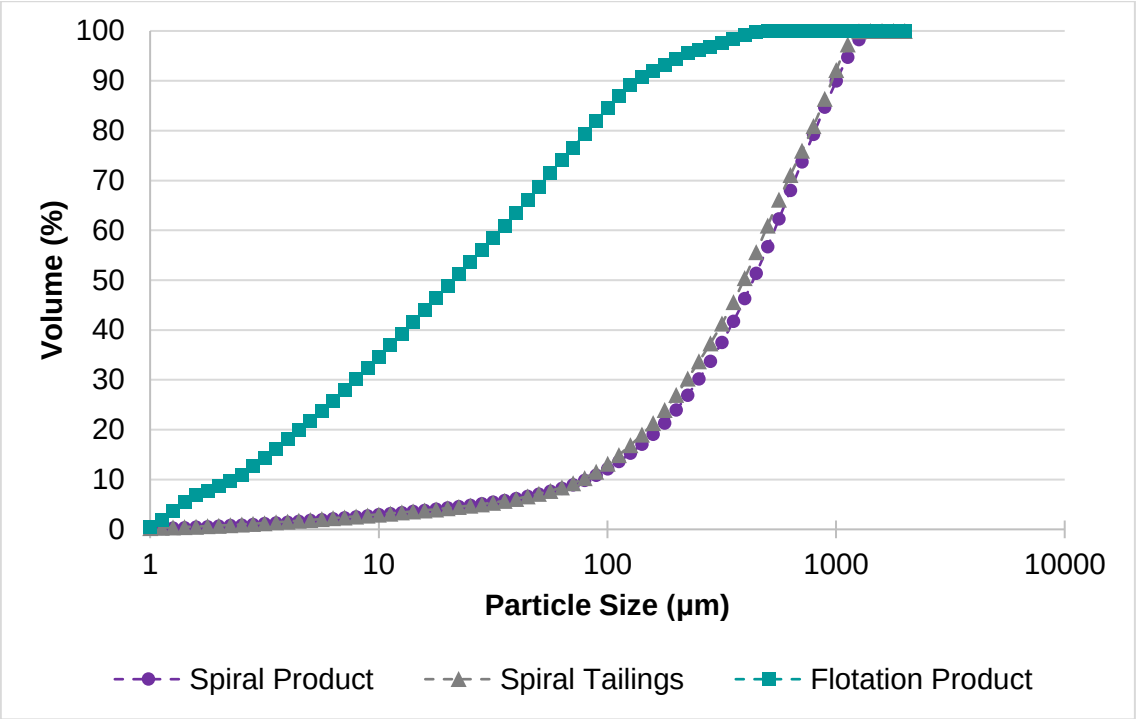

Figure 3-1 Particle size distribution of coals being investigated

The spiral product coal has a d_{50} particle size of 434 µm, and the flotation product coal has a d_{50} particle size of 21 µm which emphasizes the small particle sizes of the coal being dealt with in this study. Table 3-1 shows the particle sizes of the various coals being studied. From the table, it is clear that the coal being dealt with has fine to ultra-fine particle sizes, averaging in the range of -1003 µm to +2.3 µm. Figure 3-1 shows the cumulative PSDs of spiral product, spiral tailings, and flotation product coal.

Table 3-2 summarises the coals being investigated. The table includes total moisture, proximate analysis and heating values of the coal. The table shows the flotation coals have higher total moisture contents than spiral coals, as one would expect, considering their finer particle sizes. The spiral product has a total moisture content of 18.0 % w/w, while the flotation product has a higher total moisture content of 24.2 % w/w as received.

The spiral and flotation products have ‘as received’ calorific values of 21 MJ/kg and 19 MJ/kg, respectively, ash yields in the 18% range and volatile matter in the 22% range.

Table 3-2 Properties of coals being investigated

Property	Unit	Spiral product	Spiral tailings	Flotation product
Total moisture (*ar*)	% w/w	18.0	18.4	24.2
Surface moisture (*ar*)		16.0	16.8	19.8
Proximate analysis (*ad*)				
Inherent moisture	% w/w	2.0	1.6	4.4
Volatile matter		22.5	21.9	22.0
Ash		18.3	33.8	18.3
Fixed carbon		57.2	42.7	55.3
Ultimate analysis (*ad*)				
Carbon	% w/w	52.1	41.8	58.5
Hydrogen		2.7	2.2	3.0
Nitrogen		1.1	0.8	1.2
Sulphur		0.6	1.5	0.5
Oxygen		23.2	18.3	14.1
Heating value				
Calorific value(*ar*)	MJ/kg	21.9	16.1	19.2
Calorific value (*db*)		26.0	19.1	25.8

3.1.2 Adsorbents

This study's primary adsorbents are Porocel Dryocel 848 activated alumina (Figure 3-2), consisting of spherical, uniform ceramic beads. The adsorbent particle sizes being used included 3 mm and 5 mm beads (Figure 3-3) to compare the different particle sizes' performance.

Typical properties of Porocel Dryocel 848 can be seen in Table 3-3. The activated alumina predominantly consists of aluminium oxide with trace elements of sodium oxide and silicon dioxide. As mentioned in Section 2.5.4.3, activated alumina provides good drying performance, good regeneration ability, and good structural integrity against degradation factors such as attrition and hydrothermal ageing, hence the reason for the preferred choice of the primary adsorbent.

Figure 3-2 Intimate view of Porocel Dryocel 848 activated alumina

Figure 3-3 3 mm (left) and 5 mm (right) activated alumina

Table 3-3 Typical properties of Porocel Dryocel 848 activated alumina

Property class	**Property**	**Porocel Dryocel 848**
Chemical	Al_2O_3	93.5 % w/w
	Na_2O	0.35 % w/w
	SiO_2	0.15 % w/w
	Loss on ignition (1000°C)	6.00 % w/w
Physical	Packaged moisture	3 mm: 1.6% w/w 5 mm: 1.4% w/w
	Inherent moisture (22°C; 40% RH)	3 mm: 6.2% w/w 5 mm: 5.6% w/w
	Surface area	320 m^2/g
	Total pore volume	0.5 cm^3/g
	Abrasion (% Loss)	0.2 % w/w
	Attrition (% Loss)	0.4 % w/w
	Crush strength (5 mesh equivalent)	20 kg
	Bulk density	753 kg/m^3
Availability	Nominal sizes	1/16”, 1/8”, 3/16”, 1/4” 1.5 mm, 3 mm, 5 mm, 6 mm
	Packaging	50 lbs (22.7 kg) bags 2,000 lbs (907.2 kg) bags
Application	Spherical, uniform, dust-free desiccant for liquid and gas drying applications. High surface area for optimum dehydration and strong physical characteristics for industrial robustness.	

Secondary dewatering experiments were done using Zan-tech Zeosorb 13X APG molecular sieves (Figure 3-4), which are spherical beads, with particle sizes of 3-5 mm. Zeosorb 13X APG is a superior grade synthetic zeolite of the X-type crystal structure in sodium form, with a pore opening of 9 angstroms, allowing adsorption of molecules with critical diameters up to 8 angstroms.

Typical properties of Zeosorb 13X APG are summarised in Table 3-4. Section 2.5.4.2 discussed that molecular sieve zeolites distinguish themselves from other adsorbents by their uniform pore sizes. These uniform and precise pore sizes ensure highly selective gas separation, especially in hydrocarbon mixture separation (Tien, 2019).

Figure 3-4 Close up view of Zan-tech Zeosorb 13X APG molecular sieves

Table 3-4 Typical properties of Zan-tech Zeosorb 13X APG molecular sieves

Property class	**Property**	**Zeosorb 13X APG**
Physical	Diameter	3-5 mm
	Bulk density	610 kg/m^3
	Crush strength	60 N
	Static water adsorption (25°C; 75% RH)	28.5% w/w
	Static CO_2 adsorption (25°C; 250 mm Hg)	19.5% w/w
	Attrition (% Loss)	0.1
	Packaged moisture content	1.0% w/w
	Inherent moisture content	9.3% w/w
Availability	Adsorbent form	Beads; pellets
	Nominal sizes	Beads: 1.6-2.5 mm; 2.5-3.5 mm; 3.0-5.0 mm Pellets: 1.5-1.8 mm; 3.0-3.2 mm
	Packaging	Beads: 140 kg drums Pellets: 125 kg drums
Application	Zeosorb 13X APG is used for oxygen generation in PSA and VSA systems and the adsorption of straight and branch chain hydrocarbons, aromatics, NO_x and SO_x. It has an extreme affinity for water vapour, carbon dioxide and nitrogen.	

The maximum water adsorptive capacities of activated alumina were analysed over 48 hours, as shown in Figure 3-5. The adsorbents were drenched in water for 48 hours while the water mass retained was measured at several time intervals.

Keep in mind that the water adsorptive capacity is measured as the water mass retained as a percentage of the dry adsorbent mass and should not be confused with moisture content percentage, which is mass water retained as a percentage of the wet sample mass.

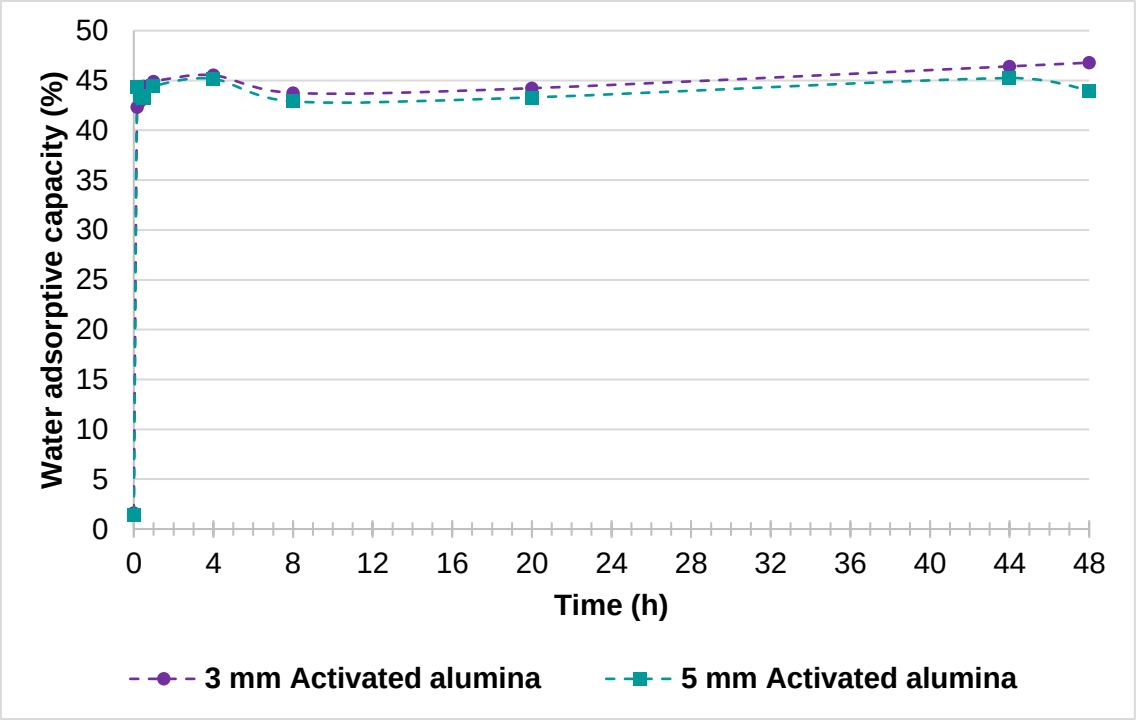

Figure 3-5 Water adsorptive capacities of Porocel Dryocel 848 activated alumina

Starting at a packaged moisture of 1.6% and 1.4% w/w for the 3 mm and 5 mm activated alumina, the 3 mm activated alumina achieved a slightly higher adsorptive capacity than the 5 mm activated alumina. Maximum water adsorptive capacities of 46% and 45% w/w were recorded for 3 mm, and 5 mm activated alumina. It was found that approximately 92% of the adsorbents' maximum adsorptive capacities were reached within 10 minutes of drenching, and the maximum water adsorptive capacity was reached within 4 hours of drenching.

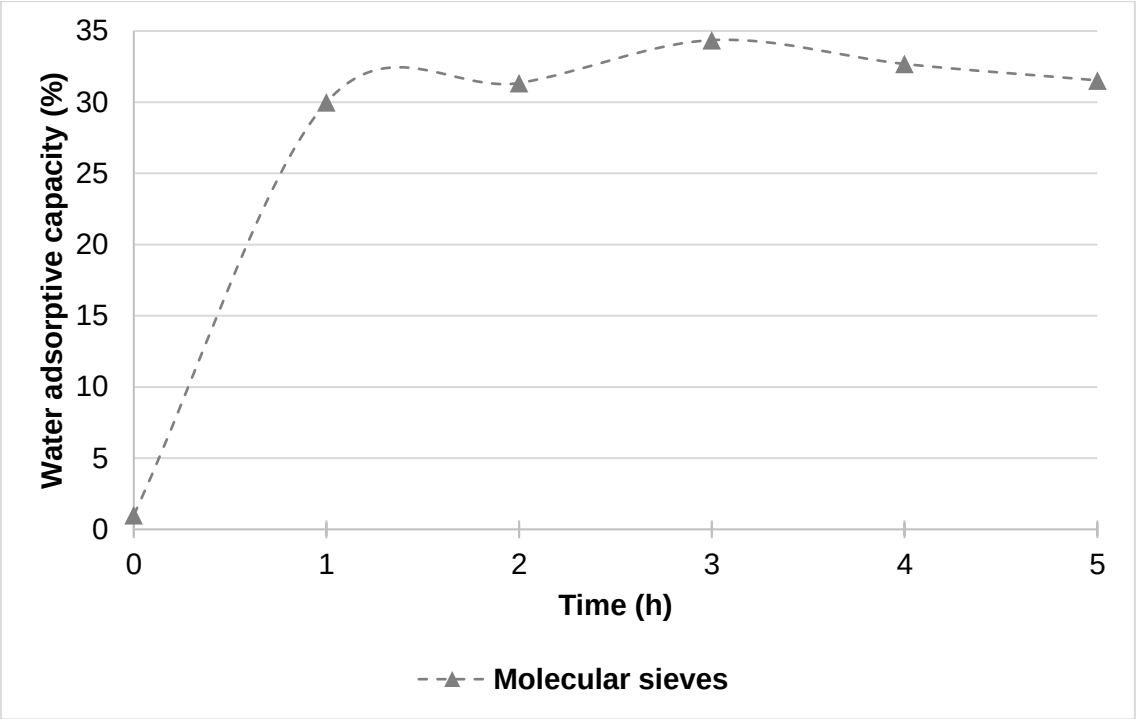

Figure 3-6 Water adsorptive capacity of Zan-tech Zeosorb 13X APG molecular sieves

The molecular sieves' water adsorptive capacity was also measured while being drenched in water for 5 hours and taking samples in 1-hour intervals. Starting at a packaged moisture of approximately 1% w/w, the molecular sieves achieved a 30% w/w adsorptivity after 1 hour and reached a maximum water adsorptive capacity of 34% w/w after 3 hours.

The apparent difference in maximum water adsorptive capacities between the activated alumina and the molecular sieves is a deciding factor, among other drives, like industrial robustness, for the choice of the primary adsorbent. Even though molecular sieves have some chemical and physical advantages above activated alumina, such as uniform pore sizes and higher selectivities, it has its limitations, discussed later in this study. Hence, the molecular sieves are investigated as a secondary adsorbent.

3.1.3 Sample storage

The coal samples and adsorbents were stored in their respective airtight plastic bucket containers in a clean closed-off sample room. The sample room was kept dust-free and moisture-free to eliminate spontaneous adsorption between the coal, adsorbents, or the environment.

3.2 Equipment

3.2.1 Rotating bed

The rotating bed (Figure 3-7) used in this study entailed a set of three rollers in tandem connected to a variable speed motor. The rollers of the bed are each 510 mm long and 40 mm in diameter. The dimensions of the cylindrical vessels (Figure 3-8) in which the contact sorption occurs is 75 mm x 55 mm ID, and each has a 10 mm baffle plate inside to enhance mixing inside the vessel.

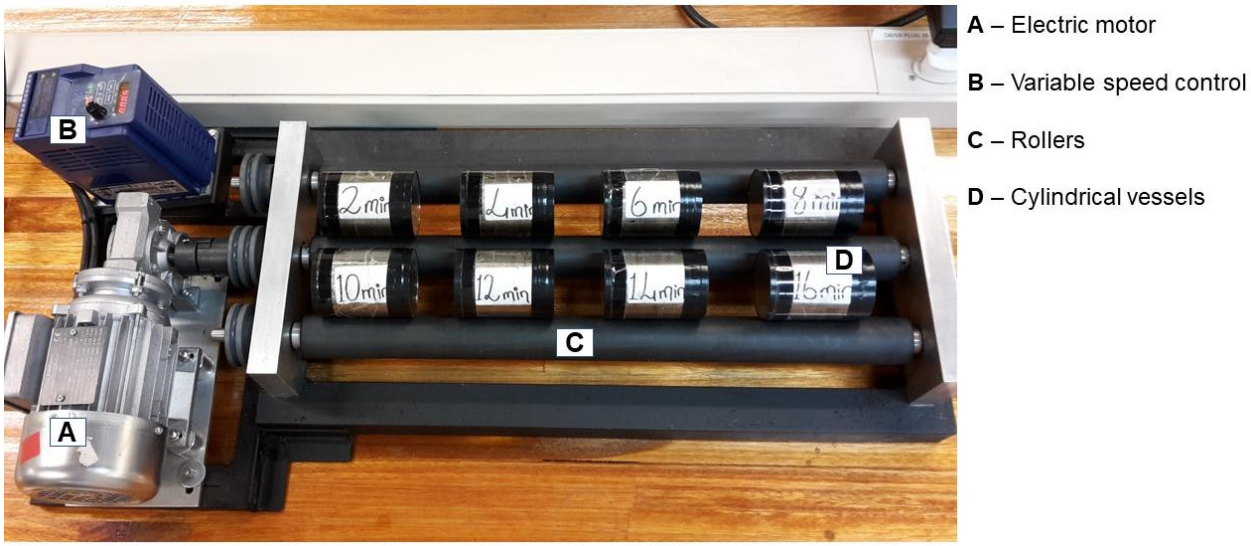

Figure 3-7 Rotating bed apparatus used

In Figure 3-7, “A” denotes the electric motor driving the rotation, “B” is the variable speed control, “C” is the rollers on which the vessels are loaded, and “D” is the cylindrical vessels in which contact-sorption takes place.

Figure 3-8 shows the cylindrical vessels in more detail. The cylindrical vessels with their baffle plates are constructed of mild steel. Circular Perspex lids are used to seal the cylindrical vessels during dewatering experiments. Insulation tape is used to seal off and attach the Perspex lids to the cylindrical vessels.

It is important to note that all adsorbent assisted drying experiments are conducted in a laboratory that is kept under ambient conditions and that no thermal heat is applied to the drying process.

Figure 3-8 Side view of cylindrical vessels used for contact-sorption

3.2.2 Adsorbent regeneration setup

For the adsorbent regeneration, conditioned airflow at 22°C and relative humidity of 70% is used to regenerate the adsorbents through a packed bed column. A CTS -40/100 Climate Control Chamber is used to condition the air at 22°C and 70% RH. A blower is connected to the CTS Climate Control Chamber, with its suction coming from inside the climate control chamber, as depicted in Figure 3-9.

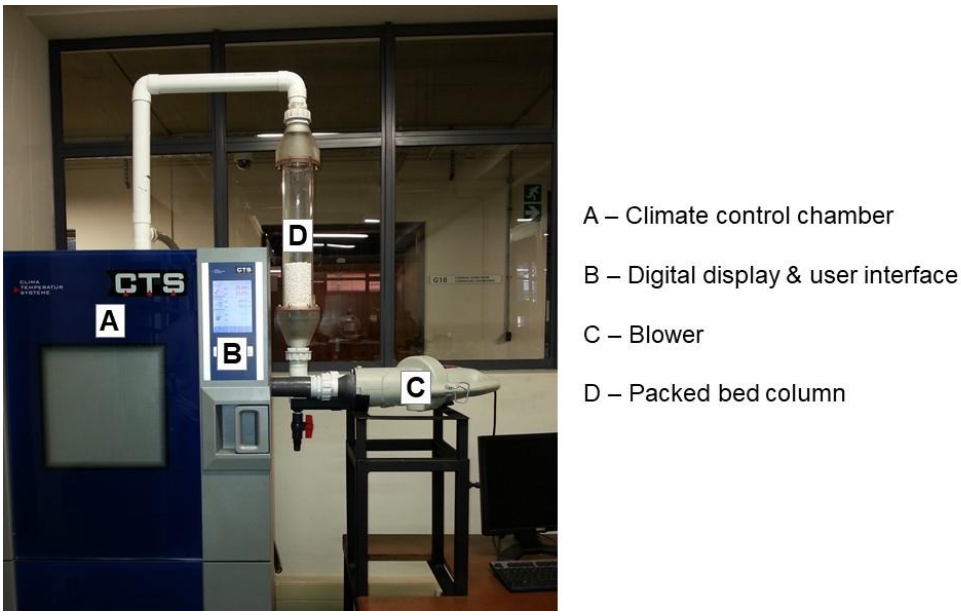

Figure 3-9 Adsorbent regeneration setup

The blower discharges to a packed bed column (Figure 3-10) that contains glass marbles situated underneath a distributor plate for even distribution of airflow. The gas exit of the packed bed

column re-enters the climate control chamber for reconditioning. The packed bed column is constructed of Perspex, and the piping of the column is constructed of PVC piping.

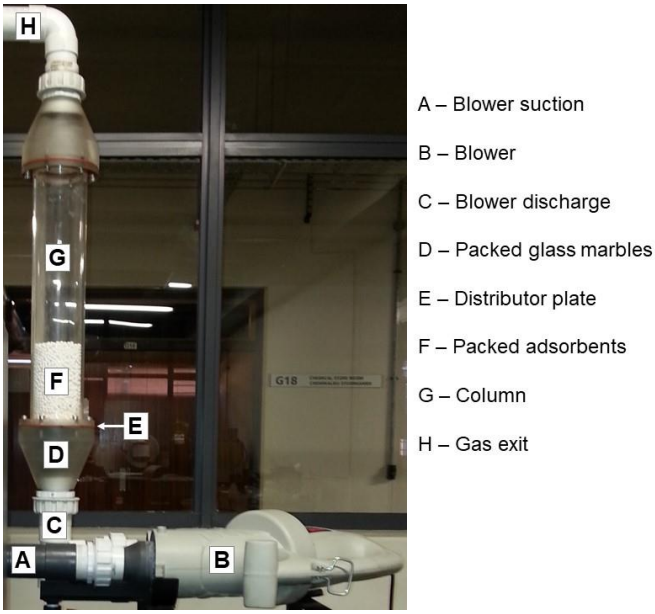

Figure 3-10 Blower with packed bed setup

It is important to note that the regeneration of the adsorbents is conducted under ambient or close to ambient conditions (22°C and 70% RH) and that no thermal heat is applied to regenerate the adsorbents. However, a relative humidity of 70% is used to simulate somewhat cloudy weather at which the adsorbents may still regenerate sufficiently.

3.3 Procedures

All experiments discussed were conducted in a clean coal laboratory, kept at a constant temperature of 22°C.

3.3.1 Adsorbent assisted drying

Adsorbent assisted drying was done on different coals and by altering several variables. These variables are summarised in Table 3-5.

Table 3-5 Variables of the adsorbent assisted drying procedure

Variable	Variations
Coal source	Medium Rank C No. 4 Seam Witbank Coalfield (No variations)
Coal beneficiation process	• Spiral product • Spiral tailings • Flotation product
Coal particle size	As received: • Spiral product (d_{50}: 434 µm) • Spiral tailings (d_{50}: 397 µm) • Flotation product (d_{50}: 21 µm)
Adsorbent type	• Activated Alumina (Primary adsorbent used for spiral and flotation coal) • Molecular Sieves (Secondary adsorbent investigated only on flotation product)

Adsorbent particle size	• Activated alumina:
	  ○ 3 mm
	  ○ 5 mm
	• Molecular sieves:
	  ○ No variation in size

Adsorbent-to-coal mass ratio	• 2:1 • 1:1 • 0.5:1
Adsorbent state	• New (fresh) • Spent • Regenerated

The adsorbent assisted drying procedure, illustrated in Figure 3-11, is discussed as follows:

1. 20 g of coal filter cake (as received) is weighed and added to the cylindrical vessels.
2. The respective pre-weighed mass of adsorbents is added with the coal in the cylindrical vessels.
3. Swiftly, the cylindrical vessels are sealed off with their Perspex lids and insulation tape.
4. The vessels are added to the rotating bed and rotated at 50 rpm for 16 minutes.
5. At each time interval of 2 minutes, the respective vessel is removed, and the coal and adsorbents are separated through sieving with a 2 mm aperture size laboratory sieve.
6. The separated coal and adsorbents for each time interval are kept in airtight sealed glass jars until the experiment is completed.
7. The moisture content of the coal and adsorbents is analysed for each time interval.
8. The coal's calorific value is measured at feed (0 min), 2 min, 8 min and 16 min time intervals.

It is important to note that steps 1, 2, 3 and 4 are carried out ever so swiftly to avoid any moisture loss from the coal or spontaneous adsorption from the adsorbents to get accurate and realistic data from the experiments. For steps 1 and 2, while working as fast as possible, the cylindrical vessels are kept closed with the Perspex lids after adding the coal and the adsorbents to avoid spontaneous moisture transport to the environment and obtain realistic and accurate results.

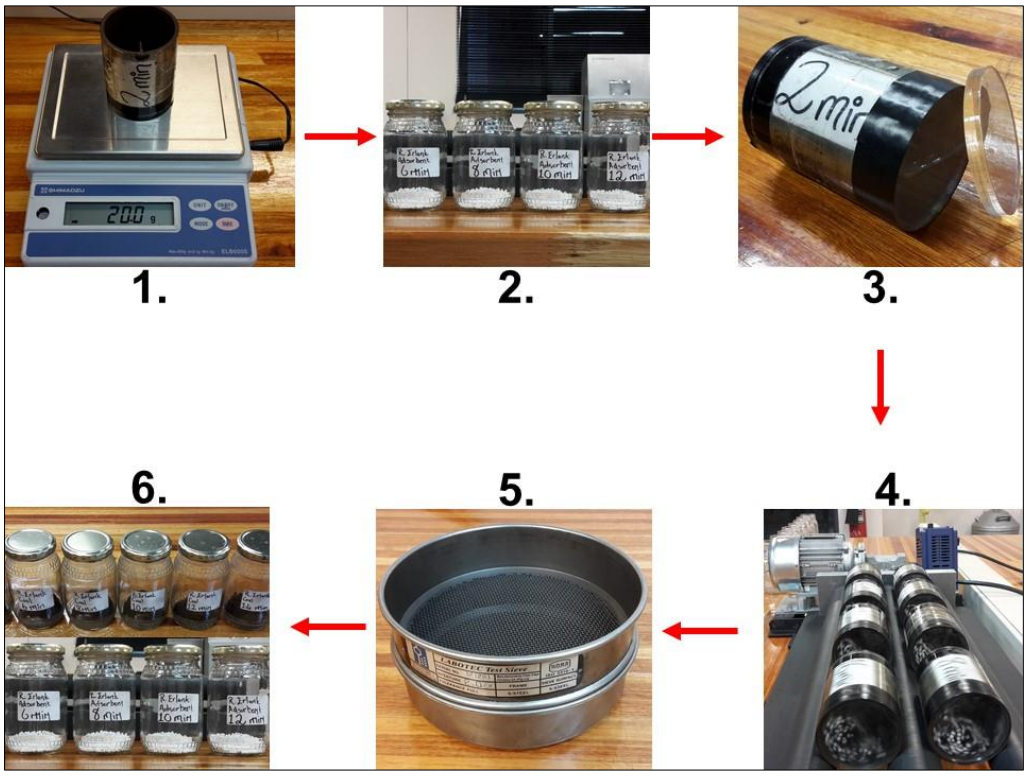

Figure 3-11 Adsorbent assisted drying procedure

3.3.2 Adsorbent regeneration

For the adsorbent regeneration, the spent adsorbents of five cycles' use are regenerated using the adsorbent regeneration setup discussed in Section 3.2.2. The regeneration procedure is discussed accordingly:

1. All spent adsorbents for a respective adsorbent-to-coal mass ratio from all sampled time intervals are mixed and rotated for 10 minutes inside a vessel on the rotating bed, for all adsorbents from different time intervals to reach equilibrium with one another.
2. Average moisture content is determined for the spent adsorbents before regeneration occurs.
3. The climate control chamber is set at 22°C and 70% RH.
4. An empty Erlenmeyer flask and glass funnel are pre-weighed and inserted inside the climate chamber, right below the blower air return entrance, to capture coal dust.
5. The empty column is weighed.
6. The spent adsorbents (of five cycles of use) are weighed and added to the column.
7. The blower is turned on, and the adsorbents are regenerated for 20 minutes.
8. In time intervals of 2 min, the blower is stopped, then the packed bed column and Erlenmeyer flask with its funnel are weighed respectively to measure mass loss and dust accumulation.

3.4 Analysis standards

All the primary analyses were done using standard methods, summarised in Table 3-6. For the calorific value analyses, an IKA C5003 Control Bomb Calorimeter was used. A Malvern Mastersizer 2000 was used for the particle size distribution analyses of the coal. Elemental analyses of carbon, hydrogen and nitrogen, was done using an Exeter Analytical CE440 Elemental Analyser.

Table 3-6 Analysis standards used in this study

Analysis	Analysis standard
Total moisture	ISO 589: 2008
Calorific value	ISO 1928: 2009
Proximate analysis	
Inherent moisture	ISO 11722: 2013
Ash yield	ISO 1171: 2010
Volatile matter	ISO 562: 2010
Fixed carbon	(by difference)
Ultimate analysis	
Carbon content	ISO 29541: 2010
Hydrogen content	
Nitrogen content	
Sulphur content	ISO 19579: 2006
Oxygen content	(by difference)

3.5 Experimental error

Three repetitions were conducted on all experiments to determine experimental errors and increase the data's integrity. Preliminary experiments (i.e. proximate analysis, PSD curves, water adsorptive capacity of the adsorbents) and main experiments (drying curves) were done three times to determine the data's integrity.

The method of determining the experimental error and relative experimental error is the T-test for a 90% confidence interval shown in Equations (3-1) & (3-2) (Devore *et al.*, 2014).

$$\boldsymbol{\epsilon = \frac{t.\sigma}{\sqrt{N}}} \tag{3-1}$$

where $\epsilon =$ experimental error

$t =$ critical t-value, 2.920 (Devore *et al.*, 2014)

$\sigma =$ standard deviation

$N =$ number of repetitions

$$\boldsymbol{\epsilon(\%) = \frac{\epsilon}{\bar{x}} \times 100} \tag{3-2}$$

where $\epsilon(\%) =$relative experimental error

$\bar{x} =$ average

Chapter 4 Drying of spiral coal

4.1 Introduction

This chapter discusses the drying ability or desorption performances of spiral coal product and tailings filter cakes using adsorbent assisted drying. The spiral coal product and tailings being investigated had d_{50} particle sizes of 434 µm and 397 µm, respectively.

Activated alumina in the form of 3 mm or 5 mm spherical beads were used as the adsorbent to dry the coal. The variables investigated were adsorbent-to-coal mass ratios, adsorbent particle sizes, and adsorbent states (new (fresh), spent, or regenerated). These variables' effect on moisture desorption from spiral coal product and tailings is discussed to determine the main driving force for optimum desorption performance.

A market specified target moisture content of 10% w/w, as stated in literature (Steyn & Minnit, 2010), was aimed at during dewatering experiments. All moisture contents referred to in this chapter, unless specified otherwise, are total moisture contents, which, as discussed in Chapter 2, account for inherent moisture and surface moisture.

In Section 4.5, qualitative remarks of unmeasured phenomena noted during experimental work receive attention while being deliberated. Qualitative remarks include difficulties, successes and keynotes experienced during experimental work.

All experimental work was conducted methodologically, as described in Section 3.3, and in a laboratory kept at a constant temperature of 22°C.

4.2 Spiral product

4.2.1 General adsorption and desorption curves

Filter cakes of spiral beneficiated coal products were dried using 3 mm and 5 mm activated alumina spherical beads. The filter cakes had a total moisture content of 18% w/w and an inherent moisture content of 2% w/w. The coal and activated alumina sorbents acted as feed to the cylindrical vessels and rotated to form a cascading motion for 16 minutes at 50 rpm, as discussed in Chapter 3. Further reference can be given to Annexure A.1 for results not discussed in this section. An example of the general adsorption and desorption curves for spiral product using 3 mm new (fresh) activated alumina in a 2:1 adsorbent-to-coal mass ratio is shown in Figure 4-1.

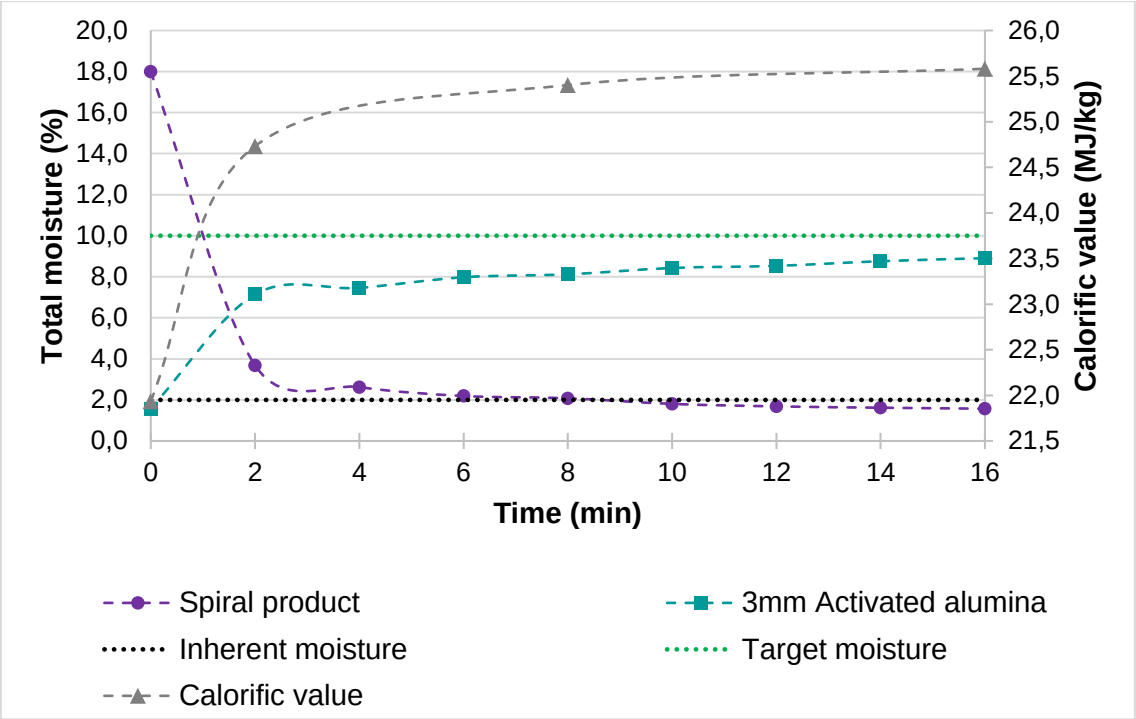

Figure 4-1 Adsorption & desorption curves of spiral product and 3 mm activated alumina

From Figure 4-1, the coal's total moisture swiftly decreased from a feed moisture content of 18% to 3.7% w/w within 2 minutes of contact-sorption at an initial desorption rate of 0.072 $g_{moisture}/g_{coal}$.min. The desorption curve's slope refers to the desorption rate measured in grams of moisture desorbed per gram wet coal per minute. The first two minutes of desorption is referred to as the initial desorption stage. A desorption rate of 0.01 $g_{moisture}/g_{coal}$.min relates to 1% w/w coal moisture reduced per minute. Market specified target moisture of 10% w/w is reached after 1 minute's contact-sorption. At 9 minutes of drying, the spiral product reaches sub inherent moisture contents. After 10 minutes of drying, the spiral product's desorption rate gradually reaches equilibrium and settles at a final moisture content of 1.6% w/w after 16 minutes.

The spiral product's total moisture content saw a 79% reduction in the first two minutes and an overall reduction of 91%. These figures conclude that 87% of the coal's dewatering is done within the first two minutes of contact sorption.

The 3 mm activated alumina was introduced with a feed moisture content of 1.6% w/w. From contact with the coal, the adsorbents' moisture content increased rapidly to 7.2% w/w within 2 minutes at an initial adsorption rate of 0.028 $g_{moisture}/g_{ads}$.min. The initial adsorption was followed by a gradual decrease in adsorption rate until a final moisture content of 8.9% w/w was reached. As expected, the desorption curve of the spiral product and the 3 mm activated alumina's adsorption curve could be said to mirror each other to a considerable extent.

The coal's calorific value was measured as received before drying occurred, during drying, after 2 minutes and 8 minutes and after drying, after 16 minutes. The spiral product had an initial heating value of 21.9 MJ/ kg, which significantly increased by 13% to 24.7 MJ/ kg within 2 minutes and increased overall by 17% to a final calorific value of 25.6 MJ/ kg after 16 minutes of drying.

As discussed in Section 3.5, all experiments with the same operating conditions were done three times to determine the experiments' reproducibility and the results' integrity. The T-test, with a 90% confidence interval, was used in determining the experimental error.

Figure 4-2 shows the average desorption curve, and the standard deviation lower and upper limit curves for the test shown in Figure 4-1. The spiral product's initial total moisture had an average of 18.0% w/w with a lower limit of 17.8% w/w and an upper limit of 18.2% w/w. After 16 minutes of drying, the spiral product had a final total moisture content averaging at 1.6% w/w with a lower limit of 1.5% w/w and an upper limit of 1.7% w/w.

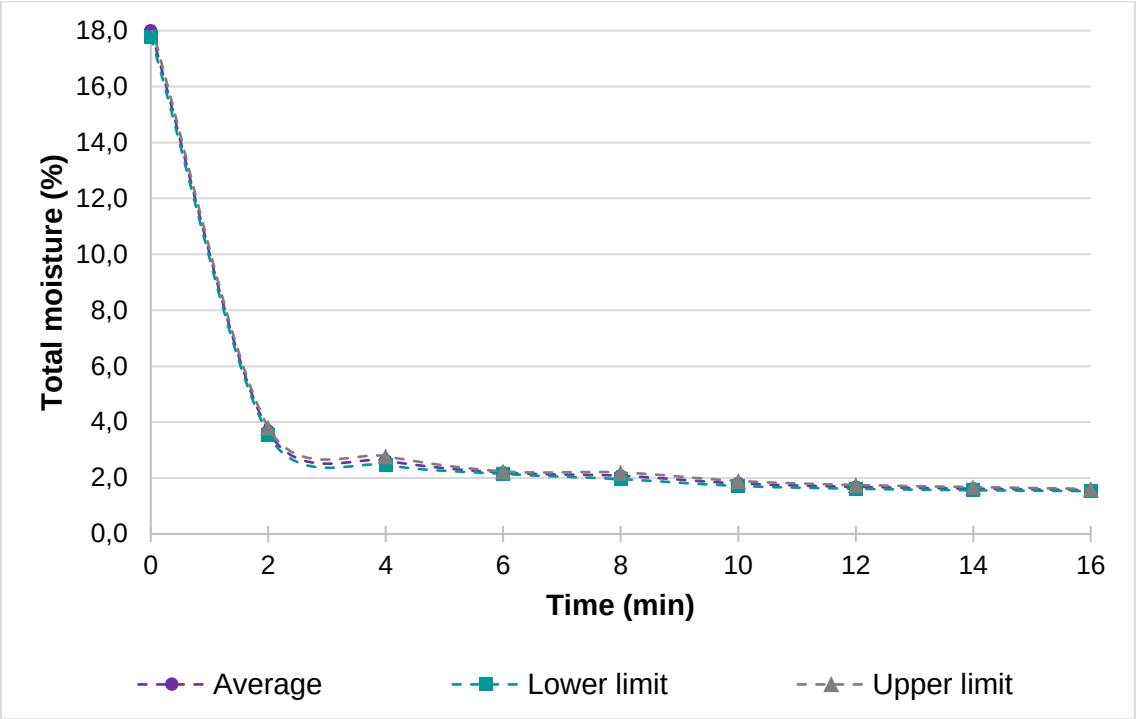

Figure 4-2 Average desorption curve of the spiral product with the standard deviation

The average, standard deviation, and relative experimental error for repeated experimental runs of spiral product drying using 3 mm activated alumina in a 2:1 adsorbent-to-coal mass ratio are summarised in Table 4-1. Low standard deviations and relative experimental errors found for the spiral product's respective moisture contents are indicative of reliable experimental data.

Table 4-1 Standard deviation and relative experimental error for spiral product moistures

Time (min)	Average (% w/w)	Standard deviation (% w/w)	Relative experimental error (%)
0 (Feed)	18.00	0.22	0.49
16 (Final)	1.57	0.04	4.29

Figure 4-3 shows the average adsorption curve, and the standard deviation lower and upper limit curves for the 3 mm activated alumina used in the test described in Figure 4-1. The activated alumina was introduced to the coal at an average equilibrium feed moisture content of 1.6% w/w with a lower limit of 1.5% w/w and an upper limit of 1.7% w/w. After 16 minutes of adsorption, the adsorbents' final moisture averaged 8.9% w/w with lower and upper limits at 8.6% and 9.3% w/w, respectively.

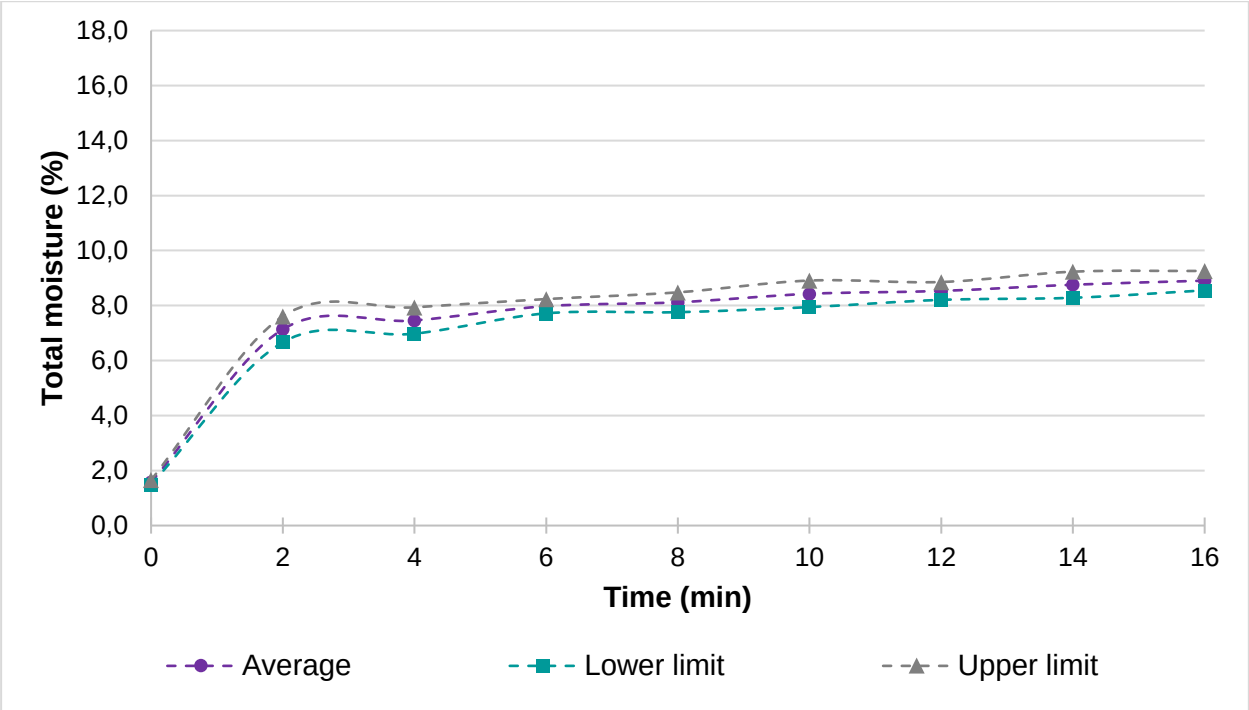

Figure 4-3 Average adsorption curve of 3 mm activated alumina with standard deviation

Table 4-2 shows the average feed and final moisture contents and its respective standard deviation and relative experimental error for the 3 mm activated alumina used on spiral product in a 2:1 adsorbent-to-coal mass ratio. The standard deviation and relative experimental error for the activated alumina were marginal, which relates to reliable results and repeatable experiments.

Table 4-2 Standard deviation and relative experimental error of 3 mm activated alumina used to dry spiral product

Time (min)	Average (% w/w)	Standard deviation (% w/w)	Relative experimental error (%)
0 (Feed)	1.57	0.08	3.21
16 (Final)	8.91	0.35	6.69

4.2.2 Effect of adsorbent-to-coal mass ratio

Higher adsorbent-to-coal mass ratios relate to higher contact surface areas between the coal particles and the adsorbents and vice versa. This higher contact surface area would mean higher adsorbent pore availability to coal moisture, which relates to higher adsorption performance. This hypothesis was tested and proven for run-of-mine coal in previous studies (Peters, 2016). In this section, the hypothesis is tested and discussed for spiral coal product.

To understand the effect of various adsorbent-to-coal mass ratios on the desorption performance of spiral product, adsorbent-to-coal mass ratios of 2:1; 1:1 and 0.5:1 were used as feed to the cylinders.

Figure 4-4 shows the desorption curves of spiral product using 3 mm activated alumina in 2:1, 1:1 and 0.5:1 adsorbent-to-coal mass ratios. The 3 mm adsorbent used in all three adsorbent-to-coal mass ratios dewatered the spiral product sufficiently to below target moisture, albeit a significant difference in initial desorption rates and final moisture contents existed between the various ratios.

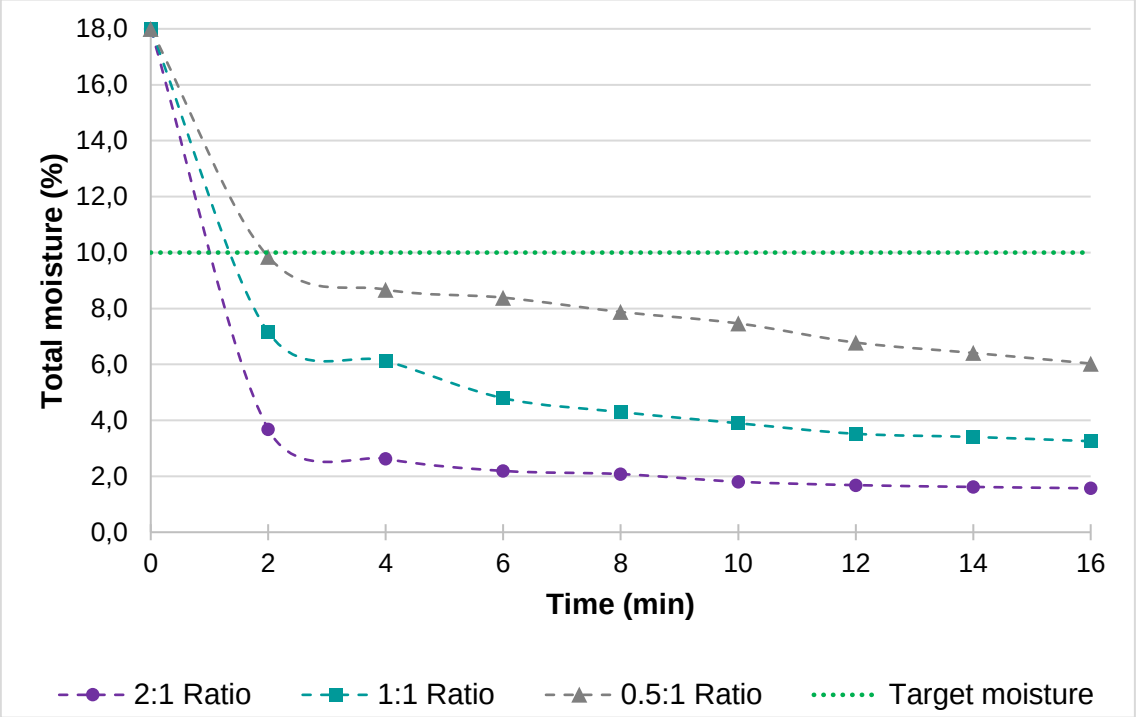

Figure 4-4 Desorption curves of spiral product using 3 mm activated alumina in various adsorbent-to-coal mass ratios

Within two minutes of dewatering (Figure 4-4), the 2:1 adsorbent-to-coal mass ratio delivered a spiral product moisture content of 3.7% w/w, followed by 7.2% and 9.9% w/w respectively by the 1:1 and 0.5:1 adsorbent-to-coal mass ratios. After 2 minutes, the desorption rates decreased, when all the setups moved towards the final equilibrium moisture content of the coal.

The various ratios' curves in Figure 4-4 settled at final coal moisture contents of 1.6%, 3.3%, and 6.0% w/w, respectively for the 2:1, 1:1, and 0.5:1 adsorbent-to-coal mass ratios. The 2:1 adsorbent-to-coal mass ratio delivered a 91% moisture reduction followed by a respective 82% and 67% moisture reduction by the 1:1 and 0.5:1 adsorbent-to-coal mass ratios.

The 2:1 adsorbent-to-coal mass ratio performed the best of all the different ratios tested, due to its higher direct contact surface area available for liquid moisture transport. This relation was also

confirmed by previous studies done on moisture transport during contact sorption drying of coals (Van Rensburg, *et al*., 2018)

Even though the effect of adsorbent particle size is discussed in detail in Section 4.2.3, further reference is given to Figure 4-5, representing the desorption curves of spiral product using 5 mm activated alumina in various adsorbent-to-coal mass ratios.

In Figure 4-5, the same relationship for increasing adsorbent-to-coal mass ratios is evident for the 5 mm activated alumina. The 5 mm adsorbent, used in a 2:1 adsorbent-to-coal mass ratio, delivered an 83% moisture reduction followed by a 61% and 48% moisture reduction for the 1:1 and 0.5:1 adsorbent-to-coal mass ratio.

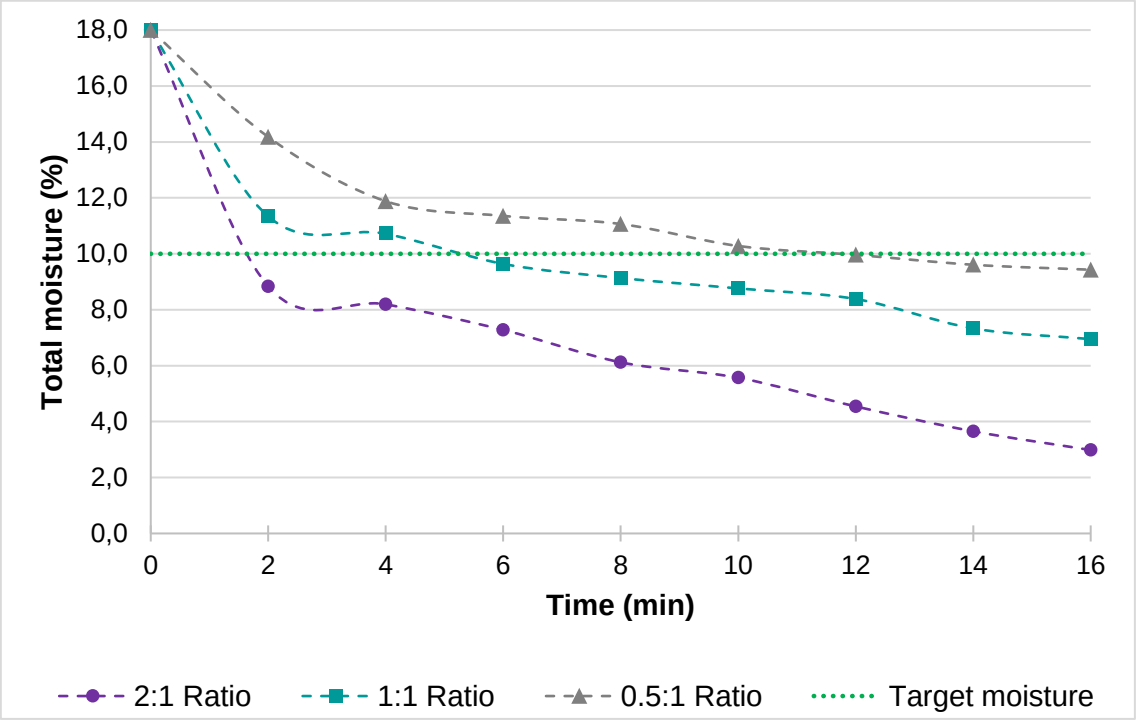

Figure 4-5 Desorption curves of spiral product using 5 mm activated alumina in various adsorbent-to-coal mass ratios

Figure 4-6 shows the adsorption curves of different adsorbent-to-coal mass ratios of 3 mm activated alumina used to dry spiral product. Even though the different adsorption curves followed similar paths, the effect of different adsorbent-to-coal mass ratios is evident in Figure 4-6 when considering the varying initial and general adsorption rates and final moisture contents. The adsorption curve's slope is referred to as the adsorption rate and measured in grams of moisture adsorbed per gram adsorbent per minute. The first two minutes of adsorption is referred to as the initial adsorption stage.

Within two minutes of adsorption, the 0.5:1 adsorbent-to-coal mass ratio yielded the highest adsorbent moisture content of 12.8% w/w, followed by an 8.6% and 7.1% w/w moisture content

for 1:1 and 2:1 adsorbent-to-coal mass ratio. After the initial adsorption stage, the adsorption rates gradually decreased with time.

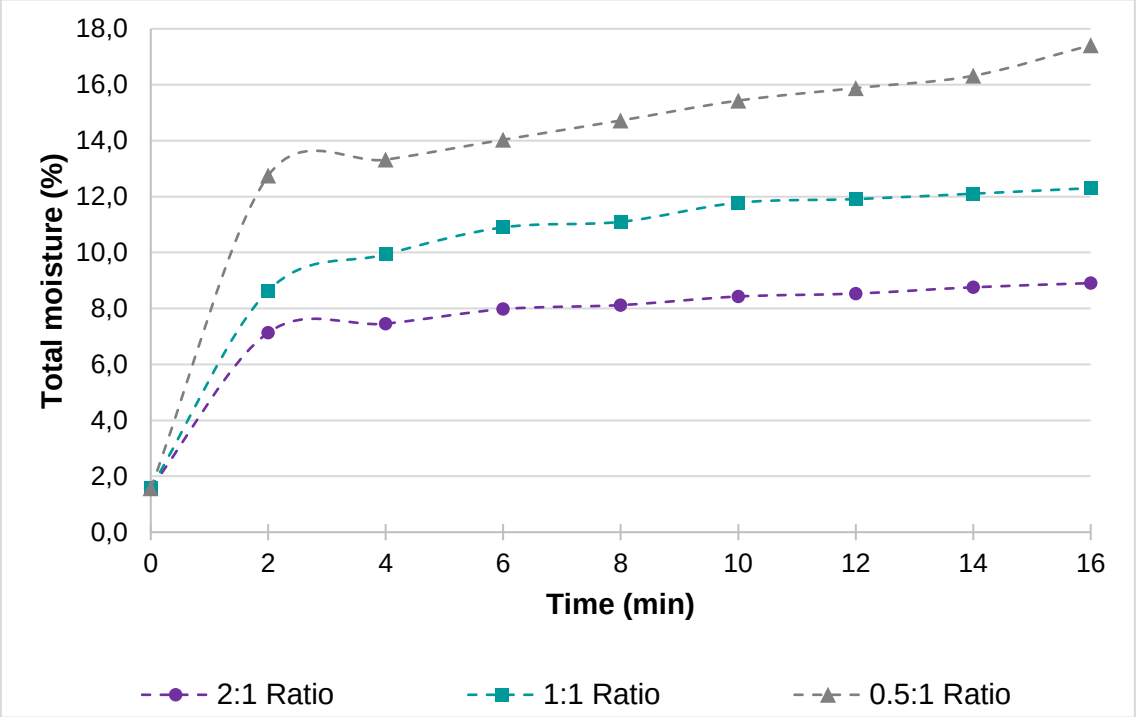

Figure 4-6 Adsorption curves of 3 mm activated alumina used on spiral product in various adsorbent-to-coal mass ratios

The various adsorbent-to-coal mass ratio curves settled at different final moisture contents. The 0.5:1 ratio settled at a 17.4% w/w final moisture content, followed by 12.3% and 8.9% w/w for the 1:1 and 2:1 adsorbent-to-coal mass ratios, respectively. The activated alumina used in all three ratios would still have the affinity to adsorb more moisture, considering the maximum adsorptive capacities discussed in Section 3.1.2. However, the affinity to adsorb more moisture would rank in descending order from 2:1 to 1:1 and, lastly, a 0.5:1 adsorbent-to-coal mass ratio.

For varying adsorbent-to-coal mass ratios, the adsorbent's initial adsorption rates relative to adsorbent mass are inversely proportional to the coal's respective initial desorption rates, relative to coal mass.

This phenomenon can be elaborated on by referring to a constant, single mass of water contained in a single mass of coal. The 0.5:1 adsorbent-to-coal mass ratio, with the smallest mass of adsorbents, will result in a higher adsorbent moisture content than the same mass of water adsorbed by a larger mass of adsorbents, i.e. 2:1 adsorbent-to-coal mass ratio. This phenomenon is also illustrated in Figure 4-7.

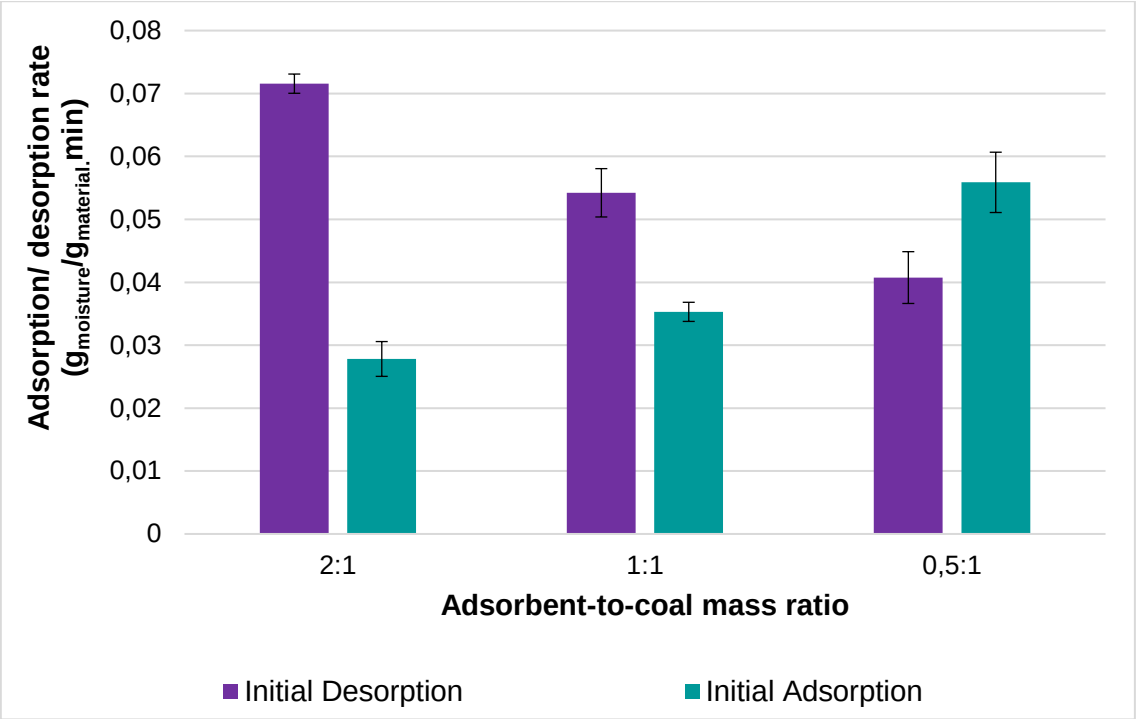

Figure 4-7 Initial adsorption/ desorption rates of 3 mm activated alumina and spiral product

Figure 4-7 compares the initial desorption rates of spiral product and adsorption rates of 3 mm activated alumina for various adsorbent-to-coal mass ratios. The figure shows that higher adsorbent-to-coal mass ratios deliver higher initial desorption rates and vice versa. The phenomenon mentioned above is also illustrated, where the higher adsorbent-to-coal mass ratios yield lower adsorption rates relative to adsorbent mass and vice versa.

From Figure 4-7, the spiral product was initially desorbed at 0.072 $g_{moisture}/g_{coal}$.min using the 2:1 ratio followed by rates of 0.054 and 0.041 $g_{moisture}/g_{coal.}$min for the 1:1 and 0.5:1 adsorbent-to-coal mass ratio. The 3 mm activated alumina had an initial adsorption rate of 0.028 $g_{moisture}/g_{ads}$.min for the 2:1 ratio followed by adsorption rates of 0.035 and 0.056 $g_{moisture}/g_{ads}$.min.

This section concludes that the adsorbent-to-coal mass ratio, using 3 mm and 5 mm activated alumina to dry spiral product coal, is directly proportional to its drying performance. Higher adsorbent-to-coal mass ratios call for better drying performances, with faster desorption and lower coal moistures, while lower adsorbent-to-coal mass ratios call for weaker drying performances.

4.2.3 Effect of adsorbent particle size

The contact surface area between adsorbent and coal particles is critical for the adsorption performances of adsorbents, as previously discussed in Section 4.2.2. Another way of varying the contact surface area is by changing the adsorbent particle size.

Although two adsorbent particle sizes of 3 mm and 5 mm may differ only by 2 mm in diameter, they can differ significantly by contact surface area per mass of adsorbent.

The difference in contact surface area becomes apparent when referring to a bulk of adsorbents, as illustrated in Figure 4-8. Assume a 1-litre cylinder is filled with uniformly spherical 3 mm and 5 mm adsorbents, respectively, with an average voidage factor of 0.4. The volume of a single 3 mm and 5 mm adsorbent particle is 14.1 mm^3 and 65.4 mm^3, respectively. With the voidage factor considered, this equates to approximately 42441 particles of the 3 mm adsorbent and 9167 particles of the 5 mm adsorbent.

Assuming all the particles' surfaces are available, the respective one litre of 3 mm and 5 mm adsorbents would have a total of 1.2 m^2 and 0.7 m^2 contact surface area, excluding the inner-pore surface areas tabulated in Table 3-3. These figures conclude the 3 mm adsorbents having a 71% higher contact surface area relative to the 5 mm adsorbents.

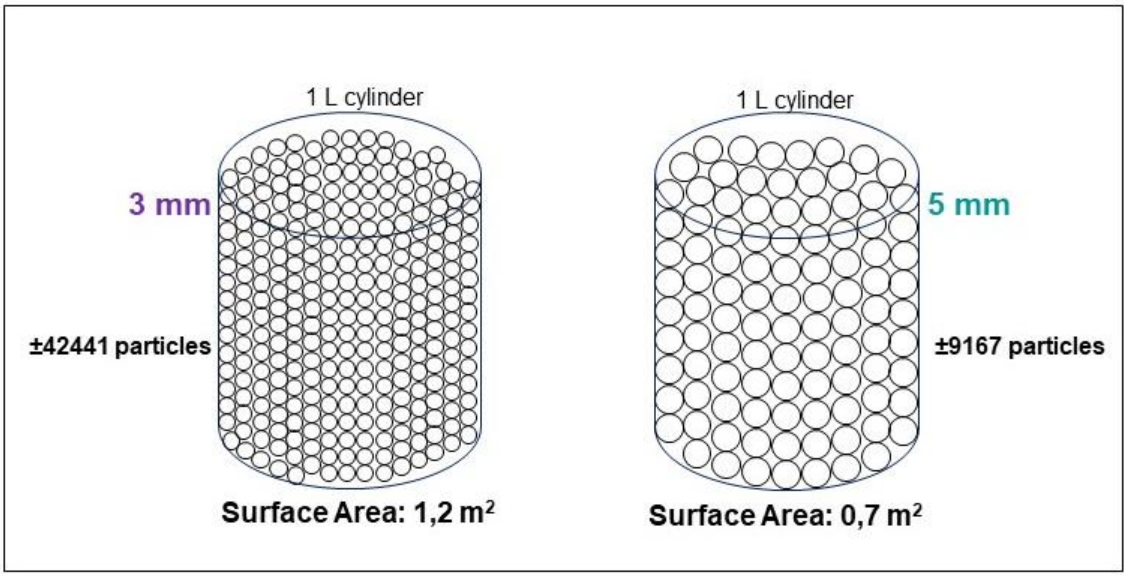

Figure 4-8 Contact surface area illustration of 3 mm and 5 mm adsorbents

Different adsorbent particle sizes used for coal drying were tested on run-of-mine coal in previous studies, which found the smaller adsorbent particles sizes to outperform the larger adsorbent particle sizes (Peters, 2016).

Similar tests were done using 3 mm, and 5 mm activated alumina to dewater the spiral coal product. Figure 4-9 represents the coal's desorption curves using 3 mm and 5 mm activated alumina in a 2:1 adsorbent-to-coal mass ratio. The figure shows that both adsorbent particles sizes dewater the spiral product sufficiently to below target moisture. It is however evident that the 3 mm adsorbent outperformed the 5 mm adsorbent in both the initial dewatering rate and the final coal moisture content.

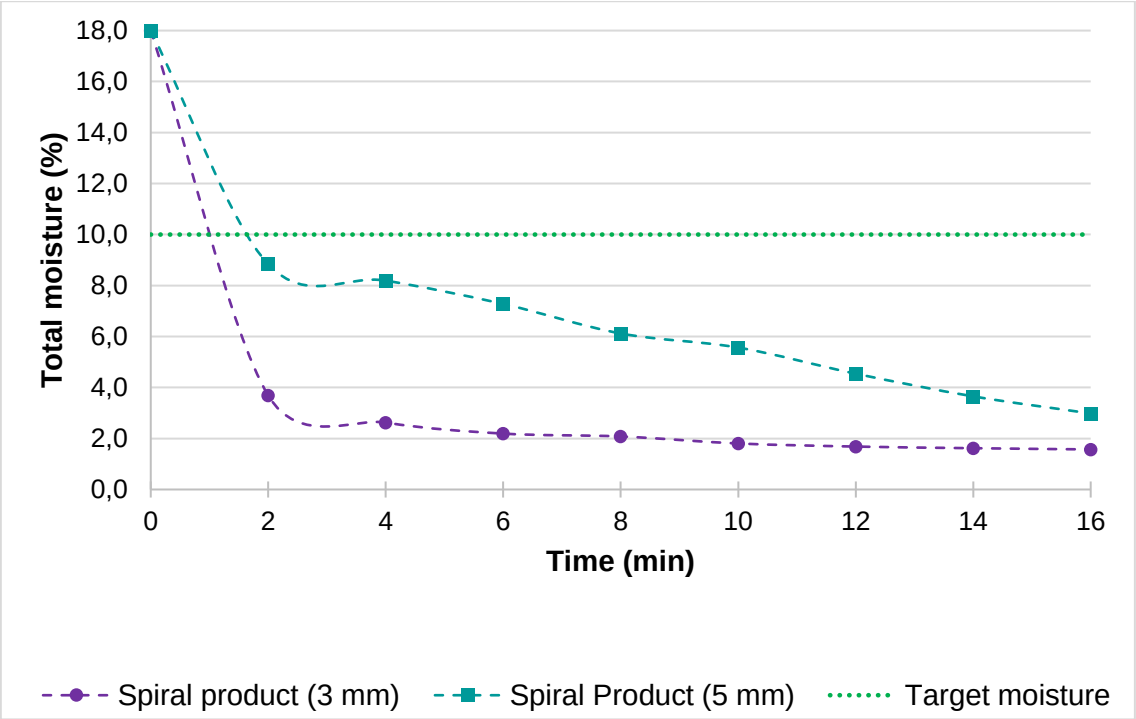

Figure 4-9 Desorption curves of spiral product using 3 mm and 5 mm activated alumina

From Figure 4-9, the desorption curve of the 3 mm adsorbent shows faster dewatering rates and lower final moisture contents than the 5 mm adsorbent desorption curve. After two minutes of dewatering, the 3 mm adsorbent achieved a spiral product moisture content of 3.7% w/w compared to 8.8% w/w achieved by the 5 mm adsorbent.

The use of 3 mm adsorbents resulted in a final coal moisture content of 1.6% w/w, while the 5 mm adsorbent achieved a final coal moisture content of 3.0% w/w. These final moisture contents conclude with the 3 mm adsorbent delivering a 91% moisture reduction and the 5 mm delivering an 83% moisture reduction.

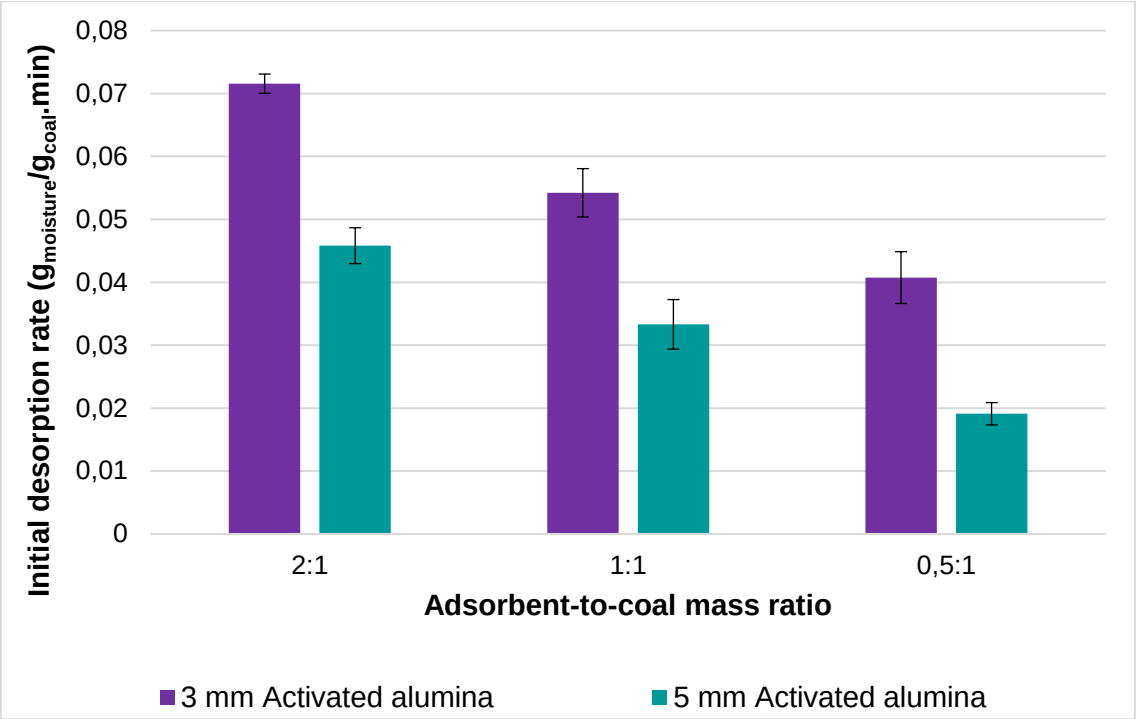

Figure 4-10 Initial desorption rates of spiral product dewatered by 3 mm and 5 mm activated alumina

Figure 4-10 shows the initial desorption rates of spiral product dewatered by 3 mm and 5 mm activated alumina in various adsorbent-to-coal mass ratios. From the figure, a clear relationship exists between adsorbent particle size and drying performance, irrespective of the adsorbent-to-coal mass ratio. For all three adsorbent-to-coal mass ratios, the 3 mm adsorbent outperformed the 5 mm adsorbent. For the 2:1 adsorbent-to-coal mass ratio, the 3 mm activated alumina outperformed the 5 mm activated alumina by 57%. Furthermore, the 3 mm adsorbent outperformed the 5 mm adsorbent by 63% and 110%, respectively, for 1:1 and 0.5:1 adsorbent-to-coal mass ratios. The 3 mm adsorbent outperformed the 5 mm adsorbent by an overall average of 77% regarding desorption rates.

Albeit a clear difference in dewatering performances exists between the 3 mm and 5 mm adsorbents, both adsorbent particle sizes resulted in sufficient dewatering of the spiral product to below the target moisture content, beneficial when considering industrial applications.

This section concludes that a noticeable relationship exists between adsorbent particle size and its dewatering performance. When considering adsorbents in bulk, an adsorbent's particle size is inversely proportional to its dewatering performance.

The hypothesis mentioned at the start of this section has been proven. Smaller adsorbent particle sizes deliver better dewatering performances than larger adsorbent particle sizes due to increased contact surface area between the adsorbent and the coal particles. The dewatering results of the spiral product, using 3 mm and 5 mm activated alumina, followed the same trends

as the previous adsorbent assisted drying studies on run-of-mine coal (Peters, 2016). Overall, considering desorption rates and final moisture contents, the 3 mm adsorbent achieved better dewatering results than the 5 mm adsorbent.

4.2.4 Effect of adsorbent state

Due to adsorbents contributing to the process' operational costs, the reuse and regeneration viability of adsorbents play a crucial part in determining this drying method's economic feasibility. For this reason, the viability of regeneration and reuse of the adsorbents were tested in this study. Adsorbent state refers to whether an adsorbent is fresh (new), spent, or regenerated. In previous studies, the viability of adsorbent reuse and regeneration has been proven successful (Peters, 2016), albeit Peters used slightly different activated alumina than this study.

In this section, the reuse, without regeneration, of activated alumina used to dewater spiral product coal is discussed. The use of regenerated adsorbents to dry spiral product is also investigated and discussed. The regeneration of the adsorbents using ambient airflow is discussed in depth in Chapter 6. A comparison is drawn between the drying performances of new, spent, and regenerated adsorbents.

The spiral product was dried using 3 mm, and 5 mm activated alumina for five consecutive cycles without regenerating the adsorbents, with the fresh (new) adsorbents being the first cycle in the series. The spiral product was dried for 10 minutes in each cycle, after which the moisture contents were measured.

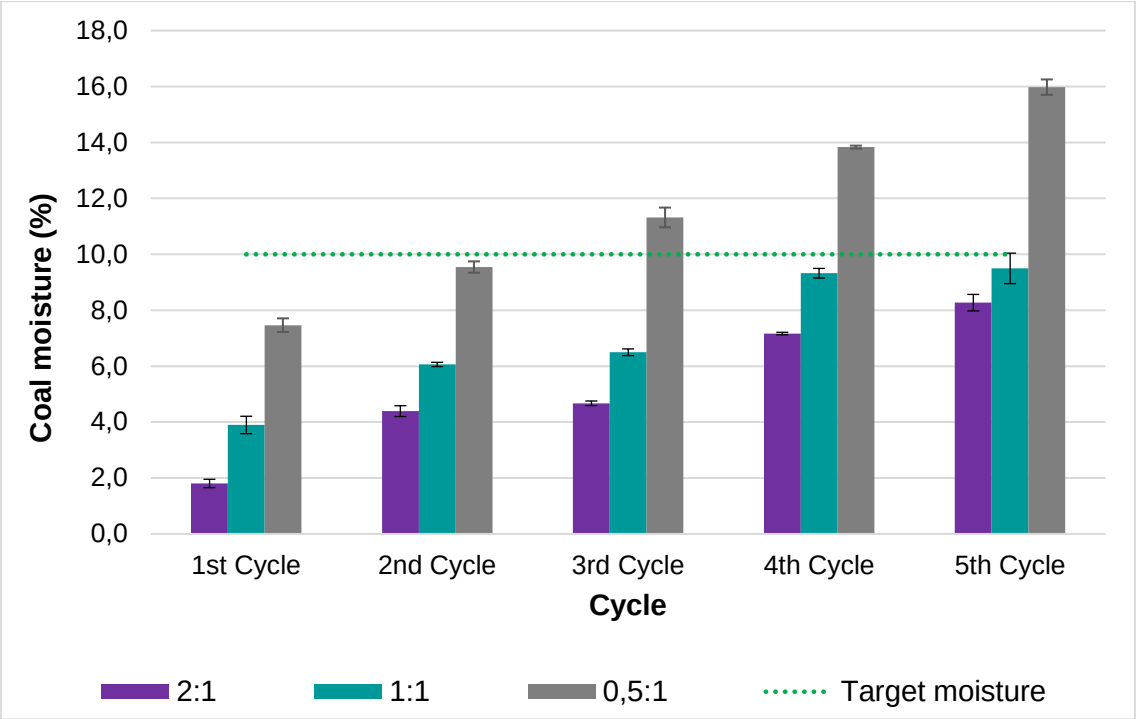

Figure 4-11 Spiral product moisture after 10 minutes using 3 mm new and spent activated alumina

Figure 4-11 shows the coal's moisture contents after 10 minutes of contact-sorption dewatering using 3 mm fresh (first cycle) and spent (second to the fifth cycle) activated alumina in various adsorbent-to-coal mass ratios. Considering a target moisture of 10% w/w, the spent 3 mm activated alumina managed to dewater the coal to below target moisture during the five cycles, tested for a 2:1 and 1:1 adsorbent-to-coal mass ratio. Until the fifth cycle of use, the 2:1 and 1:1 adsorbent-to-coal mass ratios delivered moisture contents of 8.3% and 9.5% w/w, respectively. The 3 mm adsorbent, used in a 0.5:1 adsorbent-to-coal mass ratio, achieved target moisture of 9.5% w/w only up to the second use.

Figure 4-13 shows that a correlation exists between the various cycles for each adsorbent-to-coal mass ratio, where a decrease in drying performance is realised as the adsorbent's cycle of use increases. The exact correlation discussed in Section 4.2.2, where the drying performance is directly proportional to the adsorbent-to-coal mass ratio, is also evident for each use cycle.

Figure 4-12 illustrates the moisture loads (adsorbent moisture contents) of the 3 mm activated alumina used for five consecutive cycles to dry the spiral product for 10 minutes. Figure 4-12 shows that the adsorbents' moisture load increased steadily as the cycle of use increased. Lower adsorbent-to-coal mass ratios resulted in higher adsorbent moisture loads.

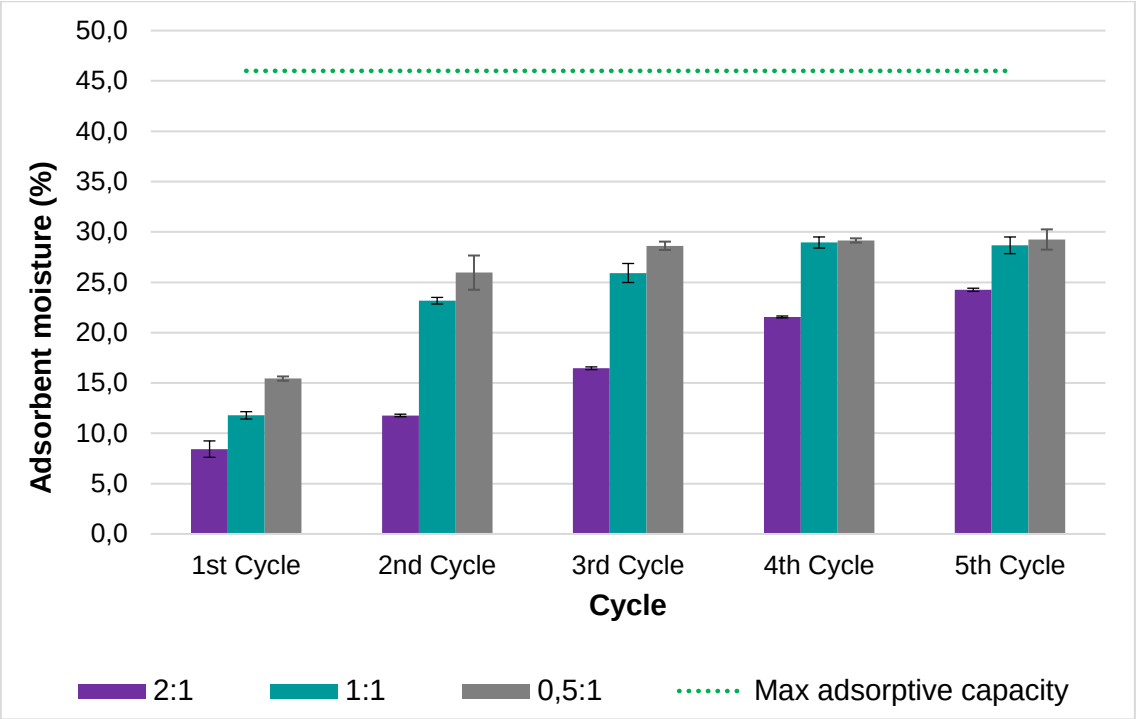

Figure 4-12 Adsorbent moisture loads of 3 mm activated alumina used to dewater spiral product consecutively

For the 2:1 adsorbent-to-coal mass ratio, the adsorbent's moisture content increased from 8.4% w/w after the 1st cycle to 24.2% w/w after the 5th cycle. A marginal difference in moisture loads exists for the fourth to the fifth cycle of the 1:1 and 0.5:1 adsorbent-to-coal mass ratios, which may contradict the statement above.

Although Figure 4-12 shows that the adsorbent did not reach its maximum pure water adsorptive capacity for either of the adsorbent-to-coal mass ratios, it does indicate a possible maximum equilibrium moisture load for the sorbents used in the process. This is evident when comparing the moisture capacity of the sorbents used in 0.5:1 mass ratio tests in cycles three to five with the sorbents used in the 1:1 mass ratio tests in cycles four to five. The moisture load for each of these cases is just below 30% w/w. Compared to maximum pure water adsorptive capacity, the adsorbents' unsaturation may also be due to competing capillary forces between the coal and the adsorbents gaining significance at certain adsorbent moisture loads or a phenomenon entailing the blinding of capillary pores due to coal dust.

The use of spent adsorbent was also tested with the 5 mm adsorbent. Figure 4-13 shows the spiral product moisture contents using 5 mm activated alumina for five consecutive cycles, without regeneration, in various adsorbent-to-coal mass ratios. The exact correlation between drying performance and the cycle of use, as seen with the 3 mm adsorbent, is valid for the 5 mm adsorbent.

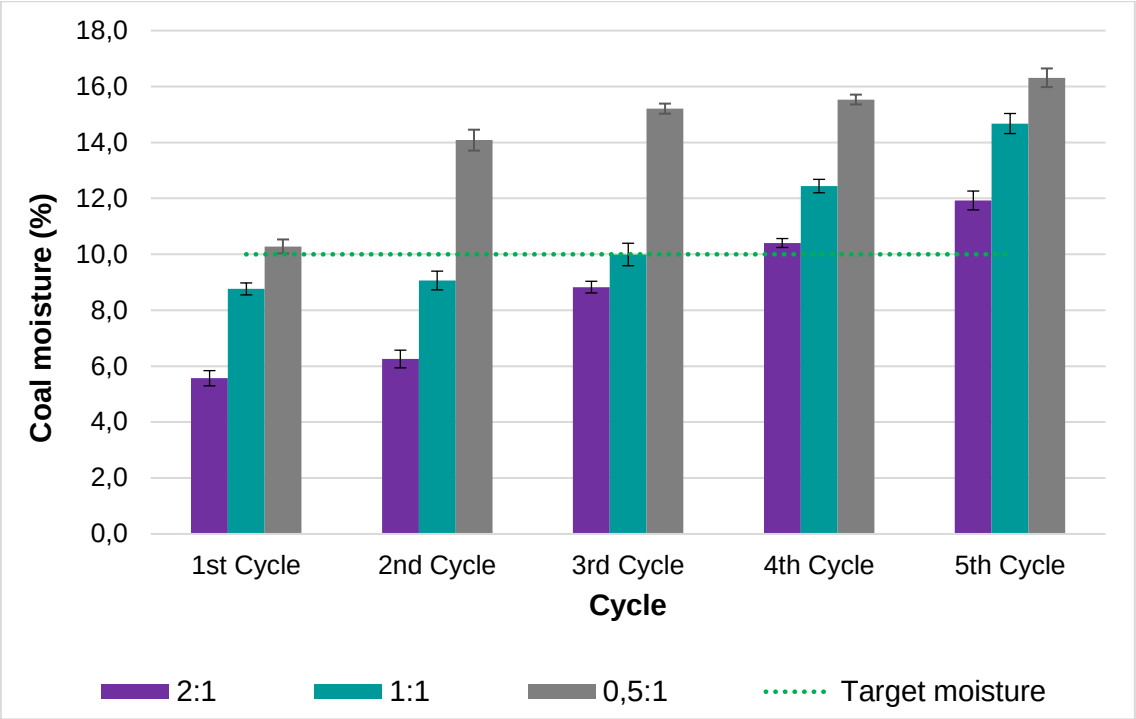

Figure 4-13 Spiral product moisture after 10 minutes using 5 mm new and spent activated alumina

Figure 4-13 shows that the 5 mm adsorbent performed weaker than the 3 mm adsorbent when reused consecutively. For the 2:1 adsorbent-to-coal mass ratio, the 5 mm adsorbent managed to dewater the coal sufficiently up to the 3rd cycle of use, delivering a coal moisture content of 8.8% w/w. However, for the 4th and 5th cycles, the 5 mm adsorbent did not sufficiently dewater the coal. For the 1:1 adsorbent-to-coal mass ratio, the 5 mm adsorbent also dewatered the coal sufficiently up to the 3rd cycle of use, reaching a coal moisture content of 10% w/w.

However, the 5 mm adsorbent used in a 0.5:1 adsorbent-to-coal mass ratio could not dewater the coal to market specification when reused consecutively, without regeneration. The 5 mm adsorbent in a 0.5:1 adsorbent-to-coal mass ratio did, however, dewater the coal to market specification after 16 minutes, but not 10 minutes, as illustrated in Figure 4-13.

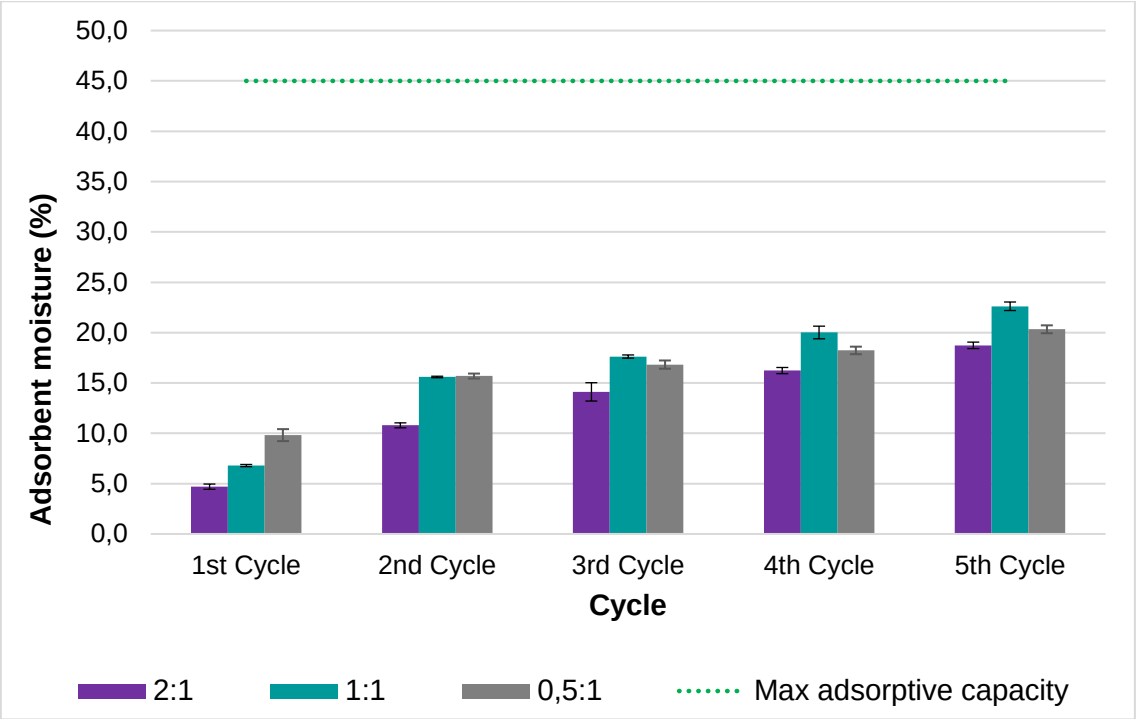

Figure 4-14 Adsorbent moisture loads of 5 mm activated alumina used to dewater spiral product consecutively

Figure 4-14 represents the 5 mm activated alumina's moisture loads used to dewater spiral product for five consecutive cycles, without regeneration, in various adsorbent-to-coal mass ratios. The same correlations discussed for the 3 mm adsorbent are seen for the 5 mm adsorbent from the figure. The adsorbent moisture loads increased gradually as the use cycle increased for each respective adsorbent-to-coal mass ratio, with the 0.5:1 adsorbent-to-coal mass ratio showing the least moisture increases.

However, a contradicting correlation is revealed between the 1:1 and 0.5:1 adsorbent-to-coal mass ratio, where the 1:1 adsorbent-to-coal mass ratio resulted in higher moisture loads than the 0.5:1 adsorbent-to-coal mass ratio. The 0.5:1 adsorbent-to-coal mass ratio also showed insignificant moisture load increases from the 2nd to the 5th cycle of use. This contradicting relationship can also be attributed to the capillary pore-blinding phenomenon, where the adsorbent used in a 1:1 ratio had fewer capillary pores blinded, and therefore, still had an affinity to adsorb moisture.

As with the 3 mm adsorbent, the 5 mm adsorbent also did not reach full saturation, which is primarily contributed to the dependency on moisture available to be adsorbed and secondarily to capillary pore-blinding.

The results discussed above concluded that even though the reuse of adsorbents, without regeneration, delivered good dewatering results for specific adsorbent-to-coal mass ratios, the need still exists for the regeneration of the adsorbents. The spent 3 mm, and 5 mm activated

alumina were regenerated using ambient airflow conditioned at 22°C and 70% RH in a packed bed column. These regeneration curves and their discussion can be found in Chapter 6.

The spent adsorbent moisture loads recorded for the 3 mm and 5 mm adsorbent, as shown in Figure 4-12 and Figure 4-14, whilst still delivering sufficient dewatering of the coal, confirmed that bone-dry adsorbents are unnecessary for sufficient dewatering of the coal to occur, which led to the use of alternative, cheaper regeneration methods compared to conventional oven-regeneration.

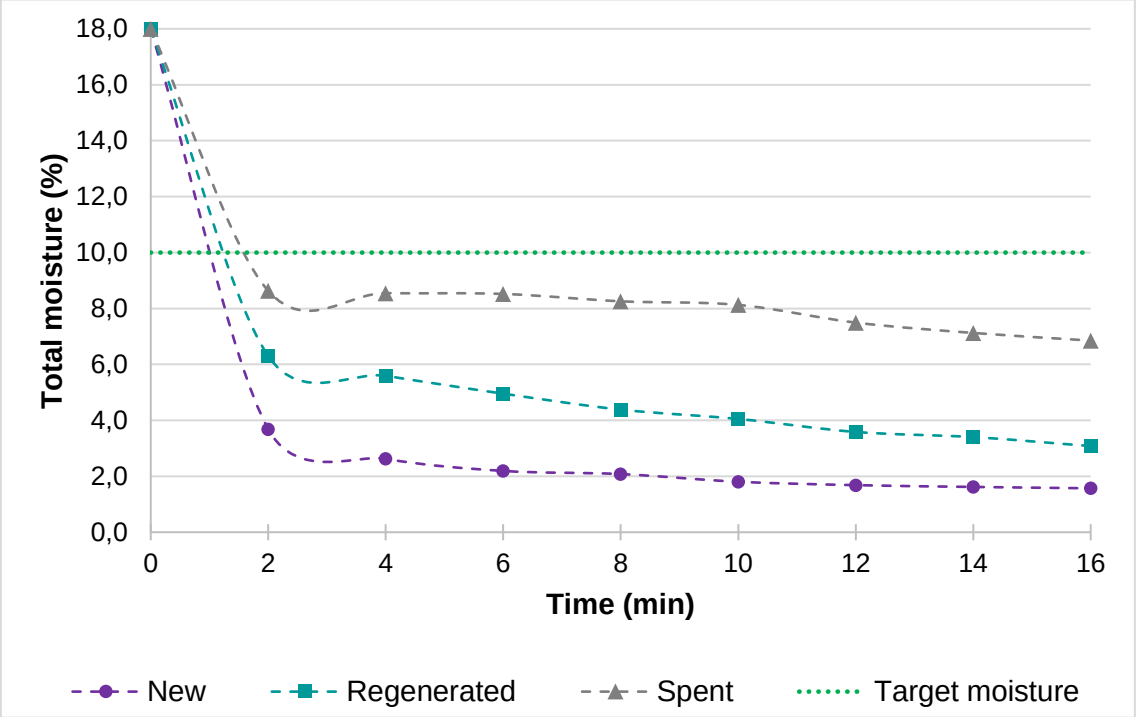

Figure 4-15 Spiral product desorption curves using new, regenerated & spent 3 mm activated alumina

Figure 4-15 shows the desorption curves of spiral product using new, regenerated and spent (5th cycle of use) 3 mm activated alumina in a 2:1 adsorbent-to-coal mass ratio. A clear difference in desorption is observed between the three curves. The regenerated adsorbent performed better than the spent adsorbent but weaker than the fresh adsorbent. The regenerated adsorbent resulted in a spiral product moisture content within target moisture of 6.3% w/w after 2 minutes and a final moisture content of 3.1% w/w.

The regenerated adsorbent had an initial desorption rate of 0.059 $g_{moisture}/g_{coal}$.min, which meant a 26% improvement over the spent adsorbent and an 18% weaker performance than the fresh adsorbent. Overall, the regenerated adsorbent achieved an 83% moisture reduction in coal, compared to a 62% moisture reduction for the spent adsorbent and a 91% moisture reduction in coal for the fresh adsorbent. It confirms that the method of regenerating the sorbent is viable for use in this application.

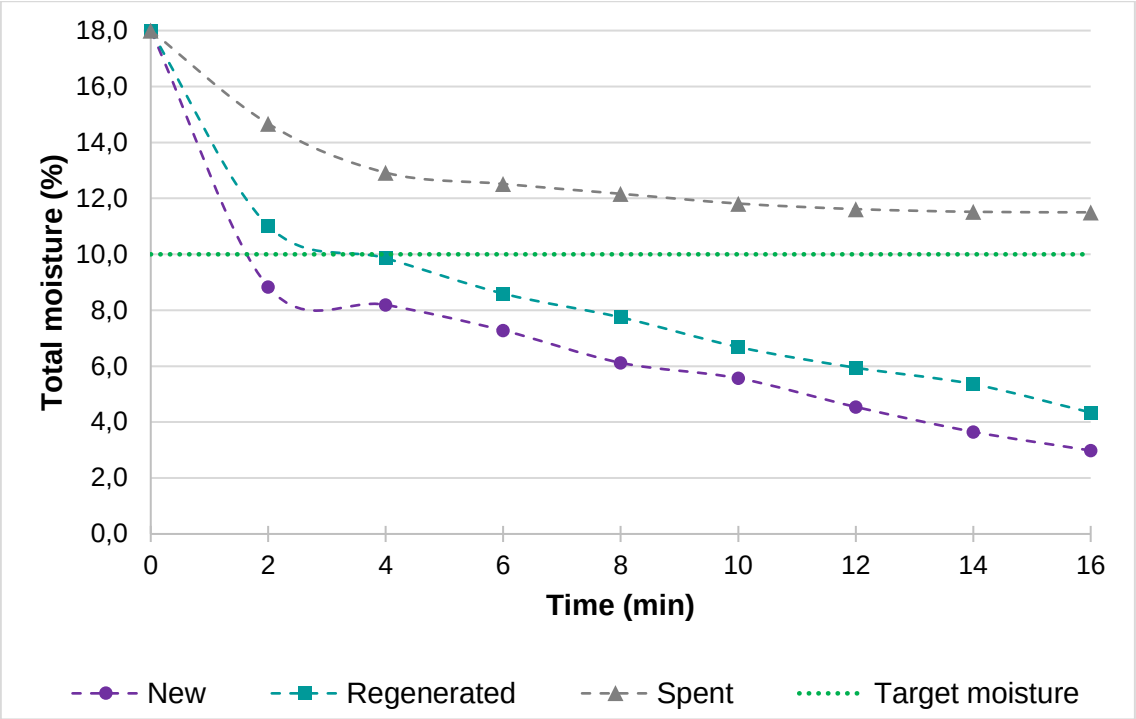

Figure 4-16 Spiral product desorption curves using new, regenerated & spent 5 mm activated alumina

Figure 4-16 displays the desorption curves of spiral product using new, regenerated and spent (5th cycle of use) 5 mm activated alumina in a 2:1 adsorbent-to-coal mass ratio. The figure shows that the regenerated 5 mm adsorbent performed similarly to the 3 mm sorbents in that the regenerated sorbents perform far better than the spent sorbents but not at the same level as their fresh feed counterparts.

In conclusion, a noticeable correlation existed in drying performances between the different adsorbent states (new, spent or regenerated). Fresh adsorbents delivered, logically, the best dewatering performance, followed closely by its regenerated version, which in turn, was a remarkable improvement on its spent version.

The reuse of adsorbents, without regeneration, to dewater spiral product was found feasible but with limitations, including eventual saturation of the adsorbents. Although adsorbent saturation was not observed in the results discussed above, it is an inevitable limitation, provided the adsorbent's capillary pores are not blinded.

The regeneration of the spent adsorbents produced noteworthy improvements in drying performances. The use of regenerated 3 mm and 5 mm adsorbents are found to be a feasible means of adsorbent assisted drying of spiral product coal.

4.3 Spiral tailings

4.3.1 General adsorption and desorption curves

Spiral coal tailings filter cake was dried using activated alumina of 3 mm and 5 mm particle sizes. The filter cake of spiral tailings had a feed total moisture content of 18.4% w/w and an inherent moisture content of 1.6% w/w. The spiral tailings were combined with the activated alumina in cylindrical vessels and rotated to create a cascading effect for 16 minutes at 50 rpm, as discussed in Chapter 3. Figure 4-17 shows the general adsorption and desorption curves for spiral tailings using 3 mm new activated alumina in a 2:1 adsorbent-to-coal mass ratio. A comparison between spiral product and tailings can be found in Section 4.4. Additional results, not discussed in this section can be found in Annexure A.2.

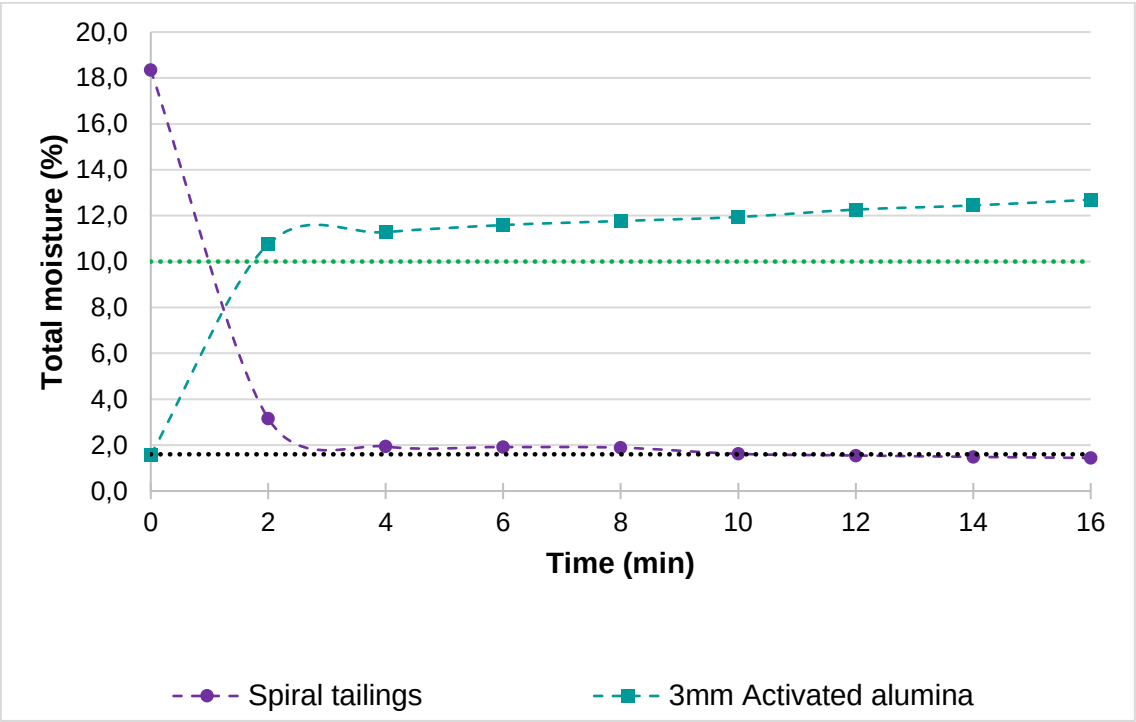

Figure 4-17 Adsorption & desorption curves of spiral tailings and 3 mm activated alumina

Figure 4-17 shows the spiral tailings' total moisture decreasing from a feed moisture content of 18.4% to 3.2% w/w within 2 minutes of dewatering at an initial desorption rate of 0.076 $g_{moisture}/g_{coal}$.min. Albeit coal tailings are not economically considered, a market specified target moisture of 10% w/w is added to the graph for helpful reference. The spiral tailings reached the target moisture within 1 minute's dewatering. After 4 minutes of dewatering, the spiral tailings' desorption rate gradually reached equilibrium and settled at a final moisture content of 1.4% w/w after 16 minutes. The spiral tailings have undergone a moisture reduction of 83% within the first

two minutes and, overall, a 92% moisture reduction after 16 minutes, which concluded that 90% of the coal's dewatering is done within the first two minutes of contact sorption.

As expected, as the moisture content of the spiral coal tailings decreased, the inverse effect can be seen on the 3mm activated alumina. The adsorbents' moisture content increased at a rate of 0.046 $g_{moisture}/g_{coal}$.min from 1.6% w/w to 10%w/w in 2 minutes, followed by a slower adsorption rate leading to a final moisture content of 12.7%w/w.

The spiral coal tailings' calorific value was not measured throughout dewatering experiments due to tailings not being economically considered. As summarised in Table 3-2, even dry-basis spiral coal tailings do not meet market specified thermal-grade or synthetic fuel-grade calorific values of 21 MJ/kg and 20 MJ/kg (Steyn & Minnit, 2010).

Very similar repeatability data was obtained for the spiral tailings as the spiral product. This was expected since the repeatability is a function of the experimental setup and not the feed material per se. Table 4-3 and Table 4-4 summarises the spiral tailings' and activated alumina's average, standard deviation, and relative experimental error of its repeated experimental drying using 3 mm activated alumina in a 2:1 adsorbent-to-coal mass ratio. These low standard deviations and relative experimental errors for the spiral tailings' moisture contents indicate reliable experimental data.

Table 4-3 Standard deviation and relative experimental error for spiral tailings' moistures

Time (min)	**Average (% w/w)**	**Standard deviation (% w/w)**	**Relative experimental error (%)**
0 (Feed)	18.35	0.11	0.36
16 (Final)	1.44	0.10	11.83

Table 4-4 Standard deviation and relative experimental error of 3 mm activated alumina used to dry spiral tailings

Time (min)	**Average (% w/w)**	**Standard deviation (% w/w)**	**Relative experimental error (%)**
0 (Feed)	1.57	0.08	3.21
16 (Final)	12.7	0.14	2.00

4.3.2 Effect of adsorbent-to-coal mass ratio

Section 4.2.2 already discussed the significance of adsorbent-to-coal mass ratios and their relation to contact surface areas between the coal particles and the adsorbents. The hypothesis in Section 4.2.2 was tested and proven for the spiral product. This section investigates the hypothesis for spiral coal tailings. The effect of various adsorbent-to-coal mass ratios on spiral tailings' desorption performance was investigated using adsorbent-to-coal mass ratios of 2:1, 1:1, and 0.5:1.

Figure 4-18 shows the desorption curves of spiral tailings dewatered by 3 mm activated alumina in 2:1, 1:1 and 0.5:1 adsorbent-to-coal mass ratios. The 3 mm adsorbent, used in all three adsorbent-to-coal mass ratios, managed to dewater the spiral tailings sufficiently to below 10% w/w moisture. However, noteworthy differences in initial desorption rates and final coal moisture contents existed for the various ratios. The various ratios' curves followed almost parallel paths but with varying desorption rates and final coal moisture contents.

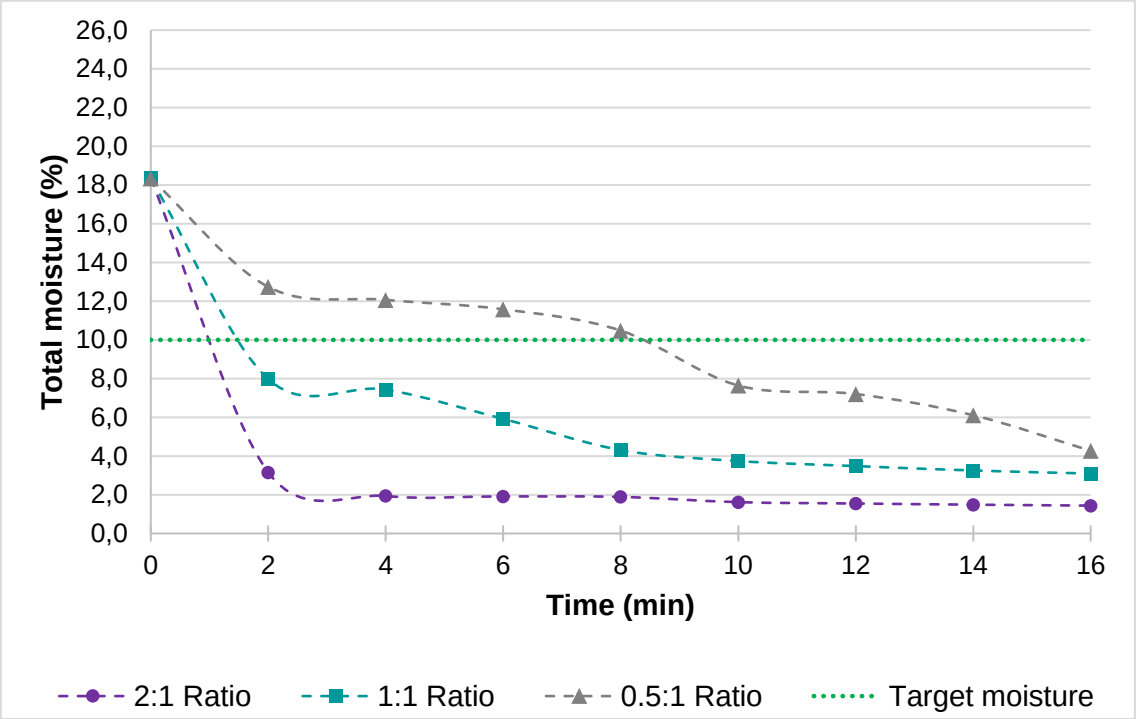

Figure 4-18 Desorption curves of spiral tailings using 3 mm activated alumina in various adsorbent-to-coal mass ratios

Figure 4-18 shows that after two minutes' dewatering, the 2:1 adsorbent-to-coal mass ratio delivered a 3.2% w/w spiral tailings moisture content, followed by 8.0% and 12.7% w/w respectively by the 1:1 and 0.5:1 adsorbent-to-coal mass ratios. The desorption rates decreased after two minutes, where the 2:1 adsorbent-to-coal mass ratio's desorption rate decreased the fastest, followed by the 1:1 ratio and the 0.5:1 ratio, respectively.

Figure 4-18 shows that the various ratios' curves settled at different final spiral tailings moisture contents of 1.4%, 3.1%, and 4.3% w/w, for the 2:1, 1:1, and 0.5:1 adsorbent-to-coal mass ratios, respectively. The 2:1 adsorbent-to-coal mass ratio delivered a 92% moisture reduction in spiral coal tailings after 16 minutes, followed by 83% and 77% moisture reductions, respectively, by the 1:1 and 0.5:1 adsorbent-to-coal mass ratios.

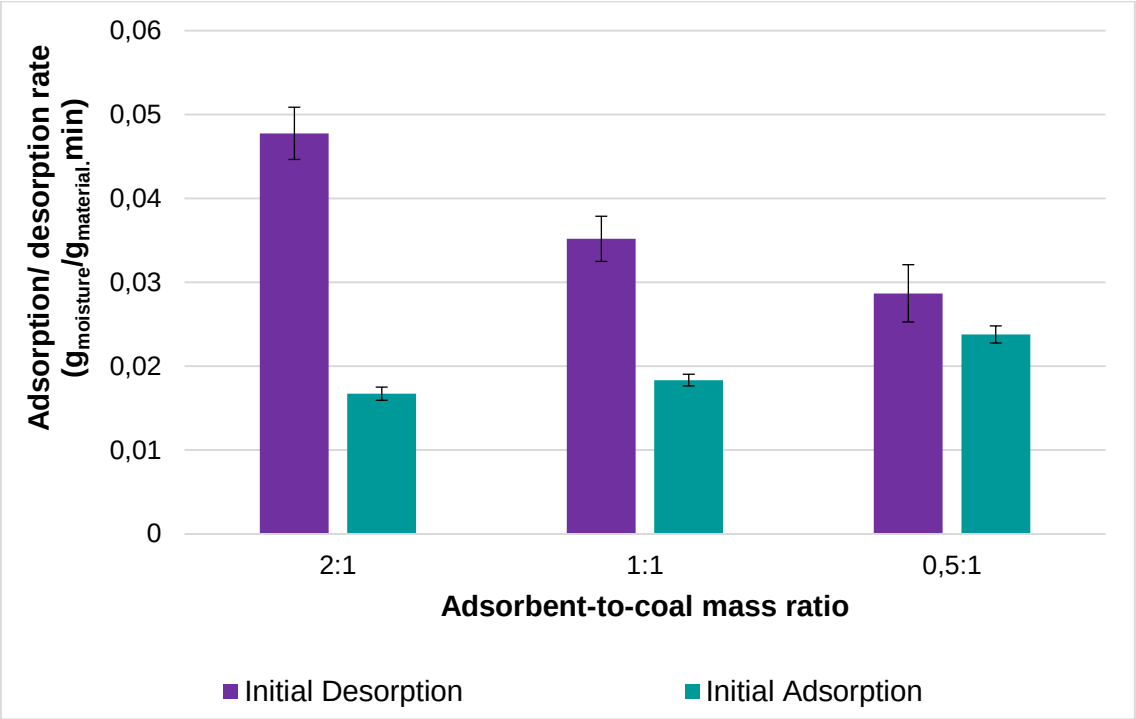

Figure 4-19 Initial adsorption/ desorption rates of 5 mm activated alumina and spiral tailings

From Figure 4-19, the spiral tailings were initially desorbed at 0.048 $g_{moisture}/g_{coal}$.min using the 2:1 ratio followed by initial desorption rates of 0.035 and 0.029 $g_{moisture}/g_{coal}$.min for the 1:1 and 0.5:1 adsorbent-to-coal mass ratios, which shows an apparent decrease in desorption rate as the adsorbent-to-coal mass ratio decreased. The 3 mm activated alumina had an initial adsorption rate of 0.017 $g_{moisture}/g_{ads}$.min for the 2:1 ratio followed by adsorption rates of 0.018 and 0.024 $g_{moisture}/g_{ads}$.min. For spiral tailings, smaller increments existed between the various ratio's adsorption rates than the desorption rates, but still, conclude the effect of the adsorbent-to-coal mass ratio on coal's dewatering performance being directly proportional to each other.

From this section, the conclusion can be drawn that the adsorbent-to-coal mass ratio, using 3 mm and 5 mm activated alumina to dry spiral tailings coal, is directly proportional to its drying performance. Higher adsorbent-to-coal mass ratios bring about better drying performances, emphasising desorption rates more than final coal moisture.

4.3.3 Effect of adsorbent particle size

To understand the part that adsorbent particle size plays in dewatering performance, this section discusses spiral tailings' dewatering using 3 mm, and 5 mm activated alumina. Figure 4-20 represents the desorption curves of spiral tailings dewatered by 3 mm and 5 mm activated alumina in a 2:1 adsorbent-to-coal mass ratio. In the figure, both adsorbent particles sizes dewater the spiral tailings sufficiently to below target moisture. A definite relationship is seen between the adsorbent particle size used and the dewatering performance of the coal when primarily considering desorption rates and, to a smaller extent, final coal moisture contents.

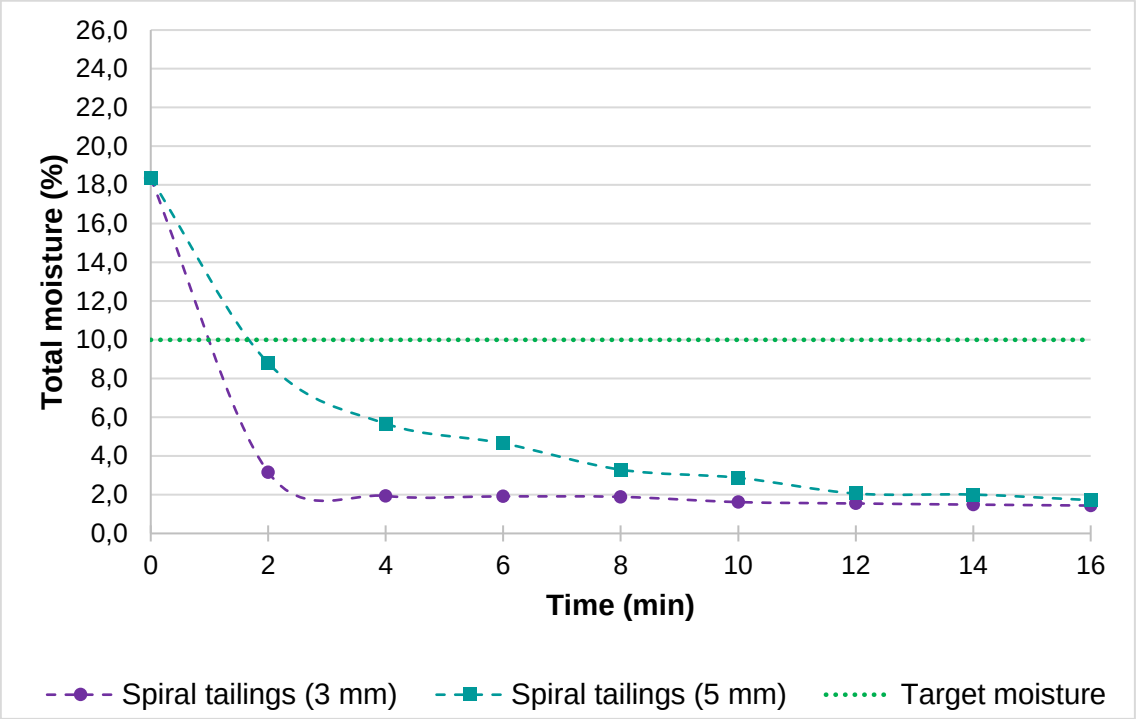

Figure 4-20 Desorption curves of spiral tailings using 3 mm and 5 mm activated alumina

In Figure 4-20, the desorption curve of the 3 mm adsorbent shows faster dewatering rates than the 5 mm adsorbent desorption curve. After two minutes, the 3 mm adsorbent achieved a spiral tailings moisture content of 3.2% w/w compared to 8.8% w/w achieved by the 5 mm adsorbent. After the initial desorption stage, the 3 mm adsorbent's desorption rate decreased faster than the 5 mm adsorbent, settling at a final coal moisture content of 1.4% w/w, while the 5 mm adsorbent achieved a final coal moisture content of 1.7% w/w.

These final moisture contents conclude that the 3 mm adsorbent delivered a 92% moisture reduction while the 5 mm delivered a 91% moisture reduction, which shows an insignificant difference. For spiral tailings, the effect of adsorbent particle size on dewatering performance is only apparent when considering the initial and overall desorption rates. After two minutes, the 3 mm adsorbent delivered an 83% moisture reduction compared to 52% for the 5 mm.

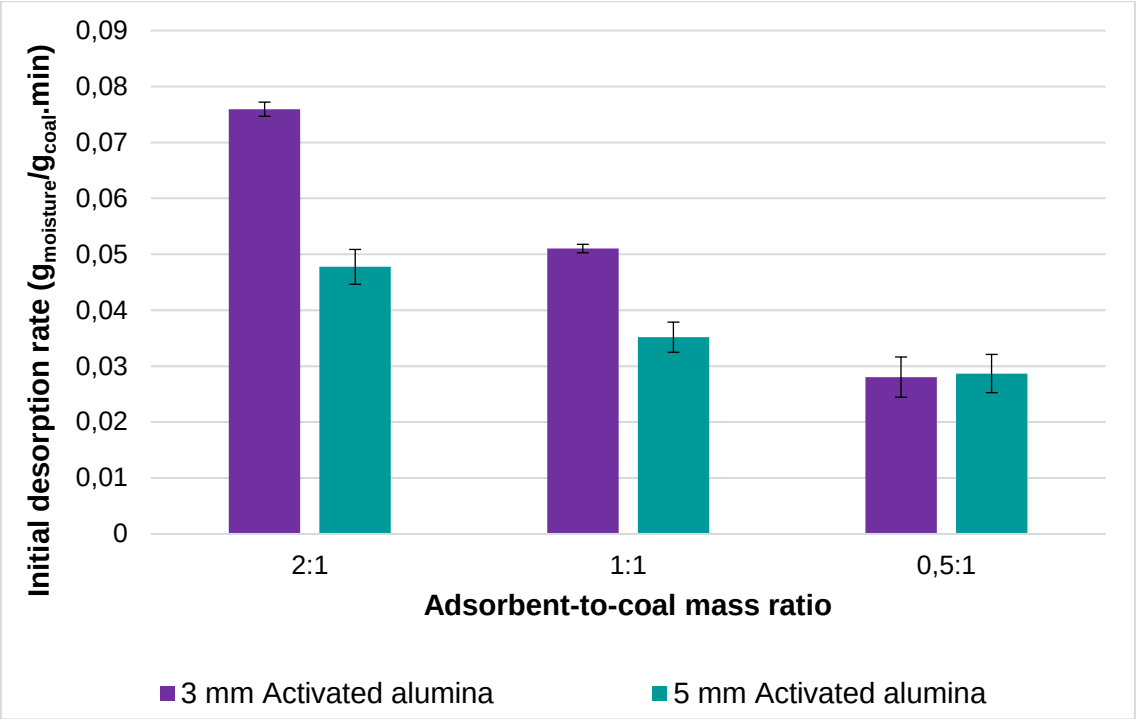

Figure 4-21 Initial desorption rates of spiral tailings dewatered by 3 mm and 5 mm activated alumina

Figure 4-21 shows the initial desorption rates of spiral tailings dewatered by 3 mm and 5 mm activated alumina in various adsorbent-to-coal mass ratios. From the figure, a clear relationship exists between adsorbent particle size and drying performance, except for the 0.5:1 adsorbent-to-coal mass ratio. For the 2:1 and 1:1 adsorbent-to-coal mass ratios, the 3 mm adsorbent outperformed the 5 mm adsorbent by 58% and 46%. The performance of the different adsorbent sizes did not differ significantly when used in a 0.5:1 ratio. With the initial desorption rates taken into account, the 3 mm adsorbent outperformed the 5 mm adsorbent by an overall average of 52%.

In conclusion, a noticeable relationship exists between adsorbent particle size and its dewatering performance when considering initial and overall desorption rates. The relationship between the adsorbent particle size and its dewatering performance can be extinguished to a lesser extent when considering the final coal moisture contents. Both particle sizes managed to dewater the spiral tailings sufficiently. When considering adsorbents in bulk, an adsorbent's particle size is inversely proportional to its dewatering performance. Therefore, the hypothesis mentioned at the start of this section again holds true. Smaller adsorbent particle sizes deliver better dewatering performance than larger adsorbent particle sizes.

4.3.4 Effect of adsorbent state

The significance of adsorbents being an expensive material to procure and the importance of their reuse and regeneration viability has already been discussed in Section 4.2.4. The practicality of regeneration and reuse of the adsorbents used on spiral coal tailings was investigated where adsorbent state refers to whether an adsorbent is new, spent, or regenerated.

In this section, the use of spent activated alumina, with and without regeneration, to dewater spiral tailings coal is discussed. A comparison is drawn between the drying performances of new, spent, and regenerated adsorbents. The regeneration process is discussed in further detail in Chapter 6. As in Section 4.2.4, the two different adsorbent sizes were used for three consecutive cycles of 10 minutes each without regeneration.

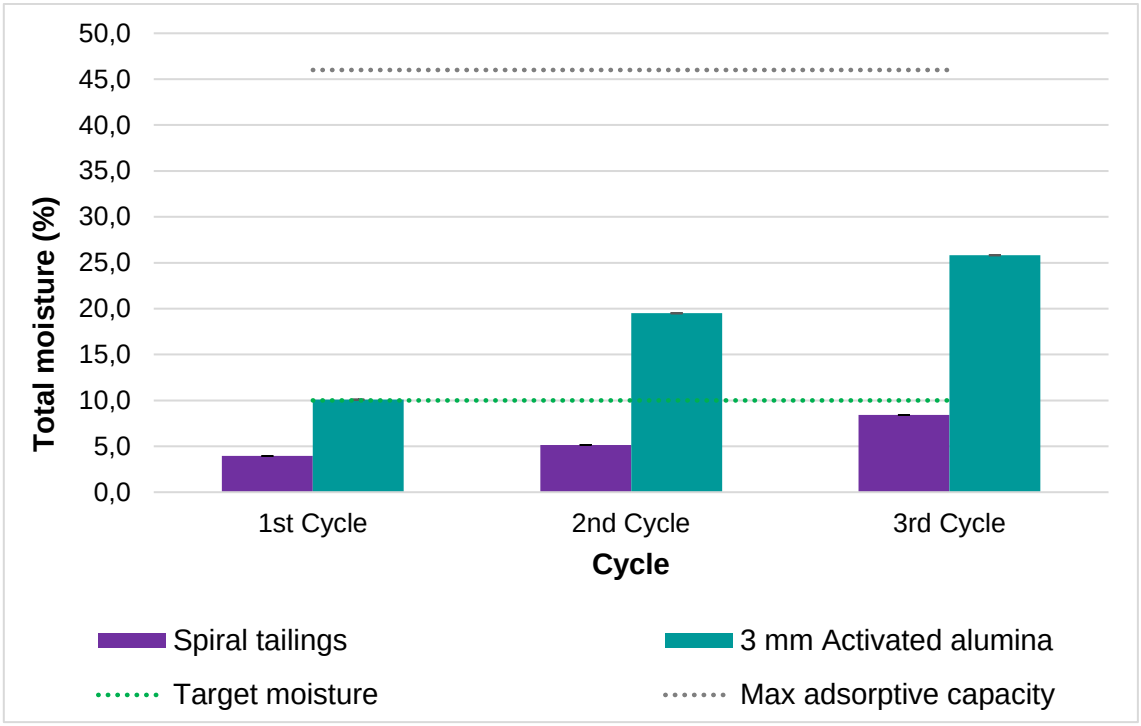

Figure 4-22 Spiral tailings and spent 3 mm activated alumina moisture after 10 minutes

Figure 4-22 shows the spiral tailings' and spent 3 mm activated alumina moisture contents after 10 minutes of dewatering using fresh (first cycle) and spent (the second and third cycle) adsorbents in a 1:1 adsorbent-to-coal mass ratio. The spent 3 mm activated alumina, when used for up to three cycles in a 1:1 adsorbent-to-coal mass ratio, dewatered the coal to below target moisture. The fresh 3 mm activated alumina resulted in a coal moisture content of 3.9% w/w, while the spent adsorbents created 5.2% and 8.4% w/w moisture contents for the second and third cycle of use.

As expected, Figure 4-22 shows a decrease in drying performance as the adsorbent's cycle of use increases. The drying performance from fresh adsorbents decreased by 9% to the 2nd cycle

of use and 24% more by the 3rd cycle. The 3 mm activated alumina's drying performance decreased overall by 31% from the first to the third cycle. The adsorbents' moisture load increased steadily as the cycle of use increased. The adsorbent's moisture content increased from 10.1% w/w, after the 1st cycle, to 19.5% w/w after the 2nd cycle and increased further to 25.8% w/w after the 3rd cycle.

Figure 4-22 also showed that the 3 mm adsorbent did not reach its maximum pure water adsorptive capacity of 46% w/w for any of the cycles of use, meaning it did not reach full saturation. This unsaturation means that the adsorbents may have had the affinity to adsorb more moisture in the consecutive 4th and 5th cycles of use or as mentioned in Section 4.2.4, competing capillary forces between the coal and adsorbents may play a role or capillary pore blinding.

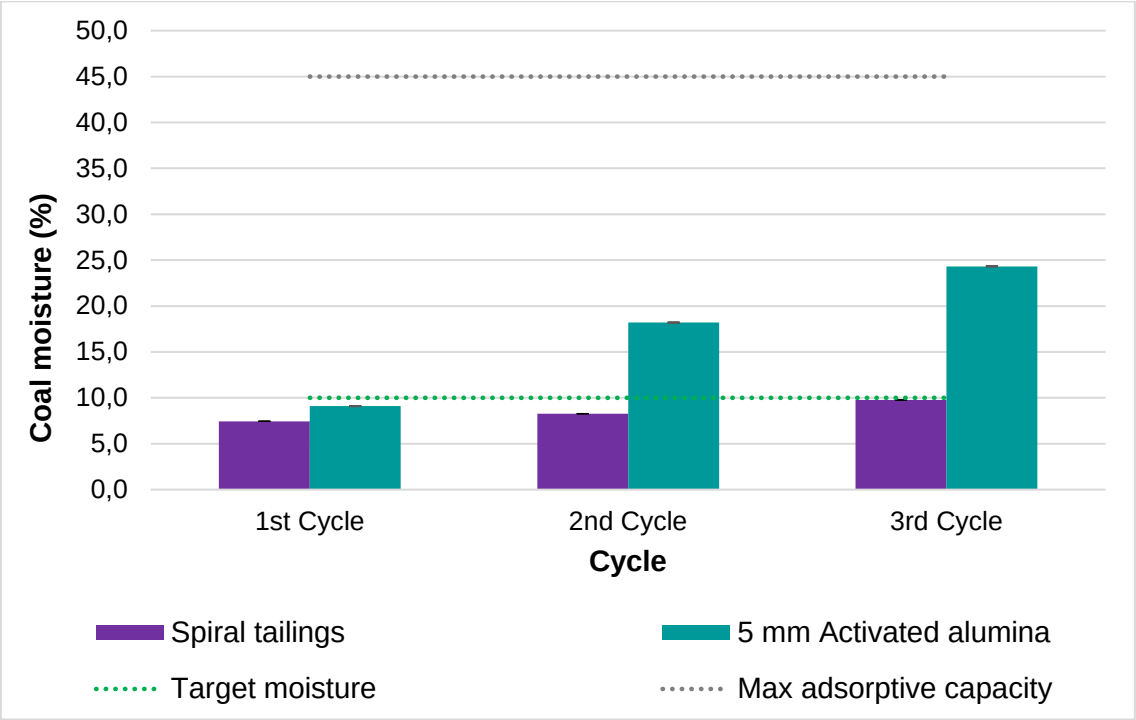

Figure 4-23 Spiral tailings and spent 5 mm activated alumina moisture after 10 minutes

Figure 4-23 shows the moisture contents of spiral tailings and spent 5 mm activated alumina used consecutively. The same trends seen with the 3 mm adsorbent exist for the 5 mm adsorbent. The spent 5 mm adsorbent was able to dry the coal to below 10% w/w. Unsaturation of the adsorbents was observed again.

The reuse of activated alumina, without regeneration, discussed above concluded that although it brought about sufficient dewatering up until the third consecutive use, the need would still exist to regenerate the adsorbents.

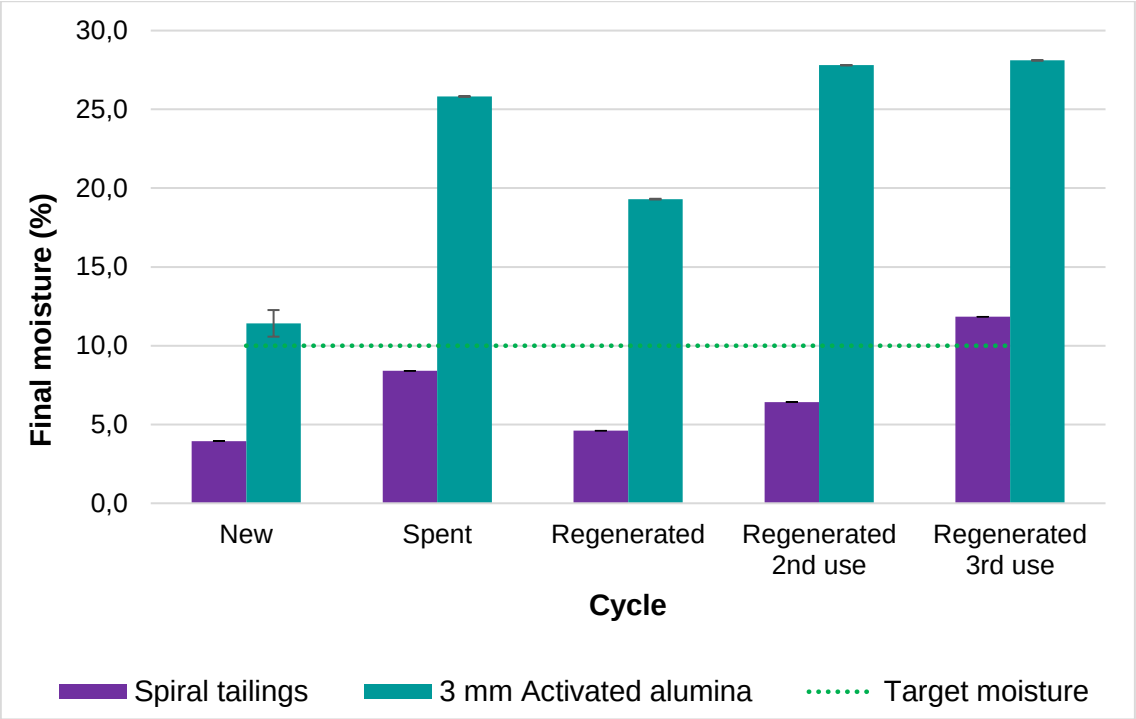

Figure 4-24 Spiral tailings moisture after 10 minutes using new, regenerated & spent 3 mm activated alumina

Figure 4-24 shows the spiral tailings' and adsorbents' final moisture contents using new, spent, and regenerated 3 mm activated alumina in a 1:1 adsorbent-to-coal mass ratio. The regenerated adsorbents were used two more times consecutively, without regenerating it between cycles resulting in the 4th and 5th column pairs seen in the Figure.

A clear difference in dewatering performance is observed between the five cycles. As anticipated, the regenerated adsorbent performed better than the spent adsorbent, and unsurprisingly, weaker than the fresh adsorbent.

The regenerated adsorbent produced a spiral tailings moisture content within target moisture of 4.6% w/w, equating to a 28% improvement over the spent adsorbent and a marginal 5% weaker performance than the fresh adsorbent. Overall, the regenerated adsorbent achieved a 75% moisture reduction in coal, compared to a 54% moisture reduction for the spent adsorbent and a 79% moisture reduction in coal for the fresh adsorbent.

Until the second cycle of use, the 3 mm regenerated adsorbent managed to dewater the spiral tailings within target moisture to 6.4% w/w, delivering even better dewatering performance than the spent adsorbent. However, when used for the third time, the regenerated adsorbent did not achieve target moisture and delivered a spiral tailings moisture content of 11.8% w/w.

Figure 4-24 shows a steady increase from 19.3% to 27.8% w/w in adsorbent moisture load was realised between the regenerated cycle and the regenerated second use cycle, which explains the sufficient dewatering of coal mentioned above. Nevertheless, from the second to the third

cycle, insignificant increases in moisture load occurred, suggesting that the adsorbents had meagre affinities left for moisture adsorption and were due for another regeneration step.

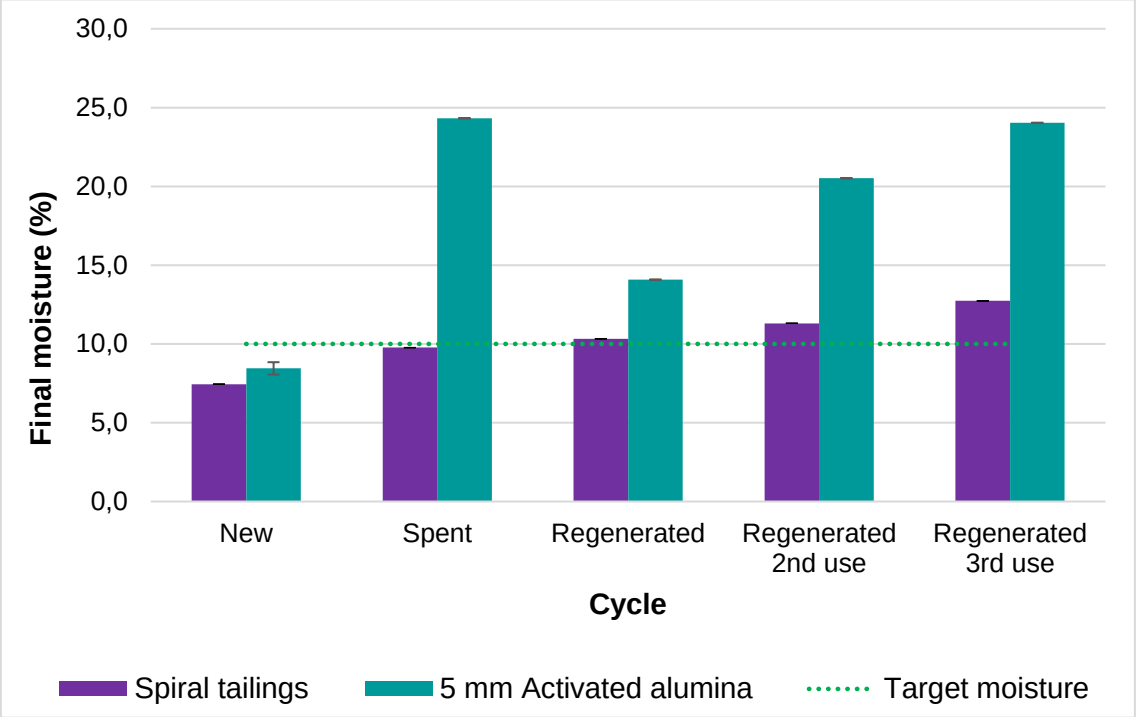

Figure 4-25 Spiral tailings moisture after 10 minutes using new, regenerated & spent 5 mm activated alumina

Figure 4-25 illustrates the spiral tailings' and adsorbents' final moisture contents using new, regenerated (used three times consecutively) and spent (3rd cycle of use) 5 mm activated alumina in a 1:1 adsorbent-to-coal mass ratio. As opposed to the 3 mm adsorbent, a less distinct difference in dewatering performance is observed between the five cycles. Contrary to the 3 mm adsorbent results, the regenerated 5 mm adsorbent performed slightly weaker than the spent adsorbent, and as expected, weaker than the fresh adsorbent.

The regenerated 5 mm activated alumina produced a bordering spiral tailings moisture content of 10.3% w/w, relating to no improvement over the spent adsorbent and a substantial 26% weaker performance than the fresh adsorbent. The regenerated 5 mm adsorbents caused a 44% moisture reduction in coal, compared to 47% moisture reduction for the spent adsorbent and 60% moisture reduction for the fresh adsorbents. None of the additional regenerated adsorbent cycles achieved target moistures, achieving coal moisture contents of 11.3% and 12.7% w/w, respectively.

Figure 4-25 shows noticeable increases in adsorbent moisture loads from 14.1% to 20.5% w/w between the regenerated cycle and the regenerated second use cycle and from 20.5% to 24.0% w/w between the second and third cycle of use. The steady increases in adsorbent moisture loads imply that it still had affinities for moisture adsorption but struggled to achieve

target moisture contents, suggesting that another regeneration step might have helped achieve the necessary coal drying.

In conclusion to this section, a visible relationship exists between the different adsorbent states (new, spent or regenerated) and their respective drying performances on spiral tailings. For the 3 mm activated alumina, fresh adsorbents delivered, understandably, the best drying performance, followed closely by its regenerated version, which in turn was a remarkable improvement to its spent version. For the 5 mm activated alumina, the fresh adsorbents also delivered the best drying performance, but contrary to the 3 mm adsorbent, the regenerated 5 mm adsorbent had little to no improvement in drying performance compared to its spent version.

The reuse of adsorbents, without regeneration, to dewater spiral tailings was viable but with limitations, due to the adsorbent's capillary pore blinding and, naturally, the eventual saturation of the adsorbents. Competing capillary forces between the coal and adsorbents may also have played a role after a certain extent of adsorbent reuse. Even though adsorbent saturation was not observed in the results discussed above, it is an inevitable limitation, provided the adsorbent's capillary pores are not blinded or trapped.

4.4 Spiral product vs tailings

4.4.1 General desorption curves

This section compares the desorption curves of spiral product and spiral tailings to understand how different quality coals' dewatering would behave. Coal products predominantly consist of carbon, whereas coal tailings predominantly contain mineral matter. The difference in composition between product and tailings may play a role in how the different coals retain water and are dewatered. A hypothetical assumption exists that the higher clay and mineral matter found in coal tailings will cause the coal to retain water stronger than the carbon-containing coal product. This section investigated this statement.

Figure 4-26 shows the desorption curves of spiral product and tailings both being dried with new 3 mm activated alumina used in a 2:1 adsorbent-to-coal mass ratio. Both coals' desorption curves followed the same trend with minute differences in moisture contents. The spiral product and tailings started with initial moisture contents of 18,0% and 18.4% w/w, respectively. Within two minutes, the product and tailings were dewatered at similar initial desorption rates of 0.072 and 0.076 $g_{moisture}/g_{coal}$.min, respectively. Halfway through drying, moisture contents of 2.1% and 1.9% w/w were recorded for the product and tailings, respectively. After 16 minutes, the product and tailings experienced 91% and 92% moisture reductions, respectively. Spiral product and tailings followed very similar dewatering behaviours. However, the spiral tailings started with a slightly higher initial moisture content and ended with a slightly lower final moisture content than the spiral product, showing a slightly greater rate of desorption.

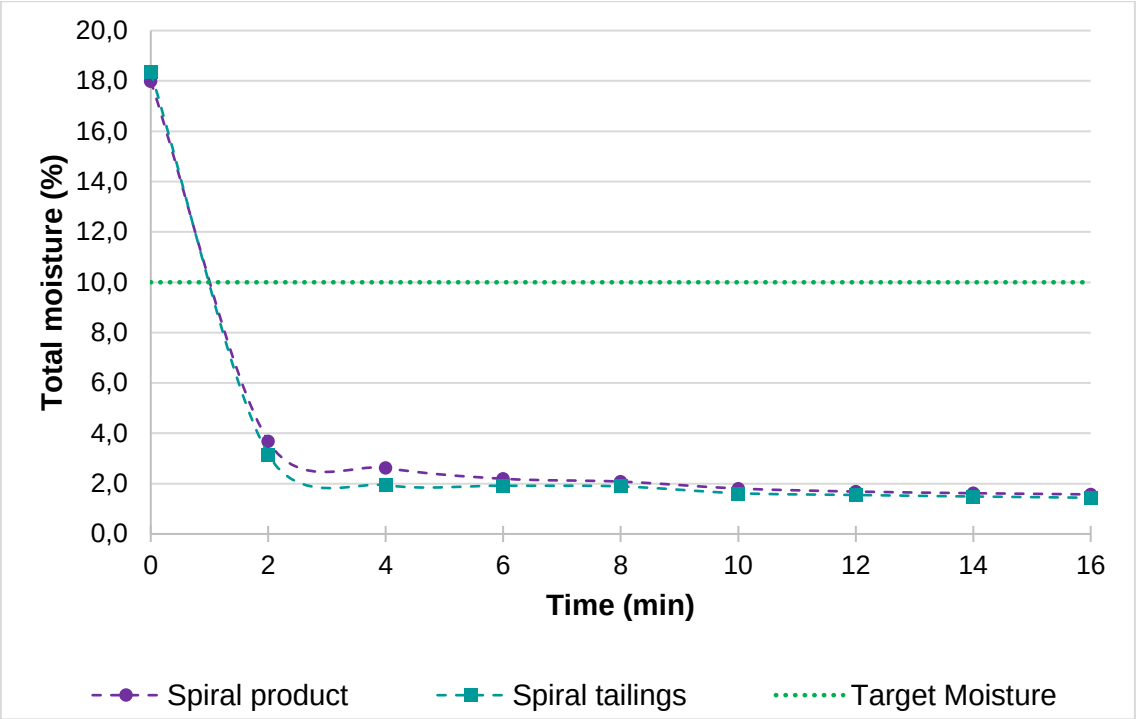

Figure 4-26 Spiral product vs tailings' desorption curves

4.4.2 Effect of adsorbent-to-coal mass ratio

This section briefly discusses the extent of the effects that various adsorbent-to-coal mass ratios may have on the dewatering performances of the spiral product and spiral tailings coal. Figure 4-27 compares the moisture reductions carried out on the spiral product and tailings using new 3 mm activated alumina in various adsorbent-to-coal mass ratios. Moisture reduction refers to the moisture removed as a percentage of the initial coal moisture content.

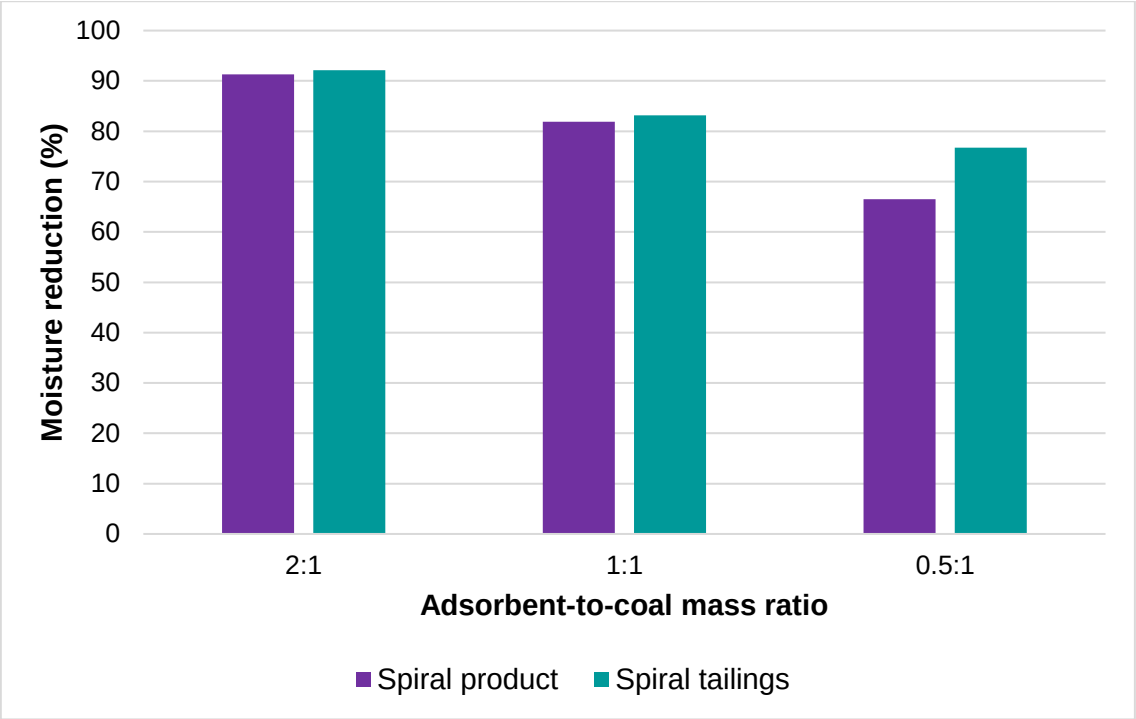

Figure 4-27 Moisture reductions of spiral product vs tailings using various adsorbent-to-coal mass ratios

In Figure 4-27, the spiral tailings experienced marginally better moisture reductions than the spiral product. For the spiral product, the 2:1 adsorbent-to-coal mass ratio was an 11% improvement over the 1:1 ratio, which in turn, was a 24% improvement over the 0.5:1 ratio. For the spiral tailings, the 2:1 ratio was an 11% improvement over the 1:1 ratio, which was an 8% improvement on the 0.5:1 ratio. From these results, it can be concluded that for the 2:1 and 1:1 ratios, the product and tailings' behaved similarly in terms of dewatering, and the differences in their moisture reduction only became evident at an adsorbent-to-coal mass ratio of 0.5:1.

4.4.3 Effect of adsorbent particle size

This section briefly discusses the extent of adsorbent particle size's effects on the dewatering of spiral product and spiral tailings. Figure 4-28 compares the moisture reductions of spiral product and tailings using new 3 mm and 5 mm activated alumina in a 2:1 adsorbent-to-coal mass ratio.

In Figure 4-28, the spiral tailings experienced slightly better moisture reductions than the spiral product. The 3 mm adsorbent delivered 10% better dewatering for the spiral product than the 5 mm adsorbent. For the spiral tailings, the 3 mm adsorbent performed 1% better than the 5 mm adsorbent. The effect of adsorbent particle size on dewatering performance was more significant for the spiral product than the tailings.

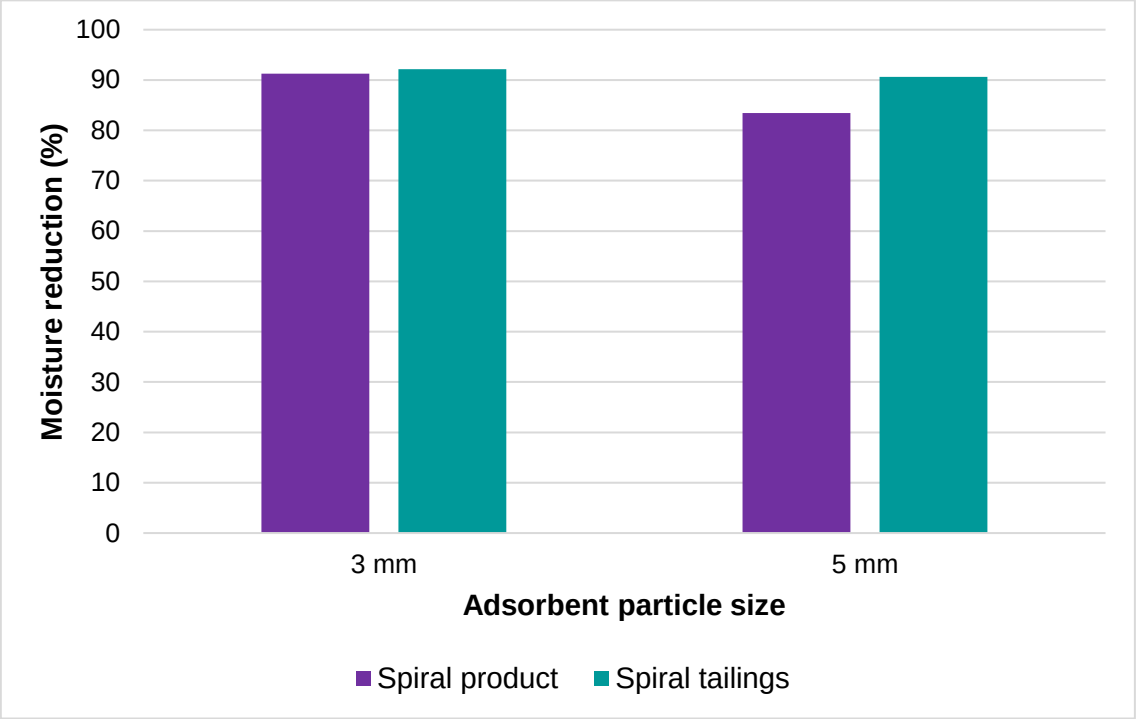

Figure 4-28 Moisture reductions of spiral product vs tailings using 3 mm and 5 mm activated alumina

4.4.4 Effect of adsorbent state

This section briefly compares the effects of the adsorbent state on the spiral product and tailings' dewatering performances. Figure 4-29 shows the spiral product and tailings' moisture reductions using new, spent and regenerated 3 mm activated alumina in a 1:1 adsorbent-to-coal mass ratio for 10 minutes.

In Figure 4-29, the spiral tailings experienced higher moisture reductions than the spiral product when using new and regenerated adsorbents. For the spiral product, the spent adsorbent performed 18% weaker than the new adsorbent, while the regenerated adsorbent had a 2% improvement in dewatering over its spent version. The spent adsorbent performed 33% weaker than the new adsorbent for the spiral tailings, while its regenerated version had a 39% improvement over its spent version. The different adsorbent states' effect on dewatering was more apparent for the spiral tailings than the spiral product.

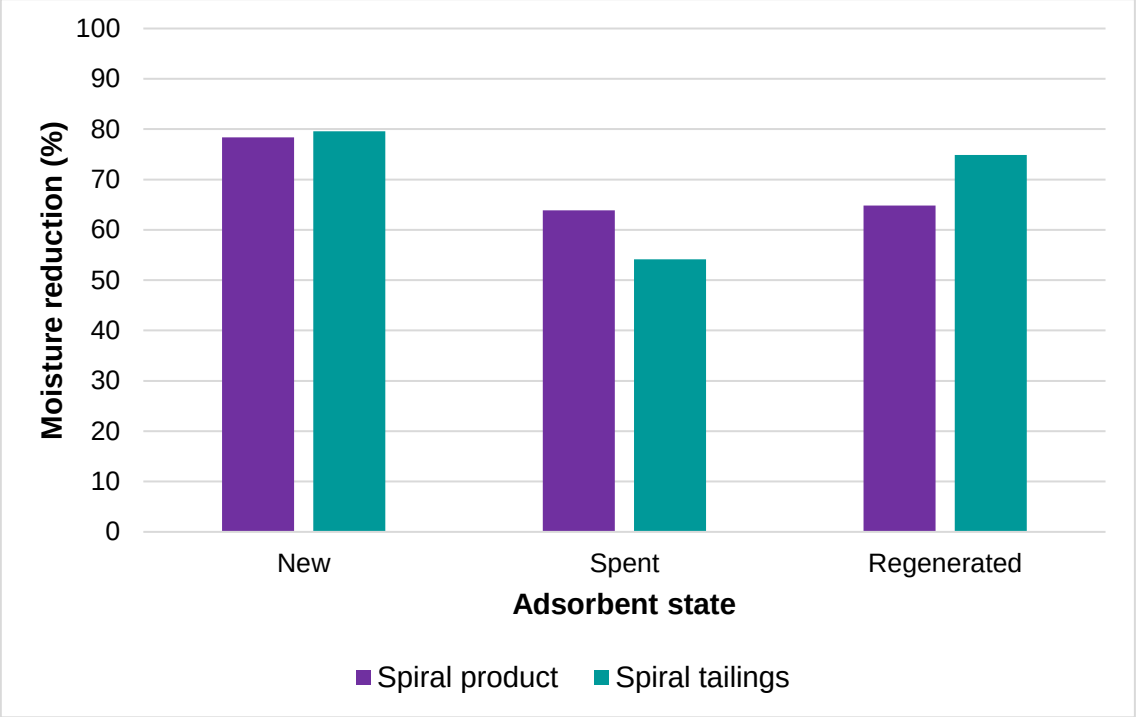

Figure 4-29 Moisture reductions of spiral product vs tailings using new, spent and regenerated activated alumina

In conclusion, although spiral product and tailings' dewatering behaved very similar to one another, spiral tailings were dewatered easier, experiencing slightly higher moisture reductions for all the scenarios above and ending with lower final moisture contents than the spiral product.

The hypothetical assumption that coal tailings, with higher mineral content and clay, would retain water stronger than carbon-containing coal product and thus having dewatering difficulties is proven wrong in this section, considering the results above.

4.5 Qualitative remarks

During experimental work, various unmeasurable phenomena were observed. All of these qualitative findings were photographed and will be discussed here.

4.5.1 Materials handling

During experimental procedures, it was noted that proper materials handling was imperative to obtain satisfactory dewatering results. The spiral coal had some affinity for caking due to the moisture retained between the coal particles. Materials handling, in this case, refers to the special care taken to sufficiently break these cakes. The looser the individual coal particles are, the better the dewatering will occur since more surface contact area is available. It is suggested to use a high-speed pugmill with an open bottom in an industrial setting to break these filter cakes, as much as possible, upstream from the cylindrical vessels.

Figure 4-30 shows a worst-case scenario where the spiral coal caked against the cylindrical vessels' inner wall, during the dewatering process. This will naturally lead to poor dewatering results, since the adsorbents will not mix with the coal, thus creating lower between the materials. This scenario can be avoided, primarily by breaking the cakes before mixing them with adsorbents and secondarily, through specially designed cylindrical vessels. Details of the suggested designs are discussed in Section 4.5.3.

Figure 4-30 Spiral coal caking against a cylindrical vessel’s inner wall

4.5.2 Adsorbent's capillary pore blinding

During experimental work, it was noted that the adsorbents' surfaces became dirtier and darker as they were used, due to the coal dust becoming entrapped on the surfaces of the adsorbents. It was also noted that the adsorbents' performance decreased as their usage increased. Figure 4-31 shows photographs in which it can be seen how the adsorbents' surfaces were coated with coal dust as they were used over time.

Figure 4-31 Coal dust entrapment on the adsorbents' surfaces as usage progresses

The connection was made that this coal dust would blind the adsorbents' capillary pores, which will inhibit their adsorption performances. Sections 4.2.4 and 4.3.4 discussed how spent adsorbents had weaker performances than new adsorbents. Figure 4-32 and Figure 4-33 compare the SEM scans, at 1000x and 5000x magnifications, of new and spent activated alumina used for dewatering spiral product coal.

In Figure 4-32, foreign particles (coal dust) can be seen on the spent adsorbent's surface compared to the new adsorbent's surface. In Figure 4-33, these foreign particles can be seen magnified, these particles appear to block openings (pores) on the adsorbent's surface. This closing down or blinding of the pore openings will inhibit moisture from being adsorbed.

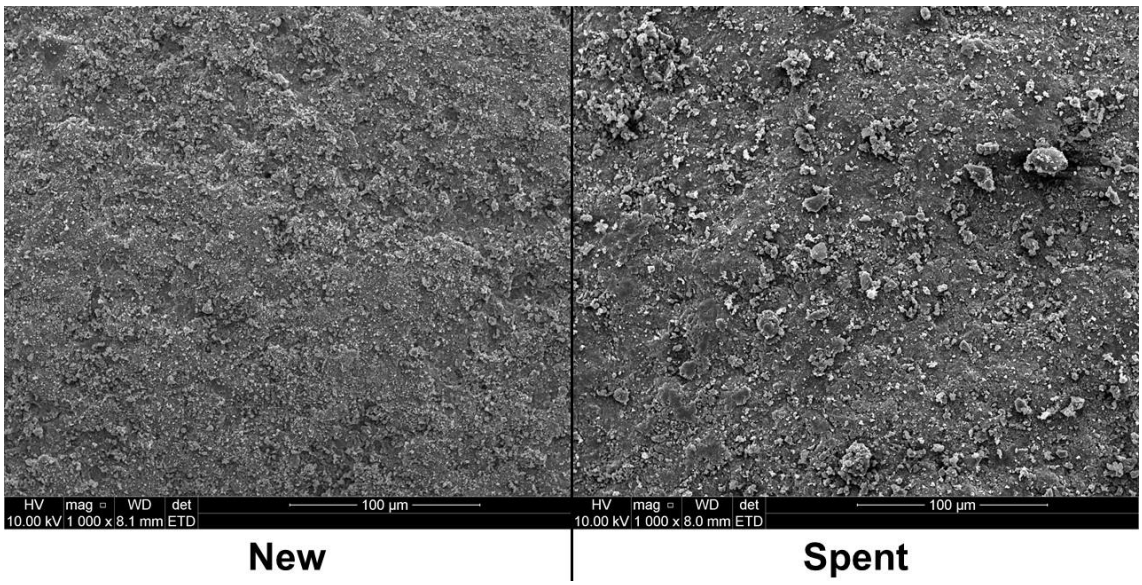

Figure 4-32 SEM scans of new and spent activated alumina used on spiral product (1000x magnified)

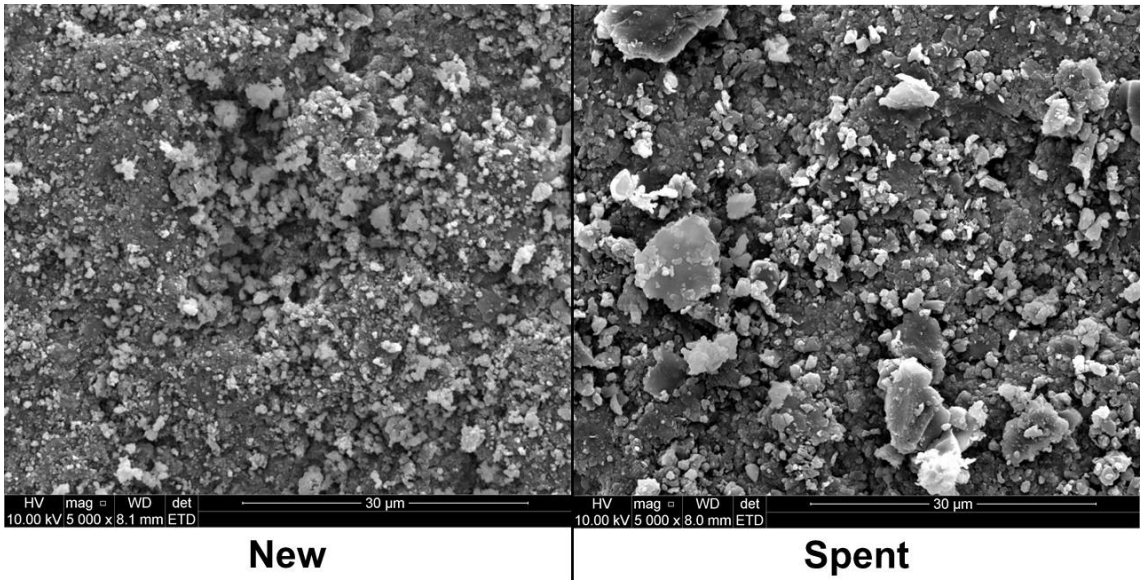

Figure 4-33 SEM scans of new and spent activated alumina used on spiral product (5000x magnified)

4.5.3 Design considerations

Sections 4.5.1 and 4.5.2 discussed phenomena and difficulties encountered during experimental procedures. This section will discuss how these phenomena and difficulties should be considered during the design of an adsorbent assisted drying plant, whether it is a pilot or industrial plant.

Regarding materials handling, it was mentioned in Section 4.5.1 that a pugmill should be installed upstream of the cylindrical vessels before the coal and adsorbents are mixed. The modified pugmill must have an open bottom so that the coal can fall through after the pugmill's rotating paddles have broken the cakes.

Figure 4-34 shows a typical pugmill that would suffice in the abovementioned application. Figure 4-35 shows a close view of the pugmill's typical paddles responsible for breaking the filter cakes.

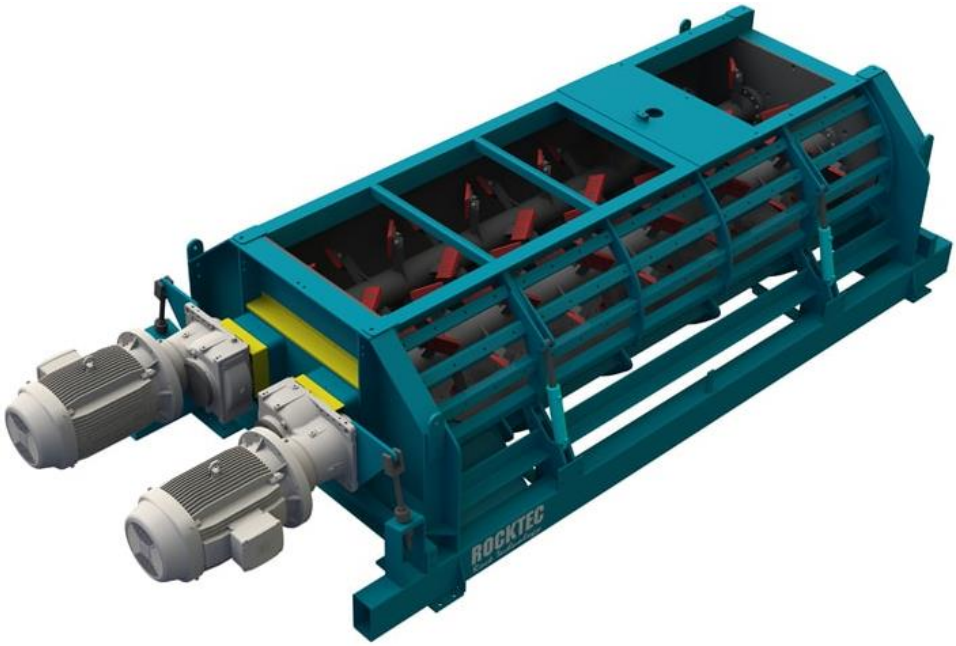

Figure 4-34 A typical pugmill, taken from (Rocktec, 2021)

Figure 4-35 A close view of the pugmill's paddles, taken from (Rocktec, 2021)

Moreover, to further aid with sufficient materials handling, specialised baffle plate design inside the cylindrical vessels will be needed. The baffle plates should ensure proper mixing of the coal and adsorbents while ensuring that the coal particles are as loose as possible without any caking occurring.

Design suggestions to overcome the capillary pore blinding are discussed in Section 6.4.4.

4.6 Conclusion

From the adsorbent assisted drying of spiral coal using activated alumina, it was concluded that spiral coal product could be dried swiftly to market specifications within two minutes of contact sorption, experiencing an overall moisture reduction of 91%. The majority of the coal's moisture reduction occurred in the first two minutes of dewatering. The spiral product also experienced a 17% increase in calorific value due to moisture reduction.

The activated alumina's drying performance, irrespective of adsorbent particle size, is directly proportional to the adsorbent-to-coal mass ratio, attributed to the higher adsorbent contact surface areas available in higher adsorbent-to-coal mass ratios.

Both the 3 mm and 5 mm activated alumina achieved successful dewatering of the spiral product. However, the activated alumina's dewatering performance is inversely proportional to its particle size, attributed to the higher contact surface area available with smaller adsorbent particles in bulk and vice versa.

The different states in which the adsorbents were had a predictable effect on drying performance, with the new adsorbents performing the best, followed closely by the regenerated adsorbents, which was a considerable improvement over the spent adsorbents. The regenerated adsorbents dewatered the spiral product to market specifications within at least 4 minutes. However, up to the fifth cycle of use, the spent adsorbents could still dry the spiral product to target moisture, suggesting that regenerated adsorbents need not be bone-dry to dewater the coal efficiently.

The spiral tailings' dewatering behaved very similarly to the spiral product's dewatering. The spiral tailings experienced the same trends as spiral product regarding the variables of adsorbent-to-coal mass ratio, adsorbent particle size and adsorbent state, with some variables' effects being slightly more prominent for the spiral product. Spent and regenerated adsorbents were able to dewater the spiral tailings sufficiently. Lastly, although very similar in dewatering behaviour, the spiral tailings experienced slightly higher moisture reductions and lower final moisture contents than the spiral product.

The main driving force for optimal drying of the coal was the contact surface area between the adsorbents and coal particles which can be altered with either adsorbent particle size or adsorbent-to-coal mass ratio. It was noted that proper materials handling is imperative to achieve satisfactory dewatering results and a phenomenon called capillary pore blinding was also observed on the adsorbents, which would inhibit their moisture adsorption.

Chapter 5 Drying of flotation coal

5.1 Introduction

In this chapter, the drying ability or desorption performance of flotation product filter cake using adsorbent assisted drying is discussed. The flotation coal product being investigated had a d_{50} particle size of 21 µm, which is an ultra-fine particle size.

As with the spiral product, activated alumina of 3 mm and 5 mm were used. In addition to the activated alumina, molecular sieves were used to dry the flotation product and draw a comparison between the two adsorbents. The experimental variables were adsorbent-to-coal mass ratios, adsorbent particle sizes and adsorbent states (new (fresh), spent, or regenerated), in an attempt to determine the main driving force for optimal desorption performance. Other means of regenerated adsorbents were also tested on flotation product coal.

The dewatering of flotation product using activated alumina as the primary adsorbent is discussed in-depth, while the dewatering using molecular sieves was approached as a secondary objective and is discussed more briefly. The desorption performances of the flotation product and the spiral product are finally compared to understand the effect that the size of the coal has on its desorption performance, as well as to determine the effects that flotation reagents would have on flotation coal's desorption performance.

As mentioned in Chapter 4, a market specified target moisture content of 10% w/w (Steyn & Minnit, 2010) was aimed at during dewatering experiments and discussing results. The moisture content referred to in the results and discussions, unless specified otherwise, is total moisture content, which, as discussed in Chapter 2, account for inherent moisture and surface moisture.

In Section 5.6, qualitative remarks of unmeasured phenomena are discussed. Qualitative remarks include difficulties, successes and keynotes experienced during experimental work.

All experimental work was conducted methodological, as described in Section 3.3, and in a laboratory kept at a constant temperature of 22°C.

5.2 Flotation product

5.2.1 General adsorption and desorption curves

Flotation beneficiated coal product's filter cake was dried using 3 mm and 5 mm activated alumina spherical beads. The flotation product's filter cake started at a total moisture content of 24.3% w/w and an inherent moisture content of 4.4% w/w. Chapter 3 discussed how the flotation product contacted the activated alumina in cylindrical vessels and was mixed in a cascading motion for 16 minutes at 50 rpm. Additional results of flotation product drying, which are not discussed here, can be found in Annexure A.3. General adsorption and desorption curves for flotation product using 3 mm fresh activated alumina in a 2:1 adsorbent-to-coal mass ratio are displayed in Figure 5-1.

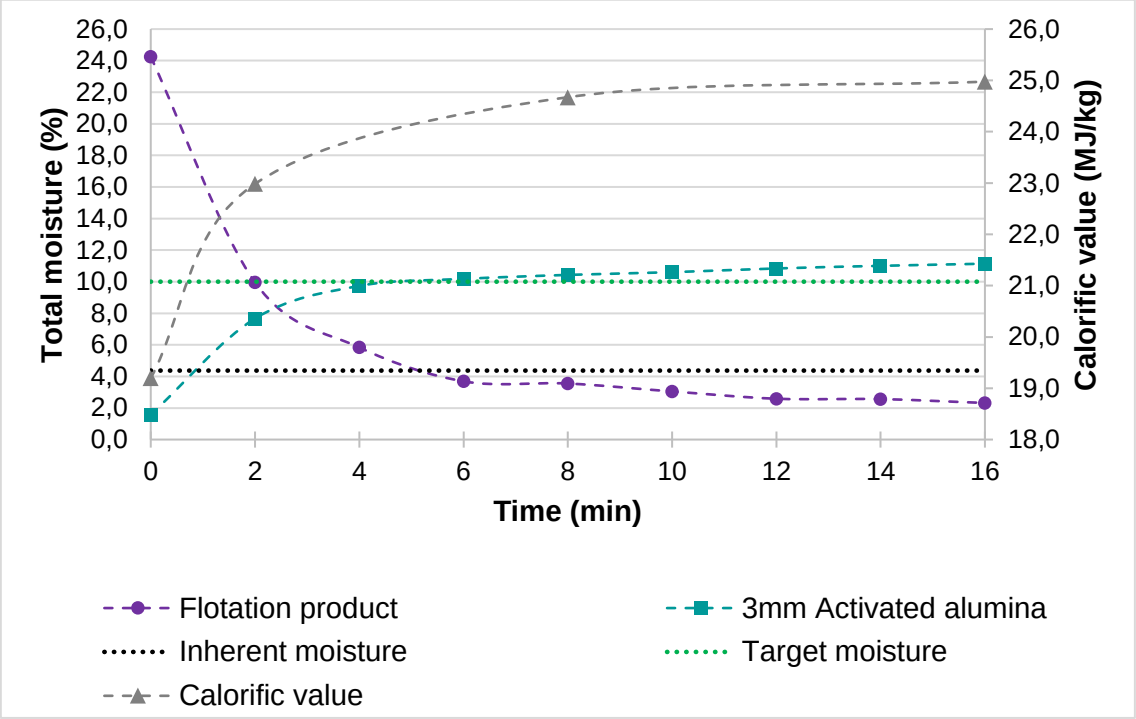

Figure 5-1 Adsorption & desorption curves of flotation product and 3 mm activated alumina

From Figure 5-1, the flotation product's moisture decreases steeply at an initial desorption rate of 0.071 $g_{moisture}/g_{coal}$.min from a feed moisture content of 24.3% to 10% w/w after 2 minutes of drying. Market specified target moisture was reached within 2 minutes, and after 5 minutes, the flotation product reached sub inherent moisture contents. The flotation product's desorption rate gradually reached equilibrium at 12 minutes, settling at a final moisture content of 2.3% w/w after 16 minutes. The flotation product reached a 59% moisture reduction in the first two minutes and an overall reduction of 91%. Almost two-thirds of the coal's dewatering was achieved within the first two minutes of contact-sorption.

The 3 mm activated alumina was fed with a packaged moisture content of 1.6% w/w and introduced to the flotation product. The 3 mm activated alumina's moisture content increased fast at an initial adsorption rate of 0.031 $g_{moisture}/g_{ads}$.min to 7.7% w/w within 2 minutes. Soon after the initial adsorption stage, the adsorption rate gradually decreased and reached a final adsorbent moisture content of 11.1% w/w. To a certain degree, the flotation product's desorption curve mirrored the adsorption curve of the 3 mm activated alumina, as would be expected from these results.

The flotation product, as received, had an initial calorific value of 19.2 MJ/ kg, which is below the market specification of 21 MJ/kg, due to its high moisture content (Steyn & Minnit, 2010). After two minutes of dewatering, the calorific value increased meaningfully by 20% to 23 MJ/ kg and overall, increased by 30% to 25 MJ/ kg after 16 minutes. Considering its moisture content and calorific value, after adsorbent assisted drying, the flotation product coal was well within market specifications, making it economically attractive.

Section 3.5 described that the experiments' reproducibility and the results' integrity were determined by conducting all experiments, with the same operating conditions, three times. The T-test, with a 90% confidence interval, was used to determine the experimental error.

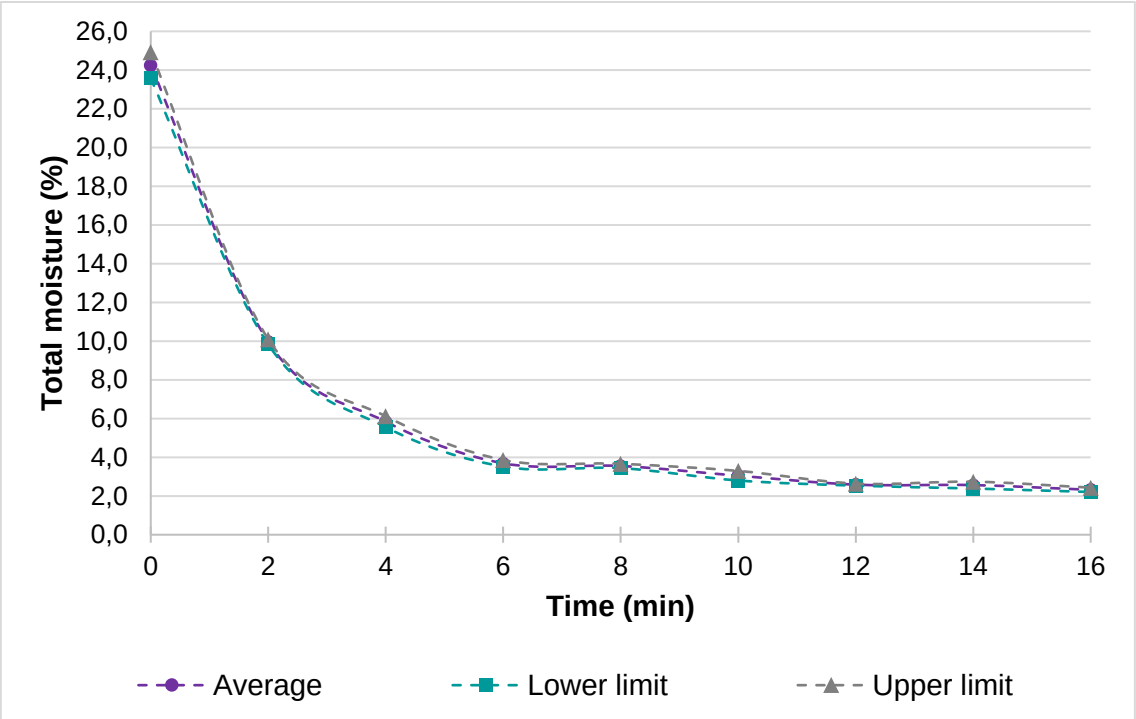

Figure 5-2 Average desorption curve of the flotation product with the standard deviation

Figure 5-2 represents the average desorption curve and the standard deviation lower and upper limit curves for flotation product dewatered with 3 mm activated alumina, used in a 2:1 adsorbent-to-coal mass ratio. The flotation product, as received, had an average initial moisture content of

24.3% w/w with a lower limit of 23.6% w/w and an upper limit of 24.9% w/w. After 16 minutes of drying, the flotation product had a final total moisture content averaging at 2.3% w/w with a lower limit of 2.2% w/w and an upper limit of 2.4% w/w.

The average, standard deviation, and relative experimental error for the experimental repeats of flotation product drying using 3 mm activated alumina in a 2:1 adsorbent-to-coal mass ratio are summarised in Table 5-1. Low standard deviations and relative experimental errors below 10% was encountered for the flotation product's respective moisture contents, which relates to reliable experimental data.

Table 5-1 Standard deviation and relative experimental error for flotation product moistures

Time (min)	Average (% w/w)	Standard deviation (% w/w)	Relative experimental error (%)
0 (Feed)	24.25	0.68	1.15
16 (Final)	2.32	0.11	8.16

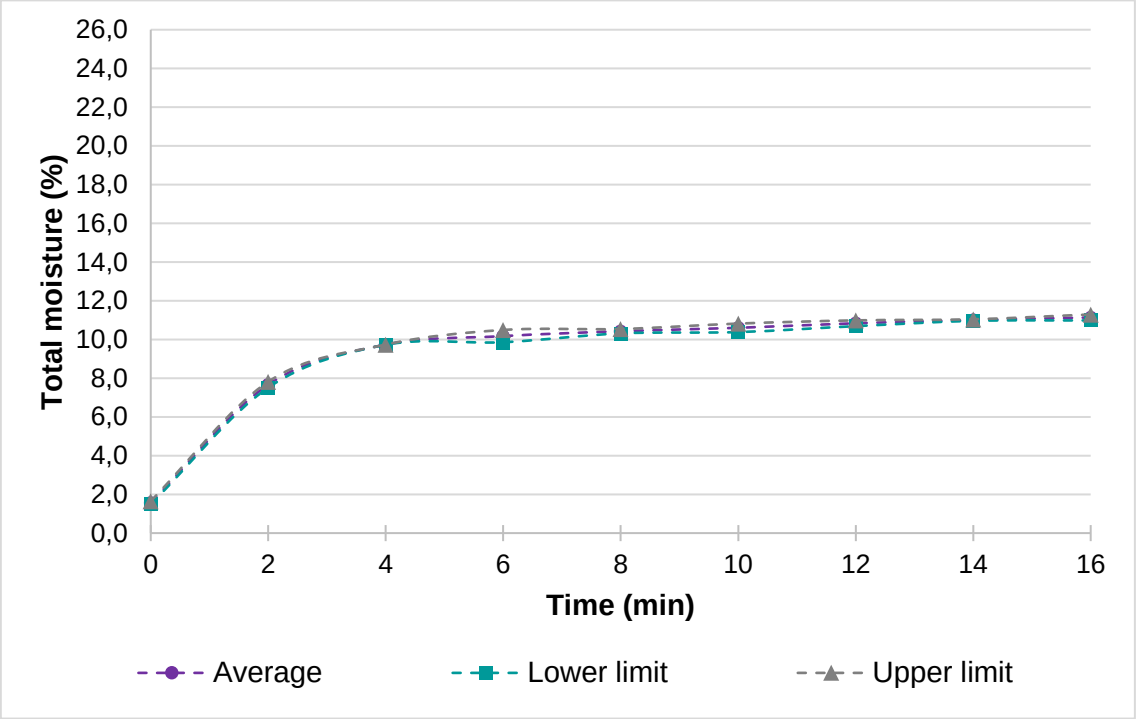

Figure 5-3 Average adsorption curve of 3 mm activated alumina used on flotation product with standard deviation

The average adsorption curve and the standard deviation lower and upper limit curves for 3 mm activated alumina used to dry flotation product in a 2:1 adsorbent-to-coal mass ratio are shown in Figure 5-3. The activated alumina was fed to the coal with an average packaged moisture content of 1.6% w/w, with a lower limit of 1.5% w/w and an upper limit of 1.7% w/w. After 16 minutes of

contact-sorption, the adsorbents reached a final average moisture content of 11.1% w/w with lower and upper limits at 11.0% and 11.3% w/w, respectively.

Table 5-2 summarises the average feed and final moisture contents, with their respective standard deviation and relative experimental error of the 3 mm activated alumina used to dry flotation product in a 2:1 adsorbent-to-coal mass ratio. The standard deviation and relative experimental error for the activated alumina's adsorption curves were marginal, relating to reliable results and repeatable experiments.

Table 5-2 Standard deviation and relative experimental error of 3 mm activated alumina used to dry flotation product

Time (min)	Average (% w/w)	Standard deviation (% w/w)	Relative experimental error (%)
0 (Feed)	1.57	0.08	3.21
16 (Final)	11.14	0.15	2.34

5.2.2 Effect of adsorbent-to-coal mass ratio

Section 4.2.2 discussed that higher adsorbent-to-coal mass ratios call for higher contact surface areas between the coal particles and the adsorbents and vice versa. This hypothesis was tested and proven for spiral product coal. In this section, the hypothesis is tested and discussed for flotation coal product.

Adsorbent-to-coal mass ratios of 2:1, 1:1, and 0.5:1 were used to comprehend the effect of various adsorbent-to-coal mass ratios on the desorption performance of flotation product.

Figure 5-4 shows the desorption curves of flotation product using 3 mm activated alumina in 2:1, 1:1 and 0.5:1 adsorbent-to-coal mass ratios. The 3 mm activated alumina, used in all three adsorbent-to-coal mass ratios, managed to dewater the flotation product well within target moisture but with noteworthy differences in initial desorption rates and final moisture contents. However, the 2:1 and 1:1 adsorbent-to-coal mass ratios differed marginally from one another concerning desorption rates and final moisture contents, which is economically appealing when considering industrial applications, with a 1:1 ratio being more economical than a 2:1 ratio. After the initial desorption stage, the various ratios' curves followed almost parallel paths but with different desorption rates and final moisture contents.

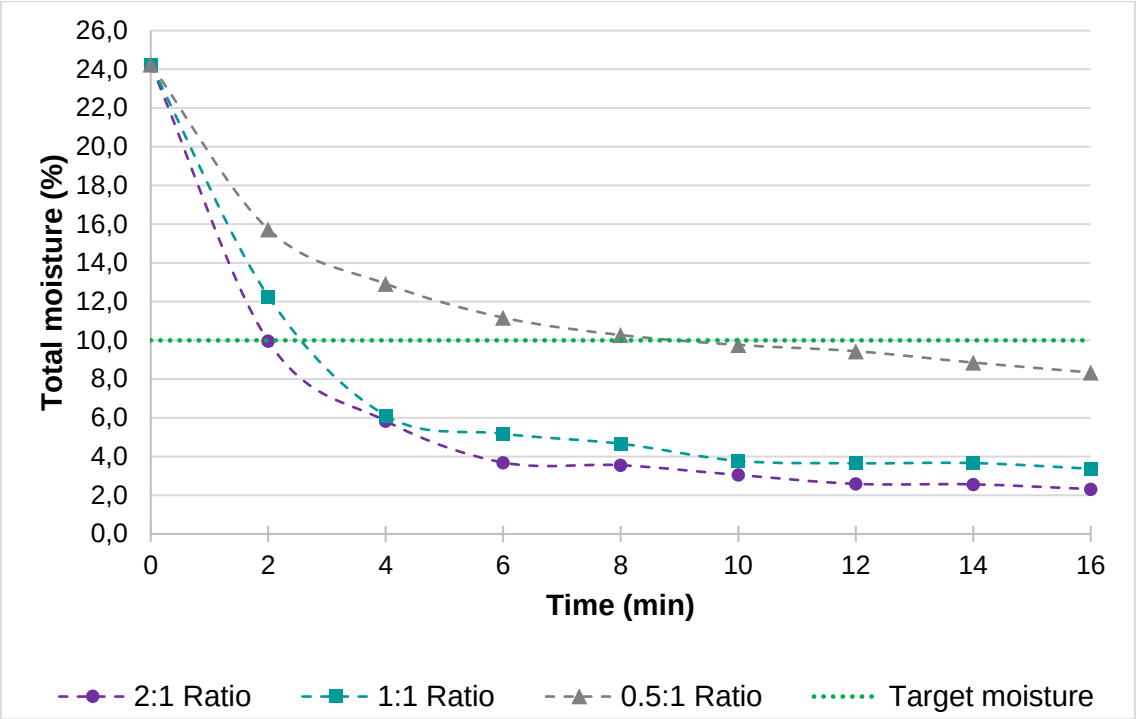

Figure 5-4 Desorption curves of flotation product using 3 mm activated alumina in various adsorbent-to-coal mass ratios

Figure 5-4 shows that within 2 minutes, the 3 mm adsorbent, used in a 2:1 adsorbent-to-coal mass ratio, caused a flotation product moisture content of 10% w/w, followed by 12.3% and 15.7% w/w respectively by the 1:1 and 0.5:1 adsorbent-to-coal mass ratios. The desorption rates gradually decreased after 2 minutes, where the 2:1 and 1:1 adsorbent-to-coal mass ratios' desorption rate decreased faster than the 0.5:1 ratio.

Figure 5-4 reveals that the various adsorbent-to-coal mass ratios' desorption curves settled at respective final flotation product moisture contents of 2.3%, 3.4%, and 8.3% w/w, for the 2:1, 1:1, and 0.5:1 adsorbent-to-coal mass ratios. The 2:1 adsorbent-to-coal mass ratio obtained a 91% moisture reduction in coal, followed by 86% and 66% moisture reduction for the 1:1 and 0.5:1 adsorbent-to-coal mass ratios.

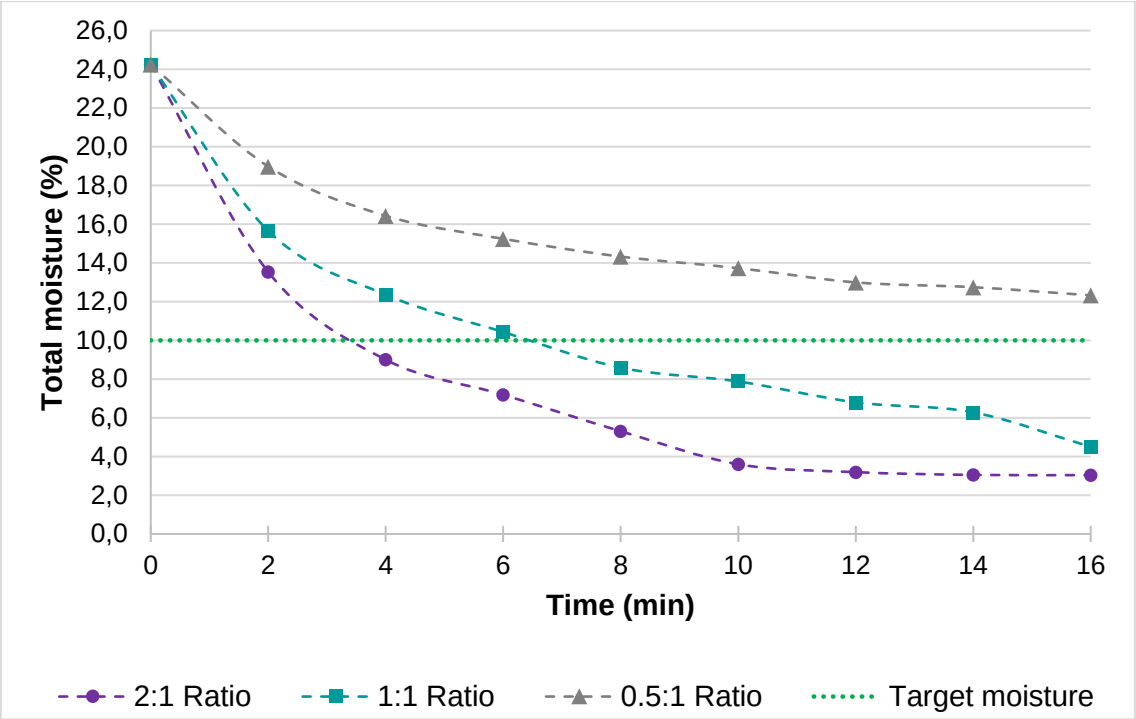

Figure 5-5 Desorption curves of flotation product using 5 mm activated alumina in various adsorbent-to-coal mass ratios

Brief attention is given to Figure 5-5, showing the desorption curves of flotation product using 5 mm activated alumina in various adsorbent-to-coal mass ratios. The effect of adsorbent particle size is, however, discussed in detail in Section 5.2.3.

Figure 5-5 shows the same correlation seen for the 3 mm adsorbent, between the adsorbent-to-coal mass ratio and drying performance manifests for the 5 mm activated alumina. The 5 mm adsorbent, used in a 2:1 adsorbent-to-coal mass ratio, delivered the best drying performance, yielding an 88% moisture reduction followed by 81% and 49% moisture reduction for the 1:1 and 0.5:1 adsorbent-to-coal mass ratios. As previously mentioned for the 3 mm adsorbent: although a difference exists, a marginal difference exists in dewatering performance for the 5 mm adsorbent between the 2:1 and 1:1 adsorbent-to-coal mass ratios, which is beneficial when considering industrial applications.

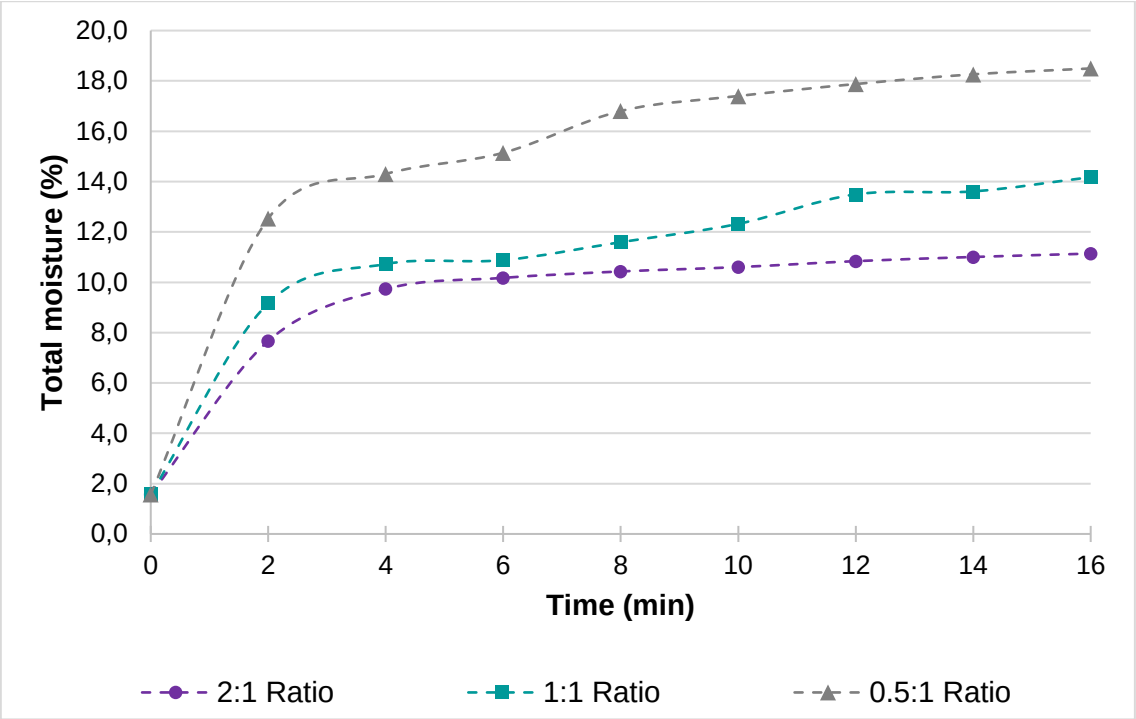

Figure 5-6 Adsorption curves of 3 mm activated alumina used on flotation product in various adsorbent-to-coal mass ratios

Figure 5-6 shows the adsorption curves of 3 mm activated alumina used in different adsorbent-to-coal mass ratios to dewater flotation product. From the figure, the effect of different adsorbent-to-coal mass ratios is apparent, considering the variable adsorption rates and final moisture contents. However, the different adsorption curves followed parallel paths to one another but with varying adsorption rates.

In Figure 5-6, the 0.5:1 adsorbent-to-coal mass ratio reached an adsorbent moisture content of 12.5% w/w after two minutes, followed by 9.1% and 7.7% w/w moisture contents for the 1:1 and 2:1 adsorbent-to-coal mass ratio. The adsorption rates gradually decreased with time, after the initial adsorption stage, as the available moisture in coal decreased with time (Figure 5-4).

Apart from different adsorption rates, the various adsorbent-to-coal mass ratios' adsorption curves also settled at different final moisture contents. The 0.5:1 ratio reached a final moisture content of 18.5% w/w, followed by 14.2% and 11.1% w/w for the 1:1 and 2:1 adsorbent-to-coal mass ratios, respectively. Considering the maximum adsorptive capacities discussed in Section 3.1.2, the activated alumina used in all three ratios would still have the affinity to adsorb more moisture. However, the affinity to adsorb more moisture would rank in descending order from 2:1 to 1:1 and, lastly, a 0.5:1 adsorbent-to-coal mass ratio.

In Chapter 4, the phenomenon stating that the adsorbents' initial adsorption rates, relative to adsorbent mass, are inversely proportional to their respective initial desorption rates, relative to

coal mass, was explained. This phenomenon is also evident for the adsorbent assisted drying of flotation product coal and is shown in Figure 5-7.

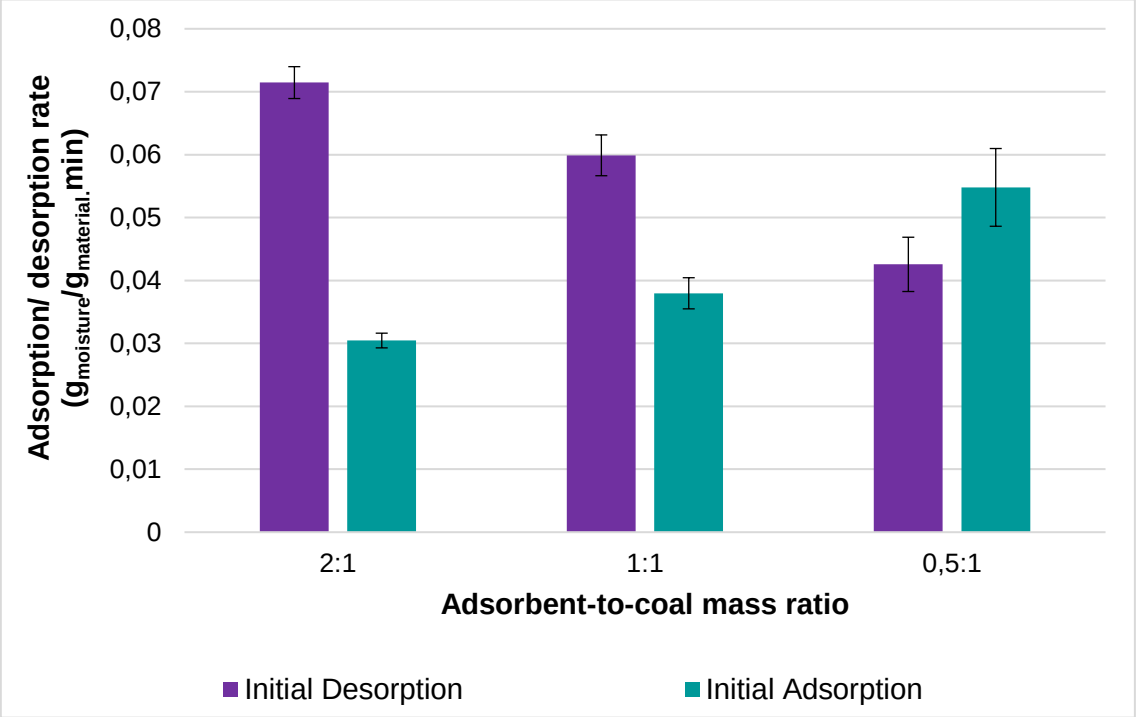

Figure 5-7 Initial adsorption/ desorption rates of 3 mm activated alumina and flotation product

Figure 5-7 draws a comparison between the initial desorption and adsorption rates of flotation product, and 3 mm activated alumina used in various adsorbent-to-coal mass ratios. From the figure, higher adsorbent-to-coal mass ratios achieved higher initial desorption rates and vice versa. Higher adsorbent-to-coal mass ratios reached lower adsorption rates relative to adsorbent mass, and vice versa, as the phenomenon described above.

Figure 5-7 shows that the flotation product had an initial desorption rate of 0.071 $g_{moisture}/g_{coal}.min$ using the 2:1 adsorbent-to-coal mass ratio followed by rates of 0.06 and 0.043 $g_{moisture}/g_{coal}.min$ for the 1:1 and 0.5:1 adsorbent-to-coal mass ratios. The 3 mm activated alumina adsorbed at an initial adsorption rate of 0.03 $g_{moisture}/g_{ads}.min$ for the 2:1 adsorbent-to-coal mass ratio followed by adsorption rates of 0.038 and 0.055 $g_{moisture}/g_{ads}.min$.

This section concludes that the adsorbent-to-coal mass ratio, using 3 mm and 5 mm activated alumina to dry flotation product coal, is directly proportional to its drying performance. Higher adsorbent-to-coal mass ratios provide better drying performances, with faster desorption and lower coal moistures, and vice versa.

5.2.3 Effect of adsorbent particle size

The significance of adsorbent particle sizes and their respective contact surface area in bulk was elaborated in Chapter 4. The hypothesis of smaller adsorbent particle sizes yielding better drying performances was investigated and proven for spiral product coal. This section investigates if this hypothesis applies to flotation product coal using 3 mm and 5 mm activated alumina.

Figure 5-8 shows the desorption curves of flotation product using 3 mm and 5 mm activated alumina in a 2:1 adsorbent-to-coal mass ratio. Both adsorbent particles sizes managed to dewater the flotation product sufficiently to market specification. A clear correlation can be seen between the adsorbent particle size used and its dewatering performance on the coal, yet a marginal difference in final coal moistures exist.

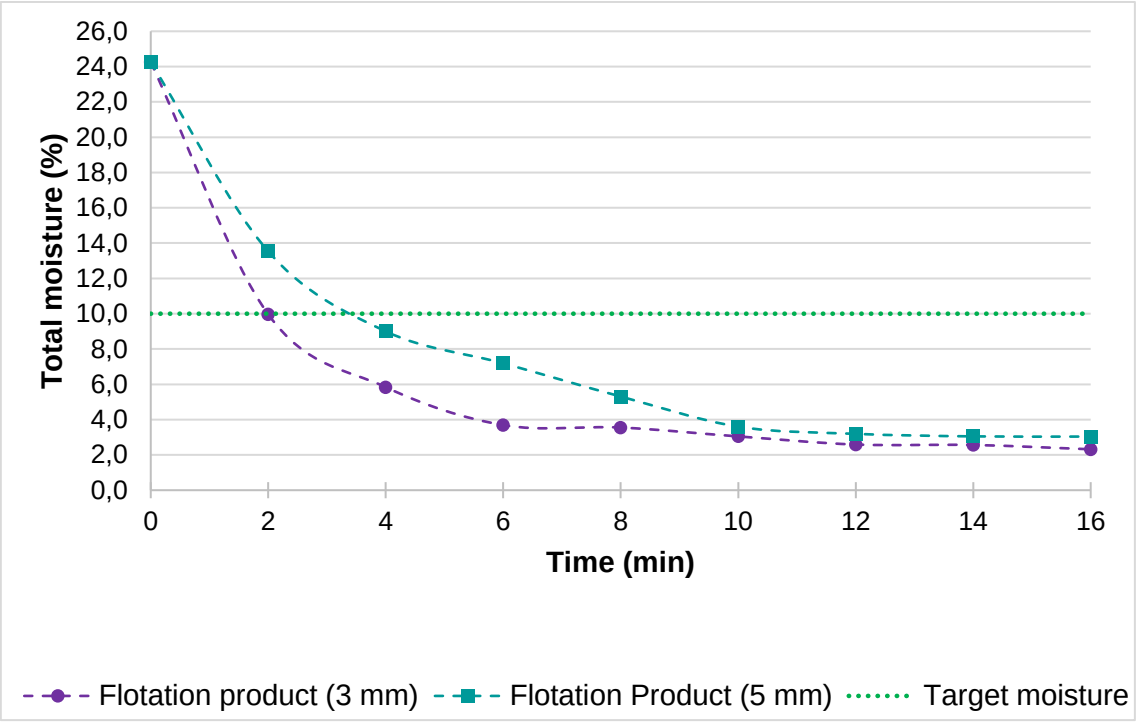

Figure 5-8 Desorption curves of flotation product using 3 mm and 5 mm activated alumina

Figure 5-8 shows that the 3 mm adsorbent showed slightly faster dewatering rates and lower final moisture contents than the 5 mm adsorbent's desorption curve. Within two minutes, the 3 mm adsorbent achieved a flotation product moisture content of 10% w/w, while the 5 mm achieved a coal moisture content of 13.5% w/w. After initial desorption, the 3 mm adsorbent's desorption rate decreased slightly faster than the 5 mm adsorbent. After 10 minutes, both adsorbents' desorption curves gradually reached equilibrium and settled almost the same moisture contents.

Figure 5-8 shows that the 3 mm adsorbent delivered a final coal moisture content of 2.3% w/w, while the 5 mm adsorbent achieved a final coal moisture content of 3% w/w. The 3 mm adsorbent produced a 91% moisture reduction, while the 5 mm caused an 88% moisture reduction.

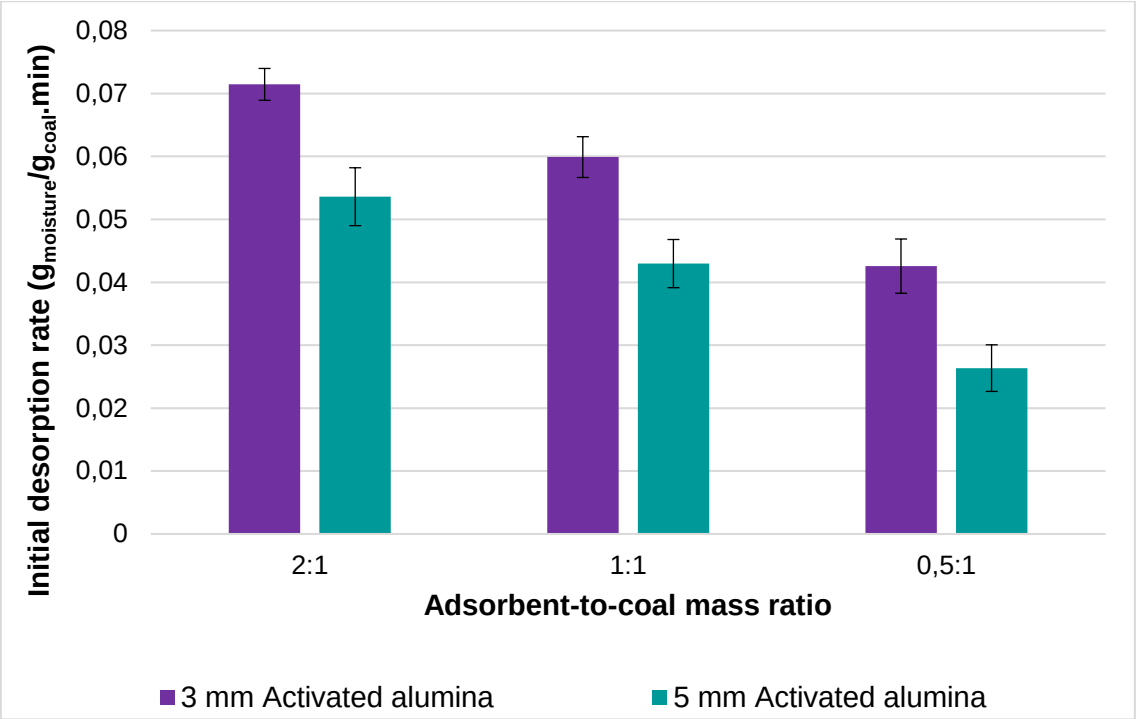

Figure 5-9 Initial desorption rates of flotation product dewatered by 3 mm and 5 mm activated alumina

Figure 5-9 illustrates the initial desorption rates of flotation product dewatered by 3 mm and 5 mm activated alumina, used in various adsorbent-to-coal mass ratios. The figure shows a clear relationship between adsorbent particle size and drying performance, irrespective of the adsorbent-to-coal mass ratio. The 3 mm adsorbent outpaced the 5 mm adsorbent for all three adsorbent-to-coal mass ratios concerning the initial desorption rates. For the 2:1 adsorbent-to-coal mass ratio, the 3 mm activated alumina outperformed the 5 mm activated alumina by 33%. Furthermore, the 3 mm adsorbent outperformed the 5 mm adsorbent by 40% and 65%, respectively, for 1:1 and 0.5:1 adsorbent-to-coal mass ratios. The 3 mm activated alumina achieved, on average, 46% better initial desorption rates than the 5 mm adsorbent.

This section is concluded for the flotation product, confirming that a visible correlation exists between adsorbent particle size and its dewatering performance. As mentioned in Chapter 4, an adsorbent's particle size is inversely proportional to its dewatering performance when considering adsorbents in bulk. The hypothesis mentioned at the start of this section has been proven for flotation product as well. Smaller adsorbent particle sizes deliver higher dewatering performances than larger adsorbent particle sizes due to their increased contact surface area available for contact sorption. Considering desorption rates and final moisture contents overall, the 3 mm adsorbent achieved 30% better dewatering results than the 5 mm adsorbent. Apart from the 0.5:1 adsorbent-to-coal mass ratio, both adsorbent particle sizes dewatered the flotation product coal to well within market specifications, which is beneficial for industrial applications, considering the industrial screening viability of 5 mm vs 3 mm particles.

5.2.4 Effect of adsorbent state

Section 4.2.4 stressed that adsorbents' reuse and regeneration viability play a decisive part in the adsorbent assisted drying method's economic feasibility because adsorbents are relatively expensive. Hence, the regeneration and reuse of adsorbents were tested in this study.

In this section, the dewatering of flotation product coal using spent and regenerated activated alumina, respectively, is discussed. The regeneration of the adsorbents using ambient airflow is discussed in depth in Chapter 6. A comparison is drawn between the drying performances of new, spent, and regenerated adsorbents. Other means of regeneration were also tested as a secondary objective and used to dewater the flotation product. These other means of regeneration are discussed in Chapter 6.

The flotation product was dried using 3 mm, and 5 mm activated alumina for five consecutive cycles without regenerating the adsorbents, with the fresh (new) adsorbents being the first cycle in the consecutive series. From the 2nd to the 5th cycle, the flotation product was dried for 10 minutes, after which the moisture contents were measured.

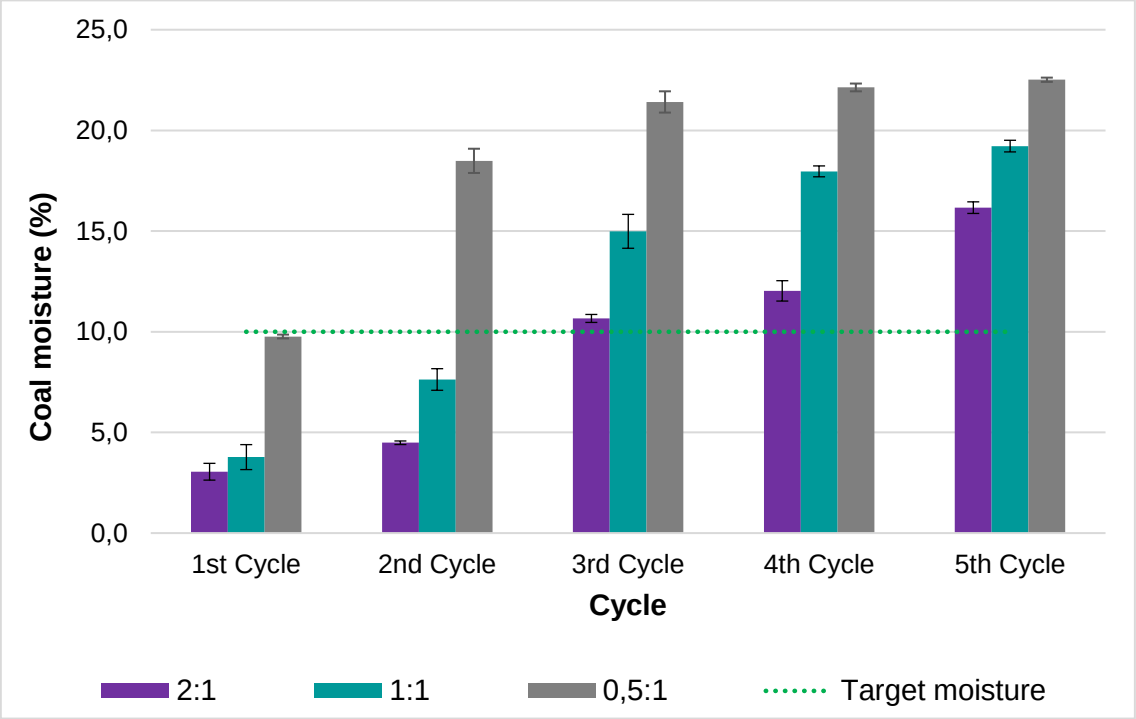

Figure 5-10 Flotation product moisture after 10 minutes using 3 mm new and spent activated alumina

Figure 5-10 shows the flotation product's moisture contents after 10 minutes of dewatering using new (1st cycle) and spent (2nd to 5th cycle) 3 mm activated alumina in various adsorbent-to-coal mass ratios. The spent 3 mm activated alumina, used in a 2:1 and 1:1 adsorbent-to-coal mass ratio, managed to dewater the flotation product, up to the 2nd cycle of use, to market specifications. Until the 2nd cycle of use, the 2:1 and 1:1 adsorbent-to-coal mass ratios produced coal moisture

contents of 4.5% and 7.6% w/w, respectively. However, the spent 3 mm activated alumina, used in a 0.5:1 adsorbent-to-coal mass ratio, did not achieve coal target moistures for any reuse cycles. Furthermore, the 2:1 and 1:1 adsorbent-to-coal mass ratios could not be reused for three or more consecutive cycles, achieving insufficient dewatering.

Figure 5-10 shows an apparent correlation between the various cycles of use for each adsorbent-to-coal mass ratio, where a decrease in drying performance is realised as the adsorbent's cycle of use increases. For each cycle of use, the same correlation discussed in Section 5.2.2 was maintained, where the drying performance is directly proportional to the adsorbent-to-coal mass ratio.

For the 2:1 adsorbent-to-coal mass ratio, the drying performance decreased by 7% from the 1st cycle to the 2nd cycle. A further 31% decrease in drying performance was obtained from the 2nd to the 3rd cycle. From the 3rd to the 4th cycle, a 10% decrease in drying performance was obtained. Lastly, a 34% decrease in drying performance was encountered for the last two cycles. Overall, the 3 mm activated alumina's drying performance decreased by 62% from the 1st cycle to the 5th cycle for the 2:1 adsorbent-to-coal mass ratio. The 1:1 adsorbent-to-coal mass ratio's dewatering performance decreased by 75% overall. Moreover, the 0.5:1 adsorbent-to-coal mass ratio's drying performance decreased overall by 88%.

Figure 5-11 shows the 3 mm activated alumina's moisture loads used for five consecutive cycles to dry the flotation product for 10 minutes. From the figure, the adsorbents' moisture content increased gradually as the cycle of use increased. With the 2:1 adsorbent-to-coal mass ratio, the adsorbent's moisture content increased from 10.6% w/w after the 1st cycle to 26.8% w/w after the 5th cycle.

As described in Section 5.2.2, lower adsorbent-to-coal mass ratios resulted in higher adsorbent moisture loads. However, peripheral differences in moisture loads existed for the 1:1 and 0.5:1 adsorbent-to-coal mass ratios, from the fourth to the fifth cycle, which may be explained with the statement below.

As explained in Section 4.2.4, the decrease in adsorption performance, as the adsorbent-to-coal mass ratio decreases, is owed to higher moisture loads and the capillary pore-blinding phenomenon. As with spiral product dewatering, this phenomenon, entailing the blinding of the adsorbents' capillary pores with coal dust, occurred for flotation product dewatering as well, and to some extent, more severe, considering its ultra-fine particle size.

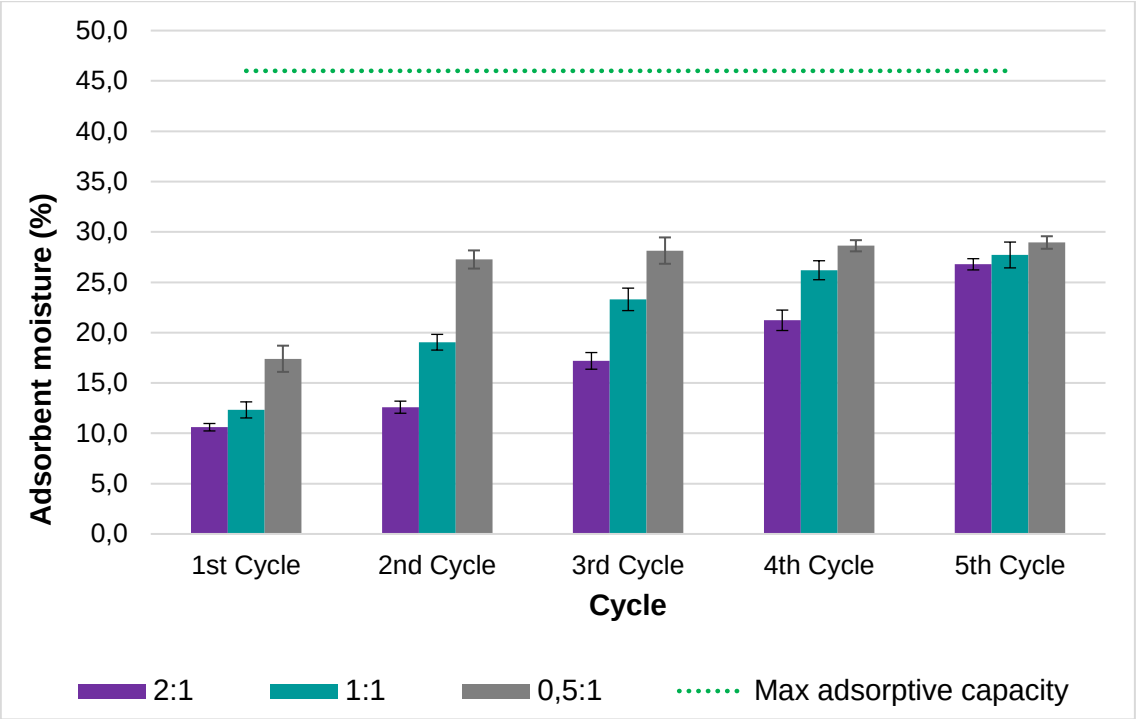

Figure 5-11 Adsorbent moisture loads of 3 mm activated alumina used to dewater flotation product consecutively

The statement above is further explained by referring to an adsorbent used in a smaller adsorbent-to-coal mass ratio, which is surrounded by more coal fines, leading to excessive contact of the adsorbents with the coal. This excessive contact can lead to the adsorbents' capillary pores being blinded easier than higher adsorbent-to-coal mass ratios. Therefore, an adsorbent, used consecutively in smaller adsorbent-to-coal mass ratios, may get blinded capillary pores sooner than an adsorbent used in higher adsorbent-to-coal mass ratios.

Figure 5-11 shows that the adsorbent did not reach full saturation, considering its maximum adsorptive capacity, for either of the adsorbent-to-coal mass ratios. This unsaturation may be attributed to two factors: primarily, the adsorbent's moisture load is dependent on the initial moisture content of the coal being dried and secondarily, the phenomenon described above; where the adsorbent's capillary pores are blinded with coal dust, inhibiting its adsorption ability.

Figure 5-11 shows the minor increases in adsorbent moisture loads from the 2nd to the 5th cycle for the 0.5:1 adsorbent-to-coal mass ratio and the 4th to 5th cycle for the 1:1 ratio, suggesting that insignificant moisture transport occurred. Because coal moisture was still available to be adsorbed, considering the moisture contents in Figure 5-10, this insignificant moisture transport can also be attributed to capillary pore-blinding due to excessive contact with the coal.

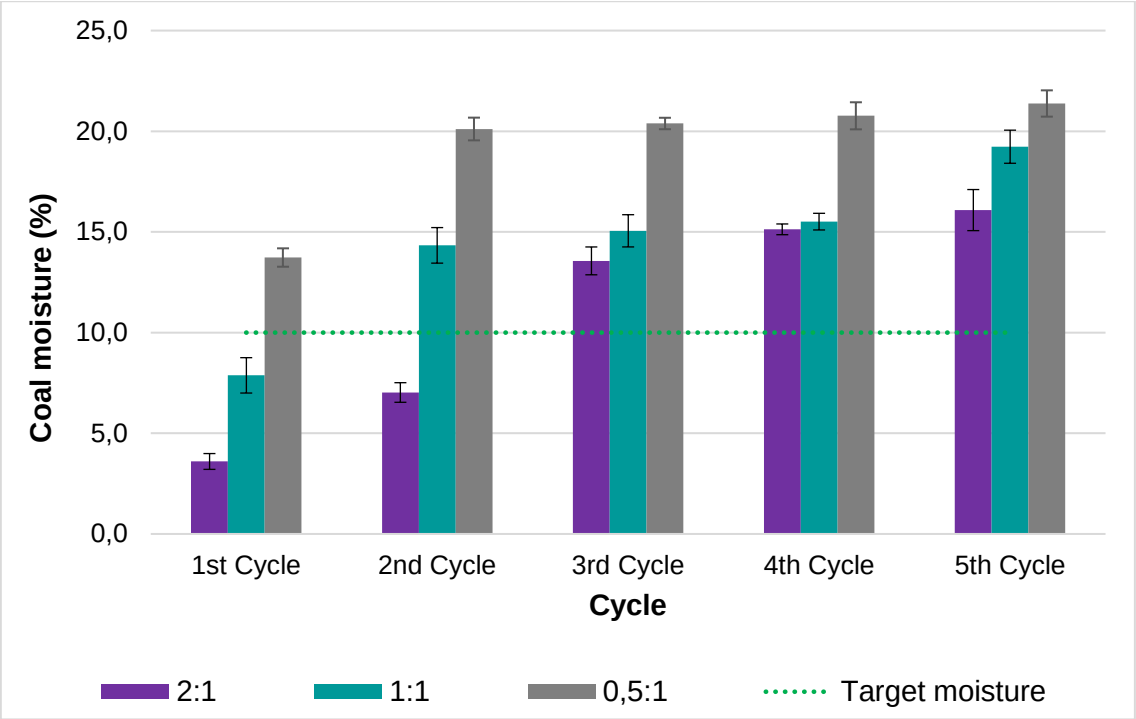

Figure 5-12 Flotation product moisture after 10 minutes using 5 mm new and spent activated alumina

Figure 5-12 represents the flotation product moisture contents after 10 minutes using 5 mm activated alumina for five consecutive cycles, without regeneration, in various adsorbent-to-coal mass ratios. As seen with the 3 mm adsorbent, the same correlations between drying performance and the cycle of use and between drying performance and the adsorbent-to-coal mass ratio exists for the 5 mm adsorbent.

Figure 5-12 shows that the 5 mm adsorbent performed weaker when reused consecutively than the 3 mm adsorbent (Figure 5-10). For the 2:1 adsorbent-to-coal mass ratio, the 5 mm adsorbent managed to dewater the coal sufficiently up to the 2nd cycle of use, delivering a coal moisture content of 7% w/w. However, from the 3rd to the 5th cycle, the 5 mm adsorbent did not achieve market specified coal moisture content. The spent 5 mm adsorbent did not achieve sufficient dewatering of the flotation product for neither the 1:1 nor the 0.5:1 adsorbent-to-coal mass ratios.

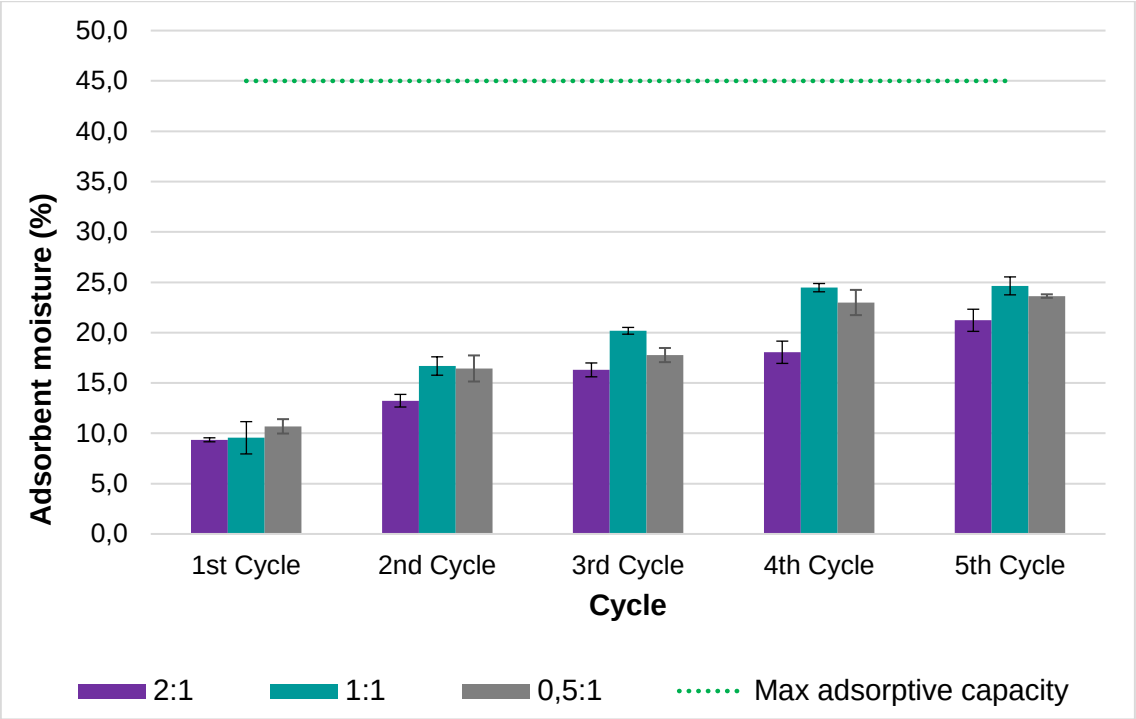

Figure 5-13 Adsorbent moisture loads of 5 mm activated alumina used to dewater flotation product consecutively

Figure 5-13 represents the 5 mm activated alumina's moisture loads used for five consecutive cycles, without regeneration, to dewater flotation product in various adsorbent-to-coal mass ratios. Figure 5-13 reveals that the same correlations discussed for the 3 mm adsorbent are valid for the 5 mm adsorbent. The adsorbent moisture loads increased steadily as the cycle of use increased for each respective adsorbent-to-coal mass ratio.

As seen with the spiral product, a contradicting correlation is revealed between the 1:1 and 0.5:1 adsorbent-to-coal mass ratios, where the 1:1 adsorbent-to-coal mass ratio achieved higher moisture loads than the 0.5:1 adsorbent-to-coal mass ratio from the 2nd cycle of use. The 0.5:1 adsorbent-to-coal mass ratio showed minor moisture load increases from the 2nd to 3rd and from the 4th to 5th cycle of use. The contradicting correlation mentioned above can be attributed to the capillary pore-blinding phenomenon, where the adsorbent used in a 1:1 adsorbent-to-coal mass ratio had less blinded capillary pores, hence, still having an affinity to adsorb moisture. Figure 5-13 shows that the 5 mm adsorbent did not reach its maximum adsorptive capacity, which is primarily contributed to its dependency on coal moisture available to be adsorbed and secondarily to capillary pore-blinding. As seen with spiral coal, competing capillary forces may also be present between the coal particles and adsorbents, reducing the adsorbents ability to reach full saturation.

For flotation product coal, the previously mentioned results conclude that without regeneration, the reuse of adsorbents to dewater the coal is viable only to the second consecutive use and primarily for the 2:1 adsorbent-to-coal mass ratio. This conclusion emphasises the need to regenerate the adsorbents.

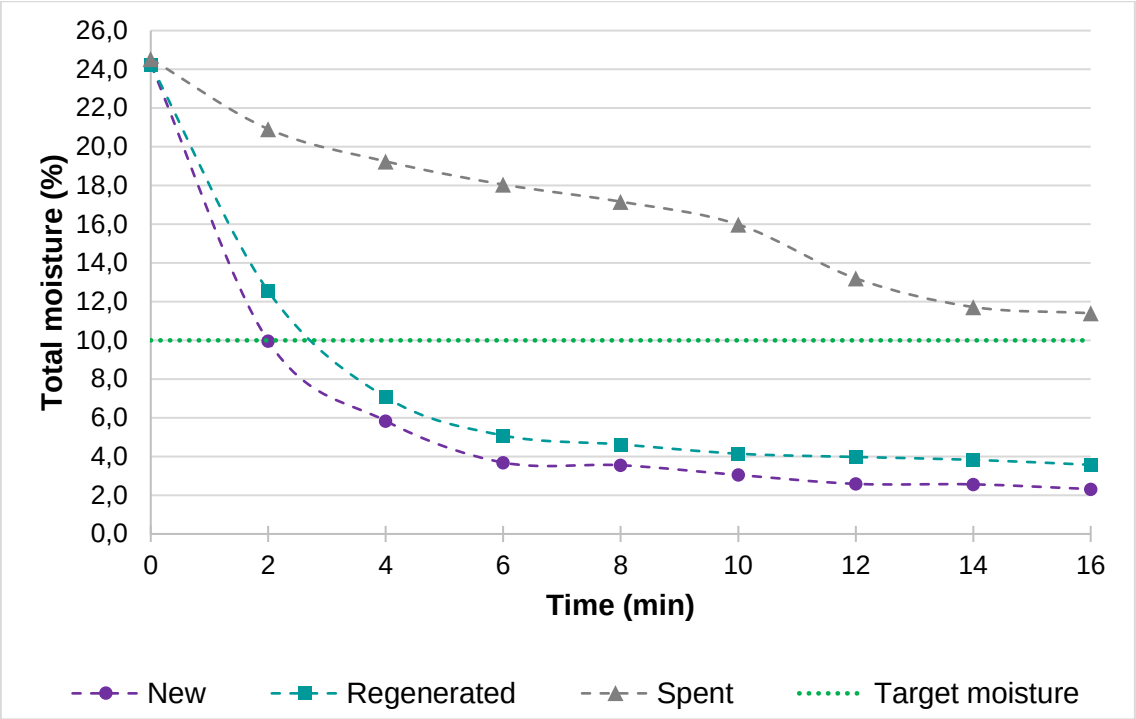

Figure 5-14 Flotation product desorption curves using new, regenerated & spent 3 mm activated alumina

Figure 5-14 shows the desorption curves of flotation product using new, regenerated and spent 3 mm activated alumina in a 2:1 adsorbent-to-coal mass ratio. Dissimilar desorption performances are observed between the three curves. The regenerated adsorbent performed significantly better than the spent adsorbent and slightly weaker than the fresh adsorbent. The regenerated 3 mm adsorbent achieved coal target moisture within 3 minutes and achieved a coal moisture content of 7.1% w/w after 4 minutes with a final moisture content of 3.6% w/w.

Figure 5-14 shows that the regenerated 3 mm adsorbent desorbed the flotation product at an initial desorption rate of 0.059 $g_{moisture}/g_{coal}$.min, which meant a 250% improvement over the spent adsorbent and an 18% weaker performance than the fresh adsorbent. Overall, the 3 mm regenerated adsorbent achieved an 85% moisture reduction in coal, compared to a 53% moisture reduction for the spent adsorbent and a 91% coal moisture reduction for the new adsorbent.

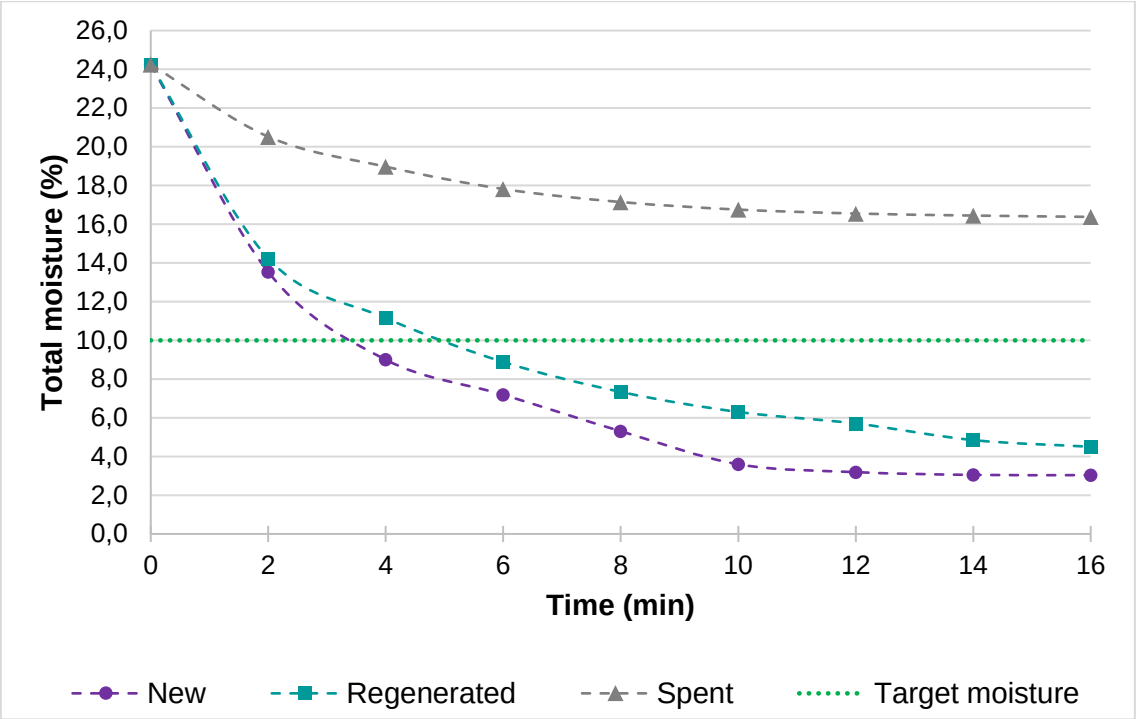

Figure 5-15 Flotation product desorption curves using new, regenerated & spent 5 mm activated alumina

Figure 5-15 shows the desorption curves of flotation product using new, regenerated and spent 5 mm activated alumina in a 2:1 adsorbent-to-coal mass ratio. The figure shows that the regenerated 5 mm adsorbent performed meaningfully better than the spent adsorbent and slightly weaker than the new adsorbent. The regenerated 5 mm adsorbent achieved target coal moisture within 5 minutes and a final coal moisture content of 4.5% w/w. The regenerated 5 mm adsorbent gave an initial desorption rate of 0.051 $g_{moisture}/g_{coal}$.min, a 200% improvement after regeneration. Overall, the regenerated 5 mm adsorbent caused an 81% moisture reduction in coal, which means a remarkable 145% improvement after regeneration.

Due to the capillary pore-blinding phenomenon discussed earlier and the adsorbents becoming grey (filled with coal dust) and less efficient over time, concern was raised to compare alternative means of regeneration as a secondary objective. The spent adsorbents were exposed to furnace temperatures of 900°C for 1 minute to combust the trapped coal dust in the capillary pores and on the surface. These furnace regenerated adsorbents were used to dry the flotation product for 10 minutes.

Figure 5-16 draws a comparison between the use of air blown regenerated and furnace regenerated 3 mm activated alumina to dewater flotation product for 10 minutes. The furnace regenerated adsorbent did, however, achieve coal target moisture after 7 minutes but performed significantly weaker than the air blown regenerated adsorbent. This unexpected correlation can be attributed to the fact that the adsorbent's surface and capillary pores may have become trapped/ blinded by the combusted coal's ash.

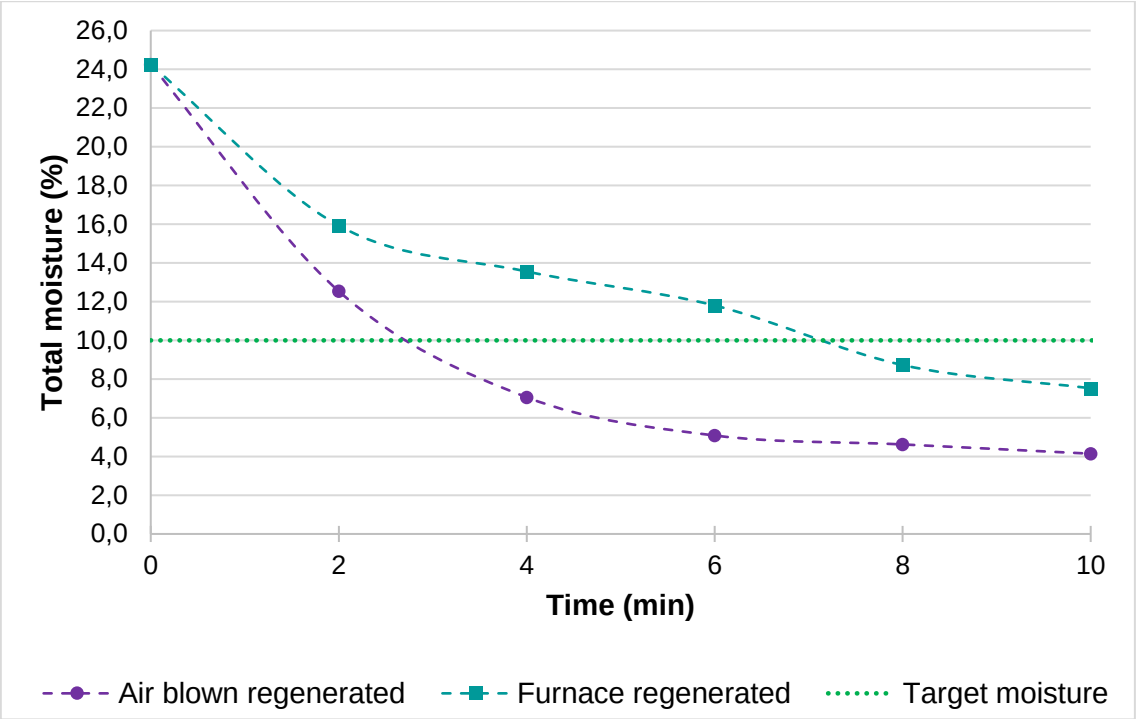

Figure 5-16 Flotation product desorption curves using air-blown regenerated and furnace regenerated 3 mm activated alumina

For the 5 mm adsorbent, another supplementary test took place where the furnace regenerated adsorbent were exposed to blown air for 5 minutes to remove the expected coal ash from the adsorbent's surface. This blown-off ash furnace regenerated adsorbent was used for dewatering the flotation product for 10 minutes and was compared against the air blown regenerated adsorbent, and the standard furnace regenerated adsorbent. This comparison is shown in Figure 5-17.

In Figure 5-17, the standard furnace regenerated 5 mm adsorbent performed slightly better than the air blown regenerated adsorbent, achieving coal target moisture within 3 minutes and delivering final coal moisture of 4% w/w compared to the 6.3% w/w delivered by the air blown regenerated adsorbent. No substantial difference in drying performance was encountered between the blown-off ash, and standard furnace regenerated adsorbent.

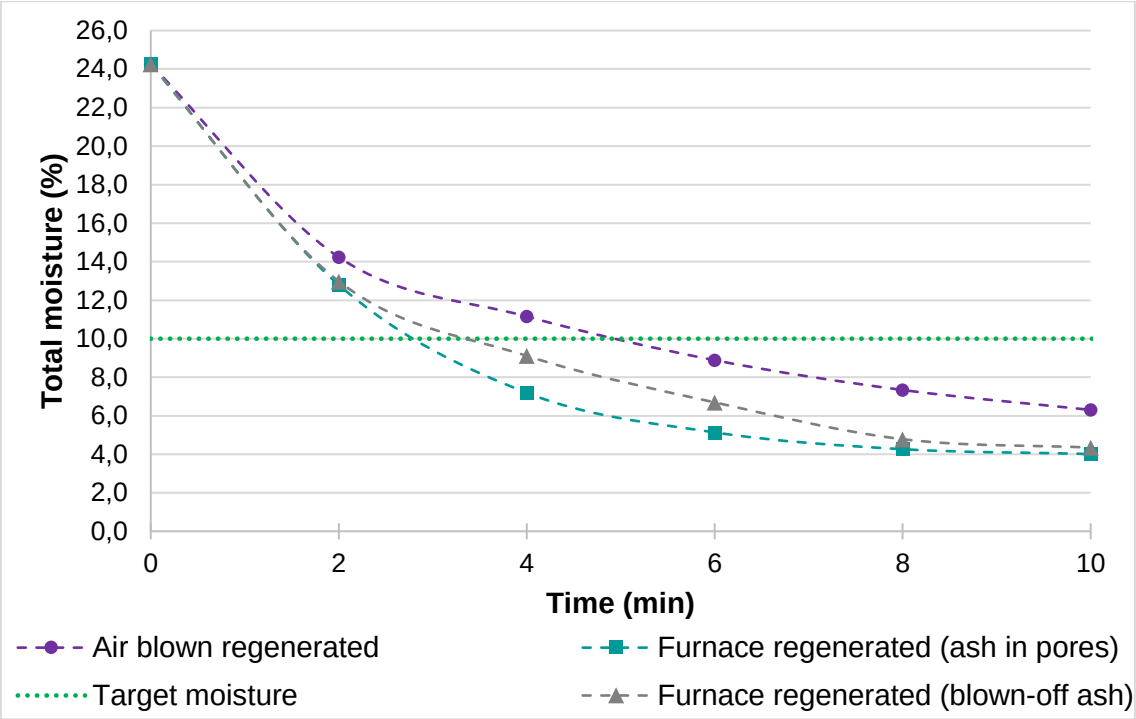

Figure 5-17 Flotation product desorption curves using air-blown regenerated and furnace regenerated 5 mm activated alumina

The furnace regenerated 5 mm adsorbent performing better and yielding significance above the furnace regenerated 3 mm adsorbent could be explained as follows: the 3 mm adsorbent's capillary pores might have been more blinded by coal dust than the 5 mm adsorbent due to its smaller size and larger contact surface area in bulk.

This section concludes that a perceptible correlation existed in drying performances between the different adsorbent states (new, spent and regenerated). Regenerated adsorbents delivered close to but slightly weaker dewatering performances than new adsorbents, but dewatered the flotation product remarkable better than its spent version.

The reuse of adsorbents, without regeneration, to dewater flotation product was found viable only up to the second cycle of use and with limitations, including capillary pore-blinding, and logically, eventual saturation of the adsorbents. Although adsorbent saturation was not observed in the previously discussed results, it is an inevitable limitation, provided the adsorbent's capillary pores are not blinded.

The regeneration of the spent adsorbents generated striking improvements in drying performances. The use of regenerated 3 mm and 5 mm adsorbents are found to be a feasible means of adsorbent assisted drying of flotation product coal, provided only the 2:1 and 1:1 adsorbent-to-coal mass ratios are used.

5.3 Flotation product dried with molecular sieves

5.3.1 General adsorption and desorption curves

The flotation product was dried using molecular sieves with a particle size of 3-5 mm. The flotation product filter cake had an initial feed moisture content of 24.3% w/w and an inherent moisture content of 4.4% w/w. The coal was mixed with the molecular sieves following the same methodology as set out in Chapter 3. Figure 5-18 shows the general adsorption and desorption curves of flotation product dewatered by new (fresh) molecular sieves in a 1:1 adsorbent-to-coal mass ratio.

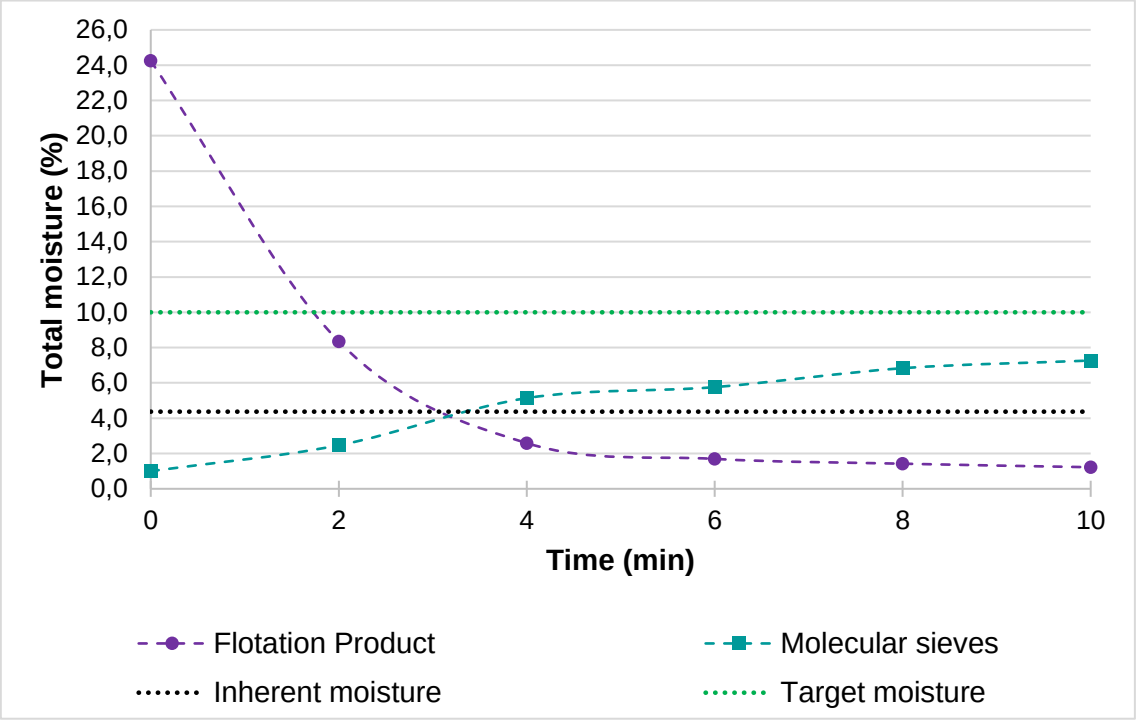

Figure 5-18 Adsorption & desorption curves of flotation product and molecular sieves

Figure 5-18 shows that the flotation product's total moisture steadily decreased from an initial moisture content of 24.3% to 8.3% w/w within 2 minutes of dewatering at an initial desorption rate of 0.080 $g_{moisture}/g_{coal}$.min. The flotation product reached target moisture within 2 minutes of dewatering, whereafter the desorption rate gradually started decreasing. After 3 minutes, the flotation product reached sub inherent moisture contents. After 4 minutes, the flotation product's desorption rate slowly reached equilibrium and settled at a final moisture content of 1.2% w/w after 10 minutes. The flotation product has undergone a moisture reduction of 66% within the first two minutes and, overall, a 95% moisture reduction after 10 minutes, concluding that 69% of the coal's dewatering is done within the first two minutes of contact sorption.

Figure 5-18 also shows that the molecular sieves were fed with a package moisture content of roughly 1.0% w/w to the flotation coal product. From contact with the flotation product, the adsorbents' moisture content increased to 2.5% w/w within 2 minutes at an initial adsorption rate of 0.008 $g_{moisture}/g_{ads}$.min. After 4 minutes, the adsorption rate gradually decreased until a final adsorbent moisture content of 7.3% w/w was reached. As seen with the previous results, the flotation product's desorption curve and the molecular sieves' adsorption curve mirrored each other to some extent.

Section 3.5 discussed that all experiments with the same operating conditions were done three times to determine the experiments' reproducibility and the results' integrity. The T-test, with a 90% confidence interval, was used to determine the experimental error.

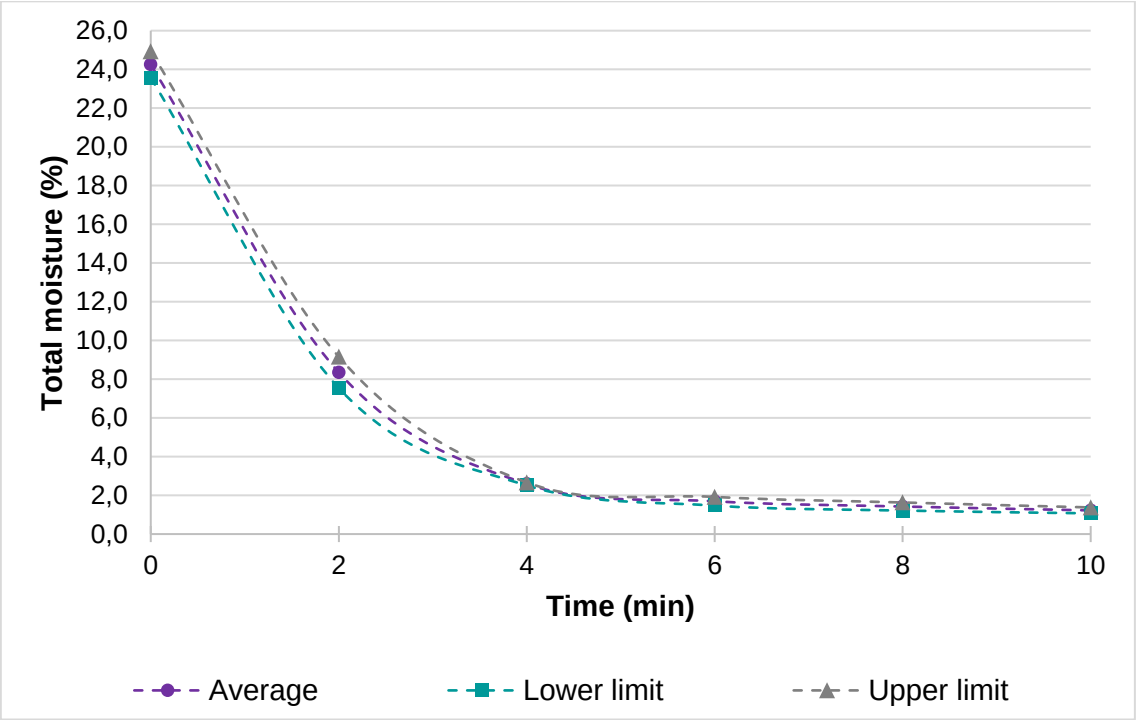

Figure 5-19 Average desorption curve of the flotation product with its standard deviation using molecular sieves

Figure 5-19 shows the flotation product's average desorption curve, with the lower and upper limit standard deviation curves using the molecular sieves in a 1:1 adsorbent-to-coal mass ratio. The flotation product's initial total moisture content averaged 24.3% w/w with a lower limit of 23.6% w/w and an upper limit of 24.9% w/w. After 10 minutes, the flotation product's final moisture content averaged at 1.2% w/w with a lower limit of 1.1% w/w and an upper limit of 1.4% w/w.

Table 5-3 summarises the flotation product's average, standard deviation, and relative experimental error of its repeated experimental runs using molecular sieves in a 1:1 adsorbent-to-coal mass ratio. Reliable experimental results are suggested by the low standard deviations and relative experimental errors found in Table 5-3 for the flotation product's moisture contents.

Table 5-3 Standard deviation and relative experimental error for flotation product moistures using molecular sieves

Time (min)	Average (% w/w)	Standard deviation (% w/w)	Relative experimental error (%)
0 (Feed)	24.25	0.68	1.15
10 (Final)	1.22	0.15	0.21

5.3.2 Effect of adsorbent-to-coal mass ratio

Sections 4.2.2 and 5.2.2 clearly defined the significance of adsorbent-to-coal mass ratios and their relation to contact surface areas between the coal particles and the adsorbents. The hypothesis in Section 5.2.2 was tested and proven for the flotation product using activated alumina as an adsorbent. This section investigates the hypothesis for flotation product using molecular sieves as the adsorbent. Adsorbent-to-coal mass ratios of 2:1, 1:1, and 0.5:1 were used to investigate the effect of various adsorbent-to-coal mass ratios on the flotation product's desorption performance.

Figure 5-20 represents the desorption curves of flotation product using molecular sieves in 2:1, 1:1 and 0.5:1 adsorbent-to-coal mass ratios. The molecular sieves managed to dewater the flotation product sufficiently to below target moisture when used in 2:1 and 1:1 adsorbent-to-coal mass ratios. However, the 0.5:1 adsorbent-to-coal mass ratio did not deliver sufficient dewatering of the flotation product to fit target moisture.

Figure 5-20 shows that striking differences in initial desorption rates and final coal moisture contents exist for the various ratios, with the dewatering performance increasing in ascending order adsorbent-to-coal mass ratios. The various ratios' curves followed almost similar paths but with different desorption rates and final coal moisture contents.

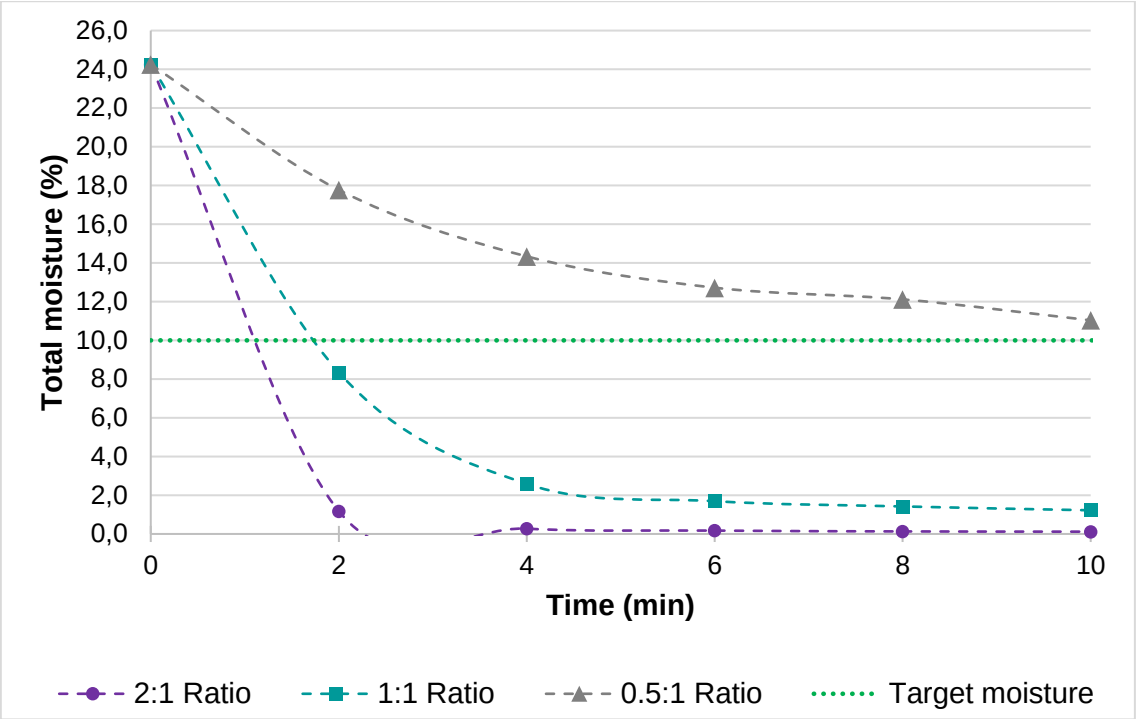

Figure 5-20 Desorption curves of flotation product using molecular sieves in various adsorbent-to-coal mass ratios

Figure 5-20 shows that, after two minutes, the 2:1 adsorbent-to-coal mass ratio yielded a 1.2% w/w flotation product moisture content, followed by 8.3% and 17.8% w/w, respectively, by the 1:1 and 0.5:1 adsorbent-to-coal mass ratios. After two minutes, the desorption rates decreased, with the 2:1 adsorbent-to-coal mass ratio's desorption rate decreasing the fastest, followed by the 1:1 ratio and the 0.5:1 ratio, respectively.

Figure 5-20 displays the various ratios' curves settling at different final flotation product moisture contents of 0.1%, 1.2%, and 11.0% w/w, for the 2:1, 1:1, and 0.5:1 adsorbent-to-coal mass ratios, respectively. The 2:1 adsorbent-to-coal mass ratio caused a 95% moisture reduction within 2 minutes, achieving a coal moisture content of 1.2% w/w. Overall, the 2:1 adsorbent-to-coal mass ratio furnished an outstanding 99% moisture reduction in flotation product after 10 minutes, followed by another remarkable 95% and 55% moisture reductions, respectively by the 1:1 and 0.5:1 adsorbent-to-coal mass ratios.

Figure 5-21 compares the flotation product's initial desorption rates using molecular sieves in various adsorbent-to-coal mass ratios. The figure shows that higher adsorbent-to-coal mass ratios deliver higher initial desorption rates and vice versa.

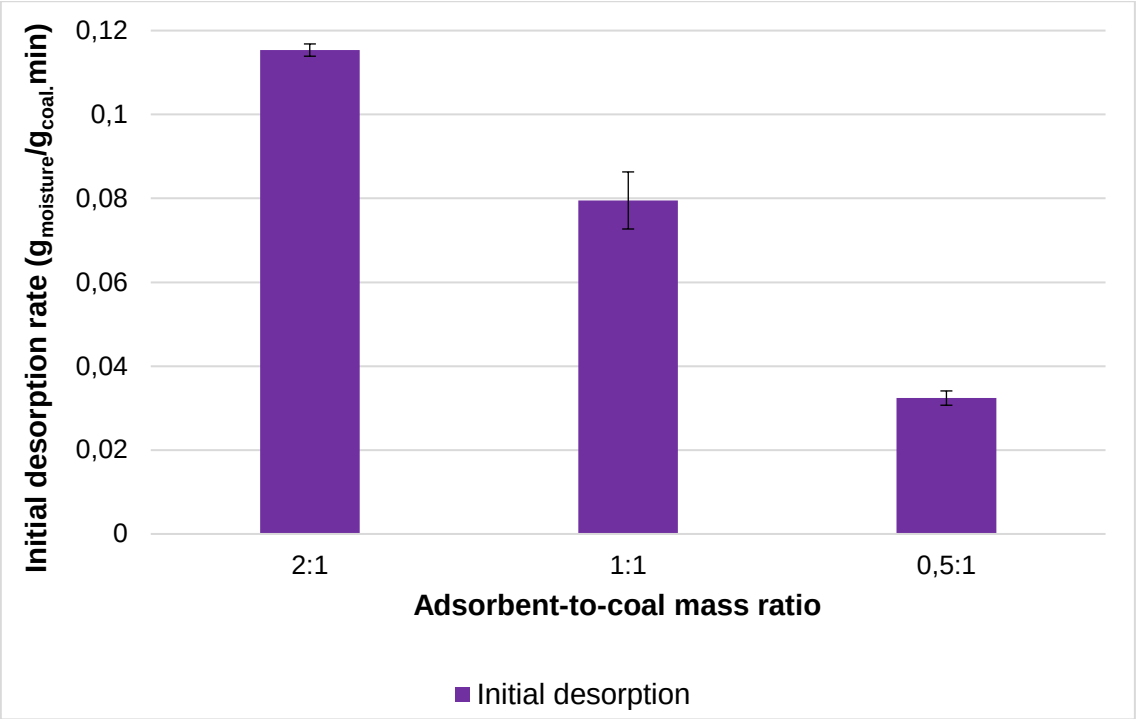

Figure 5-21 Initial desorption rates of flotation product using molecular sieves

Figure 5-21 shows that the flotation product was initially desorbed at 0.115 $g_{moisture}/g_{coal}$.min using the 2:1 ratio followed by initial desorption rates of 0.080 and 0.032 $g_{moisture}/g_{coal.}$min for the 1:1 and 0.5:1 adsorbent-to-coal mass ratios, showing an apparent decrease in desorption rate as the adsorbent-to-coal mass ratio decreased or vice versa. In terms of initial desorption rates, the 2:1 adsorbent-to-coal mass ratio performed 44% better than the 1:1 ratio, which in turn, performed 150% better than the 0.5:1 adsorbent-to-coal mass ratio.

This section concludes that the adsorbent-to-coal mass ratio, using molecular sieves to dry flotation product coal, is directly proportional to its drying performance. Higher adsorbent-to-coal mass ratios call for better drying performances and vice versa.

5.3.3 Effect of adsorbent state

Sections 4.2.4 and 5.2.4 clearly defined the importance of adsorbent's reuse and regeneration viability due to adsorbents being costly. In this section, the feasibility of using spent and regenerated molecular sieves to dry flotation coal product was investigated with the adsorbent state referring to fresh, spent, or regenerated. A comparison is drawn between the drying performances of fresh, spent, and regenerated adsorbents. Chapter 6 discusses in-depth the regeneration of the adsorbents using ambient airflow.

The flotation product was dried using molecular sieves for three consecutive cycles without regenerating the adsorbents, with the fresh adsorbents being the first cycle in the series. For each

cycle of adsorbent use, the flotation product is dried for 10 minutes, after which the moisture content was measured.

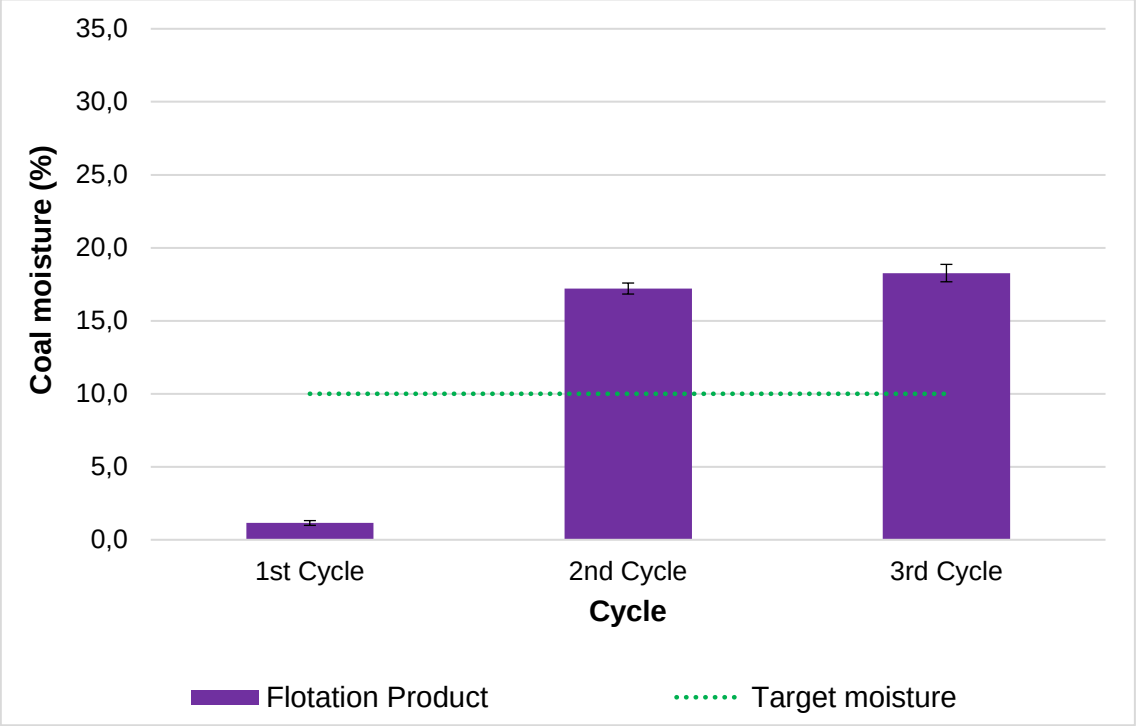

Figure 5-22 Flotation product moisture after 10 minutes using new and spent molecular sieves

Figure 5-22 shows the flotation product's moisture contents after 10 minutes' dewatering using fresh (first cycle) and spent (second and third cycle) molecular sieves in a 1:1 adsorbent-to-coal mass ratio. Unfortunately, when used twice or thrice in a 1:1 adsorbent-to-coal mass ratio, the spent molecular sieves did not dewater the coal to target moisture. The fresh molecular sieves furnished a coal moisture content of 1.2% w/w, while the spent adsorbents gave rise to 17.2% and 18.3% w/w moisture contents for the second and third cycle of use.

Figure 5-22 shows a dramatic decrease in drying performance as the molecular sieves are used twice. The drying performance decreased substantially by 69% from fresh adsorbents to the 2nd cycle of use. The 3rd cycle of use saw another 15% drop in drying performance compared to the 2nd cycle. Overall, the molecular sieves' drying performance decreased by 74% from the first cycle to the third cycle of use. The spent molecular sieves' poor drying performance, coupled with the slight decrease in drying performance between the second and third cycle of use, suggests that the spent molecular sieves were already beyond operable.

Figure 5-23 shows the adsorbent moisture loads of the molecular sieves used for three consecutive cycles to dry the flotation product for 10 minutes in a 1:1 adsorbent-to-coal mass ratio, with the first cycle being the fresh adsorbent's first use. Figure 5-23 shows the adsorbents' moisture load increasing little by little as the usage cycle increased. The molecular sieves'

moisture content increased from 7.3% w/w, after the 1st cycle, to 9.2% w/w after the 2nd cycle and increased further to 12.4% w/w after the 3rd cycle.

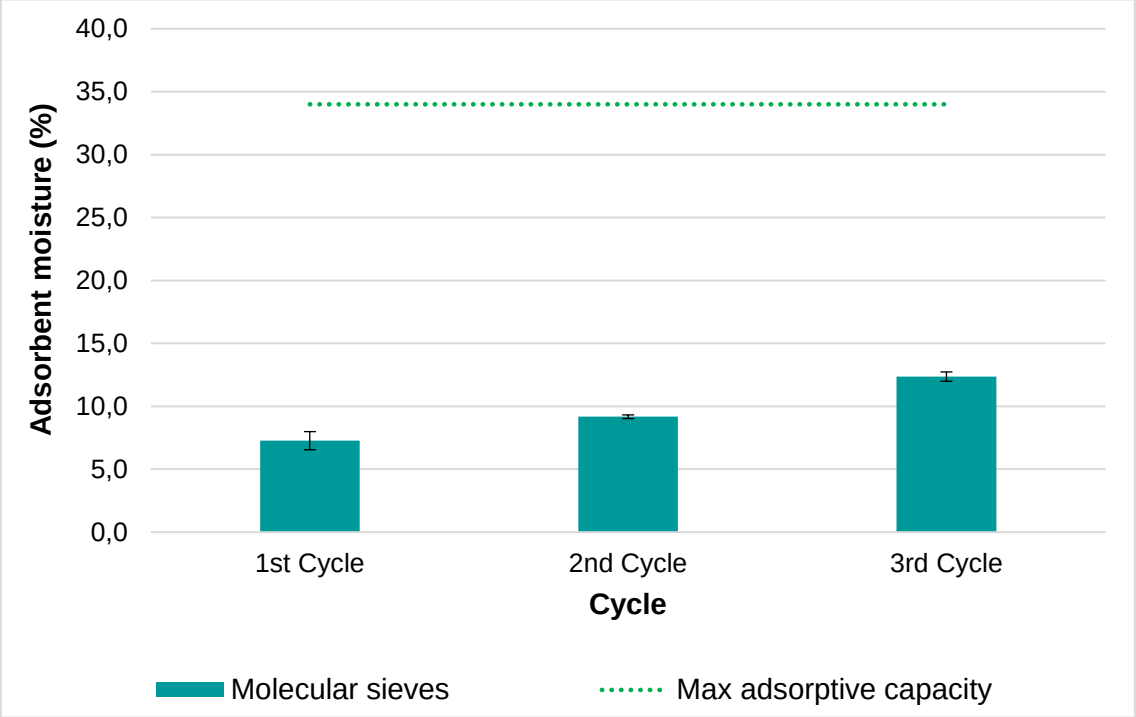

Figure 5-23 Molecular sieves' moisture loads used to dewater flotation product consecutively

Figure 5-23 also shows that the molecular sieves did not reach their maximum adsorptive capacity of 34% w/w for any usage cycles, meaning they did not reach full saturation. At most, they reached about a third of their adsorptive capacity. This unsaturation means that the adsorbents may have had the affinity to adsorb more moisture in the consecutive 4th and 5th cycles of use.

Nevertheless, referring to the spent molecular sieves' poor dewatering performance seen in Figure 5-22 and the discussions in Section 5.2.4, the unsaturation might have been due to two factors: primarily, the adsorbent's moisture load being dependent on the available moisture to be adsorbed and secondarily, the phenomenon described as capillary pore blinding; where the adsorbent's capillary pores are trapped with coal dust, inhibiting adsorption.

The reuse of molecular sieves, without regeneration, discussed above concluded that spent molecular sieves could not dewater the flotation product sufficiently to market specifications. Therefore, an even greater need existed to regenerate the molecular sieves. The spent molecular sieves were regenerated using ambient airflow conditioned at 22°C and 70% RH in a packed bed column. Chapter 6 discusses adsorbent regeneration in-depth.

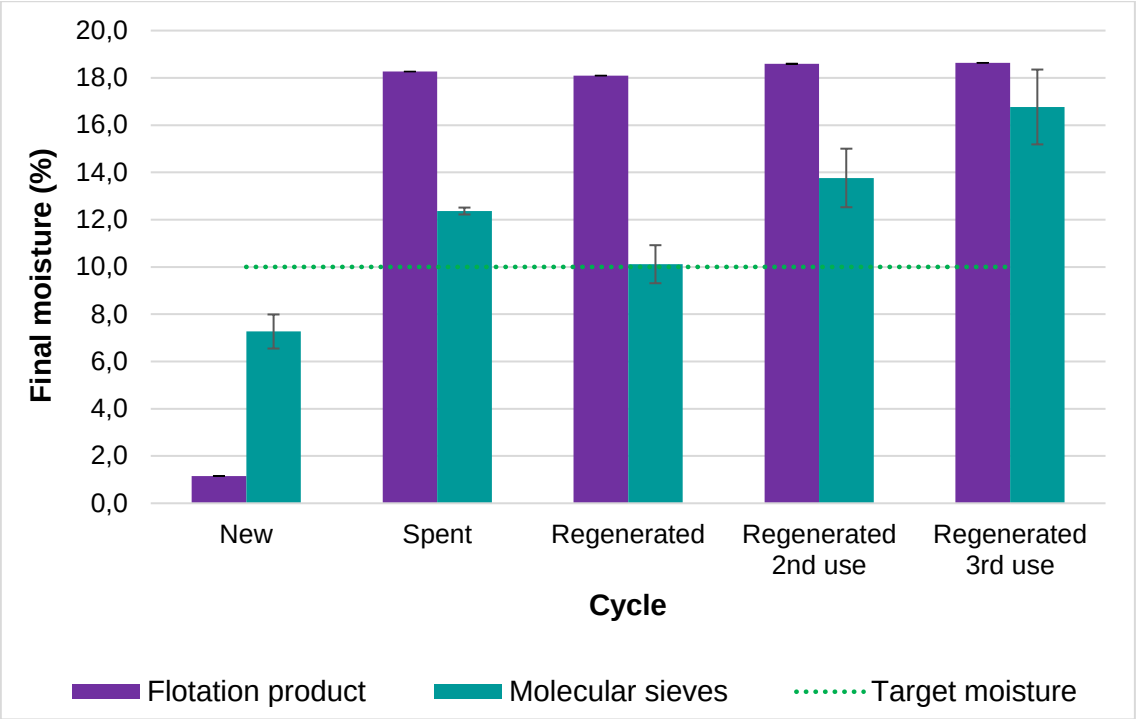

Figure 5-24 Flotation product moisture after 10 minutes using new, regenerated & spent molecular sieves

Figure 4-24 shows the flotation product's and molecular sieves' final moisture contents after 10 minutes using new, spent and regenerated molecular sieves in a 1:1 adsorbent-to-coal mass ratio. Contrary to expectation, meagre differences in dewatering performance are observed between the spent and regenerated cycles. The regenerated molecular sieves did not perform significantly better than the spent adsorbent, delivering only a 0.2% w/w lower coal moisture content.

The regenerated adsorbent delivered a flotation product moisture content of 18.1% w/w, equating to a 3% improvement over the spent adsorbent while having a significantly weaker performance of 73% than the fresh adsorbent. Overall, the regenerated molecular sieves reached a 26% moisture reduction in coal, compared to a 25% moisture reduction for the spent adsorbent and a 95% moisture reduction in coal for the fresh adsorbent.

Additionally, the regenerated adsorbent was used two more times consecutively, without regenerating it again. In both subsequent cycles, the regenerated molecular sieves achieved a similar coal moisture content of 18.6% w/w, a scanty 8% weaker dewatering performance than the first regenerated use cycle.

Steady increases in adsorbent moisture loads for the regenerated adsorbent use cycles may have suggested that the molecular sieves still had some affinity for moisture adsorption. Nonetheless, none of the regenerated adsorbent cycles achieved sufficient dewatering of flotation product coal,

indicating that the molecular sieves would be unfit to dewater the flotation product coal after regeneration.

This section completed a discernible correlation between the new molecular sieves' drying performances and the spent or regenerated adsorbents' drying performances on flotation product. The fresh molecular sieves delivered, comprehensibly, the best drying performance. Contrary to activated alumina, the regenerated molecular sieves did not achieve significantly better dewatering above its spent version.

Neither the regenerated nor the spent molecular sieves delivered sufficient dewatering of the flotation product coal to satisfy the market specification. Using regenerated or spent molecular sieves is not a feasible means of adsorbent assisted drying of flotation product coal.

5.4 Activated alumina vs molecular sieves

5.4.1 General desorption curves

In this section, the desorption curves of flotation product dewatered by activated alumina and molecular sieves are discussed, to compare how the two different adsorbents would perform. Molecular sieves have uniform and precise pore networks, suggesting that they would adsorb moisture better than activated alumina not having such precise and uniform pore networks. This hypothesis is investigated in this section.

Figure 5-25 shows the desorption curves of flotation product being dried with fresh activated alumina and molecular sieves used in a 2:1 adsorbent-to-coal mass ratio. The molecular sieves performed significantly better than the activated alumina, yielding faster desorption rates and lower coal moisture contents. In the first two minutes, the activated alumina and molecular sieves dewatered at initial desorption rates of 0.072 and 0.115 $g_{moisture}/g_{coal}$.min, respectively. The activated alumina and molecular sieves achieved moisture contents of 5.8% and 0.3% w/w after 4 minutes, and after 10 minutes, moisture contents of 3.1% and 0.1% w/w, respectively. The hypothesis stated above is proven correct, with the molecular sieves adsorbing moisture significantly better than the activated alumina due to its uniform pore networks.

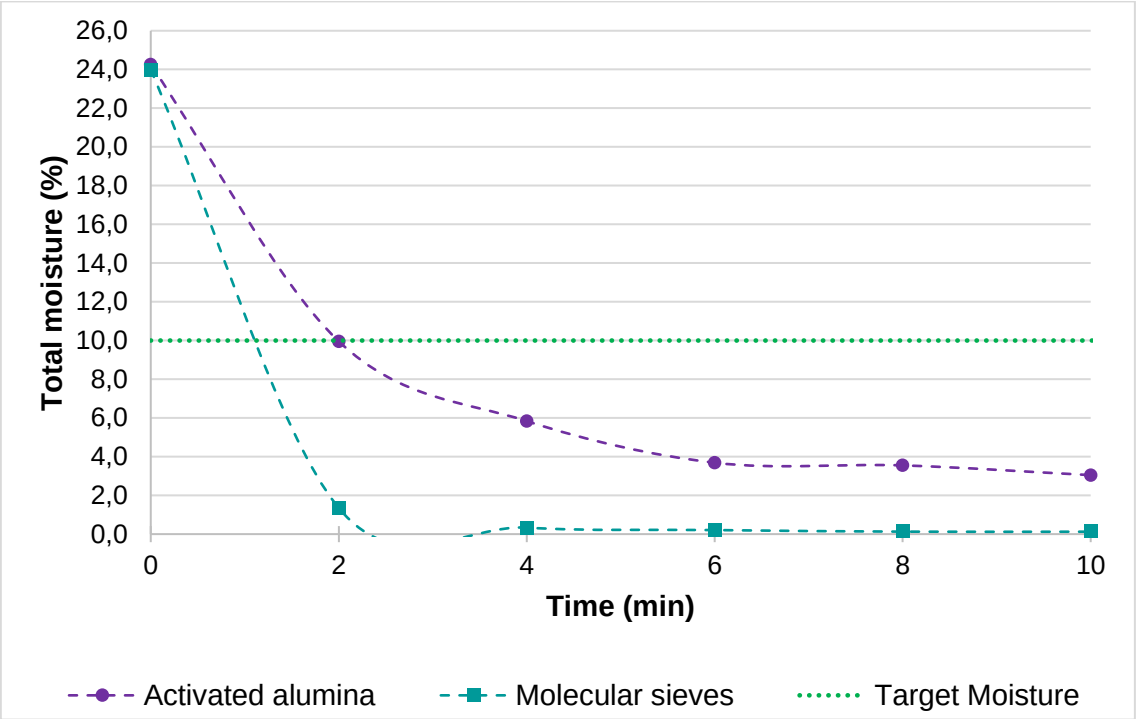

Figure 5-25 Flotation product's desorption curves using activated alumina vs molecular sieves

5.4.2 Effect of adsorbent-to-coal mass ratio

This section briefly discusses the extent of the effects that various adsorbent-to-coal mass ratios have on the desorption performance of both activated alumina and molecular. Figure 5-26 compares the moisture reduction carried out on the flotation product by the activated alumina and molecular sieves in various adsorbent-to-coal mass ratios. Moisture reduction refers to the moisture removed as a percentage of the initial coal moisture content.

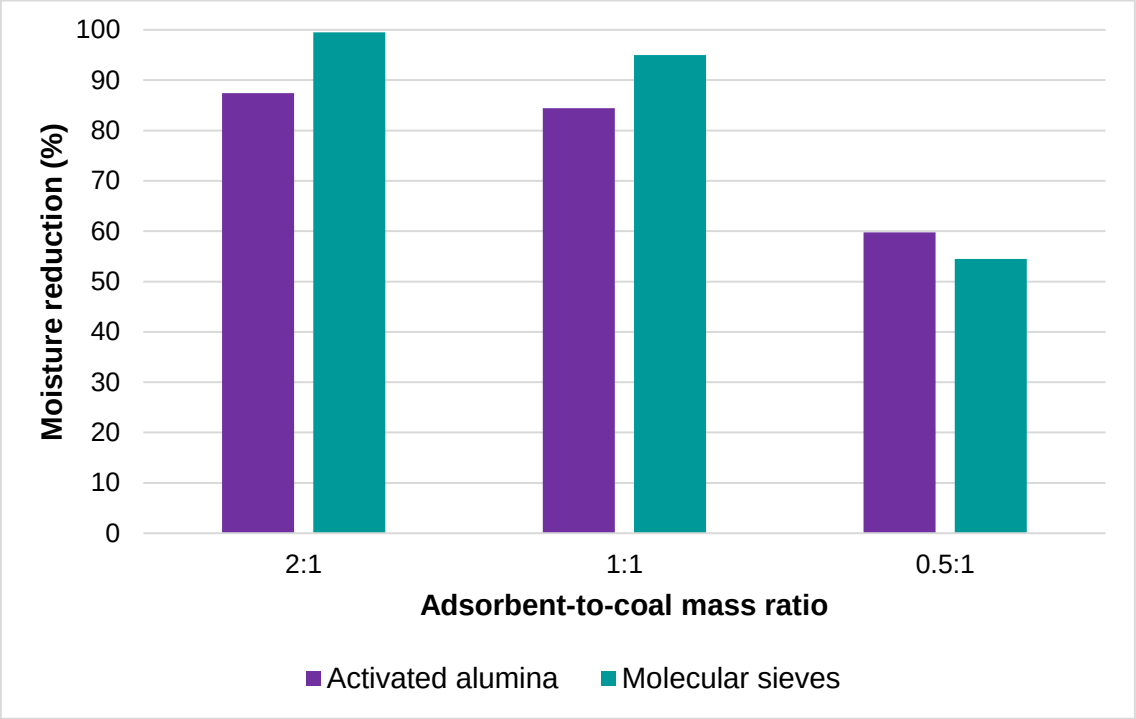

Figure 5-26 Moisture reductions of flotation product using activated alumina vs molecular sieves in various adsorbent-to-coal mass ratios

In Figure 5-26, the molecular sieves achieved significantly better moisture reductions than the activated alumina when used in 2:1 and 1:1 ratios. For the activated alumina, the 2:1 adsorbent-to-coal mass ratio had a 4% improvement over the 1:1 ratio, which in turn, was a 40% improvement over the 0.5:1 ratio. For the molecular sieves, the 2:1 ratio had a 5% improvement over the 1:1 ratio, which was a 76% improvement over the 0.5:1 ratio. From these results, it can be concluded that the two adsorbents had similar dewatering abilities for ratios of 2:1 and 1:1. The drop in adsorption for an adsorbent-to-coal mass ratio of 0.5:1 was much larger for the molecular sieves than the tailings.

5.4.3 Effect of adsorbent state

This section briefly compares the effects of adsorbent state on the activated alumina and molecular sieves' dewatering performances on flotation product. Figure 5-27 shows the flotation product's moisture reductions using new, spent and regenerated activated alumina vs molecular sieves in a 1:1 adsorbent-to-coal mass ratio, mixed for 10 minutes.

From the previous two sections, it is clear that, when using new adsorbents, the molecular sieves perform better than used adsorbents, however some interesting observations can be made when comparing this to spent and regenerated adsorbents as seen in Figure 5-27. From these results it can be seen that, the activated alumina achieved greater moisture reductions than the molecular sieves when using spent and regenerated adsorbents. The drop in the ability of adsorbents to reduce moisture is much greater for molecular sieves, at a 74% drop, than for activated alumina, which only had a drop of 55%. The improvement in moisture reduction after regeneration was also significant, given that after regeneration, the activated alumina had a 107% improvement over the spent version. Molecular sieves on the other hand could not be regenerated to the same extent, using the method laid out in Section 3.3.2, and no improvement was seen in its moisture reduction abilities, albeit its moisture reduction abilities did not decrease either.

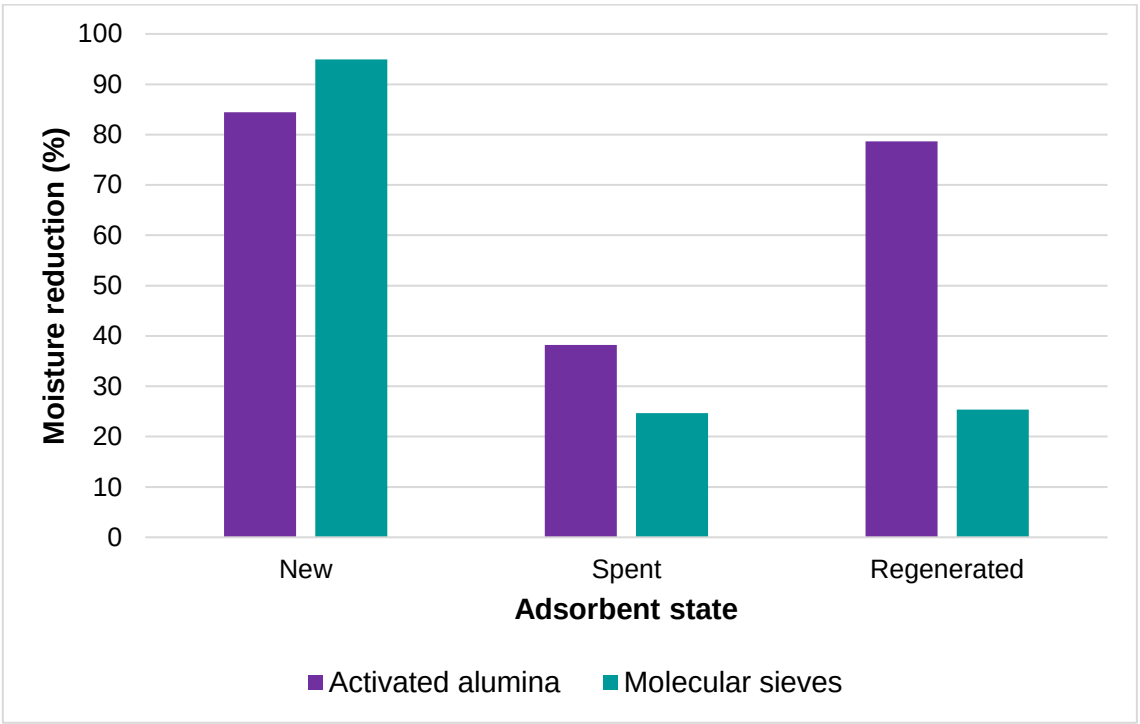

Figure 5-27 Moisture reductions of flotation product using new, spent and regenerated activated alumina vs molecular sieves

In conclusion, new (fresh) molecular sieves dewatered coal remarkably better than activated alumina. However, when spent and regenerated adsorbents were used, the molecular sieves performed significantly weaker than the activated alumina, achieving partial moisture reductions

and not delivering to coal market specifications. The hypothesis that molecular sieves with uniform pore sizes would adsorb moisture better and faster than activated alumina is proven correct, but only when using new adsorbents. The main discovery from this section was that molecular sieves are found not to be feasible for industrial use, considering how poor they performed during reuse and regeneration.

5.5 Spiral vs flotation product

5.5.1 General desorption curves

In this section, the spiral product and flotation product coal's desorption curves are discussed to comprehend how differently sized product coal types and differently beneficiated coal types would behave during dewatering. Section 3.1.1 reported that the spiral product has a d_{50} particle diameter of 434 µm while the flotation product has a significantly smaller mean particle diameter of 21 µm. From the review in Chapter 2, it is clear that finer particle size coals retain water stronger than coarser coals, making dewatering more challenging. This section aims to deliberate on the above statement and investigates any significance that the flotation reagents might have on the coal's dewatering performance.

Figure 5-28 shows the desorption curves of spiral and flotation product dewatered with new 3 mm activated alumina in a 2:1 adsorbent-to-coal mass ratio. Both product coals types' desorption curves have a similar shape and slope, following the same trend but with different moisture contents. The spiral and flotation products started with vastly different feed moisture contents of 18,0% and 24.3% w/w, respectively.

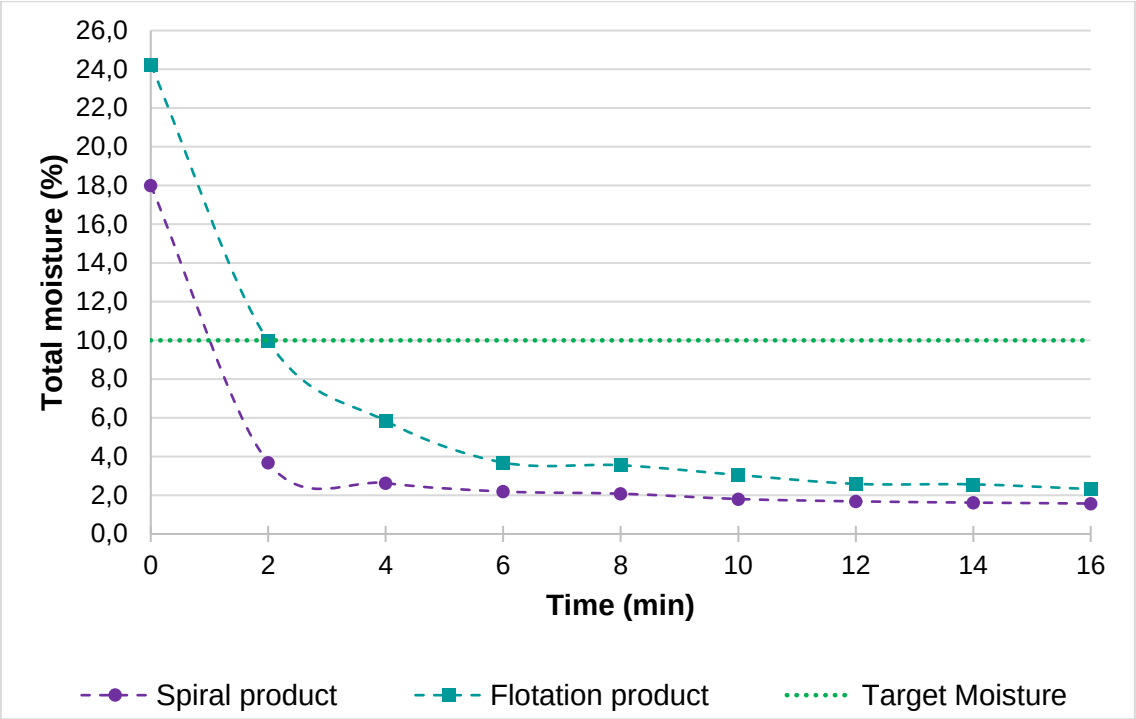

Figure 5-28 Spiral vs flotation product's desorption curves

Figure 5-28 shows that in the first 2 minutes, the spiral and flotation product had been dewatered at almost identical initial desorption rates of 0.072 and 0.071 $g_{moisture}/g_{coal}$.min, respectively. Halfway through drying, the spiral and flotation products had moisture contents of 2.1% and 3.6% w/w, experiencing 88% and 85% moisture reductions, respectively. Overall, the spiral and flotation products experienced 91% and 90% moisture reductions.

Spiral product and flotation product coal followed very similar dewatering behaviours. Although they started with vastly different feed moisture contents, they were initially desorbed at very similar desorption rates while experiencing very similar moisture reductions halfway through and overall.

These results conclude that even though vastly different coal sizes retain moisture much differently, they experience the same dewatering behaviour when using activated alumina in adsorbent assisted drying. Moreover, the reagents used during coal flotation seemed to have little to no effects on the flotation product coal's dewatering.

5.5.2 Effect of adsorbent-to-coal mass ratio

This section briefly examines how adsorbent-to-coal mass ratio dewaters coal of different particle sizes. The moisture reduction, specific to each coal is discussed in Sections 4.2.2 and 5.2.2. Figure 5-29 compares the spiral and flotation product's moisture reductions using fresh 3 mm activated alumina in various adsorbent-to-coal mass ratios.

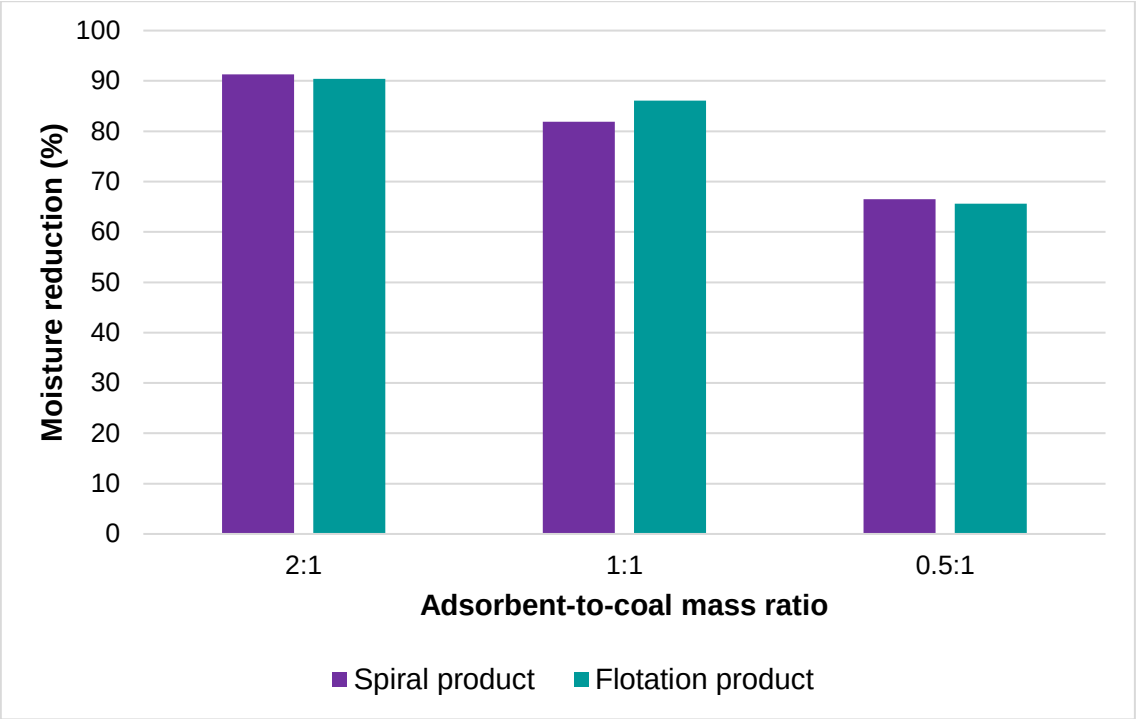

Figure 5-29 Moisture reductions of spiral vs flotation product using various adsorbent-to-coal mass ratios

In Figure 5-29, it can be seen that the flotation product experiences a slightly better moisture reduction than the spiral product for the 1:1 ratio. This can be attributed to the fact that the flotation product has a larger contact surface area because of its small particle size. These results conclude that the spiral and flotation product's dewatering behaved similarly, while the difference in effects of adsorbent-to-coal mass ratio between the two product coals was insignificant.

5.5.3 Effect of adsorbent particle size

This section briefly reviews the extent of adsorbent particle size's effects on the spiral product and flotation product's dewatering. Figure 5-30 compares the spiral and flotation product's moisture reductions dewatered by new 3 mm and 5 mm activated alumina in a 2:1 adsorbent-to-coal mass ratio.

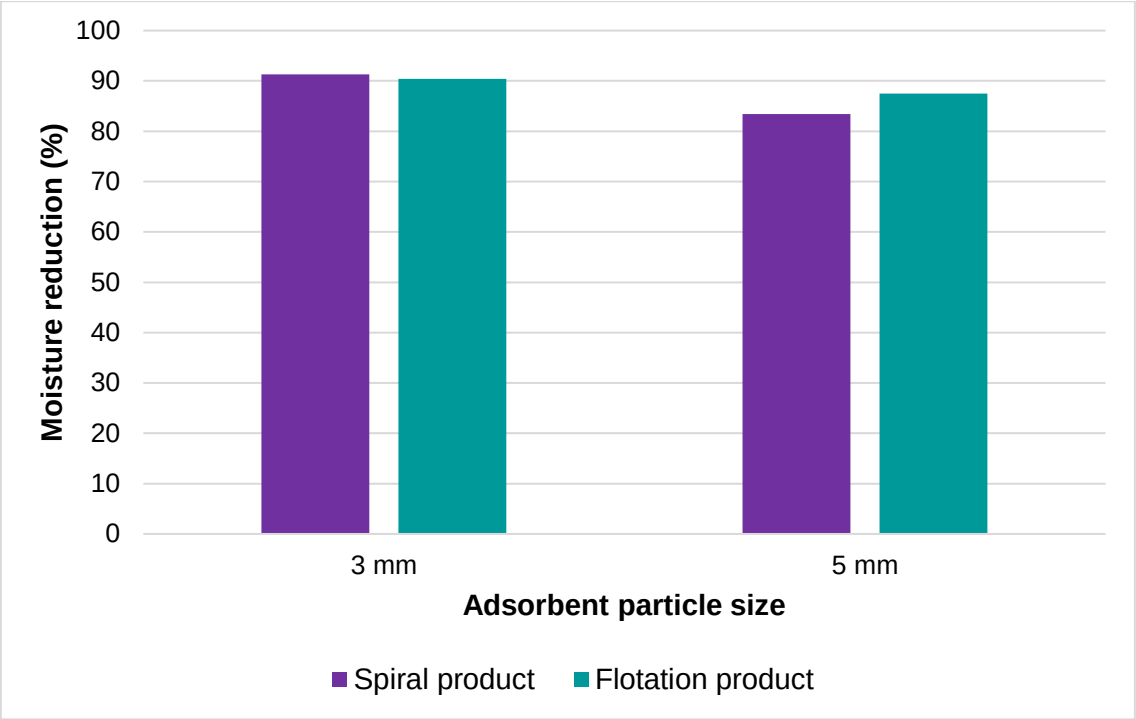

Figure 5-30 Moisture reductions of spiral vs flotation product using 3 mm and 5 mm activated alumina

In Figure 5-30, the flotation product experienced a slightly better moisture reduction than the spiral product using the 5 mm adsorbent due to the flotation product's ultra-fine particle size and larger contact surface area. The 3 mm adsorbent produced 10% better dewatering for the spiral product than the 5 mm adsorbent. For the flotation product, the 3 mm adsorbent performed 3% better than the 5 mm adsorbent. The effect of adsorbent particle size on dewatering performance was greater for the spiral product than the flotation product.

5.5.4 Effect of adsorbent state

This section briefly evaluates the spiral product and flotation product's dewatering performances affected by the adsorbent state. Figure 5-31 shows the spiral and flotation product's moisture reductions using new, spent and regenerated 3 mm activated alumina in a 2:1 adsorbent-to-coal mass ratio for 10 minutes.

In Figure 5-31, it can be seen that the spiral product experienced higher moisture reductions than the flotation product when using new and spent adsorbents. For the spiral product, the spent adsorbent performed 18% weaker than the new adsorbent, while the regenerated adsorbent had a 5% improvement in dewatering over its spent version. The spent adsorbent performed 36% weaker than the new adsorbent for the flotation product, while its regenerated version had a 48% improvement over its spent version.

The different adsorbent states' effect on dewatering could be seen more clearly for the flotation product than the spiral product. It can be seen, that the flotation product's spent adsorbents required a regeneration cycle more than the spiral product's spent adsorbents and that regeneration had a much greater improvement in dewatering abilities. Flotation product coal's dewatering is more sensitive to adsorbent states and prefers new or regenerated adsorbents.

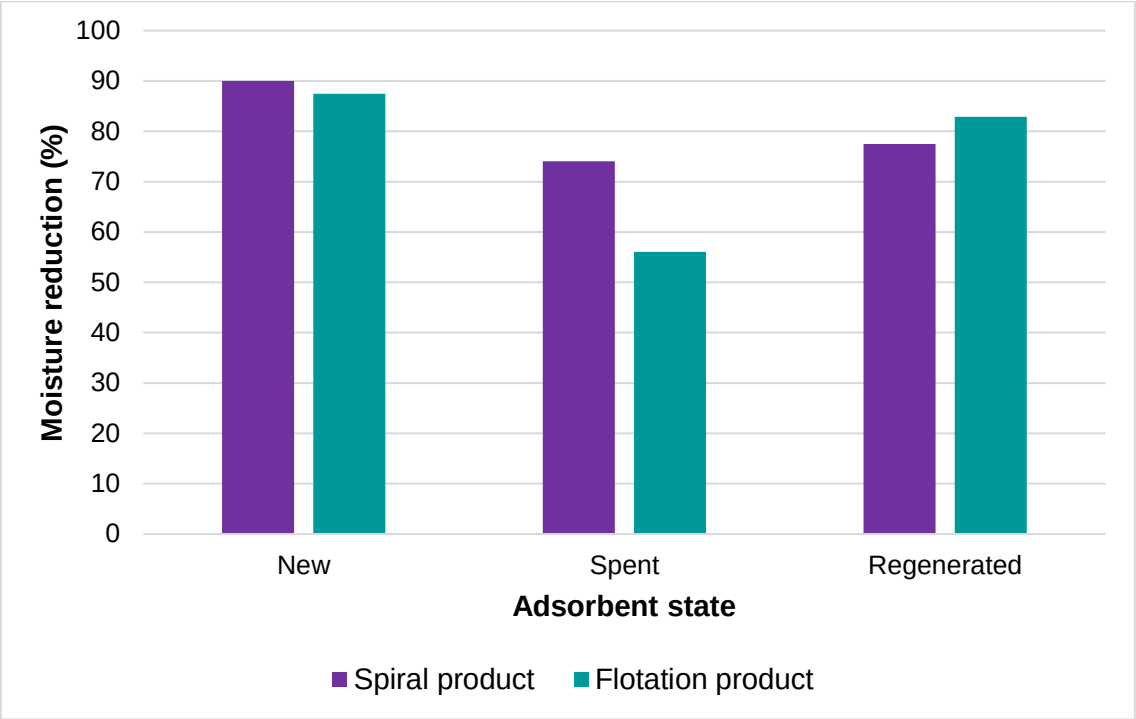

Figure 5-31 Moisture reductions of spiral vs flotation product using new, spent and regenerated activated alumina

5.5.5 Effect on calorific value

This section briefly examines how the dewatering of spiral and flotation product coal affected their calorific values. In this section, more focus is given on the calorific gains and less focus on comparing the two coals' dewatering effect. Two coals' dewatering behaviour cannot be compared based on calorific gains as the calorific values are highly sensitive to the coal's sampling.

Figure 5-32 shows the cumulative calorific gains of spiral and flotation product coals while they were dried by 3 mm activated alumina in a 2:1 adsorbent-to-coal mass ratio. The spiral product started with an initial calorific value of 21.9 MJ/kg, while the flotation product started with a significantly lower calorific value of 19.2 MJ/kg due to its higher moisture content.

In Figure 5-32, the flotation product's calorific value increased remarkably higher and faster than the spiral product, keeping in mind that it started with a lower calorific value giving more room for improvement. Within 2 minutes, the spiral and flotation product gained 2.8 and 3.8 MJ/kg, relating

to 13% and 20% increases in calorific value, respectively. Halfway through, the spiral and flotation product's calorific values increased by 16% and 29%, respectively. The spiral product and flotation product coal ended with calorific values of 25.6 and 25 MJ/kg, producing overall gains of 16% and 30%, respectively.

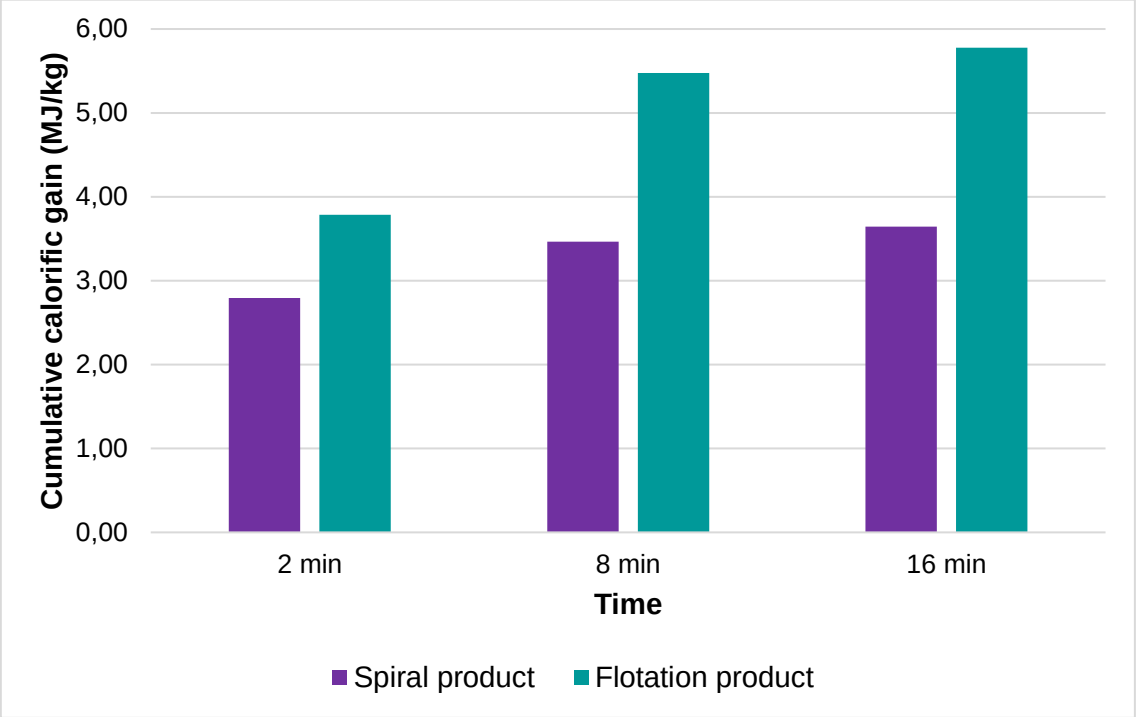

Figure 5-32 Cumulative calorific gains of spiral vs flotation product

Section 5.5 concludes that spiral product and flotation product coal's dewatering behave in a very similar manner, irrespective of adsorbent-to-coal mass ratios. The flotation product's ultra-fine particle size, availing larger contact surface area, played a significant role in its dewatering, making the effect of adsorbent particle size less prevalent than for the spiral product as it substituted the larger adsorbent's shortcoming of contact surface area.

Furthermore, the flotation product is more sensitive to the adsorbent state than the spiral product while preferring only new or regenerated adsorbents. Remarkable increases in calorific values were reported for both product coals, which will care for considerable advantages in the industrial applicability calculations.

5.6 Qualitative remarks

This section gives attention to qualitative remarks and unmeasured phenomena noted during experimental work. Photographs of various encounters receive attention and are discussed.

5.6.1 Materials handling

During experimental procedures, as in the case with spiral coal, it was noted that proper materials handling was crucial for good dewatering. The flotation coal had a considerable affinity for caking due to the moisture and possibly the flotation reagents retained between the coal particles. The flotation product coal had many lumps or clots between the ultra-fine particles. Materials handling, in this case, refers to the due care taken to sufficiently break these lumps and cakes. Looser coal particles will be dewatered easier. In practice, as with spiral coal, it is suggested to use a high-speed pugmill with an open bottom to break these lumps and cakes before mixing the adsorbents and coal.

Figure 5-33 shows a worst-case scenario of flotation product having small lumps even after dewatering. The inner coal particles within the lumps would not be dried as needed. This scenario can be avoided primarily by breaking the lumps before mixing the coal with adsorbents and secondarily through specialised designed cylindrical vessels.

Figure 5-33 Small lumps of flotation product coal with activated alumina

5.6.2 Adsorbent's capillary pore blinding

As seen with spiral coal, it was noted that the adsorbents' surfaces became dirtier and darker with usage, realising that the adsorbents' performance decreased with usage. Figure 5-34 shows a photograph of flotation product's spent adsorbents' surfaces getting coated with coal dust through continual usage.

Figure 5-34 Coal dust entrapment on flotation product's spent activated alumina

The connection was made that this coal dust entrapment would blind the adsorbents' capillary pores, inhibiting their adsorption performances. Sections 5.2.4 and 5.3.3 discussed how spent adsorbents had weaker performances than new adsorbents. Figure 5-35 and Figure 5-36 compare the SEM scans, at 1000x and 5000x magnifications, of new and spent activated alumina used for dewatering flotation product coal.

In Figure 5-35, foreign particles, presumably coal dust, can be seen on the spent adsorbent's surface compared to the new adsorbent's surface. In Figure 5-36, these foreign particles are magnified and seem to close down openings (pores) on the adsorbent's surface. This closing down or blinding of the pore openings will inhibit moisture adsorption.

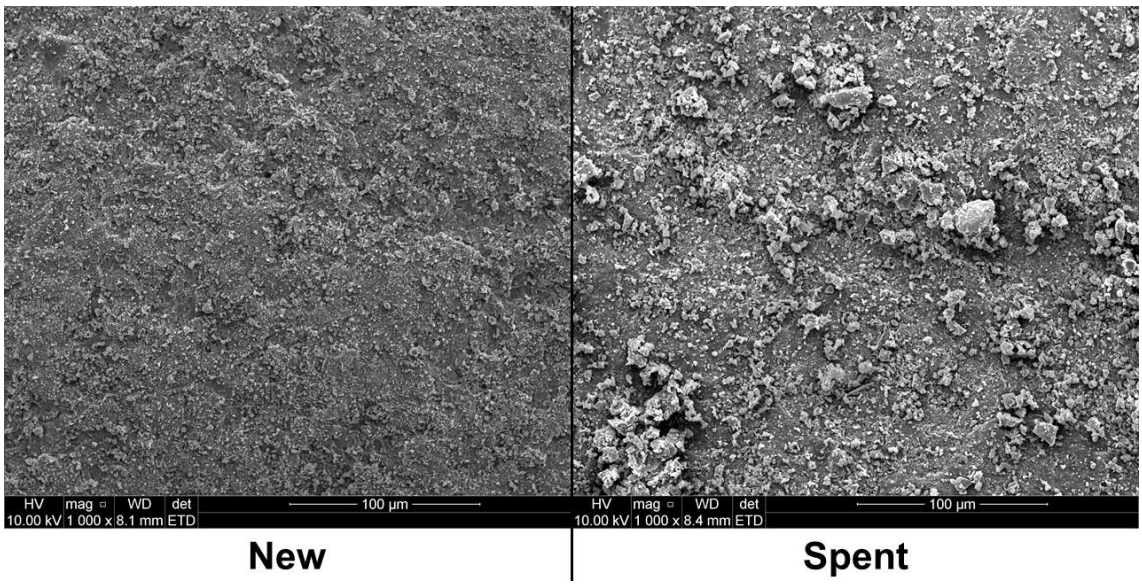

Figure 5-35 SEM scans of new and spent activated alumina used on flotation product (1000x magnified)

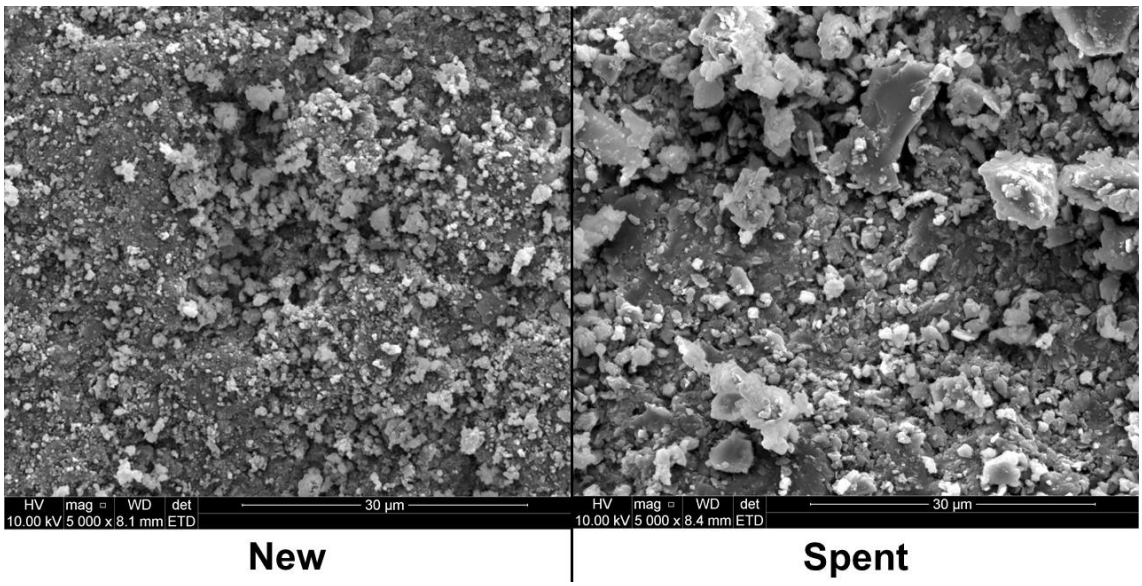

Figure 5-36 SEM scans of new and spent activated alumina used on flotation product (5000x magnified)

5.6.3 Adsorbents' robustness

During dewatering experiments, the two adsorbents, namely activated alumina and molecular sieves, behaved differently concerning their robustness during continuous use. The activated alumina performed exceptionally well regarding its industrial robustness, while the molecular sieves performed poorly.

In general, during all the dewatering experiments and general materials handling, the activated alumina showed very little to no breakage and attrition of the adsorbent particles signifying its industrial use eligibility.

On the other hand, Molecular sieves showed signs of brittleness, having considerable breakage of the adsorbent particles. Figure 5-37 shows the breakage and brittleness of the molecular sieves.

Figure 5-37 Molecular sieves' brittleness and particle breakage

5.6.4 Design considerations

This section discusses how the abovementioned concerns can be overcome during the design of an adsorbent assisted drying plant, whether pilot or industrial.

As in the case with spiral coal, a pugmill with an open bottom should be installed upstream of the cylindrical vessels before coal and adsorbent mixing for proper materials handling. Also, the rotating paddles should be designed and arranged to break small lumps and cakes, discharging only fine and loose coal particles.

Additionally, inside the cylindrical vessels, a specialised design of baffle plates will be needed, ensuring proper mixing of the coal and adsorbents and the coal particles to be as loose as possible.

Design suggestions to overcome capillary pore blinding are discussed in Section 6.4.4.

5.7 Conclusion

The section on drying of flotation coal concluded that flotation product could be dried to market specifications using activated alumina as an adsorbent. The flotation product was dried swiftly, reaching target moisture after two minutes. The moisture reduction caused the flotation product's calorific value to increase by 30% overall. As with spiral coal, optimal dewatering performance was driven by good contact surface area between the coal and adsorbents, achieved by higher adsorbent-to-coal mass ratios or smaller adsorbent particle sizes.

Spent activated alumina could dewater the flotation product confirming that a bone-dry adsorbent is not needed during regeneration. However, more than two consecutive uses of the adsorbents, without regeneration, showed insufficient dewatering. Regenerated adsorbents dewatered the flotation product to market standards within short drying times, showing substantial improvement over the spent adsorbent. Conventional furnace regenerated adsorbents did not necessarily deliver better dewatering than air-blown regenerated adsorbents considering both adsorbent particle sizes' performances.

The use of new molecular sieves to dry flotation coal showed exceptionally fast dewatering within target moisture, having the coal dewatered to near bone-dry moisture contents. However, spent molecular sieves showed poor coal dewatering, while its regenerated version showed meagre improvement and insufficient coal dewatering. These results proved molecular sieves' ineligibility for industrial use.

The comparison of spiral coal with flotation coal concluded that even though they vastly differed in particle size, their dewatering behaviours were similar, experiencing almost identical moisture desorption rates and moisture reductions. From these results, it can be concluded that the flotation reagents had little to no effects on the coal's dewatering. Lower adsorbent-to-coal mass ratios and larger adsorbent particle sizes had less weak drying effects on flotation coal than on spiral coal due to flotation coal's ultrafine particle size. The smaller particle size of flotation coal increased the contact surface area between the coal and adsorbents.

Qualitative observations showed the flotation coal having an affinity for caking and forming lumps, which inhibits dewatering performance, concluding how necessary suitable materials handling is before drying occurs. Blinding of the adsorbents' capillary pores may have played a significant role in the adsorbents' drying performance during continuous use without regeneration. Further qualitative observations showed the robustness of the activated alumina during use with negligible to no particle breakage, while the molecular sieves showed brittleness and particle breakage. Molecular sieves' brittleness added to its ineligibility for industrial use.

Chapter 6 Regeneration of adsorbents

6.1 Introduction

This chapter reflects on the regeneration of spent activated alumina and molecular sieves. The spent activated alumina being regenerated was used for dewatering of spiral product and flotation product coal, as discussed in Sections 4.2 and 5.2. The spent molecular sieves being regenerated was used for dewatering flotation product coal, as discussed in Section 5.3.

The spent activated alumina of particle sizes 3 mm and 5 mm were regenerated and investigated in detail as the primary adsorbent. The spent molecular sieves of particle size 3-5 mm were regenerated and investigated more briefly as the secondary adsorbent. Regeneration was done through a packed bed column using ambient airflow, conditioned at 22°C and 70% relative humidity. The purpose of the air's conditioning was to maintain an ambient temperature with no additional applied heat, while the relative humidity was to simulate humid weather in practice.

In this chapter, the desaturation curves of activated alumina are discussed, where new/unused activated alumina was drenched in water for five minutes, after which it was regenerated using the same regeneration process as for the spent adsorbents.

In Section 6.4, qualitative remarks of unmeasured phenomena are discussed. Qualitative remarks may include difficulties, successes, industrial applicability concerns and keynotes experienced during experimental work.

All experimental work was conducted methodological, as described in Section 3.3, and in a laboratory kept at a constant temperature of 22°C.

6.2 Activated alumina

6.2.1 Desaturation curves

This section focuses on the activated alumina's desaturation curves to comprehend how new and clean activated alumina, that is partially saturated with water, will regenerate without any external factors like dirty spent adsorbents and dust entrapment in capillary pores.

The respective 3 mm and 5 mm new/fresh activated alumina were drenched in clean water for five minutes to saturate partially. The partially saturated adsorbents were then regenerated for 60 minutes using ambient airflow provided by a blower while measuring the adsorbent moisture contents (moisture loads) at predetermined time intervals.

Additionally, adding to the industrial considerations, the short five-minute drenching duration simulates a cleaning process in which the adsorbents are cleaned of excessive coal dust entrapped on the adsorbents' surfaces which inhibits adsorption, as discussed in Chapters 4 and 5. In practice, the adsorbents can be cleaned via high-pressure water that is sparged through fine nozzles. This cleaning process forms part of a continuous adsorbent assisted dewatering plant concept design, discussed in Chapter 7.

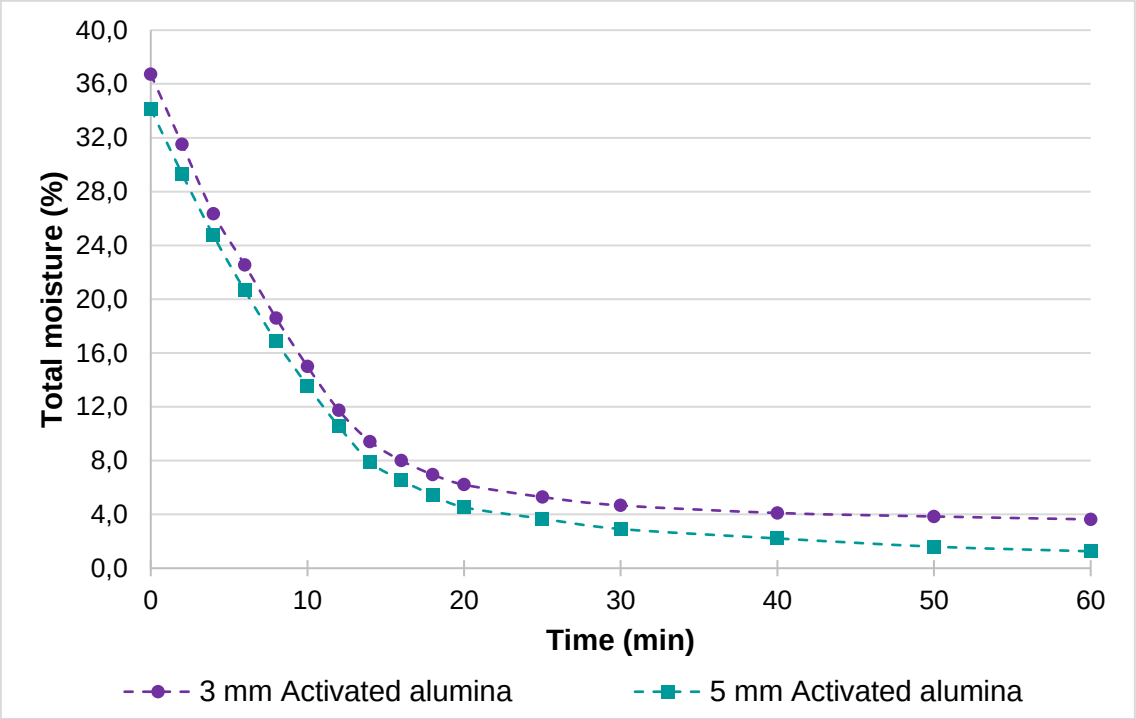

Figure 6-1 Desaturation curves of the 3 mm and 5 mm activated alumina

Figure 6-1 shows the desaturation curves of the 3 mm and 5 mm activated alumina after being regenerated for 60 minutes using ambient airflow conditioned at 22°C and 70% RH. After being

drenched in water for five minutes, the 3 mm activated alumina had a partially saturated moisture load of 36.7% w/w, while the 5 mm activated alumina had a moisture load of 34.1% w/w. During regeneration, the 3 mm and 5 mm adsorbents' desaturation curves followed almost identical paths but with different initial and final moisture loads. The desaturation followed a steep decrease in moisture loads until 12 minutes into regeneration, whereafter the desaturation rate gradually decreased until the end of regeneration.

Within two minutes of regeneration, the 3 mm adsorbent lost 5.2% w/w moisture, while the 5 mm adsorbent lost 4.8% w/w moisture at desaturation rates of 0.026 and 0.024 $g_{moisture}/g_{ads}$.min, respectively. After 10 minutes, both adsorbents lost more than half of their initial moisture, with moisture reductions in the vicinity of 60%. Both adsorbents reached the sub 10% w/w moisture mark 14 minutes into regeneration. After 20 minutes, moisture loads of 6.2% and 4.5% w/w were recorded for the 3 mm and 5 mm adsorbents. Final moisture loads of 3.6% and 1.3% w/w were recorded for the 3 mm and 5 mm activated alumina, equating to remarkable 90% and 96% moisture reductions.

Section 3.5 discussed the experiments' reproducibility and the results' integrity determined with the T-test, with a 90% confidence interval. The desaturation test was done three times to determine the experimental reproducibility. Figure 6-2 shows the 3 mm activated alumina's average desaturation curve with its upper and lower limit standard deviation curves.

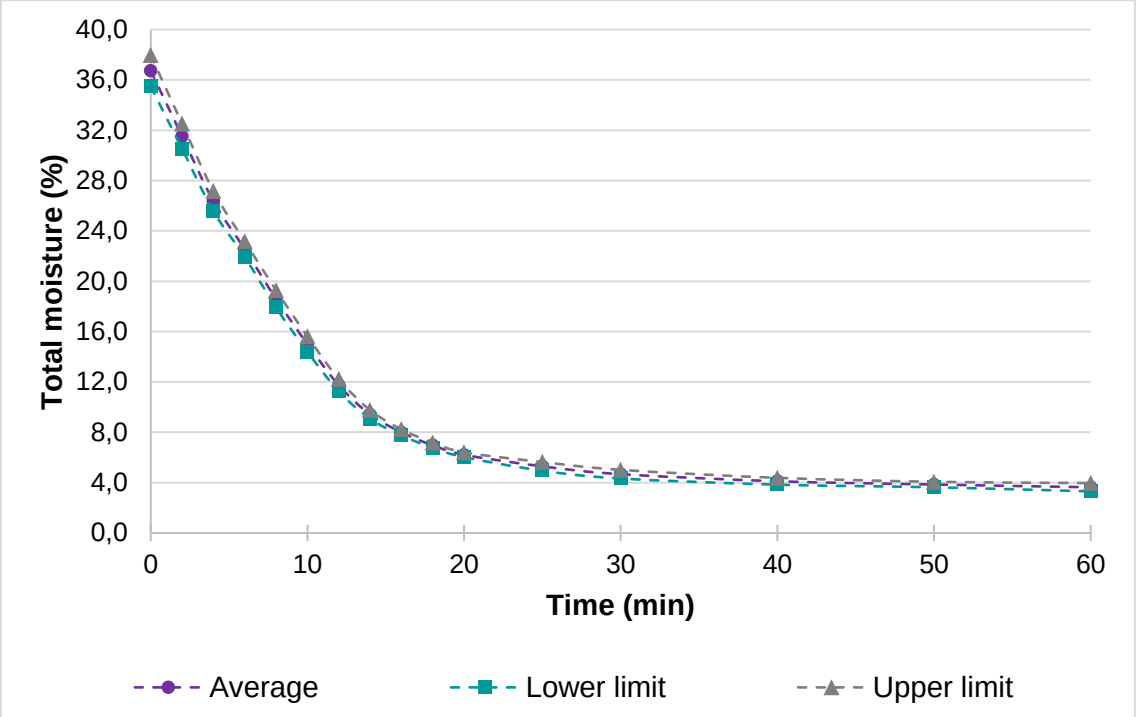

Figure 6-2 Desaturation curve of the 3 mm activated alumina with its standard deviation

In Figure 6-2, the 3 mm activated alumina started with an average moisture load of 36.7% w/w with an upper and lower limit of 38.0% and 35.5% w/w. During regeneration, the upper and lower limit standard deviation curves paralleled the average curve to a considerable extent. After 30 minutes, the moisture load averaged 4.7% w/w with upper and lower limits of 5.0% and 4.3% w/w. After regeneration of 60 minutes, the activated alumina had an average moisture load of 3.6% w/w with upper and lower limit standard deviations of 4.0% and 3.3% w/w.

Further reference can be given to Table 6-1, summarising the standard deviation and relative experimental errors for the feed and final moisture loads of the 3 mm activated alumina. The low standard deviations and relative experimental errors recorded, indicate reputable experimental data.

Table 6-1 Standard deviation and relative experimental error for the 3 mm activated alumina's desaturation

Time (min)	Average (% w/w)	Standard deviation (% w/w)	Relative experimental error (%)
0	36.72	1.25	5.74
60	3.63	0.33	15.32

6.2.2 Spiral product's spent activated alumina

This section discusses the regeneration of spent activated alumina after being used for dewatering spiral product coal. The spent 3 mm, and 5 mm adsorbents were regenerated according to their respective adsorbent-to-coal mass ratios in which they were used. For example, all the 3 mm adsorbents used in the 2:1 adsorbent-to-coal mass ratio were kept separate, while all their usage cycles' adsorbents were mixed for 10 minutes to reach equilibrium with one another. The total number of spent adsorbents, for each particle size and adsorbent-to-coal mass ratios, were then regenerated for 20 minutes.

Figure 6-3 shows the regeneration curve of spent 3 mm activated alumina after being used in a 2:1 adsorbent-to-coal mass ratio for dewatering spiral product coal. The accumulated coal dust collected from the spent adsorbents during the regeneration process is also shown in Figure 6-3. The spent adsorbents entered the regeneration process at an initial moisture load of 9.0% w/w. It is imperative to note that this initial moisture load will differ from the moisture loads recorded in Figure 4-12 due to mixing the various usage cycles' adsorbents and the possible moisture transport during materials handling.

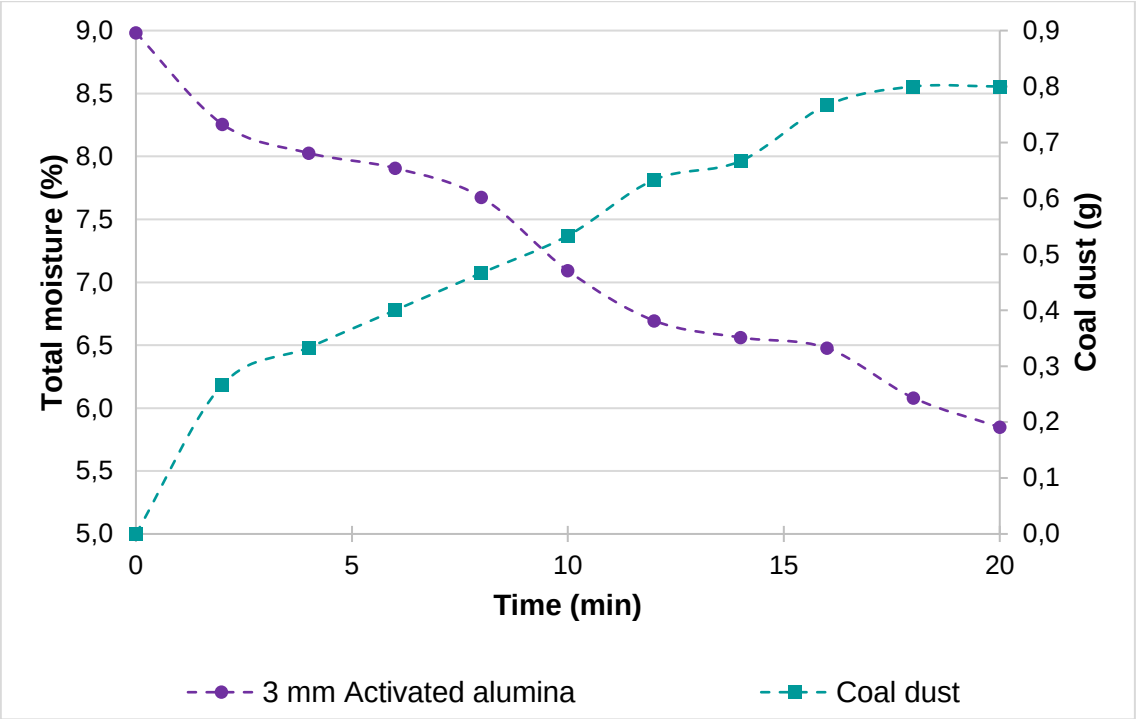

Figure 6-3 Regeneration curve of 3 mm activated alumina after spiral product drying

In Figure 6-3, the regeneration curve followed a swift decline in moisture until 2 minutes; then a more gradual decline until 8 minutes, whereafter the moisture again decreased slightly faster until 20 minutes. After two minutes, the adsorbent saw a moisture reduction of 8%. Halfway into regeneration, the adsorbent had its moisture reduced by 21%, and after 20 minutes, the adsorbent had a final moisture load of 5.9% w/w, relating to a 34% moisture reduction.

The regeneration column was filled with a bed mass of 340 g of 3 mm activated alumina in the experiment discussed above. During regeneration, the coal dust entrapped between the adsorbent particles and released due to the airflow was removed from the exit gas stream (Figure 3-10). Figure 6-3 shows that the coal dust accumulated to a meagre total of 0.8 g. The removed coal dust equates to an insignificant 0.24% of the total bed mass being regenerated. For all the other regeneration experiments in this section, even lower coal dust accumulations were recorded. These insignificant amounts of coal dust are not further reported in this section.

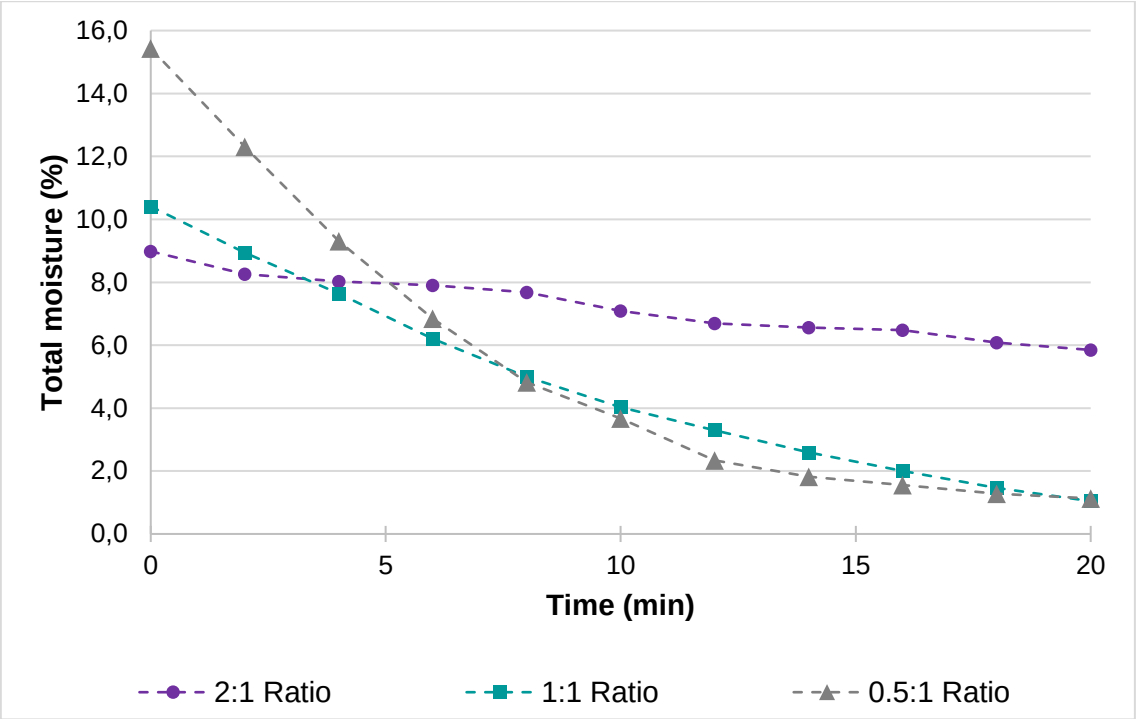

Figure 6-4 Regeneration curves of 3 mm activated alumina for various adsorbent-to-coal mass ratios after spiral product drying

At the start of this section, it was mentioned that each adsorbent-to-coal mass ratio's spent adsorbents were regenerated separately. Therefore, the regeneration column was filled with different amounts of spent adsorbent, depending on the adsorbent-to-coal mass ratio. For the 2:1 ratio, the regeneration column was filled with 340 g of spent adsorbent. For the 1:1 and 0.5:1 ratios, the column was filled with 180 g and 100 g of spent adsorbent, respectively.

Figure 6-4 shows the regeneration curves of spent 3 mm activated alumina used in various adsorbent-to-coal mass ratios for dewatering spiral product. A clear difference between the regeneration curves for each adsorbent-to-coal mass ratio is observed with different initial spent moisture loads, regeneration rates and final moisture loads. The spent adsorbents had initial moisture loads of 9.0%, 10.4% and 15.4% w/w for the 2:1, 1:1 and 0.5:1 adsorbent-to-coal mass ratios, respectively. Chapters 4 and 5 discussed how lower adsorbent-to-coal mass ratios call for higher adsorbent moisture loads relative to adsorbent mass.

Furthermore, in Figure 6-4, the lower adsorbent-to-coal mass ratios regenerated at faster regeneration rates than the higher adsorbent-to-coal mass ratios while achieving lower final moisture loads. Within two minutes, the adsorbents regenerated at initial regeneration rates of 0.004, 0.008 and 0.016 $g_{moisture}/g_{ads}$.min for the 2:1, 1:1 and 0.5:1 adsorbent-to-coal mass ratios, respectively. A precise doubling in regeneration rate occurs for each halving of the adsorbent-to-coal mass ratio. Final moisture loads of 5.9%, 1.0% and 1.1% w/w were recorded for the 2:1, 1:1 and 0.5:1 adsorbent-to-coal mass ratios.

The apparent difference in regeneration rates indicates that the adsorbents' regeneration rates are inversely proportional to the adsorbent-to-coal mass ratio or, more specifically, the bed mass in the regeneration column. Smaller bed masses in the regeneration column call for faster regeneration rates and vice versa. This correlation can best be explained while briefly referring to the Ergun Equation for fluid flow through packed beds, Equation (6-1):

$$\boldsymbol{\Delta P = \frac{150 L \mu (1-\varepsilon)^2 v}{\varepsilon^3 d_p^2} + \frac{1.75 L (1-\varepsilon) \rho v^2}{\varepsilon^3 d_p}} \qquad (6\text{-}1)$$

where $\Delta P =$ pressure differential

$L =$ bed height

$\mu =$ fluid viscosity

$\varepsilon =$ voidage factor

$v =$ superficial fluid velocity

$d_p =$ particle diameter

$\rho =$ fluid density

During the regeneration experiments, the regeneration column was a Perspex cylinder with a constant diameter, meaning that an increase in bed mass can only cause an increase in bed height. Nonetheless, assume all the variables in Equation (6-1), except the bed height, to be constant during regeneration, keeping in mind that the superficial fluid velocity is a mere calculation of the volumetric flow rate divided by the cross-sectional area and not the actual fluid velocity passing through the particles, hence superficial.

An increase in bed mass would mean an increase in bed height. According to Equation (6-1), an increase in bed height will lead to a higher pressure differential over the bed. This higher pressure differential over the bed will, in effect, cause inhibited airflow between the particles. The inhibited airflow subsequently causes slower moisture transport away from the adsorbents, causing slower regeneration rates. In return, smaller bed heights will lead to lower pressure differentials and, subsequently, faster regeneration rates. This relation is evident in Figure 6-4 and Figure 6-5. Additionally, a smaller adsorbent mass will receive the same amount of airflow as a larger adsorbent mass, causing the larger adsorbent mass to have less air per adsorbent particle to transport moisture while the smaller adsorbent mass will receive more air per adsorbent particle to transport moisture, leaving the smaller adsorbent mass to regenerate faster.

The relationship discussed above concluded the main driving force for optimal regeneration to be the adsorbent bed mass to regeneration column area ratio. Low adsorbent bed mass to regeneration column area ratios will achieve faster regeneration than high adsorbent bed mass to regeneration column area ratios.

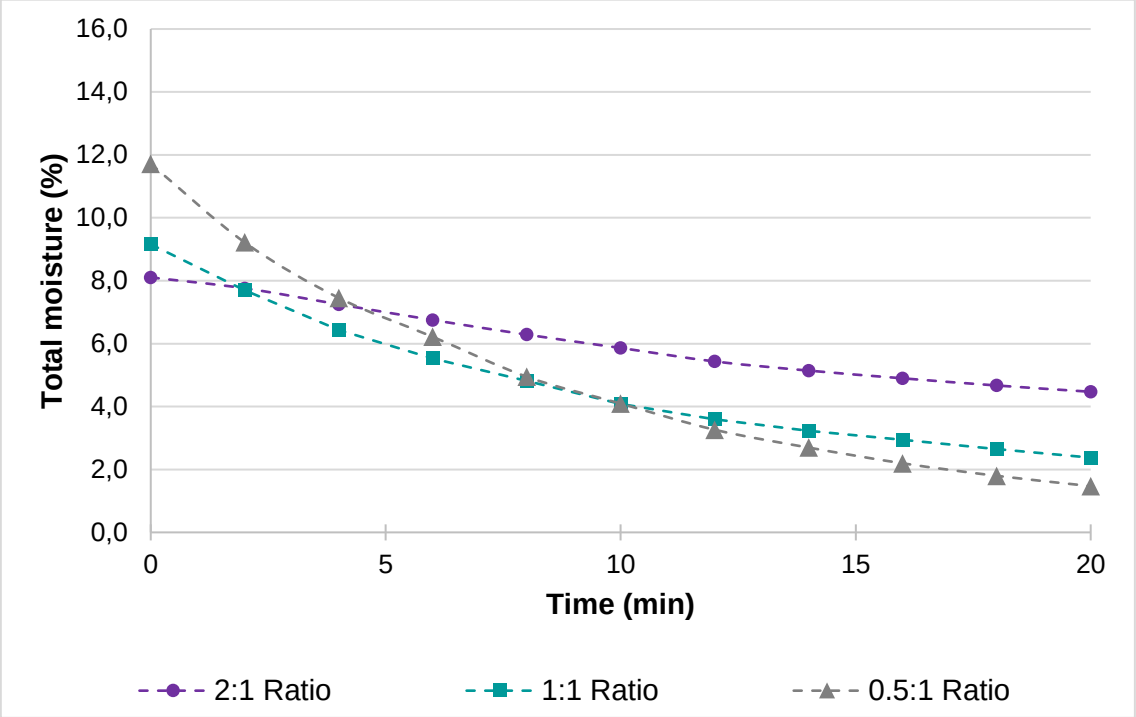

Figure 6-5 Regeneration curves of 5 mm activated alumina for various adsorbent-to-coal mass ratios after spiral product drying

Figure 6-5 receives brief attention showing the regeneration curves of spent 5 mm activated alumina used in various adsorbent-to-coal mass ratios for dewatering spiral product. The same correlations discussed for the 3 mm activated alumina exist for the 5 mm activated alumina. The lower adsorbent-to-coal mass ratios experienced faster regeneration, achieving lower final moisture loads than the higher ratios. Initial moisture loads of 8.1%, 9.2% and 11.7% w/w were recorded for the 2:1, 1:1 and 0.5:1 adsorbent-to-coal mass ratios, respectively. After 20 minutes, the 2:1 adsorbent-to-coal mass ratio experienced a 44% moisture reduction, while the 1:1 and 0.5:1 ratios saw 74% and 87% moisture reductions, respectively.

In Figure 6-6, a comparison is drawn between the 3 mm and 5 mm activated alumina's regeneration curves. The regeneration curves do not parallel each other and have different initial moisture loads, regeneration rates and final moisture loads. The 3 mm and 5 mm adsorbents started with initial moisture loads of 9.0% and 8.1% w/w, respectively. Halfway through the regeneration, the 3 mm and 5 mm adsorbent experienced moisture reductions of 21% and 27%, respectively. After 20 minutes, the adsorbents achieved moisture reductions of 34% and 44% for the 3 mm and 5 mm adsorbents, respectively.

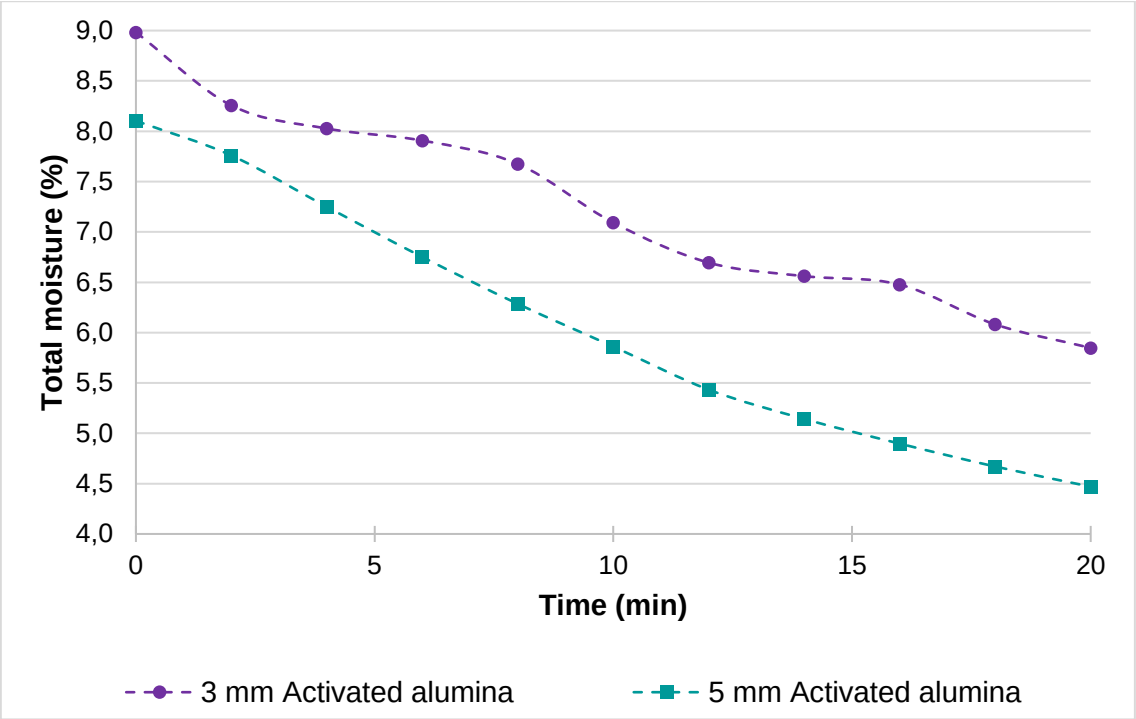

Figure 6-6 Regeneration curves of 3 mm vs 5 mm activated alumina after spiral product drying

Halfway through and overall, the 5 mm activated alumina showed faster regeneration than the 3 mm activated alumina. This relation is once again explained by briefly referring to Equation (6-1). Assume all the variables in Equation (6-1), except the particle diameter, to be constant while assuming the bed height difference, due to bulk density difference caused by particle diameter difference, to be negligible.

According to Equation (6-1), a larger particle diameter will cause a lower pressure differential over the bed. This lower pressure differential will, in effect, alleviate the airflow through the bed. The alleviated movement of air between the particles will, in turn, improve the moisture transport from the adsorbents. The improved moisture transport subsequently calls for faster regeneration rates and lower final moisture loads. Therefore, an adsorbent's regeneration rate is directly proportional to its particle diameter. Larger particle sizes call for faster regeneration and vice versa.

The regeneration of the spent activated alumina was experimentally done three times, as discussed in Section 3.5, to determine the experimental results' integrity. Figure 6-7 shows the average regeneration curve of 3 mm activated alumina used to dewater spiral product with lower and upper limit standard deviations.

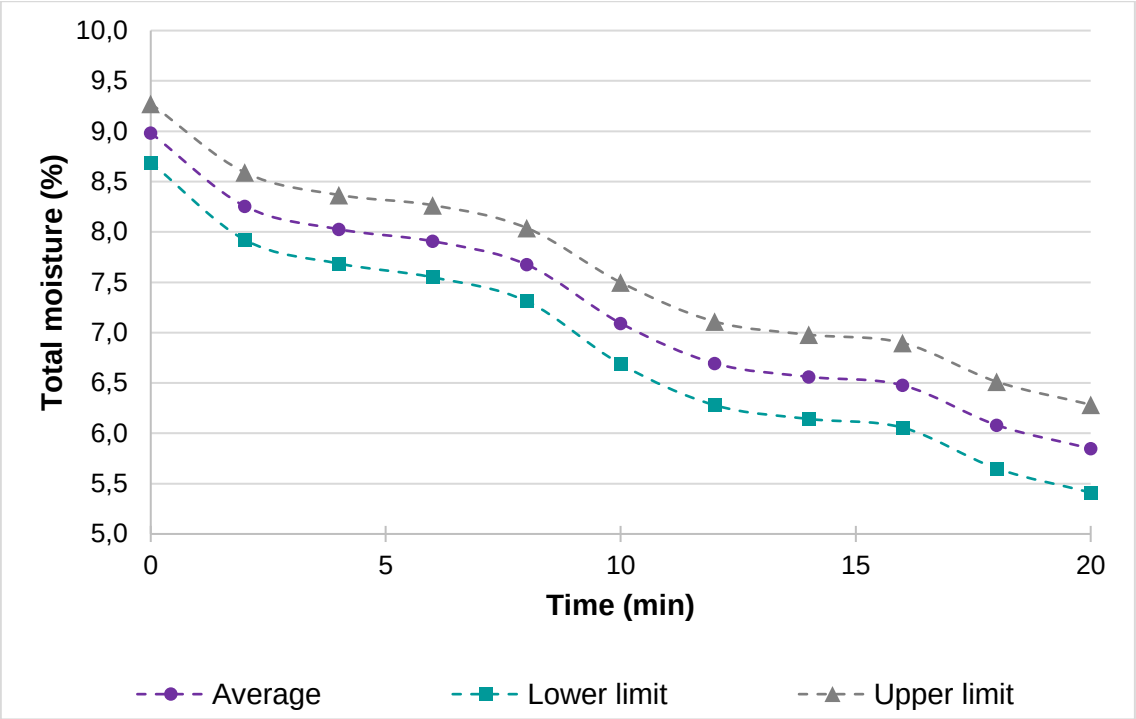

Figure 6-7 Regeneration curve of 3 mm activated alumina with its standard deviation after spiral product drying

In Figure 6-7, the 3 mm adsorbent starts with an average moisture load of 9.0% w/w with upper and lower limit standard deviations of 9.3% and 8.7% w/w. After regeneration, the final moisture load averaged at 5.9% w/w with upper and lower limit standard deviations of 6.3% and 5.4% w/w. Further reference is given to Table 6-2, showing the standard deviation and relative experimental error for the 3 mm activated alumina's regeneration after spiral product dewatering. The low standard deviations and experimental error are indicative of reliable results.

Table 6-2 Standard deviation and relative experimental error for 3 mm activated alumina's regeneration after spiral product drying

Time (min)	Average (% w/w)	Standard deviation (% w/w)	Relative experimental error (%)
0	8.98	0.29	5.46
20	5.85	0.44	12.58

6.2.3 Flotation product's spent activated alumina

This section discusses the regeneration of spent activated alumina used for dewatering flotation product coal. The spent 3 mm, and 5 mm adsorbents were regenerated according to their respective adsorbent-to-coal mass ratios in which they were used, as explained in Section 6.2.2. Additional results of the regeneration of flotation product's spent adsorbents, which were not discussed in this section can be found in Annexure B.1.

Figure 6-8 reveals the regeneration curve of spent 3 mm activated alumina used in a 2:1 adsorbent-to-coal mass ratio for dewatering flotation product coal. The accumulated coal dust collected from the spent adsorbents during regeneration is also shown in Figure 6-8. The regeneration process started with the spent adsorbents having an initial moisture load of 9.1% w/w. As mentioned in Section 6.2.2, it is to be noted that this initial moisture load will differ from the moisture loads recorded in Figure 5-11 due to the mixing of the various usage cycles' adsorbents and the natural moisture transport during materials handling.

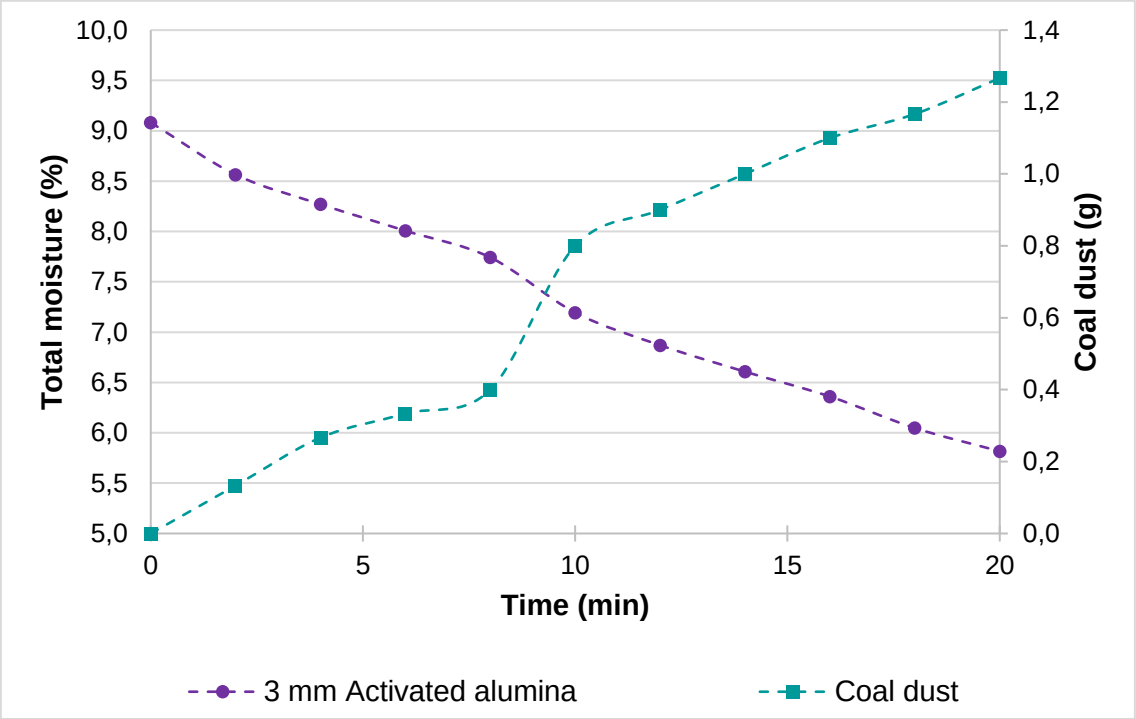

Figure 6-8 Regeneration curve of 3 mm activated alumina after flotation product drying

In Figure 6-8, the regeneration curve followed an almost linear decline in moisture until the end. Within two minutes, the adsorbent underwent a moisture reduction of 5%. Halfway into regeneration, the adsorbent saw a moisture reduction of 21%, and after 20 minutes, the adsorbent had a final moisture load of 5.8% w/w, relating to a 36% moisture reduction.

During regeneration, the coal dust entrapped between the adsorbent particles and released due to the airflow accumulated to a meagre total of 1.3 g, as shown in Figure 6-8. The removed coal

dust equates to a trivial 0.38% of the total bed mass being regenerated. To show the experimental results' integrity, Figure 6-9 shows the average regeneration curve of 3 mm activated alumina used for dewatering flotation product with lower and upper limit standard deviations.

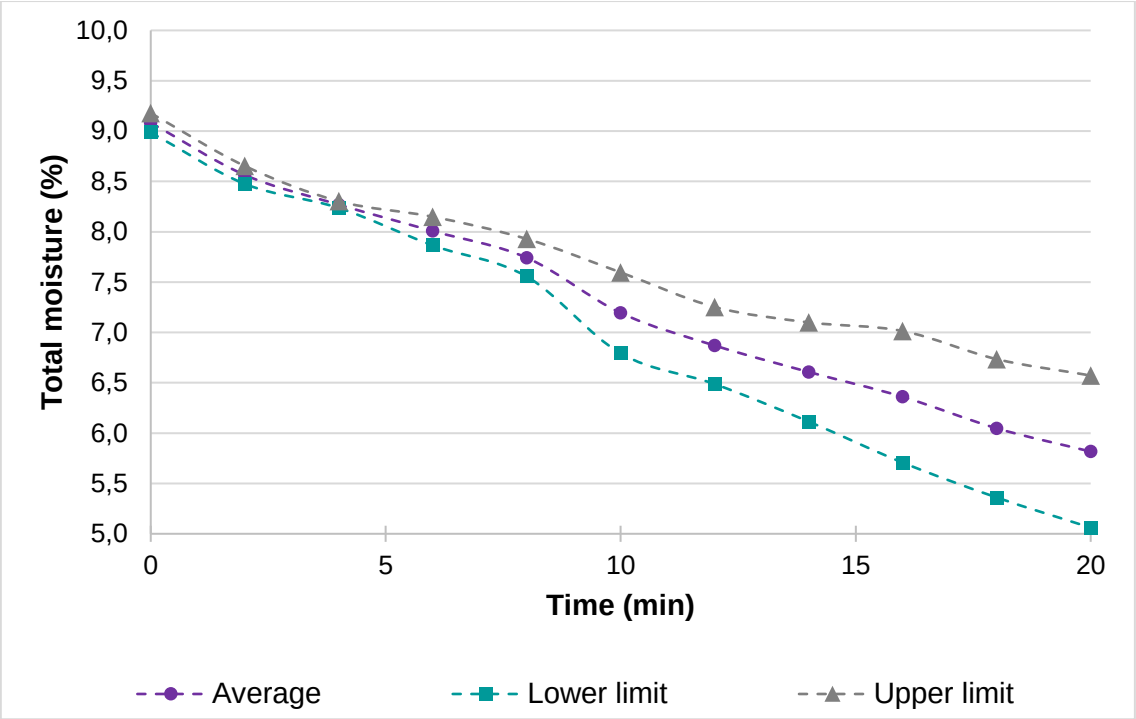

Figure 6-9 Regeneration curve of 3 mm activated alumina with its standard deviation after flotation product drying

Figure 6-9 shows the 3 mm adsorbent starting with an average moisture load of 9.1% w/w with upper and lower limit standard deviations of 9.2% and 9.0% w/w. After regeneration, the final moisture load averaged at 5.8% w/w with upper and lower limit standard deviations of 6.6% and 5.1% w/w. Table 6-3 shows the standard deviation and relative experimental error for the 3 mm activated alumina's regeneration after flotation product dewatering. Low standard deviations and experimental errors were recorded at the start of the regeneration process, with somewhat more significant standard deviations and relative experimental errors at the end of the regeneration process, which can be expected.

Table 6-3 Standard deviation and relative experimental error for 3 mm activated alumina's regeneration after flotation product drying

Time (min)	Average (% w/w)	Standard deviation (% w/w)	Relative experimental error (%)
0	9.08	0.10	1.78
20	5.82	0.76	21.9

6.3 Molecular sieves

6.3.1 Flotation product's spent molecular sieves

Even though Section 5.3.3 concluded that regenerated molecular sieves did not dewater flotation product coal to market specifications, this section briefly discusses the regeneration of spent molecular sieves after being used for dewatering flotation product coal. The spent molecular sieves were regenerated for 20 minutes using ambient airflow as per Section 3.3.2.

Figure 6-10 shows the regeneration curve of spent molecular sieves after being used in a 1:1 adsorbent-to-coal mass ratio for dewatering flotation product coal. The accumulated coal dust collected from the spent adsorbents during regeneration is also shown in Figure 6-10. The spent adsorbents had an initial moisture load of 10.9% w/w. This initial moisture load will differ from the moisture loads recorded in Figure 5-23 due to the mixing of the various usage cycles' adsorbents and the possible moisture transport during materials handling.

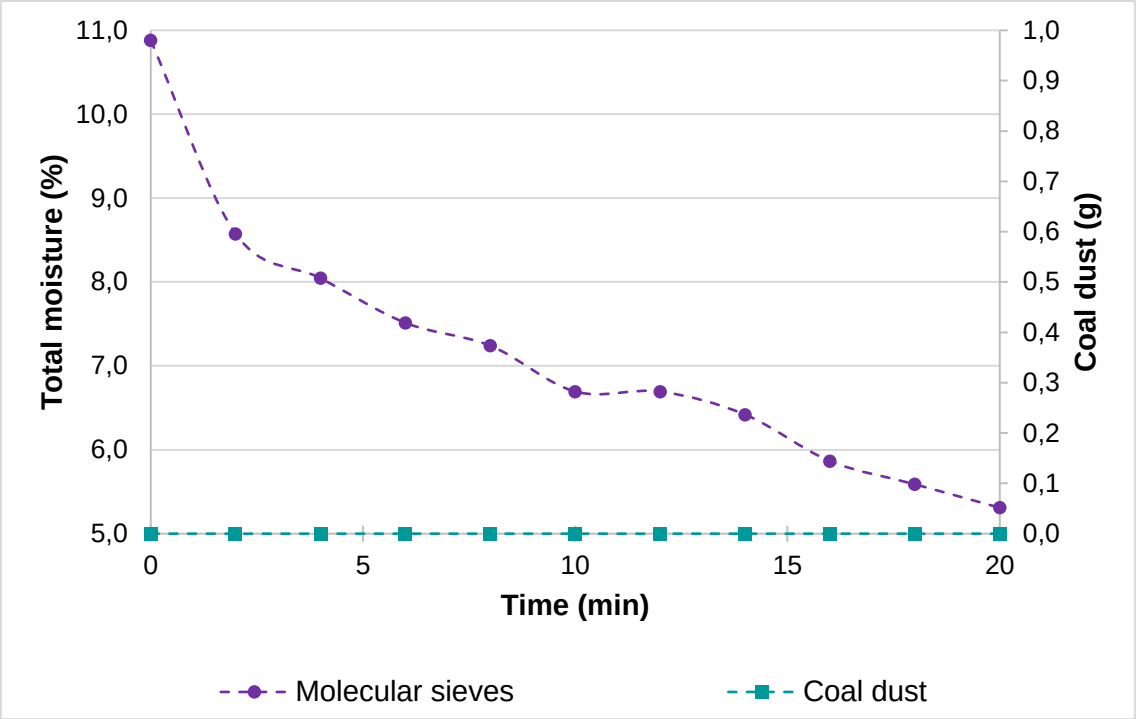

Figure 6-10 Regeneration curve of molecular sieves after flotation product drying

Figure 6-10 shows the molecular sieves' moisture load swiftly decreasing for 2 minutes, after which it gradually decreased until 20 minutes. Within 2 minutes, the adsorbent experienced a 21% moisture reduction. Halfway into regeneration, the adsorbent experienced a 39% moisture reduction, and after 20 minutes, the adsorbent had a final moisture load of 5.3% w/w, relating to a 51% moisture reduction. Figure 6-10 reveals that, during regeneration, no coal dust entrapped between the adsorbent particles was removed from the exit gas stream.

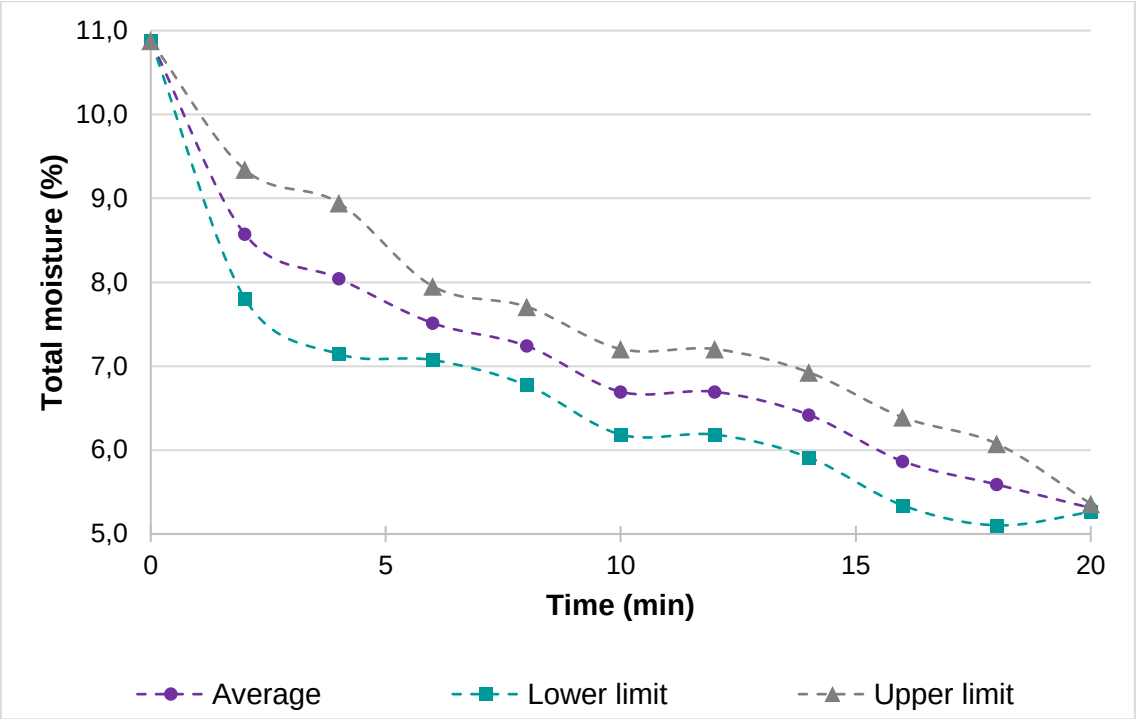

Figure 6-11 Regeneration curve of molecular sieves with standard deviation after flotation product drying

As per Section 3.5, the spent molecular sieves' regeneration was experimentally done three times to determine the experimental results' integrity. Figure 6-11 shows the average regeneration curve of molecular sieves used for dewatering flotation product with lower and upper limit standard deviations.

Figure 6-11 shows the molecular sieves with an average initial moisture load of 10.9% w/w with an upper and lower limit standard deviation of 10.9% w/w. After regeneration, the final moisture load averaged at 5.3% w/w with upper and lower limit standard deviations of 5.4% and 5.3% w/w. Table 6-4 shows the standard deviation and relative experimental error for the molecular sieves' regeneration. Very low standard deviations and experimental errors were recorded for the regeneration of the molecular sieves, indicative of reliable experimental results.

Table 6-4 Standard deviation and relative experimental error for molecular sieves' regeneration after flotation product drying

Time (min)	Average (% w/w)	Standard deviation (% w/w)	Relative experimental error (%)
0	10.88	0.00	0.00
20	5.31	0.05	1.58

6.4 Qualitative remarks

This section gives attention to qualitative remarks and unmeasured phenomena noted during experimental work. Photographs of various encounters receive attention and are discussed.

6.4.1 Fluidisation

Supplementary to the regeneration of the adsorbents, it was noted that higher air flow rates fluidised the adsorbents to a certain extent. This fluidisation might have helped with the regeneration because of the adsorbent particles' rotation, ensuring that moist air does not get trapped between the particles. Figure 6-12 shows the 3 mm, and 5 mm activated alumina fluidising to a certain extent using higher air velocities. No adsorbent particle breakage was observed during these additional tests.

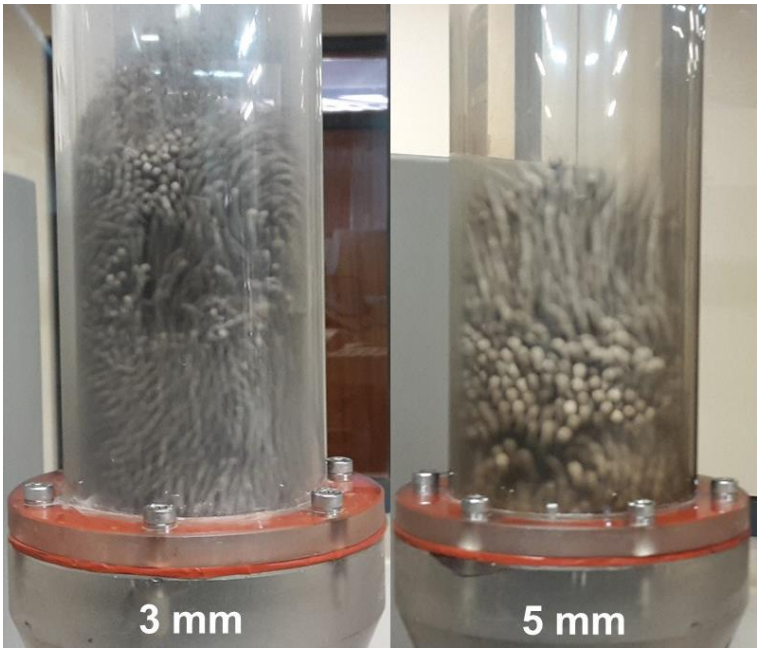

Figure 6-12 Fluidisation of the 3 mm and 5 mm activated alumina during regeneration

6.4.2 Adsorbent robustness

During regeneration, it was observed that the activated alumina performed remarkably well concerning robustness. Even with the fluidisation factor, which might have promoted particle breakage, negligible to no breakage and attrition was encountered during regeneration, signifying activated alumina's eligibility as an industrial adsorbent.

It was already discussed in Section 5.6.3 that molecular sieves behaved weaker and were more brittle than the activated alumina.

6.4.3 Furnace regeneration

Section 5.2.4 discussed how alternative means of regeneration were investigated as a secondary objective and how the furnace regenerated adsorbents would perform. This section briefly discusses and graphically illustrates how the furnace regeneration cleaned and regenerated the adsorbents.

Figure 6-13 compares the spent and furnace regenerated adsorbents from a close view. A clear difference can be seen with the furnace regenerated adsorbents seeming almost like new adsorbents. All the coal dust entrapped on the surfaces was combusted and removed from the surfaces. However, the ash yielded from the coal may still be found on the surfaces of the adsorbents.

It should be kept in mind that furnace regeneration is not an economical method of regeneration and was only secondarily tested in this study for comparison purposes.

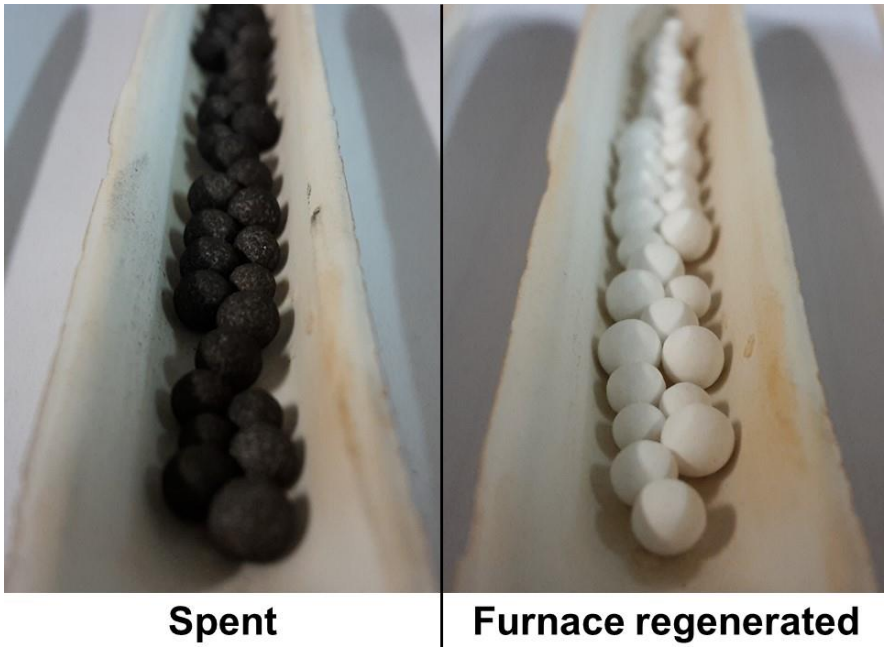

Figure 6-13 Spent vs furnace regenerated activated alumina

6.4.4 Design considerations

Sections 6.2 and 6.3 discussed how the adsorbents were regenerated in a regeneration column that was closed off with bolted flanges on the inlet stream and outlet stream. However, this closed-off regeneration column means that the regeneration will remain a batch process. Regeneration of the adsorbents in a continuous process will need a different approach in regeneration column design.

Since fluidisation was present during regeneration while the particle breakage was little to none, it is suggested to use a horizontal, long-length rectangular fluidised bed to regenerate the adsorbents. The fluidised bed should have an ever so slight decline for the adsorbents to move naturally down the bed. Furthermore, the bed's length and decline slope will comprehensibly affect the adsorbents' residence time in the regeneration process. Therefore, extra care should be taken to design the fluidised bed's length and decline slope. Perhaps a variable and manoeuvrable decline slope of the bed will be beneficial for extra control. Lastly, the fluidised bed's bottom platework, being perforated for upwards airflow, should have a lip or weir plate at the discharge end of the bed to maintain a buffer and controlled flow of the adsorbents in the regeneration column.

In addition to the regeneration column design, Sections 6.2.2 and 6.2.3 discussed that the smaller adsorbent bed masses regenerated faster than the larger bed masses. Because the regeneration rate will be critical in plant economics, attention should be given to the adsorbent bed mass to perforated/ distributor plate area ratio. A smaller adsorbent bed mass, regenerated on a larger distributor plate area, will be more beneficial than a large bed mass regenerated on a small distributor plate area.

Regarding the adsorbents' capillary pore blinding discussed in Sections 4.5.2 and 5.6.2, it is suggested to briefly clean the adsorbents' surfaces with high-pressure water through fine nozzles before regeneration. The cleaning can be achieved with the screened and separated adsorbents travelling on an ever so slightly declined and almost horizontal long-length chute where fine high-pressure nozzles briefly clean the adsorbents before entering the regeneration column. Cleaning of the adsorbents should only be done intermittently when necessary. Adding more moisture to the adsorbents will increase regeneration times and subsequently operational costs.

Figure 6-14 Spent vs briefly washed activated alumina

The chute's platework at the bottom must be perforated for the water to drain fast. The cleaning water can be collected below the chute, filtered and recycled to the high-pressure cleaning water pumps. Figure 6-14 compares the surfaces' cleanliness of spent and briefly washed and rinsed adsorbents. In Figure 6-14, the adsorbents were only rotated in clean water in a flask for 5 minutes, screened and rinsed. The washed adsorbents' surfaces seemed remarkably cleaner than the spent adsorbents. The dark colour of the water retained signifies the amount of coal dust being washed off from the spent adsorbents.

6.5 Conclusion

From the results shown in this Chapter, it was concluded that the regeneration of spent adsorbents, using ambient airflow, is a feasible means of reducing the adsorbents' moisture load, without applying heat.

Previous chapters discussed that regeneration does not have to provide a bone-dry adsorbent, which is beneficial for the regeneration times required for sufficient moisture load reductions. The desaturation of partially saturated activated alumina using ambient airflow showed the adsorbents' moisture load was reduced by more than half within 10 minutes of regeneration.

The regeneration of spent adsorbents showed sufficient moisture load reductions. Regeneration rates can be increased by lowering the adsorbent bed mass and, consequently, bed height. Lower adsorbent-to-coal mass ratios, having smaller bed masses, had higher initial spent moisture loads and experienced faster regeneration rates than the higher adsorbent-to-coal mass ratios. The main driving force for optimal regeneration times is the bed mass to regeneration column area ratio, which stressed the importance of intelligent regeneration column design. Lower bed mass to regeneration column area ratios will regenerate faster. Finally, the larger adsorbent particle sizes regenerated faster than the smaller adsorbent particle sizes due to the lower bed pressure drop.

The regeneration of molecular sieves proved successful in achieving sufficient moisture load reductions of 39% and 51% after 10 minutes and 20 minutes, however, as was discussed in Sections 5.3.3 and 5.4.3, neither regenerated nor spent molecular sieves achieve acceptable dewatering.

During regeneration, negligible amounts of coal dust entrapped between the adsorbents and on the adsorbent particle surfaces were removed from the exit gas stream of activated alumina or molecular sieves' regeneration.

Qualitative observations confirmed the activated alumina's robustness once again, showing negligible to no particle breakage during regeneration, even in the supplementary fluidisation cases. Although the adsorbents' supplementary furnace regeneration showed adequate removal of the coal dust from the adsorbents' surfaces, Chapter 5, fortunately, found this regeneration method to be no improvement over air-blown regeneration as this is not an economically viable method. Finally, briefly washing and rinsing the adsorbents, to clean the coal dust entrapped in capillary pores, delivered a remarkably cleaner adsorbent.

Chapter 7 Industrial applicability

7.1 Introduction

This chapter discusses the industrial applicability of adsorbent assisted drying using activated alumina as an adsorbent. Sections 5.3 and 5.6.3 discussed molecular sieves' shortcomings, therefore disqualifying it as a suitable adsorbent. Molecular sieves will, therefore, not be considered for discussion in this chapter.

The energy balance of adsorbent assisted drying will be evaluated in this chapter, to determine whether the process is energy-positive or negative. Furthermore, the process' industrial applicability is reviewed, considering critical factors like adsorbent robustness and other factors that may make the process practical or impractical.

Most importantly, the process' economic feasibility is reviewed at a high level to determine the typical operational costs of the process and the potential financial gain it might hold. Lastly, a concept design of a continuous adsorbent assisted drying plant is shown and discussed.

7.2 Energy considerations

In process design, one of the leading factors that determine a process' economic viability, regarding operational expenditure, remains energy. Especially with processes involving energy commodities like oil, gas & coal, the aim is to utilise less energy during operation than the process produces in terms of the commodity's calorific value gain.

Previous studies found the adsorbent assisted drying of ROM coal fines with the regeneration of its spent adsorbents to be a cost-effective and energy positive process (Peters, 2016; Van Rensburg *et al.*, 2020). Peters also reported the adsorbent assisted drying process to be one of the least energy-consuming applications of emerging drying technologies.

This section examines the high-level energy balance of the adsorbent assisted drying discussed in this study. The energy consumed during the drying process is compared to the coal's calorific gains due to drying. The energy calculations included only the laboratory-scale equipment's energy consumption and the spiral and flotation product coal's calorific gains recorded for a 2:1 adsorbent-to-coal mass ratio. Details and assumptions of the energy calculations can be found in Annexure C.1.

Table 7-1 Summarised energy balance on adsorbent assisted drying of spiral and flotation product

Property	Unit	Spiral product	Flotation product
Drying time (new)	min	2	2
Drying time (regenerated)	min	2	4
Regeneration time	min	10	10
ΔE_{drying} (new adsorbents)	kJ/kg	2727.5	3719.8
ΔE_{drying} (drying & regeneration)	kJ/kg	1242.4	1650.4

Table 7-1 shows the drying times required for the coals to reach target moisture, the required regeneration time for the moisture content of the adsorbents to be halved and the process's general energy balance. Short drying times required for the coal to reach target moisture signifies an economically attractive process. The table shows that both coals' drying process using new adsorbents is remarkably energy-positive, with energy gains of 2727.5 kJ/kg and 3719.8 kJ/kg, respectively. The unit kJ/kg refers to kilojoules gained/consumed per kilogram of coal dried.

Even for the more realistic, continuous approach (the process with drying and regeneration of its spent adsorbents), the process was still found to be energy positive for both coals, with energy gains of 1242.4 kJ/kg and 1650.4 kJ/kg. The significant difference between the drying process

and the continuous drying process with regeneration, is that even though the second process is still energy-positive, regeneration leads to a lower energy gain. This is due to the regeneration process's energy consumption, which emphasises the importance of intelligent regeneration column design for fast regeneration rates and energy savings.

7.3 Industrial applicability

This section briefly discusses activated alumina's industrial applicability in terms of robustness and the screening of adsorbents from coal. Sections 5.6.3 and 6.4.2 qualitatively discussed the robustness of activated alumina and that little to no particle breakage and attrition occurred during drying and regeneration. In this section, more detail is added to the adsorbents' robustness.

7.3.1 Effect of low pH on the adsorbents

Supplementary experiments done during this study showed that the activated alumina is chemically stable and retain its structural integrity when exposed to low pHs, as reported in the literature that activated alumina is chemically inert (Ducreux & Nedez, 2011).

The activated alumina was drenched in $H_2SO_{4(aq)}$ solutions of pH=1, 2 and 3, respectively, for 30 minutes while the mass loss in adsorbent was determined. No degradation or mass loss of the adsorbents was recorded after being drenched in the $H_2SO_{4(aq)}$ solutions.

Even more tests were done on the activated alumina. The adsorbents were drenched in an $H_2SO_{4(aq)}$ solution of pH=1.5 for 168 hours (7 days), where the mass loss in the adsorbent was recorded to be insignificant. Figure 7-1 shows a close-up view of the dry adsorbents before and after the drenching. No significant damage or degradation can be seen on the adsorbents.

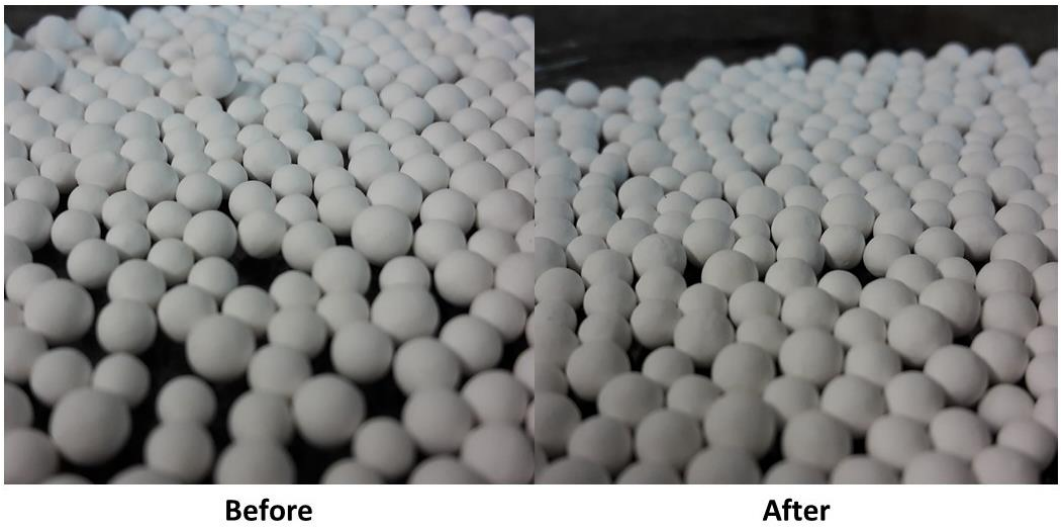

Figure 7-1 Close up view of untreated vs H_2SO_4(aq) treated activated alumina

7.3.2 Attrition and compressive strength

Further supplementary experiments were done to quantify the adsorbents' attrition through Richards' tumbler test (Richards, 1990), while the adsorbents' compressive strength was measured with the Japanese standard for compressive strength tests.

The tumbler tests done on the activated alumina showed no mass loss due to attrition, which ties in with the low attrition shown in the product's technical data sheet (Table 3-3). The insignificant to non-existing attrition is a deciding factor in industrial applications.

Moreover, the compressive strength tests (England, 2000) revealed that the activated alumina could withstand compressive forces of 35-50 N and 50-85 N for the 3 mm and 5 mm particles, which equates to compression pressures of 5.0-7.1 MPa and 2.5-4.3 MPa, respectively. These compressive strengths show suitability for stockpiling and handling of the adsorbent particles.

7.3.3 Screening separation of coal and adsorbents

During experiments, it was qualitatively observed that the screening of spiral and flotation coal from activated alumina was done with ease, provided proper coal materials handling was done beforehand, as discussed in Sections 4.5.1 and 5.6.1. The coal fines' particle sizes differ vastly from the adsorbents' particle sizes; hence they are easily separated with sieving screens due to no near-size particles between the coal and adsorbents. The negligible coal dust removed from the adsorbents during regeneration, as discussed in Chapter 6, also confirms the efficient separation of adsorbent and coal via basic sieving.

Furthermore, the activated alumina is also available in larger particle sizes like 5 mm, which proved successful at dewatering in this study, and a 6 mm size that was not investigated in this study. The larger particle sizes may show better suitability for industrial screening than the smaller adsorbent particle sizes.

7.4 Economic feasibility

This section discusses a high-level economic feasibility study of the adsorbent assisted drying of spiral and flotation coal product. The economic feasibility calculations include only adsorbent consumption and coal sales income. The electricity consumption was not added to the calculations due to data unavailability on such a continuous and industrial plant's electricity consumption. The energy needed per mass of coal dried in a laboratory-scale setup will vastly differ from an industrial-scale setup. The energy calculations in Section 7.2 cannot be upscaled or extrapolated for this purpose.

Sections 4.2.4 and 5.2.4 discussed that the activated alumina could be reused and regenerated to dry the spiral and flotation product sufficiently, which is beneficial for industrial use since it is not necessary to procure new adsorbents for every fresh feed of wet coal. Furthermore, an adsorbent-to-coal mass ratio of 1:1 was found adequate to dry the coal, which is also beneficial for industrial use since fewer adsorbents should be procured than for the 2:1 ratio.

The high-level economic feasibility calculations are based on a typical coal beneficiation plant in South Africa producing 65 tph spiral and flotation coal product (Harmse, 2020). Bulk sale figures of activated alumina can be in the vicinity of $1400/tonne (Wong, 2020). Details of the economic feasibility calculations can be found in Annexure C.2.

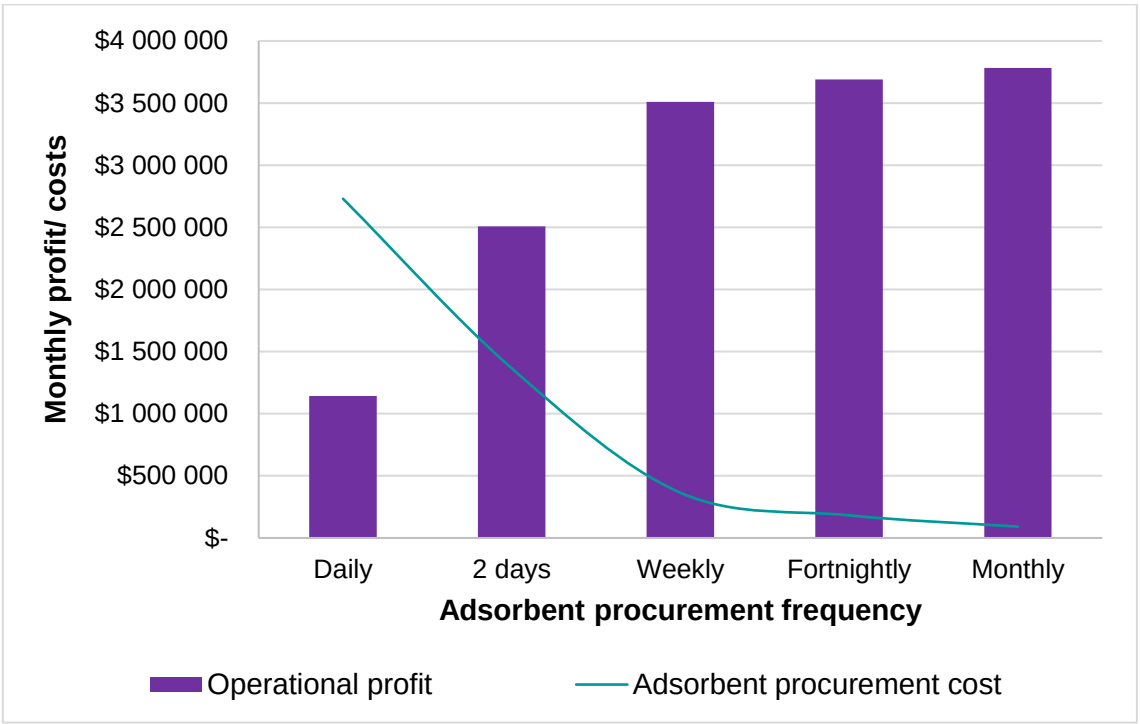

Figure 7-2 High-level economic feasibility of adsorbent assisted drying

Figure 7-2 shows the monthly operational profit and adsorbent procurement costs at a high level for a typical adsorbent assisted drying plant with a wet coal feed rate of 65 tph. The frequency at which new adsorbents are procured is a determining factor for plant economics; hence various procurement frequencies are shown in the figure.

Figure 7-2 shows the adsorbent assisted drying process of being economically feasible at a high level with operational profits as high as $3.8 million per month when adsorbents are procured monthly and profits as low as $1.1 million per month when adsorbents are procured daily. The fresh adsorbent procurement frequency needs to be adjusted, depending on the adsorbents' degradation and prolonged efficiencies. The less frequent fresh adsorbents need to be procured, the higher profit margins will be.

Therefore, it is imperative to ensure that process design provides precautionary measures to retain spent or regenerated adsorbents as long as possible in a closed-loop, provided that the adsorbents' performance allows it. This can be achieved with intelligent materials handling, rotating vessel and regeneration column designs that will prolong the adsorbents lifespan as long as possible.

7.5 Concept continuous adsorbent assisted drying plant

7.5.1 Process flow diagram

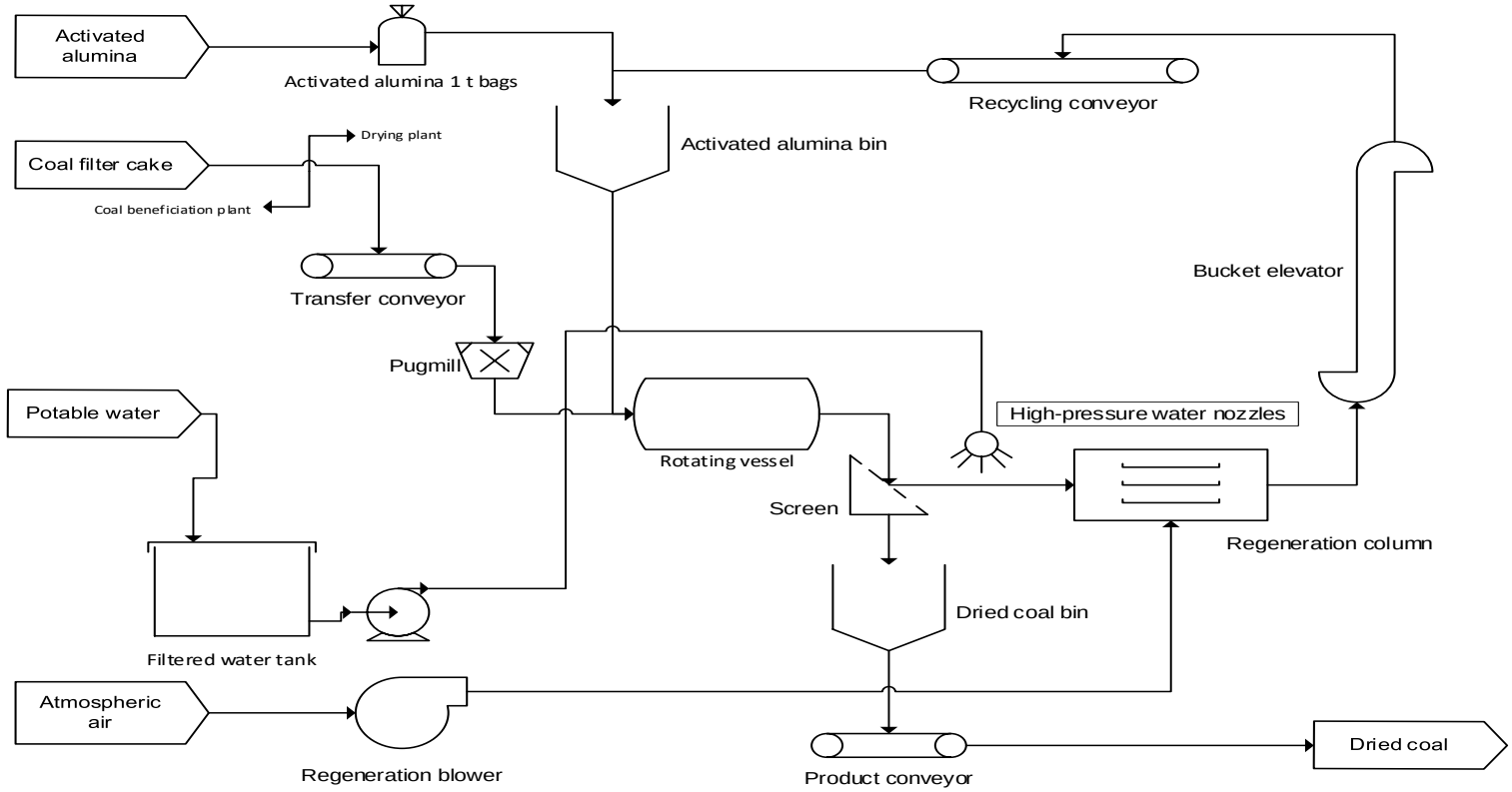

Figure 7-3 High-level process flow diagram of a concept adsorbent assisted drying plant

7.5.2 Process description

Figure 7-3 shows the process flow diagram of a concept continuous adsorbent assisted drying plant. Conveyor head chutes and other chutes are not shown in Figure 7-3 for clarity purposes.

In Figure 7-3, the wet coal filter cake is conveyed from the coal beneficiation plant onto a transfer conveyor that discharges through a head chute into a pugmill with an open bottom. The pugmill breaks down the filter cakes and lumps to ensure the coal particles are as loose as possible. From the pugmill, the coal is discharged through a chute into the rotating vessel.

Fresh feed and regenerated activated alumina collect in the activated alumina bin. The activated alumina is discharged from the bin through a chute into the rotating vessel, where it is combined with the coal particles. Inside the rotating vessel, contact-sorption occurs between the coal particles and the activated alumina, delivering a dried coal product and moisture loaded adsorbent. The rotating vessel discharges through a chute onto a vibrating screen where the coal fines, as the undersized particle, are discharged directly into a dried coal bin. From the dried coal bin, the coal is conveyed on the product conveyor to be shipped via trucks or railway.

The spent activated alumina is discharged from the screen as oversize through a long, slightly declined chute where it can be either directly regenerated or briefly washed with high-pressure fine water nozzles to clean off coal dust entrapped on the adsorbents' surfaces. The washing with high-pressure water should only be done intermittently when it is evident that the adsorbents' surfaces are covered in coal dust.

From the long, slightly declined chute, the spent activated alumina enters the regeneration column, where the adsorbents are slightly fluidised and regenerated with upwards airflow. The airflow is supplied by the regeneration blower that uses atmospheric air. Inside the regeneration column, the regenerated adsorbents will overflow over a small weir plate and discharge into another slightly declined chute that will discharge onto a bucket elevator. At the end of the slightly declined chute, an actuated flapper controls the adsorbents' flow onto the bucket elevator.

Finally, the bucket elevator elevates the regenerated activated alumina upwards and discharges it through a chute onto a horizontal recycling conveyor. The recycling conveyor conveys it further and discharges the activated alumina through a chute into the activated alumina bin.

7.6 Conclusion

Reviewing the industrial applicability of the adsorbent assisted drying process using activated alumina revealed some striking figures and contributions. These figures and contributions can benefit and assist any upscaling of this process as well as further research.

The adsorbent assisted drying process was found energy-positive on a laboratory scale, gaining more energy from the dried coal than what was consumed to dry the coal. The more continuous and realistic approach considering regeneration and drying with regenerated adsorbents was also an energy-positive process. The fact that this process was found to be energy positive contributes significantly to its industrial applicability due to energy consumption being a discerning factor in plant economics.

The activated alumina also showed robustness with chemically inertness and stability against low pHs. The adsorbent showed negligible to no attrition during operation and suitability for stockpiling and materials handling with sufficient compressive strengths. The adsorbents and coal can also be easily screened and separated due to their vastly different particle sizes.

Furthermore, the adsorbent assisted drying process was found economically feasible on a high level with varying profit margins depending on the frequency of fresh adsorbent procurement. The need for intelligent materials handling, rotating vessel and regeneration column design is emphasised to retain adsorbents as long as possible in a closed-loop operation.

In conclusion, the adsorbent assisted drying process is found industrially applicable, considering the contributions made in this chapter. A concept adsorbent assisted drying plant was draughted and discussed.

Chapter 8 Conclusions and recommendations

8.1 Conclusions

Although humanity is trying to foster a greener future, coal will remain a primary energy source for many years to come. Coal researchers have only shifted their focus to greener coal utilisation concerning water, energy and the environment. This section will discuss and conclude the results obtained from the research conducted.

8.1.1 Adsorbent assisted drying

The adsorbent assisted drying of spiral and flotation coal fines using activated alumina as an adsorbent concluded that the coal could be dried swiftly to market-specified moisture content within two minutes' contact sorption, experiencing overall moisture reductions in the vicinity of 91%. The majority of the coals' moisture reduction occurred in the first two minutes of dewatering. Due to moisture reduction, the spiral and flotation product experienced 17% and 30% increases in calorific value respectively. The first experiments were done only on the spiral product, varying the adsorbent-to-coal mass ratio, adsorbent size and adsorbent state as discussed below.

The activated alumina's drying performance, irrespective of adsorbent particle size, is directly proportional to the adsorbent-to-coal mass ratio, attributable to the higher adsorbent contact surface areas available in higher adsorbent-to-coal mass ratios. Higher adsorbent-to-coal mass ratios delivered faster dewatering and lower coal moisture contents and vice versa. The 0.5:1 adsorbent-to coal mass ratio showed insufficient dewatering in some cases during this study.

Both the 3 mm and 5 mm activated alumina delivered adequate drying of the spiral and flotation coal. Nevertheless, the activated alumina's dewatering performance is inversely proportional to its particle size, attributed to the higher contact surface area available with smaller adsorbent particles in bulk. Smaller adsorbent particle sizes achieved faster dewatering and lower coal moisture contents than larger adsorbent particle sizes.

The new, spent and regenerated adsorbent states showed predictable correlations regarding drying performance, with the new adsorbents performing the best, followed closely by the regenerated adsorbents, which showed considerable improvement over the spent adsorbents. The regenerated adsorbents dewatered the spiral and flotation product to market specifications within at least 4 and 6 minutes, irrespective of adsorbent particle size. However, up to the fifth cycle of use, the spent adsorbents could still dry the spiral product to target moisture, while the

flotation product could be dried up to the second cycle of use. The spent adsorbent moisture loads suggested that continuous adsorbent use does not require bone-dry regenerated adsorbents to dewater the coal efficiently.

The main driving force for optimal drying of coal fines is the contact surface area between the adsorbent and coal particles. Therefore, drying efficiency can be optimised by using either smaller adsorbent particle sizes or higher adsorbent-to-coal mass ratios or both. However, larger adsorbent particle sizes and some lower adsorbent-to-coal mass ratios still showed sufficient dewatering of the coal fines.

8.1.2 Comparison of different adsorbents and coals

Three repetitions were done on the original experiment, each time varying one of the experiment's core facets. Firstly the adsorbent type was varied. When compared to activated alumina, molecular sieves showed extraordinarily fast dewatering of the flotation product, having the coal dewatered to near bone-dry moisture contents within two minutes using new adsorbents. However, spent molecular sieves showed poor coal dewatering, while its regenerated version showed meagre improvement suggesting molecular sieves' ineligibility for industrial use.

Secondly, the product was exchanged for tailings in experiments and when compared, spiral product and tailings were dewatered similar to one another. The variables of adsorbent-to-coal mass ratio, adsorbent particle size and adsorbent state had the same trends for spiral tailings as with spiral product but with most variables' effects being slightly more prominent for the spiral product. Spent and regenerated adsorbents were able to dry the spiral tailing as with the spiral product. Albeit similar in dewatering behaviour, the spiral tailings experienced slightly higher moisture reductions and lower final moisture contents than the spiral product, proving the hypothetical assumption that the mineral matter in the coal tailings would retain water stronger than the carbon-containing coal product wrong.

Thirdly, the spiral product was exchanged for entirely new coal, flotation coal product. The differences in the dewatering of the two types of coal were evaluated. Spiral coal has a much larger particle size than flotation coal giving the spiral coal a smaller contact surface. From the experiments, it was found that, regardless of their differences, the two coals were dewatered very similarly. The different coals showed almost identical moisture desorption rates and total moisture reduction. Only minute differences were seen, such as a smaller adsorbent-to coal mass ratio and larger adsorbent particle sizes had less weak drying effects on flotation coal than on spiral coal. These small differences can be attributed to the flotation coal's smaller particles. From the previous discussion, it is clear that adsorbent regeneration plays a major role in adsorbent assisted drying since regeneration allows the adsorbents to be reused rather than discarded.

From Chapter 6, it was concluded that regeneration of spent adsorbents using ambient airflow is a feasible means of reducing the adsorbents' moisture load without applying heat.

Since adsorbents do not have to be completely dry after regeneration to achieve sufficient moisture load reduction, it was found that the moisture load of partially saturated adsorbents could be halved within 10 minutes of regeneration. It was also found that this regeneration rate is increased by lowering the adsorbent bed mass. A lower adsorbent-to-coal mass ratio, smaller bed masses, higher initial moisture load and larger adsorbent particle sizes all contributed to a faster regeneration rate. The larger particle sizes played a part in creating a lower bed pressure drop, but the driving factor was still the bed mass to regeneration column area ratio. It was found that a lower bed mass to regeneration column area led to faster regeneration.

Regeneration of molecular sieves was also done, delivering sufficient moisture load reductions, however, this did not allow the regenerated adsorbents to dewater coal better than spent adsorbents.

During regeneration, negligible amounts of coal dust entrapped between the adsorbents and on the adsorbent particle surfaces were removed from the exit gas stream of either activated alumina or molecular sieves' regeneration.

8.1.3 Qualitative observations

Some qualitative observations were made through the different experiments. Both spiral and flotation coal have an affinity for caking that can be broken up using pugmills with open bottoms before the coal is combined with adsorbents.

When continuously using adsorbents, their dewatering ability diminished. This might be due to capillary pore blinding due to coal dust found to become entrapped on the surface of each adsorbent. Although the adsorbents' supplementary furnace regeneration showed adequate removal of the coal dust from the adsorbents' surfaces, Chapter 5, fortunately, found this regeneration method to be no improvement over air-blown regeneration as this is not an economically attractive method. Finally, brief washing and rinsing of the adsorbents to clean the coal delivered a remarkably cleaner adsorbent.

Activated alumina was particularly robust, making it usable in industrial situations, especially compared to molecular sieves that were brittle.

8.1.4 Industrial applicability

Reviewing the industrial applicability of the adsorbent assisted drying process using activated alumina can be used when wanting to upscale the process of adsorbent assisted drying. The most positive result here is that the adsorbent assisted drying process was found to be energy-positive on a laboratory scale, gaining more energy from the dried coal than what was consumed to dry the coal. This was even true for the more continuous and realistic approach of considering regeneration and drying with regenerated, making adsorbent assisted drying an attractive drying method for the industry.

More experiments on the activated alumina found it to be robust with chemical inertness and stability against low pHs. This also adds to the industrial usability of these adsorbents, given that the negligible attrition found during operation will make it suitable for stockpiling. Another observation made that adds to industrial usability is that the adsorbents can be easily separated from coal with sieves, due to their vastly different particle sizes.

Furthermore, the adsorbent assisted drying process was found economically feasible on a high level with varying profit margins depending on the frequency of fresh adsorbent procurement. In a conceptual design for an adsorbent assisted drying plant, seen in Section 7.5, the need for intelligent materials handling, rotating vessel and regeneration column design was emphasised to retain adsorbents as long as possible in a closed-loop operation.

Finally, the adsorbent assisted drying process is found industrially applicable, considering the contributions made by this study.

8.2 Recommendations

From the conclusions drawn for this study, several recommendations exist for future research work in this field. This section discusses these recommendations and other relevant research suggestions.

The adsorbent assisted drying of spiral and flotation coal fines proved successful in this study, which was investigated on a laboratory scale and in a batch process approach. It is strongly recommended to investigate this process on a continuous pilot-plant scale in further research.

The concept design for a continuous adsorbent assisted drying plant discussed in Section 7.5 should be used and investigated for future research. This will enable the drying process' energy balance and economic feasibility to be determined more accurately while investigating the industrial applicability in depth. Moreover, the mechanical design suggestions regarding intelligent rotating vessel, baffle plate and regeneration column designs discussed in Sections 4.5.3, 5.6.4 and 6.4.4 should be considered and investigated for effectiveness as part of the continuous pilot-plant approach.

The capillary pore blinding phenomenon encountered during continuous use of the adsorbents should be investigated in-depth while investigating ways to eliminate or overcome the occurrence. Moreover, optimising the adsorbents' regeneration should receive attention in future research to develop energy-saving and prolonged adsorbent usage designs.

Bibliography

Badenhorst, M.J.G. 2009. A Study of The Influence of Thermal Drying on Physical Coal Properties. Potchefstroom: Nort-West University. (M.Eng).

Baruya, P. 2014. Coal reserves in a carbon constrained future: IEA Clean Coal Centre. (IEACCC/233).

Baruya, P. 2018. Production and Supply Chain Costs of Coal. London: IEA Clean Coal Centre. (IEACCC/289).

Bland, R.W. & McDaniel, B. 2011. Coal Drying Method and System. (Patent: United States of America. US 2011/0247233 A1).

Bland, R.W. & McDaniel, B. 2014. Coal Drying Method and System. (Patent: United States of America. US 2014/0144072 A1).

Bonsu, A.K. 1983. Influence of pulp density and particle size on spiral concentration efficiency. Camborne School of Mines. (M.Phil).

Bourgeois, F.S. & Barton, W.A. 1998. Advances in the Fundamentals of Fine Coal Filtration. *Coal Preparation*, 19(1-2):9-31.

Bratton, R., Ali, Z., Luttrell, G., Bland, R. & McDaniel, B. 2012. Nano Drying Technology: A New Approach for Fine Coal Dewatering. *(In* Klima, M.S., Arnold, B.J. & Bethell, P.J., *eds*. Challenges in Fine Coal: Processing, Dewatering and Disposal. Society for Mining, Metallurgy, and Exploration, Inc. p. 345-359).

Buckley, G.L. 2004. History of Coal Mining in Appalachia. (*In* Encyclopedia of Energy:495-505).

Campbell, Q.P. 2006. Dewatering of fine coal with flowing air using low pressure drop systems. Potchefstroom: North-West University. (PhD).

De Korte, G.J. Division of Mining Technology. 2001. Dewatering and drying of fine coal: Survey of dewatering costs. Pretoria: Csir. (Coaltech 2020 project no. Y3675).

De Korte, G.J. Coal prices vs moisture content in South Africa [23 May 2019.

De Korte, G.J. The current market specifications and demand for coal fines in South Africa [14 February 2019].

Department of Energy (RSA). Energy. 2018. Coal Resources.

Department of Mineral Resources (RSA). Resources, M. 2016. Directorate: Mineral Economics.

Devore, J.L., Farnum, N.R. & Doi, J. 2014. Applied Statistics for Engineers and Scientists. Third: Cengage Learning.

Doheim, M.A., Gawad, A.F.A., Mahran, G.M.A., Abu-Ali, M.H. & Rizk, A.M. 2013. Numerical simulation of particulate-flow in spiral separators: Part I. Low solids concentration (0.3% & 3% solids). *Applied Mathematical Modelling*, 37:198-215.

Drytech Engineering. 2008. Drying Technology. https://www.drytecheng.com/Drytech.htm Date of access: 08 July 2019.

Ducreux, O. & Nedez, C. 2011. Air and Gas Drying With AxSorb Activated Alumina. https://india.axens.net/component/axensdocuments/875/air-and-gas-drying-with-axsorb-activated-alumina/english.html Date of access: 15 July 2019.

Dunn, M.B. 1980. Richards Bay Coal Terminal. *Journal of the South African Institute of Mining and Metallurgy*, 80(1):57-61.

Dzinomwa, G.P.T., Wood, C.J. & Hill, D.J.T. 1997. Fine Coal Dewatering Using pH- and Temperature-sensitive Superabsorbent Polymers. *Polymers for Advanced Technologies*, 8:767-772.

England, T., 2000. The Economic Agglomeration of Fine Coal For Industrial and Commercial Use.: Coaltech 2020.

ESI Africa. 2014. The economic possibilities of South Africa's coal fines. https://www.esi-africa.com/the-economic-possibilities-of-south-africas-coal-fines/ Date of access: 12 March 2018.

Eskom. 2016. Coal in South Africa. http://www.eskom.co.za/AboutElectricity/FactsFigures/Pages/Facts_Figures.aspx Date of access: 18 April 2018.

Eskom. 2017a. Generation Plant Mix. http://www.eskom.co.za/AboutElectricity/FactsFigures/Pages/Facts_Figures.aspx Date of access: 18 April 2018.

Eskom. 2017b. How electricity is produced at a coal fired power station. http://www.eskom.co.za/AboutElectricity/FactsFigures/Pages/Facts_Figures.aspx Date of access: 18 April 2018.

Falcon, R.M.S. 2013. Coal Geology, Types, Ranks and Grades. Johannesburg.

Falcon, R.M.S. & Ham, A.J. 1988. The characteristics of Southern African coals. *Journal of the South African Institute of Mining and Metallurgy*, 88(5):145-161.

Falcon, R.M.S. & Snyman, C.P. 1986. An Introduction to Coal Petrography: Atlas of Petrographic Constituents in the Bituminous Coals of Southern Africa. *Review Paper Series of The Geological Society of South Africa*(Issue).

Falconer, K.W. 1990. Spotlight on 100 years of coal mining in Witbank. *Journal of the South African Institute of Mining and Metallurgy*, 90:78.

FLSmidth. 2019. KREBS Coal Spirals. https://www.flsmidth.com/en-gb/products/centrifugation-and-classification/krebs-spirals Date of access: 26 September 2019.

Galloway, R.L. 1882. A History of Coal Mining in Great Brittain. London: Macmillan and Co.

Hancox, P.J. & Götz, A.E. 2014. South Africa's coalfields — A 2014 perspective. *International Journal of Coal Geology*, 132(6):170-254.

Hand, P.E. 2000. Dewatering and drying of fine coal to a saleable product.: Coaltech 2020.

Harmse, J., 2020. The throughput of a typical coal beneficiation plant operating spiral classifiers and flotation cells [14 August 2020].

Holland-Batt, A.B. 1993. The Effect of Feed Rate on the Performance of Coal Spirals. *Coal Preparation*, 14(3-4):199-222.

IEA. 2018. World Energy Outlook. https://www.iea.org/weo/ Date of access: 04 April 2019.

Kudra, T. & Mujumdar, A.S. 2009. Advanced Drying Technologies: CRC Press.

Laskowski, J.S. 2001. Coal Flotation and Fine Coal Utilization. Vancouver: Elsevier.

Le Roux, M. 2003. An Investigation into an Improved method of Dewatering Fine Coal. Potchefstroom: P.U. for C.H.E. (M.Eng).

Le Roux, M. & Campbell, Q.P. 2003. An investigation into an improved method of fine coal dewatering. *Minerals Engineering*, 16(10):999-1003.

Le Roux, M., Campbell, Q.P., Watermeyer, M.S. & de Oliveira, S. 2005. The optimization of an improved method of fine coal dewatering. *Minerals Engineering*, 18(9):931-934.

Lemley, A., Wagenet, L. & Kneen, B. 1995. Activated Carbon Treatment of Drinking Water.

Lester, E. & Kingman, S. 2004. The effect of microwave preheating on five different coals. *Fuel*, 83(14-15):1941-1947.

Marland, S., Merchant, A. & Rowson, N. 2001. Dielectric properties of coal. *Fuel*, 80(13):1839-1849.

Mills, C. 1978. Mineral Processing Plant Design. New York: AIMME.

Minerals Council South Africa. 2019. Mining in SA (Coal). https://www.mineralscouncil.org.za/sa-mining/coal Date of access: 04 April 2019.

Mohanty, M.K., Akbari, H. & Luttrell, G.H. 2012. Fine Coal Drying and Plant Profitability. *(In* Klima, M.S., Arnold, B.J. & Bethell, P.J., *eds*. Challenges in Fine Coal: Processing, Dewatering and Disposal. Society for Mining, Metallurgy, and Exploration, Inc. p. 329-344).

Motengwe, C. & Alagidede, P. 2017. The Nexus between Coal Consumption, CO2 Emissions and Economic Growth in South Africa. *Geography Research Forum*, 37:80-110.

Osborne, D.G. 2012. Perspectives on Coal Fines. *(In* Klima, M.S., Arnold, B.J. & Bethell, P.J., *eds*. Challenges in Fine Coal: Processing, Dewatering and Disposal. Society for Mining, Metallurgy, and Exploration, Inc. p. 3-45).

Osborne, D.G. 1988. Coal Preparation Technology. Vol. 1. Oxford: Graham Trotman Limited.

Peer, F. & Venter, T. 2003. Dewatering of coal fines using a super absorbent polymer. *Journal of the Southern African Institute of Mining and Metallurgy*, 103(6):403-409.

Peters, E.S. 2016. Adsorbent assisted drying of fine coal. Potchefstroom: North-West University. (M.Eng).

Petrick, A.J. 1969. Moisture in coal: Its occurrence, its implications and some of the problems met in practice. (No. 16).

Prat, G. 2012. Dewatering Fine Coal and Tailings with a Filter Press. *(In* Klima, M.S., Arnold, B.J. & Bethell, P.J., *eds*. Challenges in Fine Coal: Processing, Dewatering and Disposal. Society for Mining, Metallurgy, and Exploration, Inc. p. 279-292).

Reddick, J.F., von Blottnitz, H. & Kothuis, B. 2007. A cleaner production assessment of the ultra-fine coal waste generated in South Africa. *Journal of the Southern African Institute of Mining and Metallurgy*, 107(12):811-816.

Richards, S., 1990. Physical Testing of Fuel Briquettes. *Fuel Processing Technology,* 25(2):89-100.

Richards Bay Coal Terminal. 2018. Infrastructure. https://rbct.co.za/operations-6/infrastructure/ Date of access: 14 June 2018.

Rocktec, 2021. Materials handling. https://rocktec.co.nz/materials-handling/products/rocktec-pugmills/pugmill Date of access: 14 March 2021

SACPS. 2015. Coal Preparation in Southern Africa. Fifth: The Southern African Coal Processing Society.

SANEDI. 2011. Coal Road Map. https://www.sanedi.org.za/coal-roadmap/ Date of access: 04 April 2019.

Seehra, M.S., Kalra, A. & Manivannan, A. 2007. Dewatering of fine coal slurries by selective heating with microwaves. *Fuel*, 86(5-6):829-834.

Stavrakis, N. 1986. Sedimentary environments and facies of the Orange Free State Coalfield. *Mineral Deposits of Southern Africa*, 2:1939-1952.

Steyn, M. & Minnit, R.C.A. 2010. Thermal coal products in South Africa. *Journal of the Southern African Institute of Mining and Metallurgy*, 110(10):593-599.

Tao, D., Groppo, J.G. & Parekh, B.K. 2000. Enhanced ultrafine coal dewatering using flocculation filtration processes. *Minerals Engineering*, 13(2):163-171.

Tien, C. 2019. Introduction to Adsorption: Basics, Analysis and Applications: Elsevier.

Van Rensburg, M.J., Le Roux, M., Campbell, Q.P. & Peters, E.S. 2018. Moisture transport during contact sorption drying of coal fines. *International Journal of Coal Preparation and Utilization*:1-16.

Van Rensburg, M.J., Le Roux, M., Campbell, Q.P. & Peters, E.S. 2020. Contact sorption: a method to reduce the moisture content of coal fines. *International Journal of Coal Preparation and Utilization*, 40(4-5):266–280.

Venter, P. & Naude, N. 2015. Evaluation of some optimum moisture and binder conditions for coal fines briquetting. *Journal of the Southern African Institute of Mining and Metallurgy*, 115(4):329-333.

Wills, B.A. & Napier-Munn, T. 2006. Wills' Mineral Processing Technology. Queensland: Elsevier Ltd.

Wong, E., 2020. What is the bulk sale figures of activated alumina [14 December 2020].

Yang, X. 2015. Suitability evaluation of emerging drying technologies for fine clean coal drying. Illinois: Southern Illinois University at Carbondale. (PhD).

Young, R.W. 2017. Maps and Mining of Coal in the Wollongong District since 1797. *The Globe*, 82:1-11.

Zarzycki, R. & Chacuk, A. 1993. Absorption: Fundamentals & Applications. First: Pergamon Press Ltd.

Annexure A: Drying results

A.1 Spiral product drying

Further reference can be given in this annexure for spiral product drying results not discussed in Section 4.2.

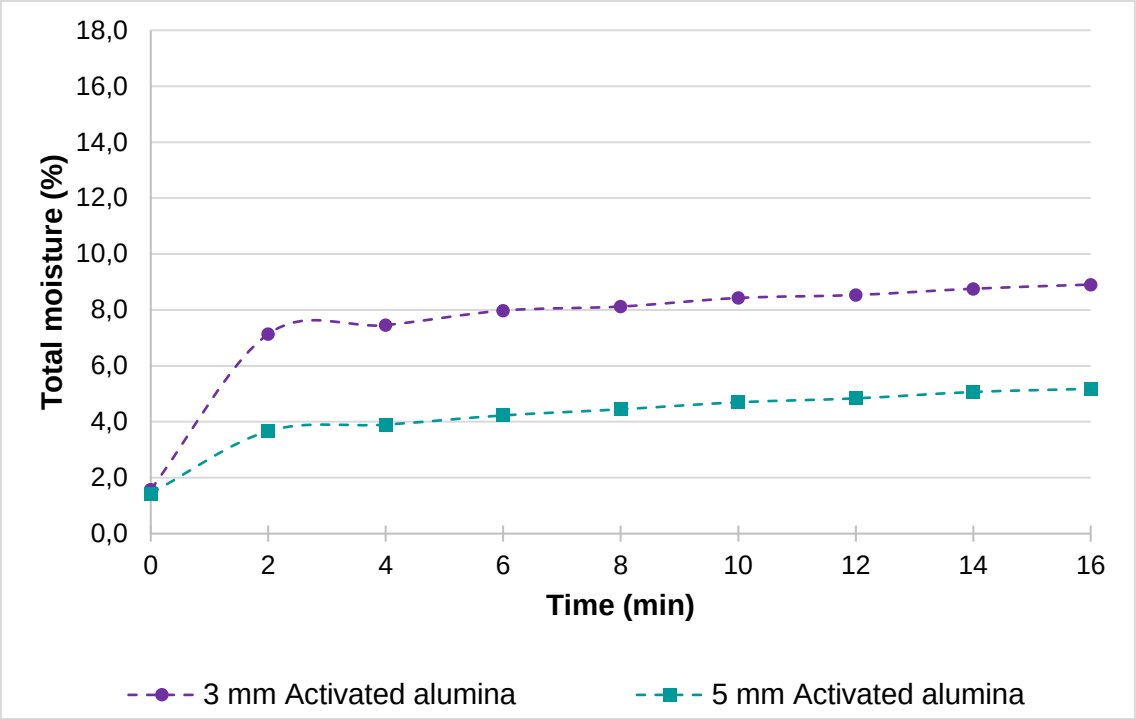

Figure A-1 Adsorption curves of 3 mm and 5 mm activated alumina used to dry spiral product

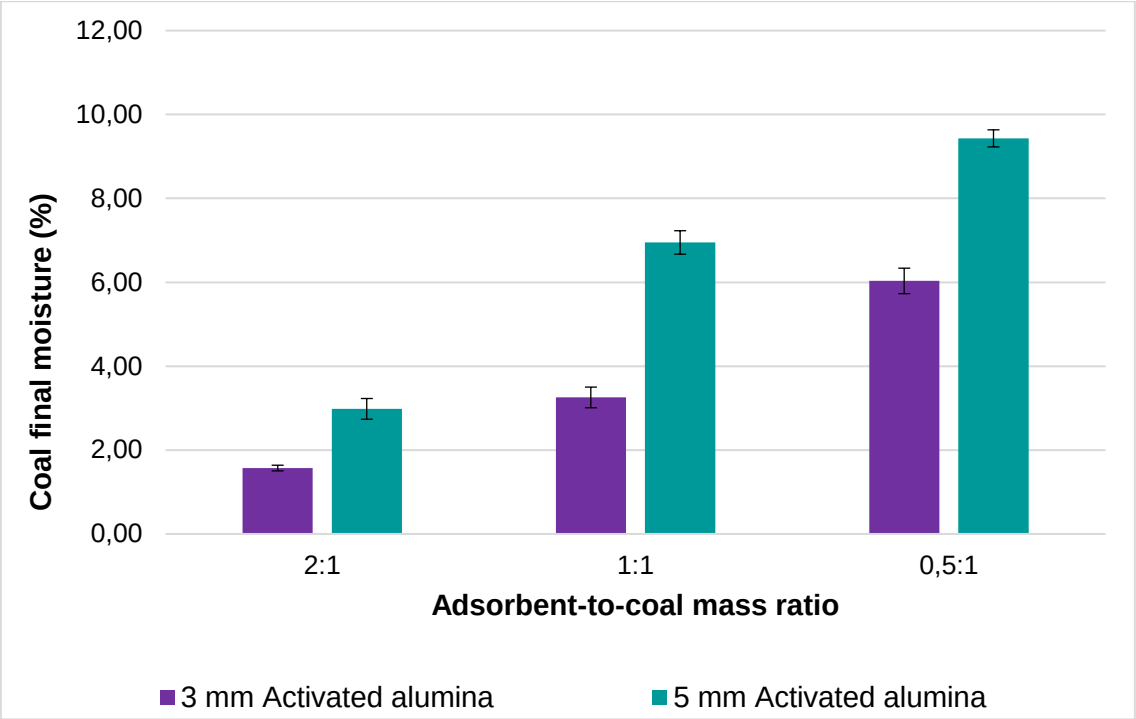

Figure A-2 Final spiral product moisture contents using 3 mm and 5 mm activated alumina

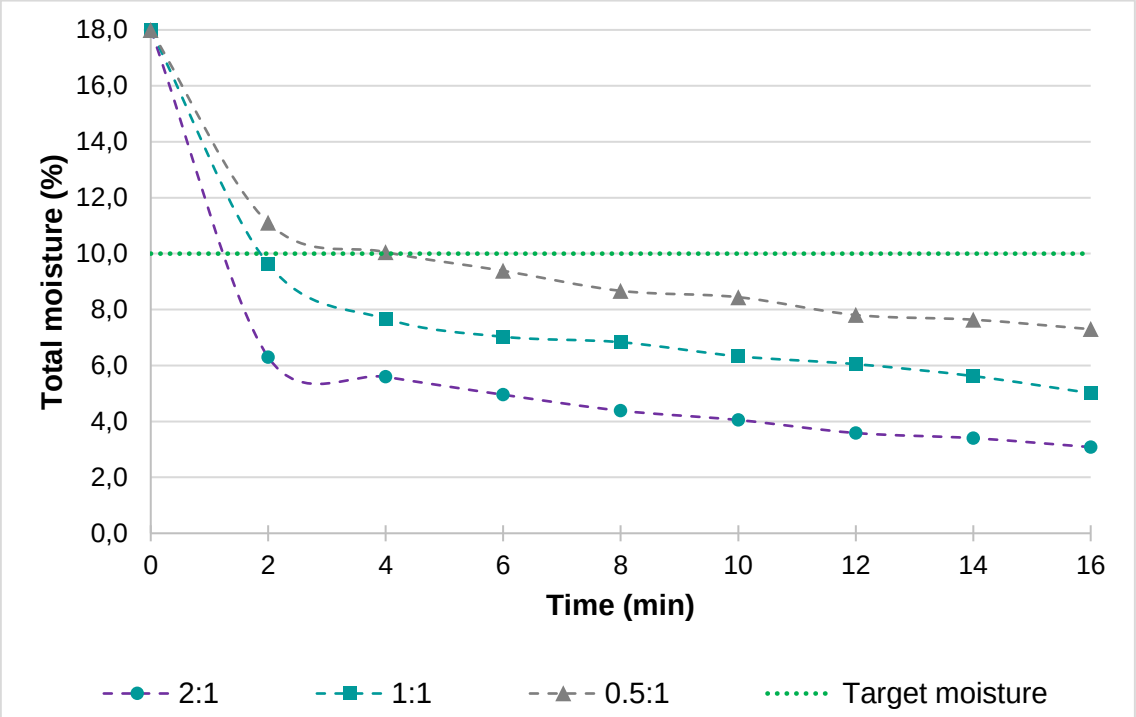

Figure A-3 Desorption curves of spiral product using regenerated 3 mm activated alumina

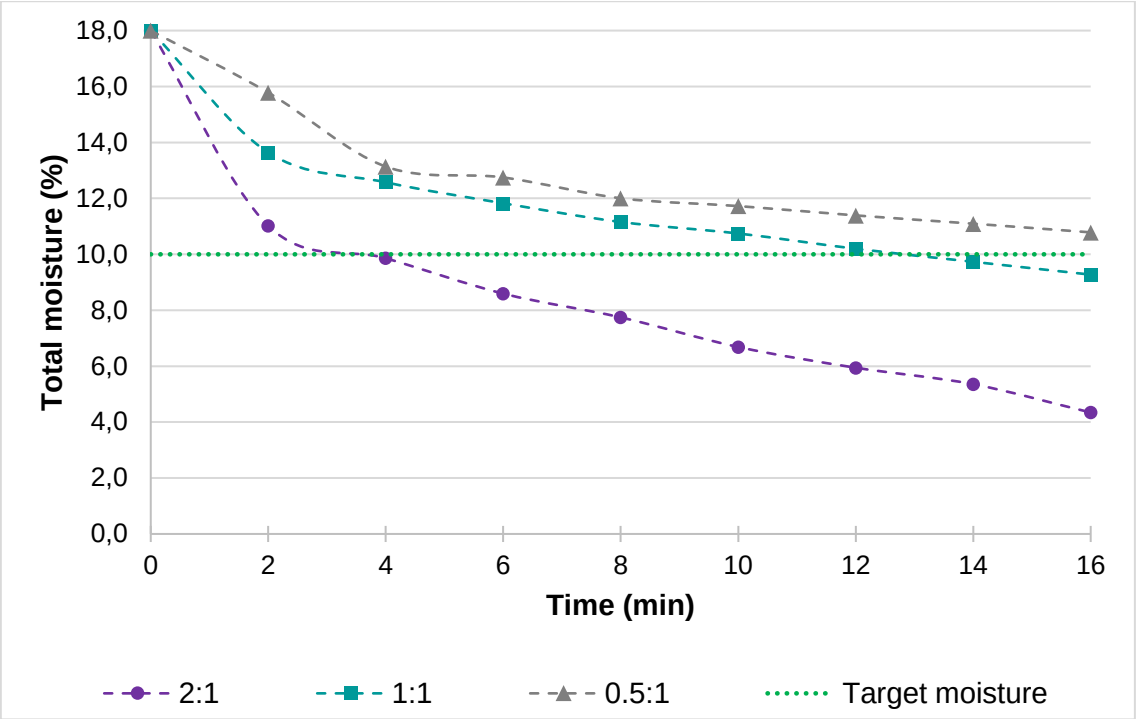

Figure A-4 Desorption curves of spiral product using regenerated 5 mm activated alumina

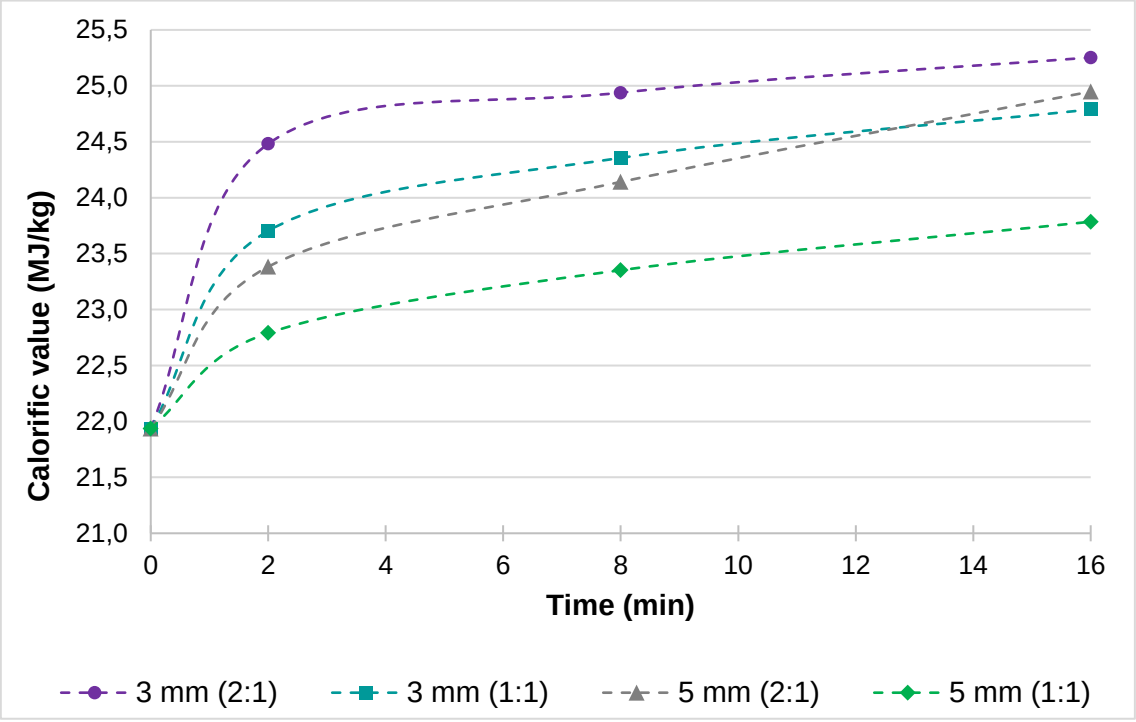

Figure A-5 Calorific gains of spiral product using regenerated 3 mm activated alumina

A.2 Spiral tailings drying

Additional results of spiral tailings drying, not discussed in Section 4.3 can be found in this annexure.

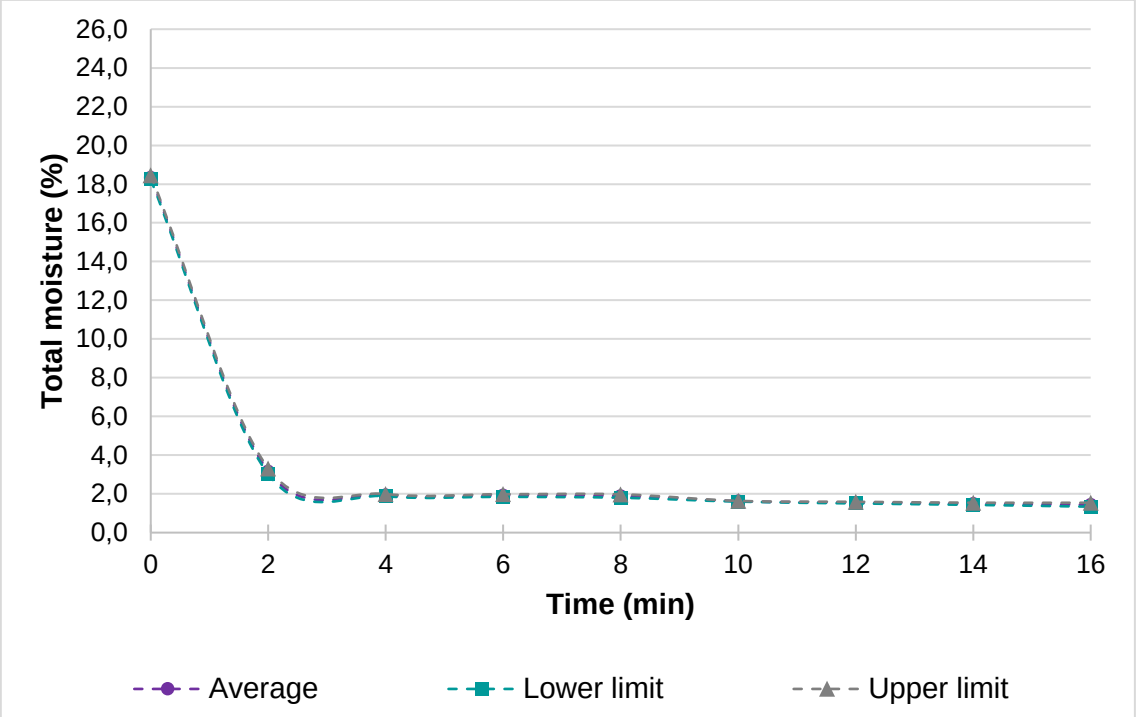

Figure A-6 Average desorption curve of spiral tailings with standard deviations

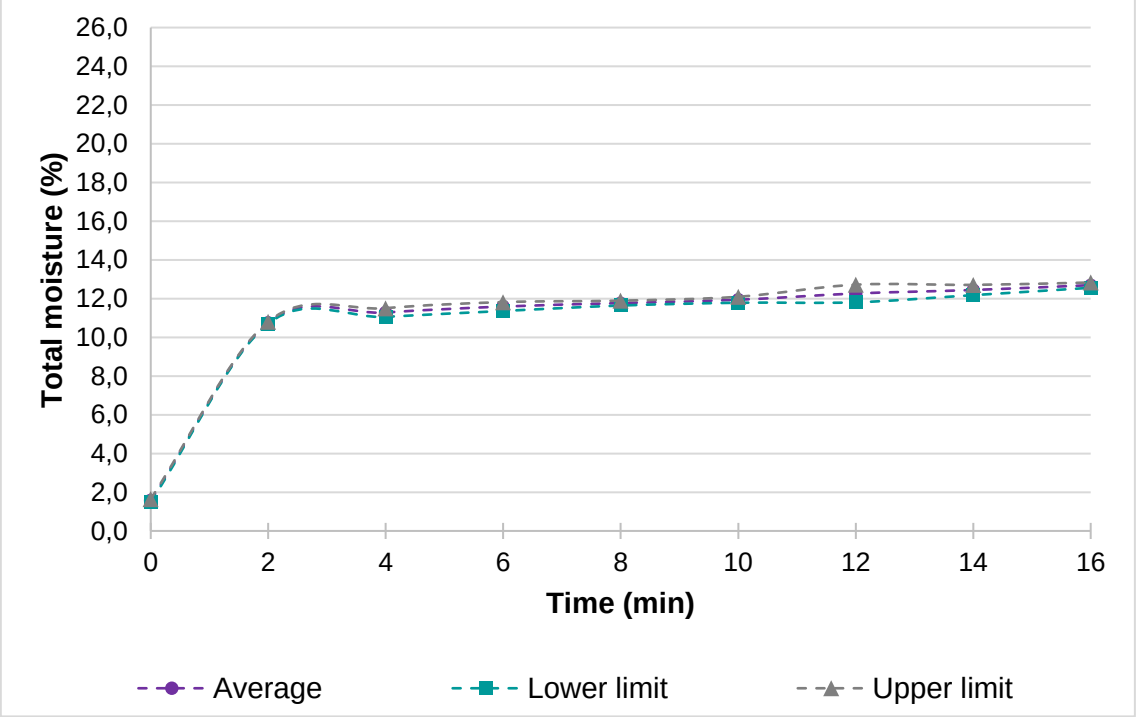

Figure A-7 Average adsorption curve of 3 mm activated alumina used on spiral tailings with standard deviations

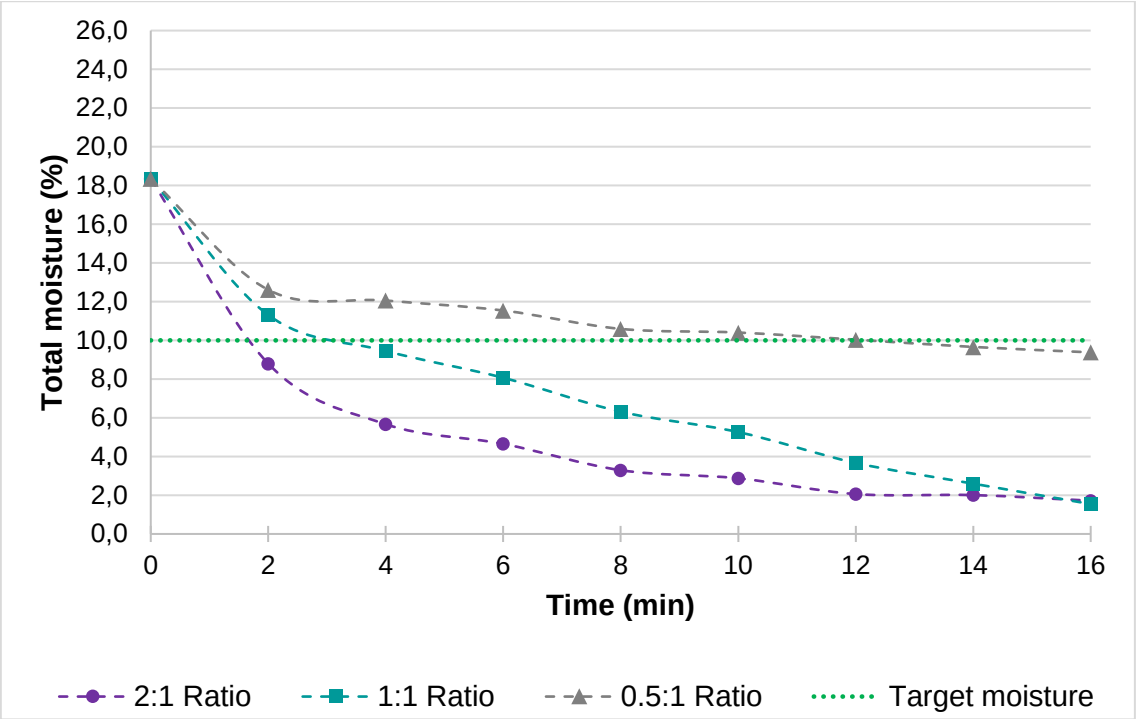

Figure A-8 Desorption curves of spiral tailings using 5 mm activated alumina in various adsorbent-to-coal mass ratios

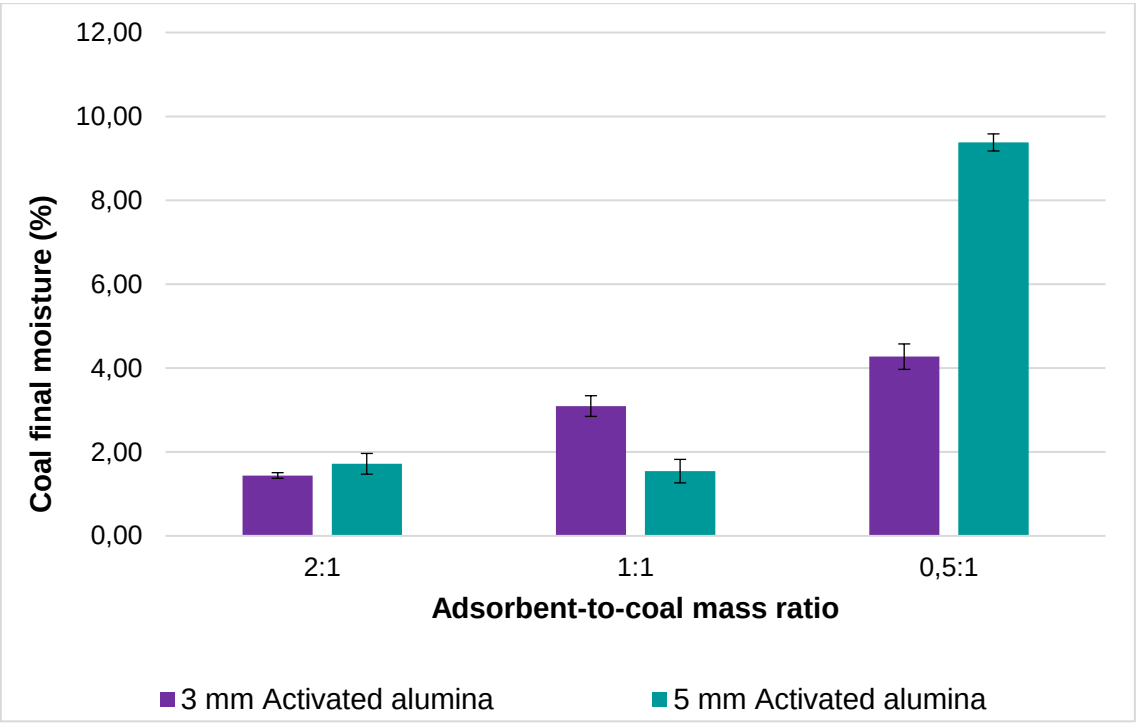

Figure A-9 Final spiral tailings moisture contents using 3 mm and 5 mm activated alumina

A.3 Flotation product drying

This annexure can be referenced for additional flotation product drying results, that were not discussed in Section 5.2.

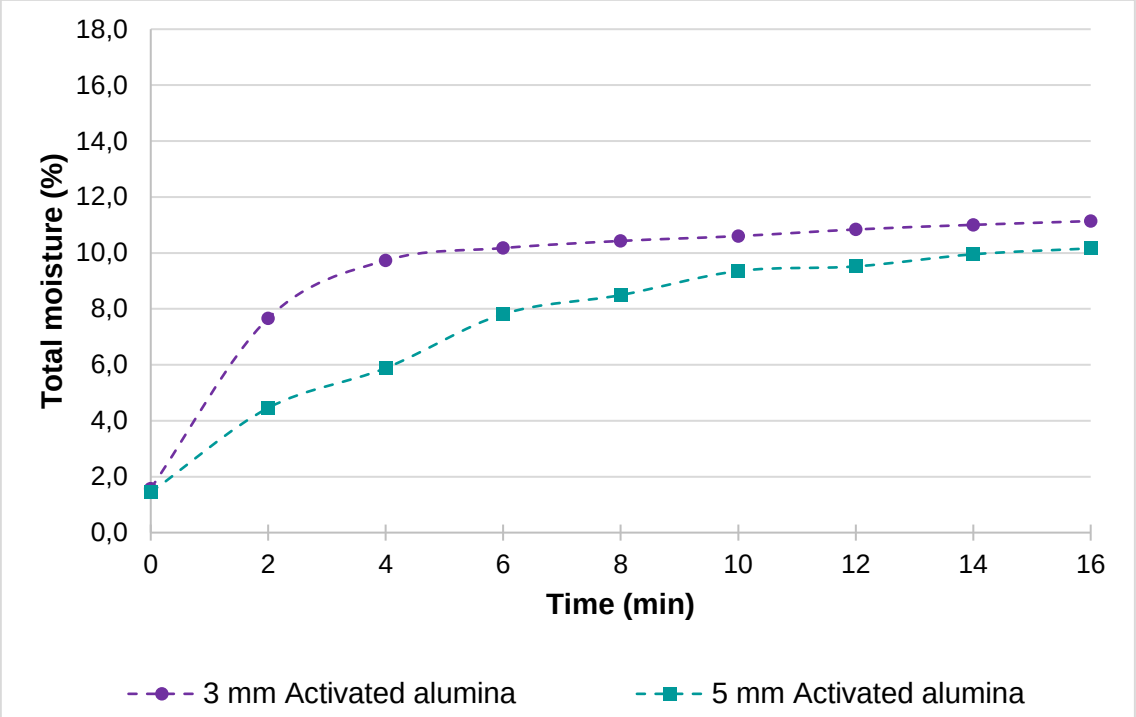

Figure A-10 Adsorption curves of 3 mm and 5 mm activated alumina used to dry flotation product

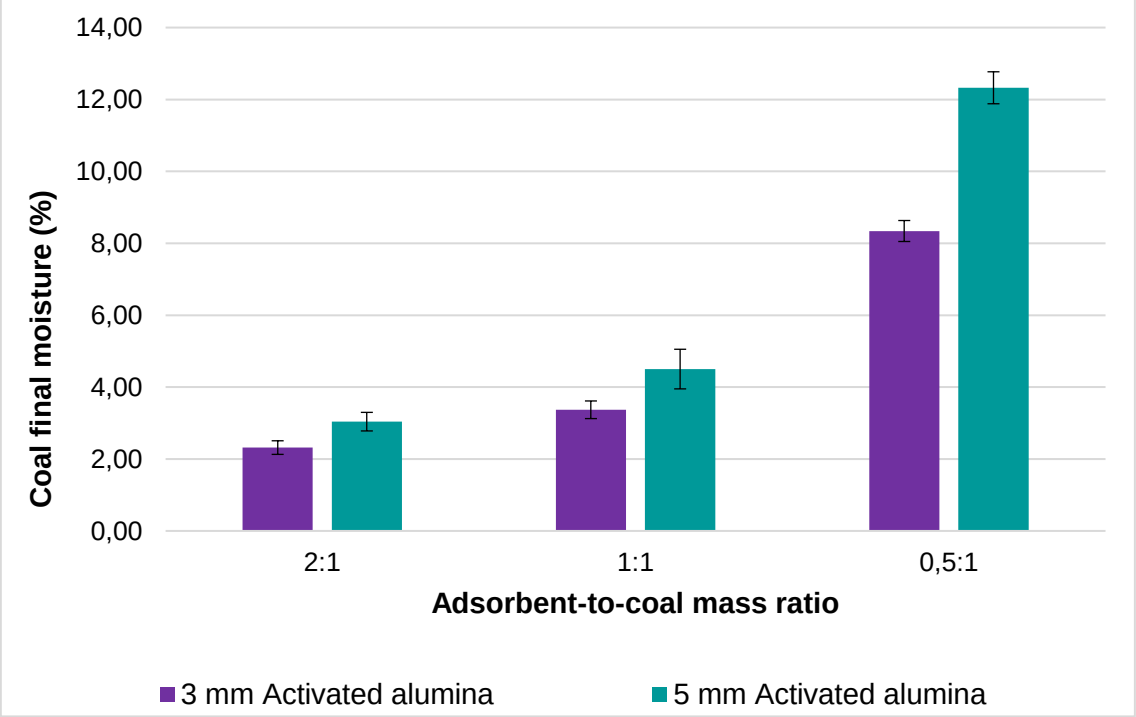

Figure A-11 Final flotation product moisture contents using 3 mm and 5 mm activated alumina

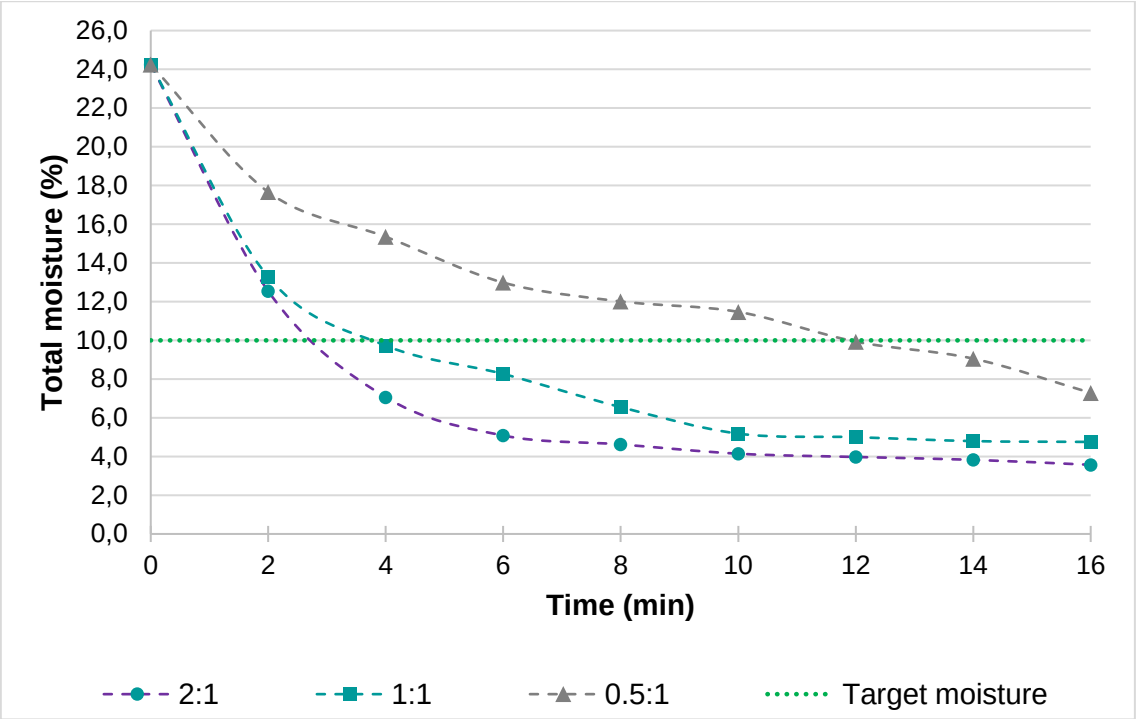

Figure A-12 Desorption curves of flotation product using regenerated 3 mm activated alumina in various adsorbent-to-coal mass ratios

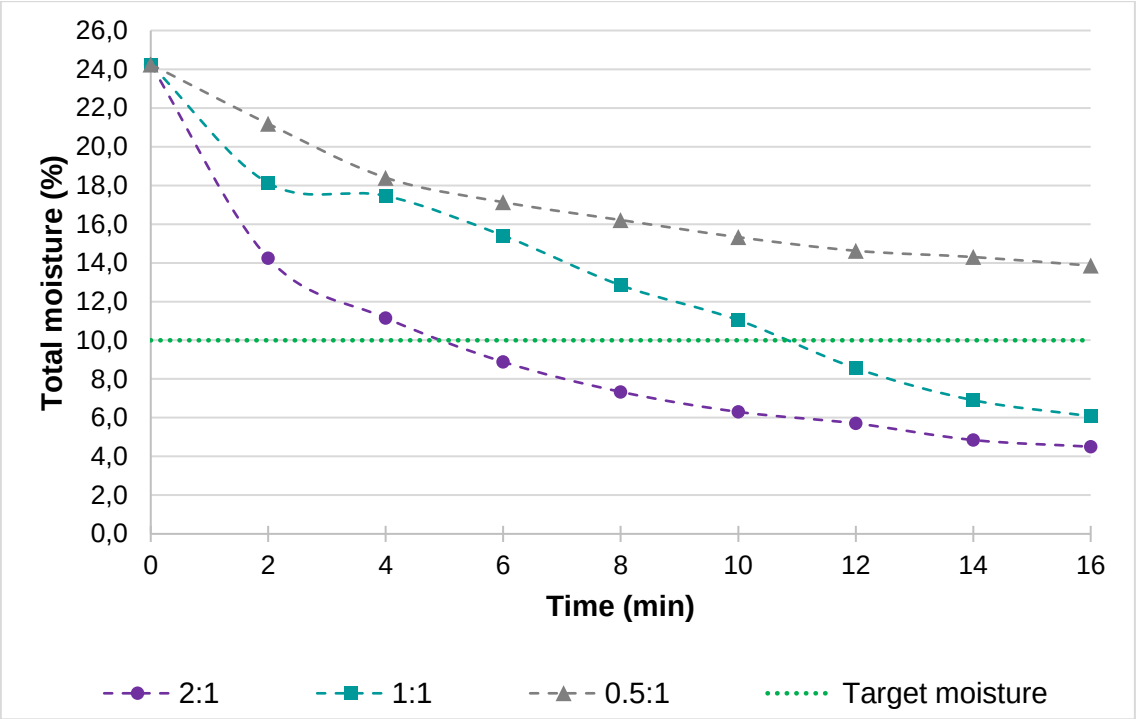

Figure A-13 Desorption curves of flotation product using regenerated 5 mm activated alumina in various adsorbent-to-coal mass ratios

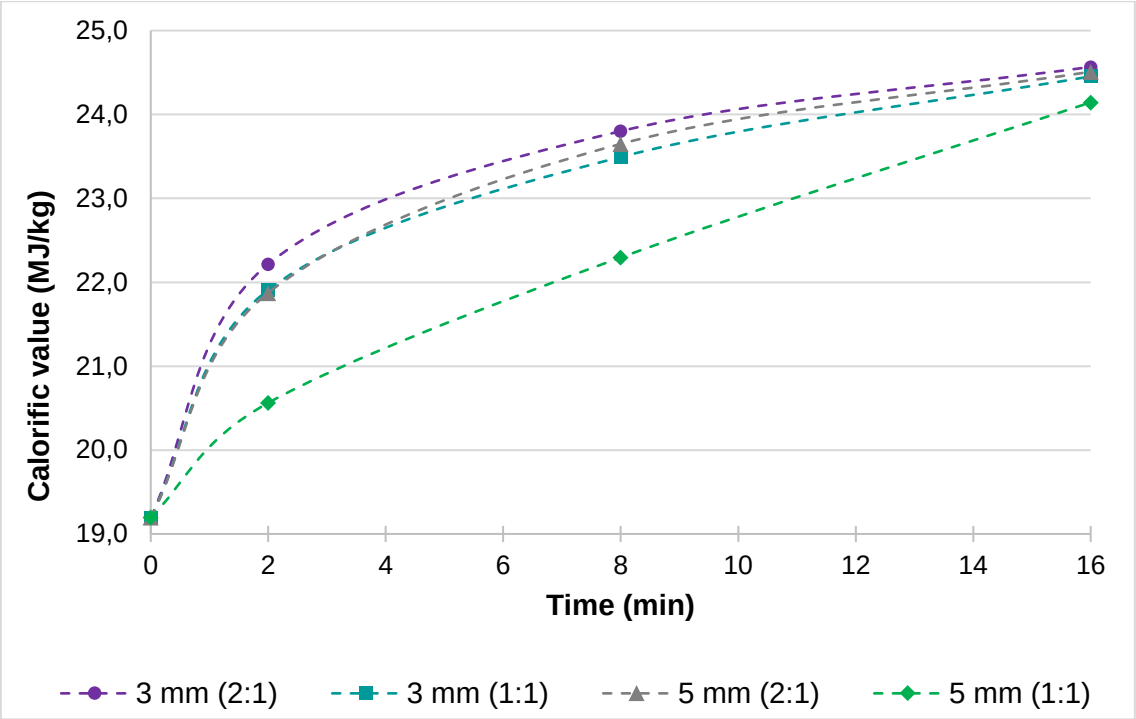

Figure A-14 Calorific gains of flotation product using regenerated 3 mm activated alumina

Annexure B: Regeneration results

B.1 Flotation product's spent activated alumina

Results of the regeneration of flotation product's spent activated alumina not discussed in Section 6.2.3 can be referenced in this annexure.

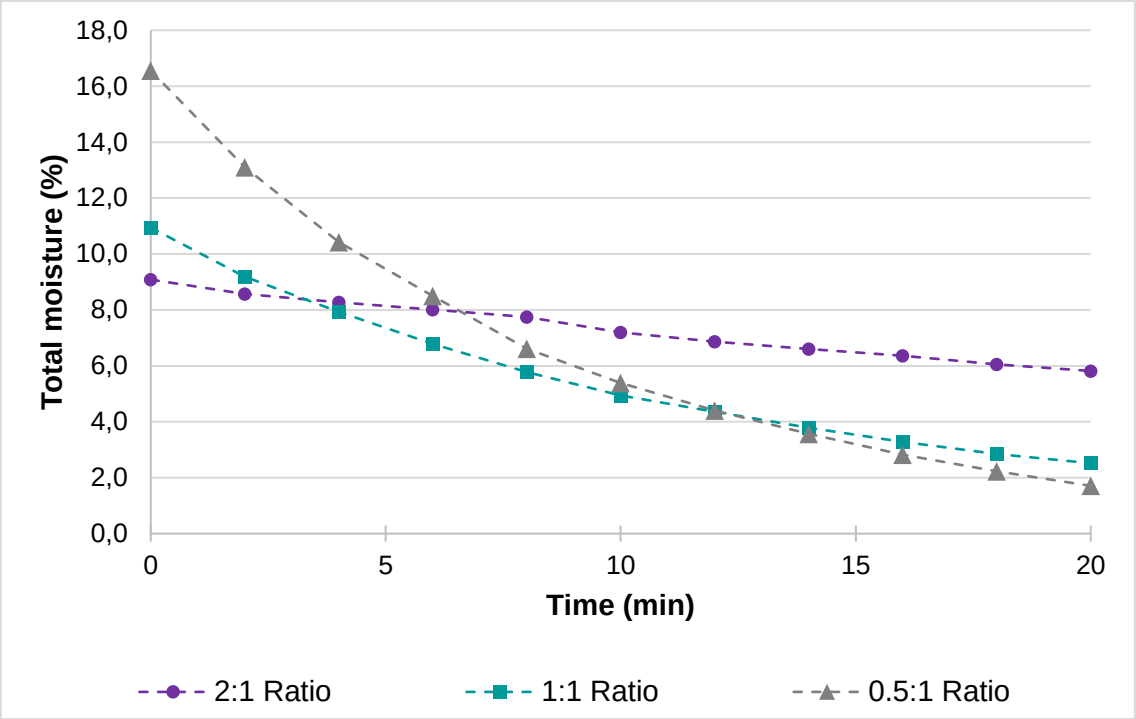

Figure B-1 Regeneration curves of 3 mm activated alumina used to dry flotation product in various adsorbent-to-coal mass ratios

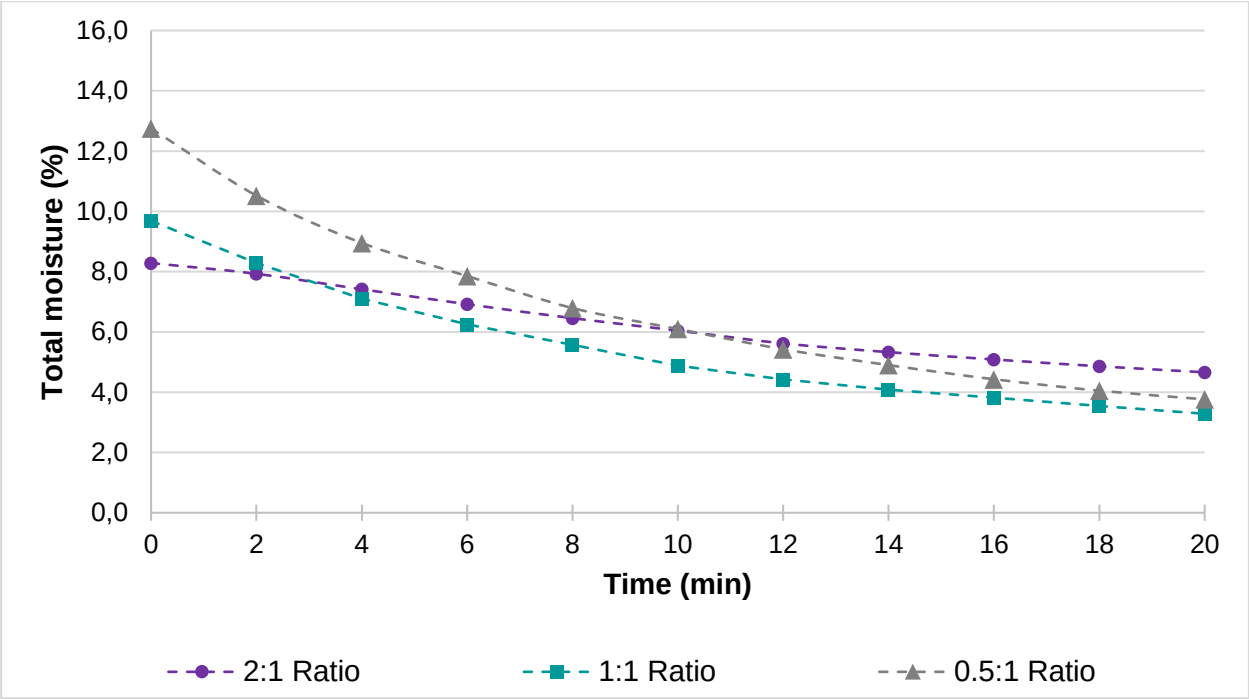

Figure B-2 Regeneration curves of 5 mm activated alumina used to dry flotation product in various adsorbent-to-coal mass ratios

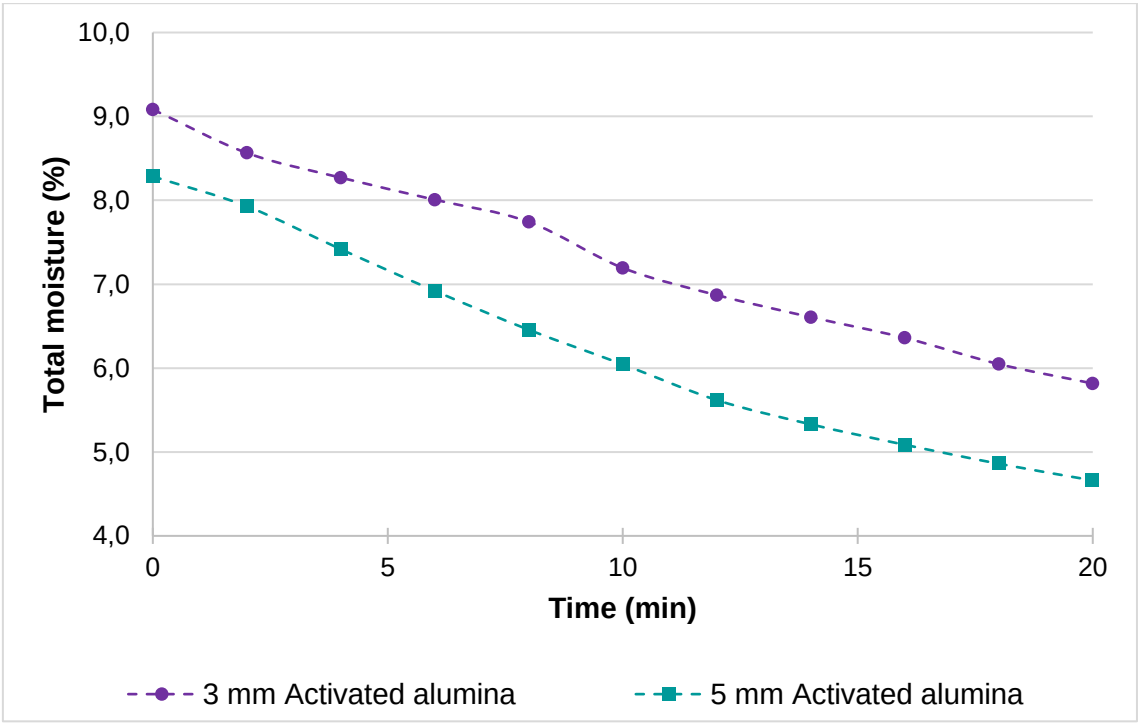

Figure B-3 Regeneration curves of 3 mm and 5 mm activated alumina used to dry flotation product

Annexure C: Industrial applicability

C.1 Energy calculations

Energy calculations for the adsorbent assisted drying of spiral and flotation products were based on two scenarios: drying using new activated alumina and drying using regenerated adsorbents. For the new activated alumina usage, only the rotating bed's energy consumption and the coal's calorific gains were considered. For the more continuous, realistic and industrial approach, using regenerated adsorbents, the rotating bed and regeneration blower's energy consumption and the coal's calorific gains were considered. Calorific gain refers to the gain in coal calorific value due to moisture reduction.

The following assumptions were used during energy calculations:

- Only the rotating bed's energy consumption on which the cylindrical vessels rotated and the regeneration blower were included for energy consumption.
- The climatic chamber's energy consumption and air and moisture enthalpy changes were not included because this was only used for simulation purposes. Air conditioning will not occur in practice, while normal atmospheric air will be fed at the regeneration blowers' suction.
- The adsorbents' adsorption enthalpy was disregarded in the energy calculations because it did not contribute to electrical energy consumption or calorific gains in coal. Therefore, no water enthalpies were considered.
- The calorific gains of spiral and flotation products were considered using new and regenerated adsorbents, respectively.
- The energy calculations were based on the parameters recorded during drying and regeneration using a 2:1 adsorbent-to-coal mass ratio.

For the general energy balance of the drying process, Equation (C-1) applies:

$$\boldsymbol{\Delta E_{drying} = E_{gain} - E_{consumption}} \qquad \text{(C-1)}$$

Where ΔE_{drying} System energy of the drying process in kJ/kg

E_{gain} System energy gain in kJ/kg

$E_{consumption}$ System energy input in kJ/kg

The energy balance of the drying process using new adsorbents equates to Equation (C-2):

$$\boldsymbol{\Delta E_{drying} = E_{coal} - E_{rotation}} \quad \text{(C-2)}$$

The realistic, continuous operation energy balance equates to Equation (C-3):

$$\boldsymbol{\Delta E_{drying} = E_{coal} - E_{rotation} - E_{blower}} \quad \text{(C-3)}$$

For the energy consumption of the rotating bed, Equation (C-4) applies:

$$\boldsymbol{E_{rotation} = \frac{W_{rotation} . t}{m_{coal}}} \quad \text{(C-4)}$$

Where $E_{rotation}$ Energy consumption of the rotating bed in kJ/kg

$W_{rotation}$ Power consumption of the rotating bed in kJ/s

t Rotation time in seconds

m Mass of coal being dried in kg

For the energy consumption of the regeneration blower, Equation (C-5) applies:

$$\boldsymbol{E_{blower} = \frac{W_{blower} . t}{m_{adsorbents}}} \quad \text{(C-5)}$$

Where E_{blower} Energy consumption of the blower in kJ/kg

W_{blower} Power consumption of the blower in kJ/s

t Regeneration time in seconds

m Mass of adsorbents being regenerated in kg

For the energy gain of the coal, Equation (C-6) applies:

$$\boldsymbol{E_{coal} = 1000 . \Delta Q_{coal}} \quad \text{(C-6)}$$

Where E_{coal} Energy gain of the coal in kJ/kg

ΔQ_{coal} Calorific gain of the coal in MJ/kg

For the calorific gain of the coal, Equation (C-7) applies:

$$\boldsymbol{\Delta Q_{coal} = Q_{coal(dried)} - Q_{coal(wet)}} \quad \text{(C-7)}$$

Where ΔQ_{coal} Calorific gain of the coal in MJ/kg

$Q_{coal(dried)}$ Coal calorific value after drying in MJ/kg

$Q_{coal(wet)}$ Coal calorific value before drying in MJ/kg

For this study, the following equipment power consumptions and coal and adsorbent masses were applicable:

$W_{rotation} = 0.09\ kW$

$W_{blower} = 0.7\ kW$

$m_{coal} = 0.16\ kg$

$m_{adsorbents} = 0.34\ kg$

Table C-1 shows the summarised energy calculations for the adsorbent assisted drying of this study. The drying time refers to the drying time required to reach target moisture for the respective coals and scenarios (new or regenerated adsorbents). The required regeneration time for sufficient regeneration was based on an approximate 50% adsorbent moisture reduction.

Table C-1 Summarised energy calculations for adsorbent assisted drying

Property	Unit	Spiral product	Flotation product
Drying time (new)	min	2	2
Drying time (regenerated)	min	2	4
Regeneration time	min	10	10
E_{coal} (new adsorbents)	kJ/kg	2795.0	3787.3
E_{coal} (regenerated adsorbents)	kJ/kg	2545.2	3020.7
$E_{rotation}$ (new adsorbents)	kJ/kg	67.5	67.5
$E_{rotation}$ (regenerated adsorbents)	kJ/kg	67.5	135
E_{blower}	kJ/kg	1235.3	1235.3
ΔE_{drying} (new adsorbents)	kJ/kg	2727.5	3719.8
ΔE_{drying} (drying & regeneration)	kJ/kg	1242.4	1650.4

C.2 Economic feasibility calculations

The high-level economic feasibility calculations were based on the following assumptions:

- Operational expenditure included only adsorbent consumption.
- The process income included coal sales.

The following parameters were applicable for the calculations:

Adsorbent-to-coal mass ratio:	1:1
Coal feed rate:	65 tonnes per hour
Adsorbent bulk sale price:	$1400/tonne (Wong, 2020)
Coal price:	$82.76/tonne (Indexmundi, 2021)
Coal sales per month:	$3,873,168.00
Adsorbent procurement frequency:	Daily, every second day, weekly, fortnightly, monthly
Adsorbent procurement cost:	$91,000/ coal feed

$$Operational\ profit = montly\ coal\ sales - montly\ adsorbent\ procurement$$